## Supplementary Information

# Integrating artificial intelligence and optogenetics for Parkinson's disease diagnosis and therapeutics in male mice

Bobae Hyeon[1,2,3], Jaehyun Shin[4#], Jae-Hun Lee[5#], Woori Kim[2,3], Jea Kwon[6], Heeyoung Lee[1], Dae-gun Kim[7,8], Choong Yeon Kim[9,10], Sang Kun Choi[1], Jae-Woong Jeong[9,11,12], Kwang-Soo Kim[2,3], C. Justin Lee[5*], Daesoo Kim[7*] and Won Do Heo[1,7,13*]

[#] These authors contributed equally
[*] Corresponding authors

C. Justin Lee: cjl@ibs.re.kr
Daesoo Kim: daesoo@kaist.ac.kr
Won Do Heo: wondo@kaist.ac.kr

This PDF includes the following;

high-resolution Supplementary Figure file is available via Figshare (see Data Availability).

Supplementary Figures (45)

Supplementary Tables (22)

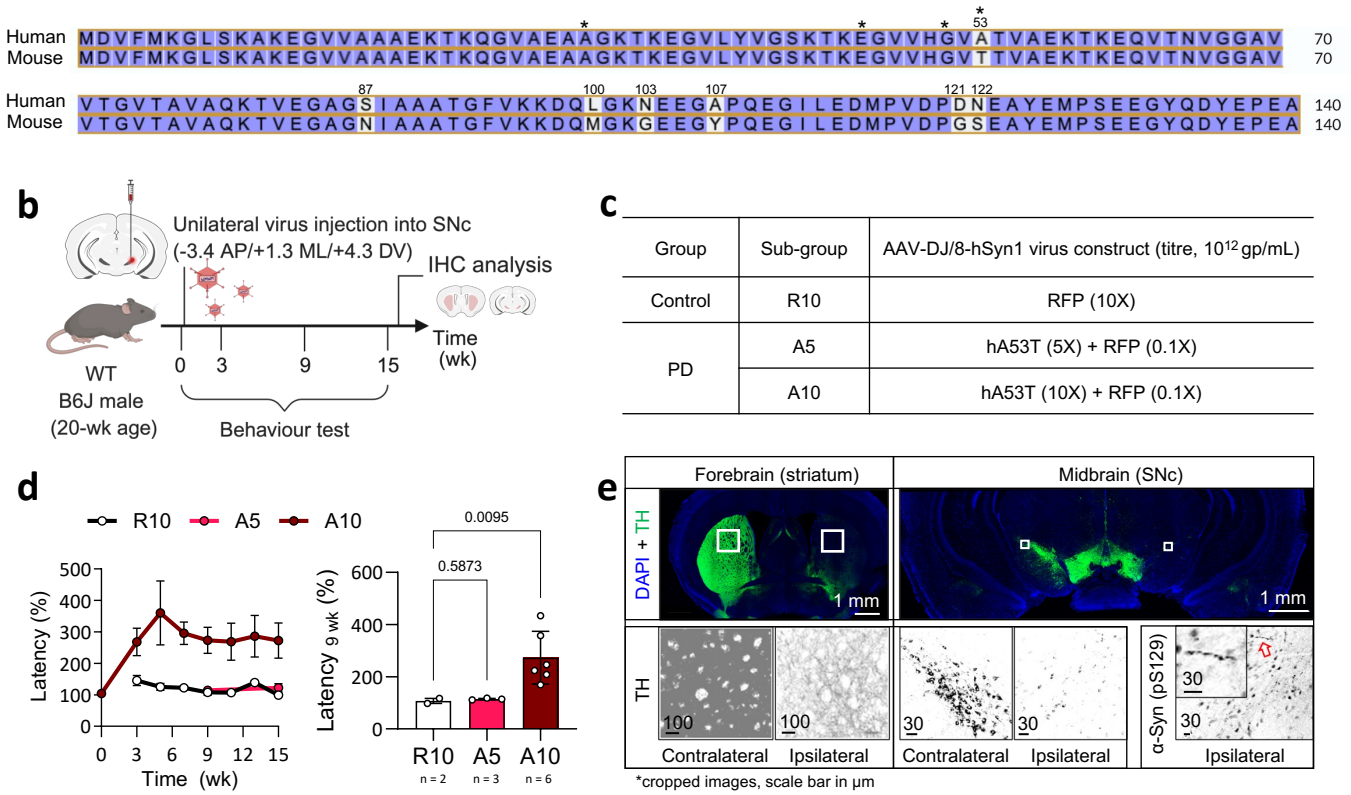
Supplementary Notes (8)

Supplementary References

# Supplementary Figures

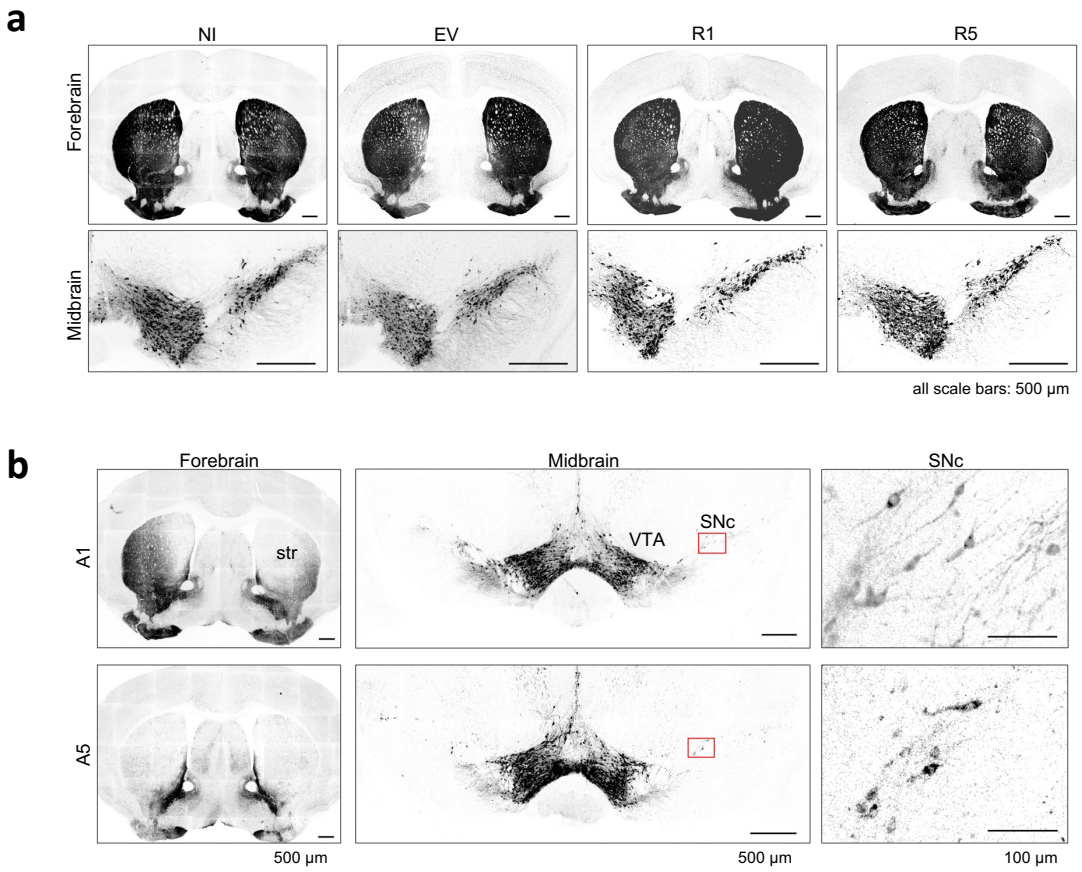
List of Supplementary Figures:


1. Unilateral hA53T PD mouse model failed to show dose-dependent PD severity.
2. Immunohistochemistry (IHC) images of the CT and PD groups.
3. Bilateral hA53T PD mouse model exhibited diverse phenotypes.
4. Comparison temporal variabilities with t-SNE datasets.
5. Description of features engineered to develop AI models for PD diagnosis in mice.
6. Development and comparison of AI models for PD diagnosis.
7. Comparison of cross-view (CV) and cross-subject (CS) validation methods.
8. Comparison of APS, RRS, and BWS for early PD detection at 2 wk.
9. Validation of APS for PD specificity using an amyotrophic lateral sclerosis (ALS) mouse model.
10. Detailed plots of correlation analysis with varied dataset filtering at group level.
11. Summary of correlation analysis.
12. Comparison train-validation (TV) and unseen datasets for top 20 feature importances.
13. Comparison of body lengths across non-PD (NP) and PD groups.
14. CT group's longitudinal analysis of the top 20 features (XGB model) in the KDE plots.
15. PD (A5) group's longitudinal analysis of the top 20 features (XGB model) in the KDE plots.
16. Longitudinal comparison of KL divergences (XGB model) between the CT and PD (A5) groups.
17. Longitudinal comparison of feature values (XGB model) between the CT and PD (A5) groups.
18. NALS group's longitudinal analysis of the top 20 features (XGB model) in the KDE plots.
19. ALS group's longitudinal analysis of the top 20 features (XGB model) in the KDE plots.
20. Longitudinal comparison of KL divergences (XGB model) between the NALS and ALS groups.
21. Longitudinal comparison of feature values (XGB model) between the NALS and ALS groups.
22. Endpoint comparison of PD and ALS groups for the top 20 features identified by the XGB model.
23. SHAP dependence plots of the top 20 features (XGB model).
24. Summary table of SHAP dependence plots for the top 20 features (XGB model).
25. Behavioural assessments (RRS, BWS, and APS) in PD mice treated with optogenetic stimulation (optoRET).
26. Behavioural assessments (RRS, BWS, and APS) in A1 PD mice treated with L-DOPA or RET agonist (BT44).
27. Group comparison of the decision tree plots (XGB model) at 10 wk.
28. Group comparison of the top 20 features (XGB model) in the KDE plots at 10 wk.
29. Comparison of KL divergences of the top 20 features (XGB model) between groups at 10 wk.
30. Group comparisons of the feature values (XGB model) at 10 wk.
31. Comparisons of treatment response and PD symptomatic evaluations in A1 PD mice with different treatments.
32. Summary table of the features engineered and extracted for the spectro-temporal analysis.
33. Model evaluation and SHAP dependence plots of top 20 features (TSFEL model).
34. CT group's longitudinal analysis of the top 20 features (TSFEL model) in the KDE plots.
35. PD (A5) group's longitudinal analysis of the top 20 features (TSFEL model) in the KDE plots.
36. Longitudinal comparison of KL divergences (TSFEL model) between the CT and PD (A5) groups.
37. Longitudinal comparison of feature values (TSFEL model) between the CT and PD (A5) groups.
38. Group comparison of the KDE plots of the top 20 features (TSFEL model) at 10 wk.
39. Group comparison of the top 20 features (TSFEL model) at 10 wk.
40. Group comparison of the turning features at 10 wk.
41. Group comparison of the rearing features at 10 wk.
42. Model evaluation and SHAP dependence plots of top 20 features (Gait model).
43. Group comparison of the top 20 features (Gait model) in KDE plots at 10 wk.
44. Group comparison of the top 20 features (Gait model) in bar plots at 10 wk.
45. Snapshot video images of CT and PD mice in walking.




**Supplementary Figure 1. Unilateral hA53T PD mouse model failed to show dose-dependent PD severity.**

**(a)** Sequence alignment of human (UniProt ID: P37840) and mouse (UniProt ID: O55042) alpha-synuclein (aSyn) amino acid sequences, highlighting seven mismatches (A53T, S87N, L100M, N103G, A107Y, D121G, and N122S). Positions of familial PD-associated substitutions (A30P, E46K, G51D, A53E, and A53T) are indicated by asterisks (*). Notably, substitutions in the C-terminal region of mouse aSyn (G121 and S122) effectively dampen membrane-induced aSyn aggregation and vesicle permeabilisation, protecting rodents from the deleterious effects exerted by the A53T mutation in humans. **(b)** Schematic illustration of the experimental setup used to characterise the unilateral hA53T PD mouse model. **(c)** Table summarising three experimental groups injected with RFP or different doses of hA53T virus. **(d)** Line and bar graphs showing traverse latency in the elevated-beam walking test (BWT), analysed longitudinally and at the midpoint (9 wk), respectively (R10 = 107.4% ± 9.38, A5 = 114.5% ± 2.17, A10 = 273.0% ± 41.26; traverse time normalised by mean baseline of A10). **(e)** Representative TH-stained immunohistochemistry (IHC) images of forebrain and midbrain sections, highlighting the striatum and SNc following unilateral injection of hA53T at the 5X dose (A5 group). An additional SNc image stained for phospho-aSyn (pS129) reveals aSyn aggregates and Lewy-like fibrils (indicated by a red arrow). Data are shown as mean ± SEM; sample sizes (n) are indicated in plots. Schematic was created in Schematics were created in BioRender. Heo, W. (2025) https://BioRender.com/cykyauz. Statistical analysis was performed using Brown–Forsythe and Welch one-way ANOVA tests followed by Dunnett's T3 post hoc corrections for multiple comparisons. Source data are provided in the Source Data file.

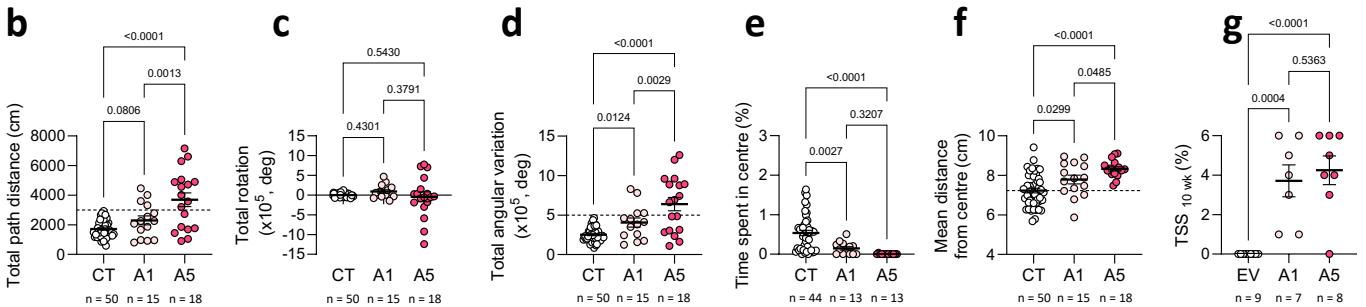



**Supplementary Figure 2. Immunohistochemistry (IHC) images of the CT and PD groups.**

**(a)** Representative TH-stained IHC images of the forebrain and midbrain from CT subgroups. **(b)** Representative TH-stained IHC images of the forebrain and midbrain from PD subgroups. Red boxes indicate the SNc regions shown in the enlarged images on the right. Abbreviations: CT, control; NI, no virus injection; EV, empty vector; R1, RFP (1X); R5, RFP (5X); A1, hA53T (1X); A5, hA53T (5X); str, striatum; SNc, substantia nigra pars compacta; VTA, ventral tegmental area; TH, tyrosine hydroxylase.

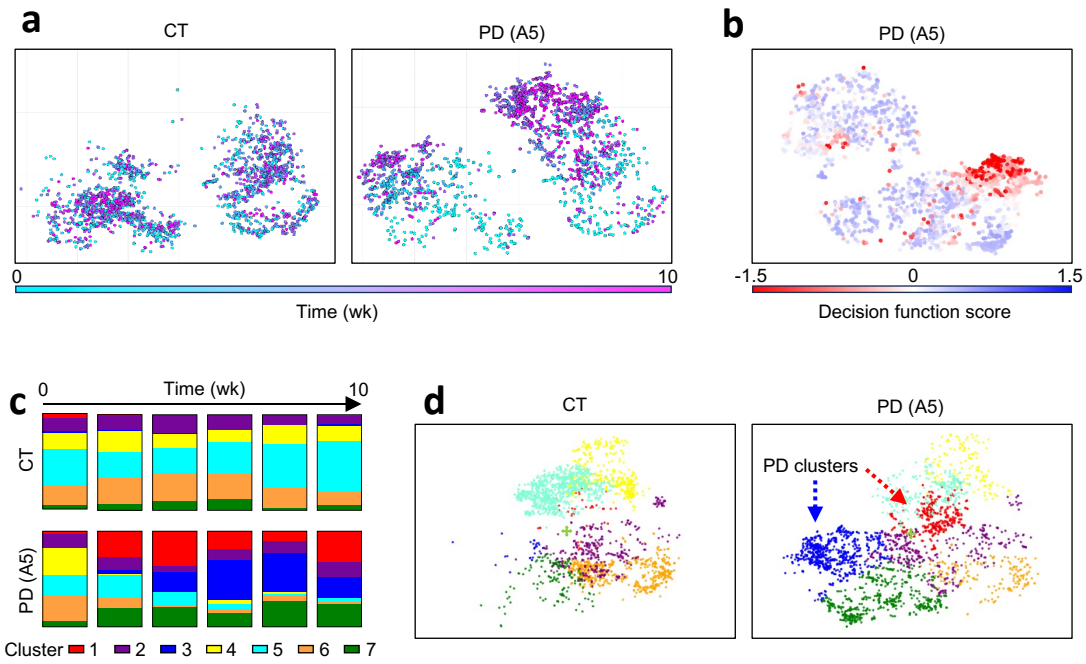
**a**

| Observed phenotype | Behaviour assessment | Observation in A5 | Examples |
|---|---|---|---|
| Hyperactivity | OFT | 61% (11/18) | CT: Total distance: 2358.35 cm; Total rotation: 13416.89 deg; Time in center: 0.57%; Mean: 6.73 cm |
| Directional movement (rotation) | OFT | 56% (10/18) | A1: Total distance: 2254.29 cm; Total rotation: 123376.96 deg; Time in center: 0.20%; Mean: 7.47 cm |
| Thigmotaxis | OFT | 67% (12/18) | A5: Total distance: 5057.69 cm; Total rotation: -57164.36 deg; Time in center: 0.00%; Mean: 8.51 cm |
| Tremor (hands) | OFT | 100% (16/16) | Supplementary_Movie_01_Tremor |
| Increased wall-touching in rearing | OFT | 94% (15/16) | Supplementary_Movie_02_Rearing |
| Lagging/trailing feet in walking | OFT | 63% (10/16) | Supplementary_Movie_03_Trailing |
| Distracted (stop and look downward) | BWT | 87% (13/15) | Distracted; Sandwiching; Collapsed |
| Collapsed (plantar on the beam over 50% of total testing distance) | BWT | 67% (10/15) | |
| Freezing or dragging feet on the beam | BWT | 87% (13/15) | |
| Thighs sandwiching the beam | BWT | 80% (12/15) | Supplementary_Movie_04_EBWT |
| Hindlimb clasping | TST | 88% (7/8) | Class 0; Class 1; Class 2; Class 3 |




**Supplementary Figure 3. Bilateral hA53T PD mouse model exhibited diverse phenotypes.**

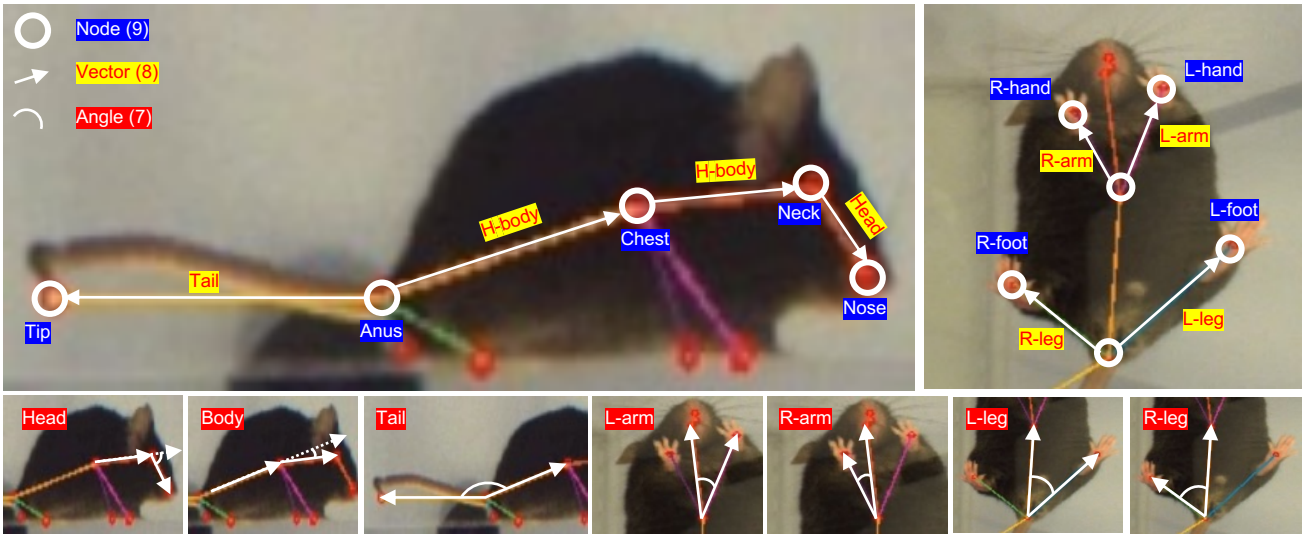
**(a-g)** Altered locomotion, motor coordination, tremor, and dystonia observed during the open-field test (OFT), elevated-beam walking test (BWT), and tail suspension test (TST). In panel a, percentages represent the proportion of mice in the A5 group exhibiting each behavioural phenotype, determined by defined thresholds. **(b-f)** Metrics of body centre position measured in the OFT, assessing altered locomotion. Dashed horizontal lines in panels (b, d, f) indicate the thresholds for hyperactivity, rotation, and thigmotaxis in PD, respectively. **(g)** Assessment of hindlimb clasping measured as TST score (TSS, see Methods). Abbreviations: Control (CT), EV (non-PD), A1 (mild) and A5 (severe) PD groups. Data are shown as mean ± SEM; sample sizes (n) are indicated in plots. All statistical analyses were performed using one-way ANOVA followed by Holm–Sidak post hoc corrections for multiple comparisons. Source data are provided in the Source Data file.




**Supplementary Figure 4. Comparison temporal variabilities with t-SNE datasets.**

**(a)** Temporal dynamics of t-SNE datasets (3D) for the Control (CT) and PD (A5) groups, shown in 2D flatted plots. **(b)** Anomaly detection results for the PD (A5) group, compared to the CT group. Each group contains dataset, covering the entire experimental period (0–10 wk). **(c)** Time-series bar graphs of the proportionality of *k*-means clustering labels for the CT and PD groups. **(d)** *K*-means clustering results, labelled with cluster 1–7 for the CT and A5 groups (0–10 wk). The PD specific clusters (dots in red [label 1] and blues [label 5]) are indicated with the dashed arrows.

**a**




**b**

| Name of Engineered feature | | |

**a**

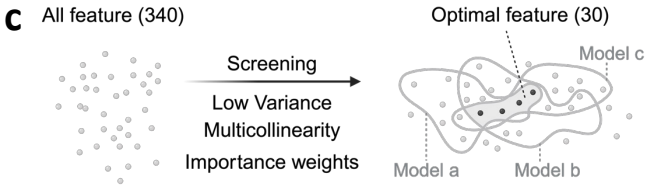
| | CT | A5 |
|---|---|---|
| Number of mice used for ML | 10 | 11 |
| Dataset included wk | 0 - 10 wk | 4 - 10 wk |
| Number of clips | 5,855 | 11,066 |
| + Additional clips (0 wk) | 5,249 | 0 |
| Number of clips for ML (train/validation) | 7,661/3,444 | 7,616/3,449 |

**b**

Parameter setting for training Extreme Gradient Boosting (XGB)

- learning_rate: 0.3
- n_estimators: 100
- max_depth: 6
- Subsample: 1
- Colsample_bytree: 1
- gamma: 0
- booster: "gbtree"
- reg_lambda: 1
- reg_alpha: 0

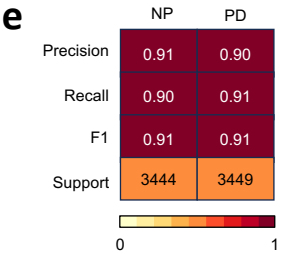
**c**



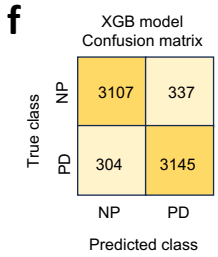

**d**

| Model | All features | Optimal features |
|---|---|---|
| Extreme Gradient Boosting | 0.93 | 0.90 |
| Extra Trees Classifier | 0.89 | 0.90 |
| Random Forest Classifier | 0.90 | 0.89 |
| Light Gradient Boosting Machine | 0.91 | 0.89 |
| Gradient Boosting Classifier | 0.88 | 0.86 |
| Ada Boost Classifier | 0.85 | 0.83 |
| Decision Tree Classifier | 0.81 | 0.81 |
| Logistic Regression | 0.87 | 0.81 |
| Quadratic Discriminant Analysis | 0.79 | 0.81 |
| Linear Discriminant Analysis | 0.88 | 0.81 |
| Ridge Classifier | 0.88 | 0.81 |
| K Neighbors Classifier | 0.75 | 0.80 |
| SVM - Linear Kernel | 0.82 | 0.76 |
| Naive Bayes | 0.73 | 0.76 |
| Dummy Classifier | 0.49 | 0.50 |

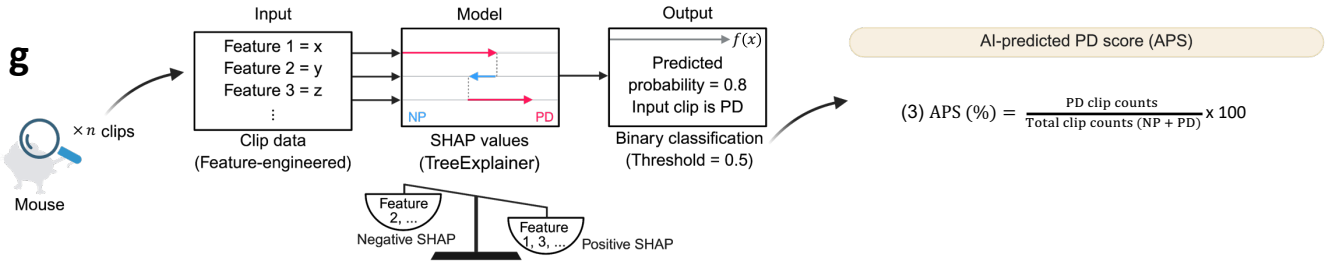
**e**




**f**




**g**




**Supplementary Figure 6. Development and comparison of AI models for PD diagnosis.**

**(a)** Summary table of balanced dataset compositions, prepared from Control (CT) and PD (A5) groups for AI model development for PD diagnosis. **(b)** Summary table of parameter settings applied for XGB model training with PyCaret (version 2.3.10). See Supplementary Table 2 for default parameter settings of other classifiers. Default parameters may differ in more recent PyCaret versions. **(c)** Schematic illustration of the feature selection process, outlining the screening criteria and how the optimal features were identified from the comparison of various classifiers. **(d)** Comparison of various classifiers' performance when trained with full feature set (n = 340) and the optimal feature set (n = 30), detailing accuracy on the classification of validation dataset. **(e)** Summary of the XGB model evaluation metrics. **(f)** Confusion matrix of the XGB model in the classification of the cross-view (CV) validation dataset. **(g)** Schematic illustration, detailing the derivation of PD scores from the AI model's predictions on motion clips (as non-PD [NP] or PD), for each mouse. Abbreviations: ML, machine learning; NP, non-PD. Schematics were created in BioRender. Heo, W. (2025) https://BioRender.com/cykyauz.

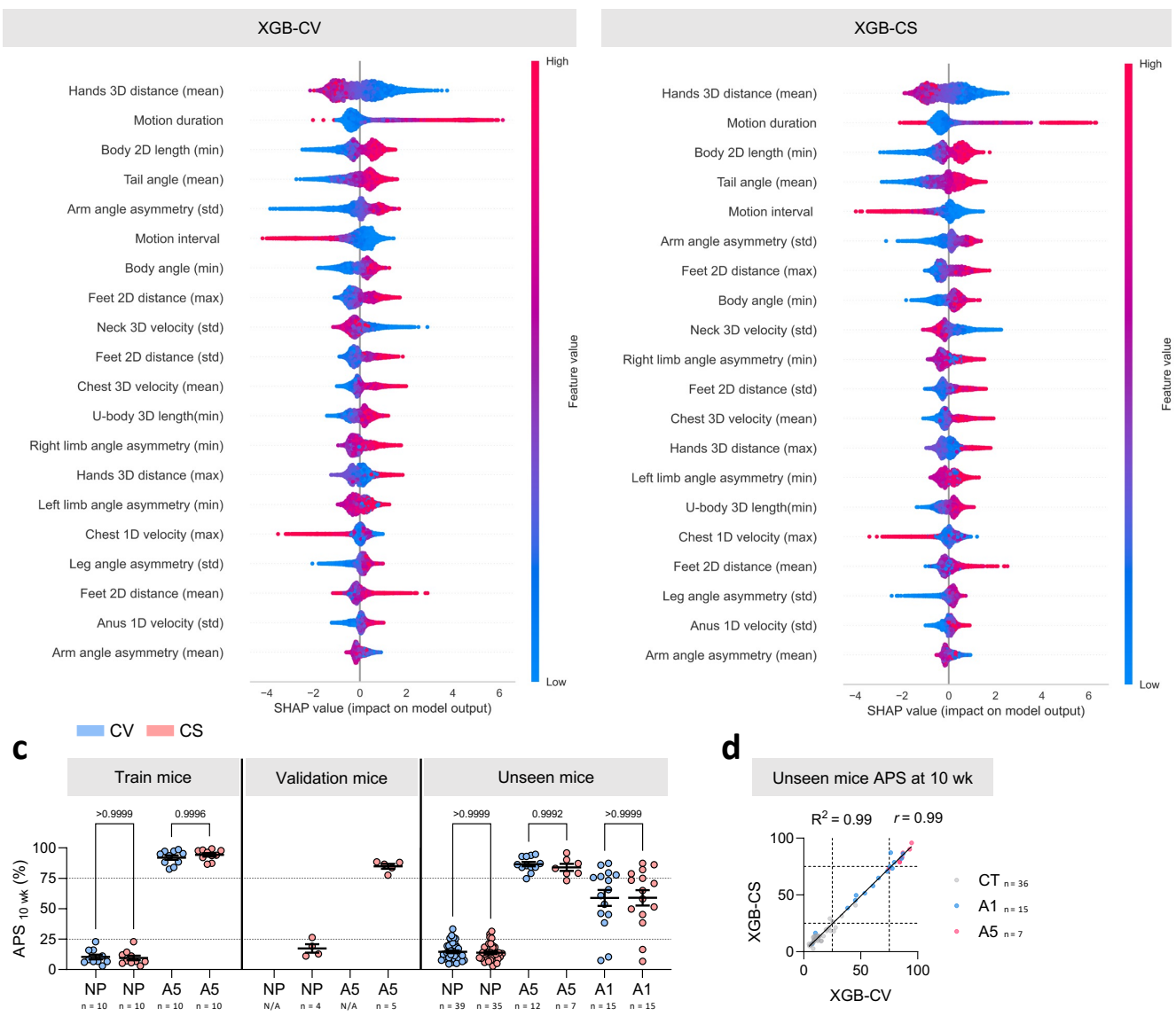
**a**

Cross-view (CV)

| | Model | Accuracy | AUC | Recall | Prec. | F1 | Kappa | MCC | TT (Sec) |
|---|---|---|---|---|---|---|---|---|---|
| xgboost | Extreme Gradient Boosting | 0.9029 | 0.9635 | 0.9086 | 0.8978 | 0.9031 | 0.8057 | 0.8059 | 4.218 |
| et | Extra Trees Classifier | 0.8951 | 0.9618 | 0.8713 | 0.9142 | 0.8921 | 0.7901 | 0.7911 | 0.854 |
| rf | Random Forest Classifier | 0.8942 | 0.959 | 0.8895 | 0.8972 | 0.8933 | 0.7883 | 0.7884 | 2.208 |
| lightgbm | Light Gradient Boosting Machine | 0.8884 | 0.9566 | 0.8836 | 0.8915 | 0.8875 | 0.7768 | 0.7769 | 0.466 |
| gbc | Gradient Boosting Classifier | 0.8621 | 0.9373 | 0.8514 | 0.8693 | 0.8602 | 0.7243 | 0.7246 | 5.591 |
| ada | Ada Boost Classifier | 0.8293 | 0.9127 | 0.8205 | 0.8343 | 0.8272 | 0.6585 | 0.6589 | 1.248 |
| dt | Decision Tree Classifier | 0.811 | 0.8111 | 0.8366 | 0.795 | 0.8152 | 0.6221 | 0.6231 | 0.633 |
| lr | Logistic Regression | 0.8101 | 0.8851 | 0.7991 | 0.816 | 0.8073 | 0.6202 | 0.6205 | 2.631 |
| qda | Quadratic Discriminant Analysis | 0.8069 | 0.8836 | 0.731 | 0.8606 | 0.7903 | 0.6136 | 0.6208 | 0.195 |
| lda | Linear Discriminant Analysis | 0.8064 | 0.8818 | 0.7909 | 0.8151 | 0.8027 | 0.6127 | 0.6132 | 0.214 |
| ridge | Ridge Classifier | 0.8058 | 0 | 0.7915 | 0.8137 | 0.8023 | 0.6115 | 0.612 | 0.222 |
| knn | K Neighbors Classifier | 0.7973 | 0.873 | 0.7554 | 0.8234 | 0.7878 | 0.5946 | 0.5968 | 0.475 |
| svm | SVM - Linear Kernel | 0.764 | 0 | 0.7624 | 0.7775 | 0.762 | 0.5281 | 0.5391 | 0.338 |
| nb | Naive Bayes | 0.757 | 0.8422 | 0.657 | 0.8196 | 0.7292 | 0.5136 | 0.524 | 0.193 |
| dummy | Dummy Classifier | 0.5017 | 0.5 | 0 | 0 | 0 | 0 | 0 | 0.176 |

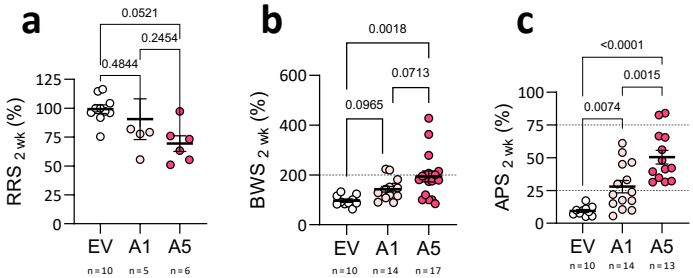
Cross-subject (CS)

| | Model | Accuracy | AUC | Recall | Prec. | F1 | Kappa | MCC | TT (Sec) |
|---|---|---|---|---|---|---|---|---|---|
| xgboost | Extreme Gradient Boosting | 0.8959 | 0.9612 | 0.8882 | 0.8996 | 0.8913 | 0.7916 | 0.7948 | 5.068 |
| rf | Random Forest Classifier | 0.89 | 0.9551 | 0.8722 | 0.901 | 0.8839 | 0.7797 | 0.7828 | 2.831 |
| et | Extra Trees Classifier | 0.8892 | 0.9574 | 0.8451 | 0.9227 | 0.8787 | 0.7781 | 0.7836 | 0.993 |
| lightgbm | Light Gradient Boosting Machine | 0.8762 | 0.9516 | 0.8642 | 0.8814 | 0.8693 | 0.7521 | 0.7559 | 0.553 |
| gbc | Gradient Boosting Classifier | 0.8553 | 0.9318 | 0.8377 | 0.8627 | 0.846 | 0.7103 | 0.7144 | 6.558 |
| ada | Ada Boost Classifier | 0.8287 | 0.9085 | 0.8141 | 0.8331 | 0.8203 | 0.6571 | 0.6605 | 1.601 |
| dt | Decision Tree Classifier | 0.8105 | 0.8106 | 0.8222 | 0.7995 | 0.8096 | 0.6209 | 0.6226 | 0.611 |
| lr | Logistic Regression | 0.8066 | 0.88 | 0.7926 | 0.8088 | 0.7982 | 0.613 | 0.6153 | 2.045 |
| qda | Quadratic Discriminant Analysis | 0.8045 | 0.8798 | 0.7223 | 0.8538 | 0.7765 | 0.6081 | 0.6175 | 0.314 |
| lda | Linear Discriminant Analysis | 0.8025 | 0.8773 | 0.783 | 0.8077 | 0.7923 | 0.6047 | 0.6073 | 0.294 |
| ridge | Ridge Classifier | 0.8019 | 0 | 0.7839 | 0.8061 | 0.7922 | 0.6035 | 0.6059 | 0.313 |
| svm | SVM - Linear Kernel | 0.7872 | 0 | 0.7787 | 0.7848 | 0.7757 | 0.5741 | 0.58 | 0.617 |
| knn | K Neighbors Classifier | 0.7865 | 0.8649 | 0.7446 | 0.8059 | 0.7708 | 0.5726 | 0.5765 | 0.552 |
| nb | Naive Bayes | 0.7574 | 0.8382 | 0.6582 | 0.8088 | 0.721 | 0.5137 | 0.5236 | 0.326 |
| dummy | Dummy Classifier | 0.5053 | 0.5 | 0 | 0 | 0 | 0 | 0 | 0.295 |



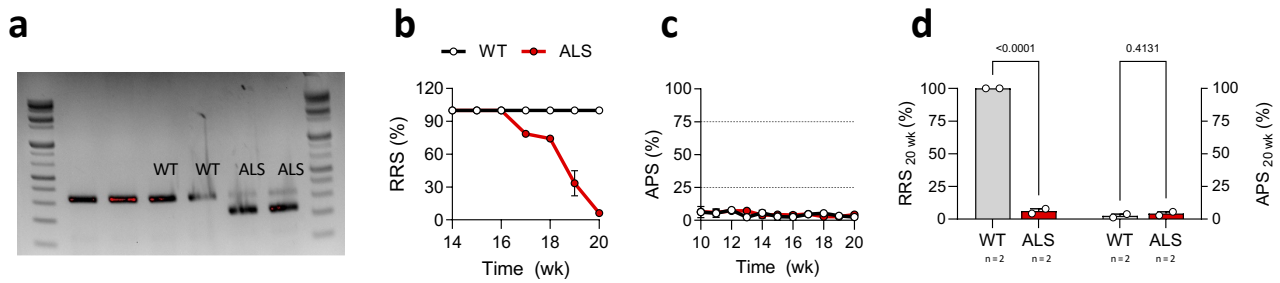

**Supplementary Figure 7. Comparison of cross-view (CV) and cross-subject (CS) validation methods.**

**(a)** Tables summarising the evaluation metrics for the models trained and validated using CV (left) and CS (right) methods. **(b)** SHAP summary plots of the XGB models computed on the CV (left) and CS (right) validation datasets. The top 4 features are identically ranked, with 100% of the top 20 features overlapping between the two methods. Comparisons of the feature order, Spearman correlation was ≈ 0.9789 ($p$ ≈ 7.15e-14) and of the absolute SHAP values, the Pearson correlation was ≈ 0.9999 ($p$ ≈ 4.81e-114). **(c)** Prediction results (AI-predicted PD scores; APS) for the mice across datasets, as predicted by the XGB-CV model (blue) and the XGB-CS model (red). No significant differences were found across all groups. Importantly, XGB-CV model assessed all unseen A5 mice into the severe PD category (APS > 75% in rounded values). **(d)** Comparison of the APS for each mouse by the two models. The dashed line indicates the simple linear regression of the all data plotted. Two model predictions were highly correlated (Pearson's correlation, $r$ = 0.99). Collectively, these findings robustly confirm the generalisability and stability of the CV-based XGB model. Data are shown as mean ± SEM; sample sizes (n) are indicated in plots. Statistical analysis was performed using one-way ANOVA followed by Holm–Sidak post hoc corrections for multiple comparisons. Source data are provided in the Source Data file.



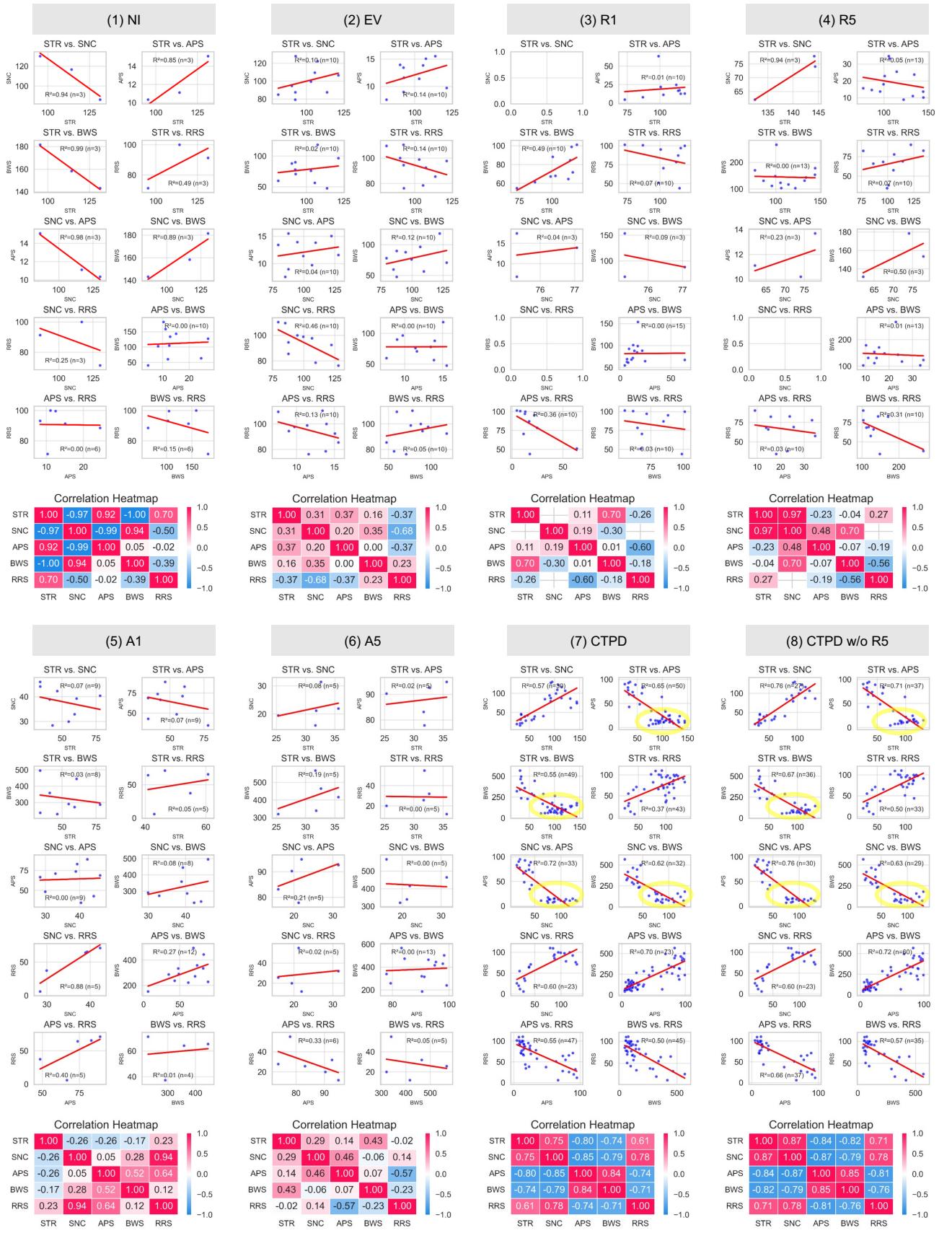

**Supplementary Figure 8. Comparison of APS, RRS, and BWS for early PD detection at 2 wk.**

**(a–c)** Comparisons of RRS, BWS and APS assessments for the EV, A1 and A5 groups at 2 wk post-surgery (RRS [%]: EV = 99.22 ± 3.67, A1 = 90.56 ± 17.62, A5 = 69.37 ± 6.84; BWS [%]: EV = 96.74 ± 6.69, A1 = 142.9 ± 11.16, A5 = 194.2 ± 22.37; APS [%]: EV = 9.42 ± 1.15, A1 = 27.94 ± 4.70, A5 = 50.41 ± 5.23). Data are shown as mean ± SEM; sample sizes (n) are indicated in plots. Statistical analysis was performed using one-way ANOVA followed by Holm–Sidak post hoc corrections for multiple comparisons. Source data are provided in the Source Data file. Abbreviations: RRS, rotarod test score; BWS, elevated beam walking test score; APS, AI-predicted PD score.



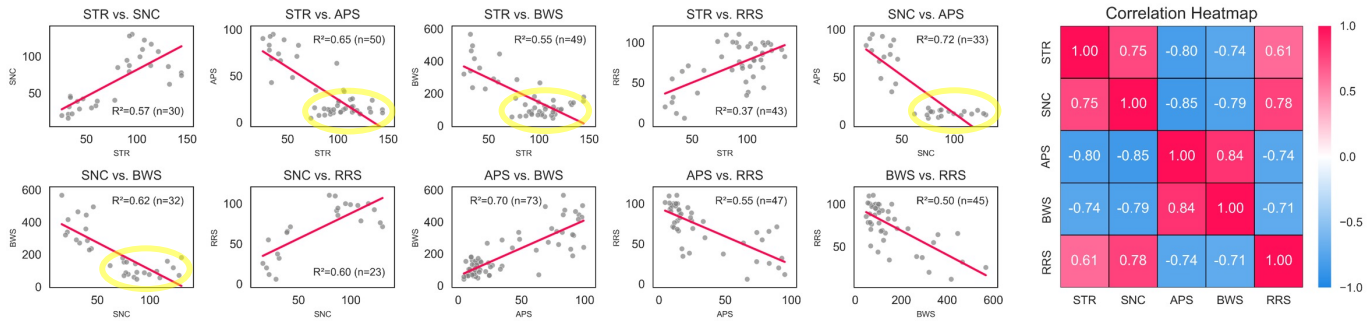

**Supplementary Figure 9. Validation of APS for PD specificity using an amyotrophic lateral sclerosis (ALS) mouse model.**

**(a)** Genotyping results of wild-type (WT) and ALS model (SOD1-G93A heterozygous transgenic) mice. **(b–d)** Comparisons of rotarod test score (RRS) and AI-predicted (XGB model) PD score (APS) assessments between WT and ALS mice, shown as fitted line and dot graphs for both longitudinal (10 or 14 - 20 wk of age) and endpoint (20 wk of age) analyses (RRS [%]: WT = 100 ± 0.00, ALS = 6.11 ± 1.85; APS: WT = 2.52 ± 1.33, ALS = 4.24 ± 1.38; n = 2 per group). ALS mice exhibit clear motor dysfunction as assessed by RRS, while APS remains comparable to WT. Note that ALS mice have shorter lifespans (50% survival at 128.9 ± 9.1 days), so the experimental scheme was adjusted to the 10–20 wk age range. Data are shown as mean ± SEM; sample sizes (n) are indicated in plots. Statistical analysis was performed using two-way ANOVA followed by Fisher's LSD post hoc tests without correction for multiple comparisons. Source data are provided in the Source Data file.



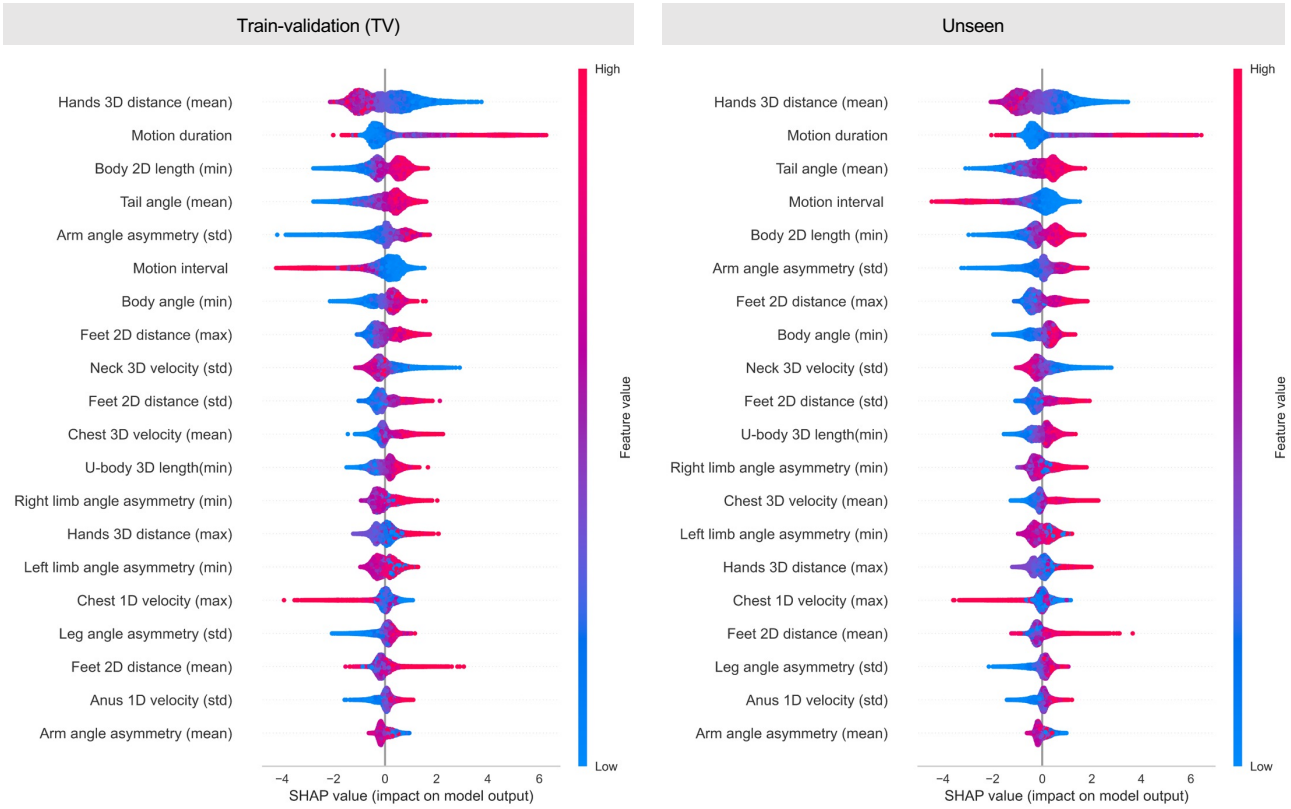

**Supplementary Figure 10. Detailed plots of correlation analysis with varied dataset filtering at group level.**

Line graphs (fitting line in red) of pairs of metrics and a heatmap of Pearson's correlation values. Datasets, including all CT and PD groups were filtered by group(s) and then filtered by each pair of metrics for the computation of Pearson's correlation (not by all metrics). Individual group filtered plot sets (#1-6), highlight variabilities in the correlation of different pairs of metrics as a characteristic for the group. Plot set #7 shows the overall data correlations between metrics. In plot set #8, the R5 group was excluded to show the effect of this group on decreasing the magnitude of correlations, particularly STR vs SNc. Yellow ovals on set #7 and #8 highlight the buffering capacity of DA system, reflected in flat clusters of APS and BWS. Abbreviations: STR, striatal TH intensity; SNC, SNc TH cell counts, RRS, rotarod test score; BWS, elevated beam walking test score; APS, AI-predicted PD score.



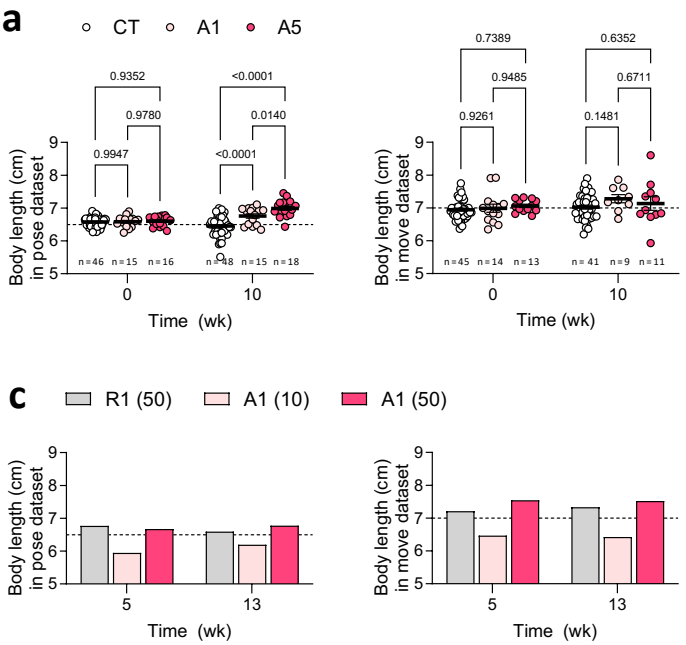

**Supplementary Figure 11. Summary of correlation analysis.**

Line graphs (fitting line in red) of pairs of metrics and a heatmap of Pearson's correlation values. For each computation, dataset (CT and PD groups) are filtered for each pair of metrics. Yellow ovals highlight the buffering capacity of DA system, reflected in flat clusters of APS and BWS. Abbreviations: STR, striatal TH intensity; SNC, SNc TH cell counts, RRS, rotarod test score; BWS, elevated beam walking test score; APS, AI-predicted PD score.



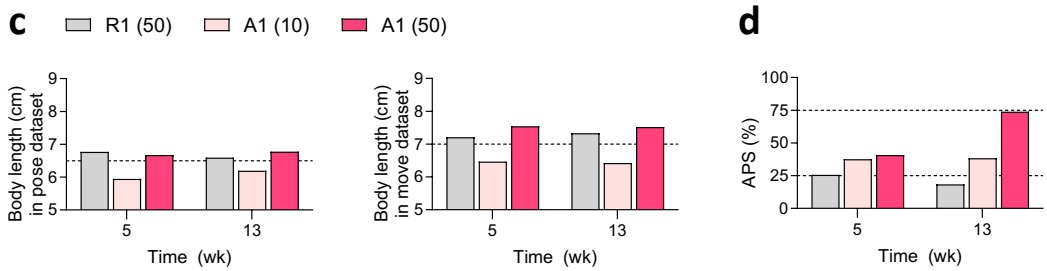

**Supplementary Figure 12. Comparison train-validation (TV) and unseen datasets for top 20 feature importances.**

Bar charts display the absolute mean SHAP values of the XGB models computed on the TV (left; NP = 10, A5 = 11 mice) and the unseen (right; NP = 40, A5 = 13 mice) datasets. The analysis revealed a 100% overlap in the top 20 features, with a Spearman correlation of ≈ 0.9835 ($p$ ≈ 8.29e-15). A separate comparison of the absolute SHAP values for these top 20 features yielded a Pearson correlation of about 0.2013 ($p$ ≈ 0.3948), indicating some variability in the absolute magnitudes; however, given the near-perfect consistency in ranking, this variation in magnitudes is considered of lesser concern. Together, these results provide robust quantitative evidence that the top 20 features remain highly relevant across the TV and unseen datasets, thereby confirming the stability and generalisability of the feature selection approach.
Abbreviations: NP, non-PD



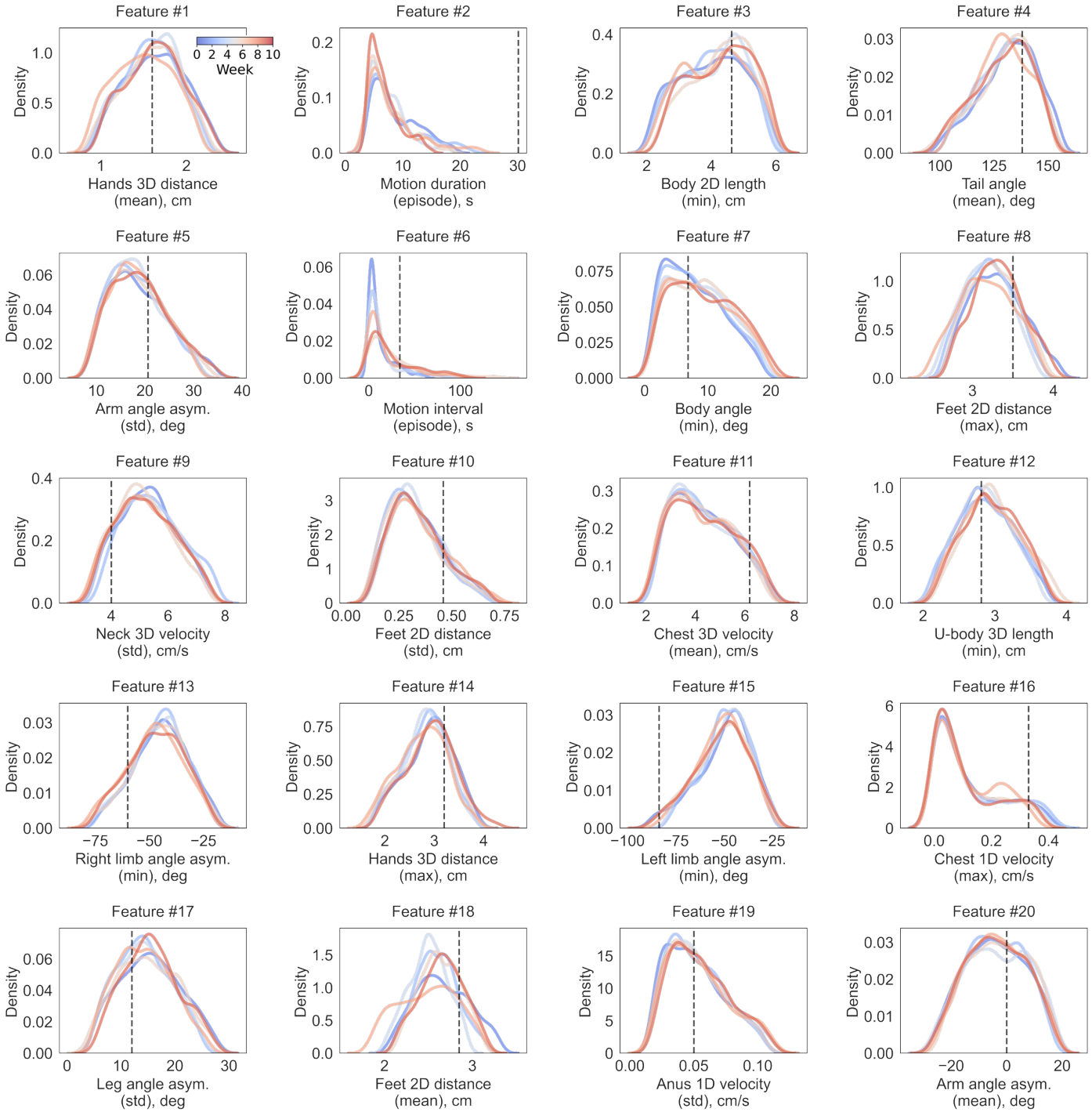

**b**

| Parameters | P-value in 2-way ANOVA test | |
|---|---|---|
| | Pose dataset | Move dataset |
| Time | 0.0006 | 0.0456 |
| Group | <0.0001 | 0.2201 |
| Time x Group | <0.0001 | 0.4359 |



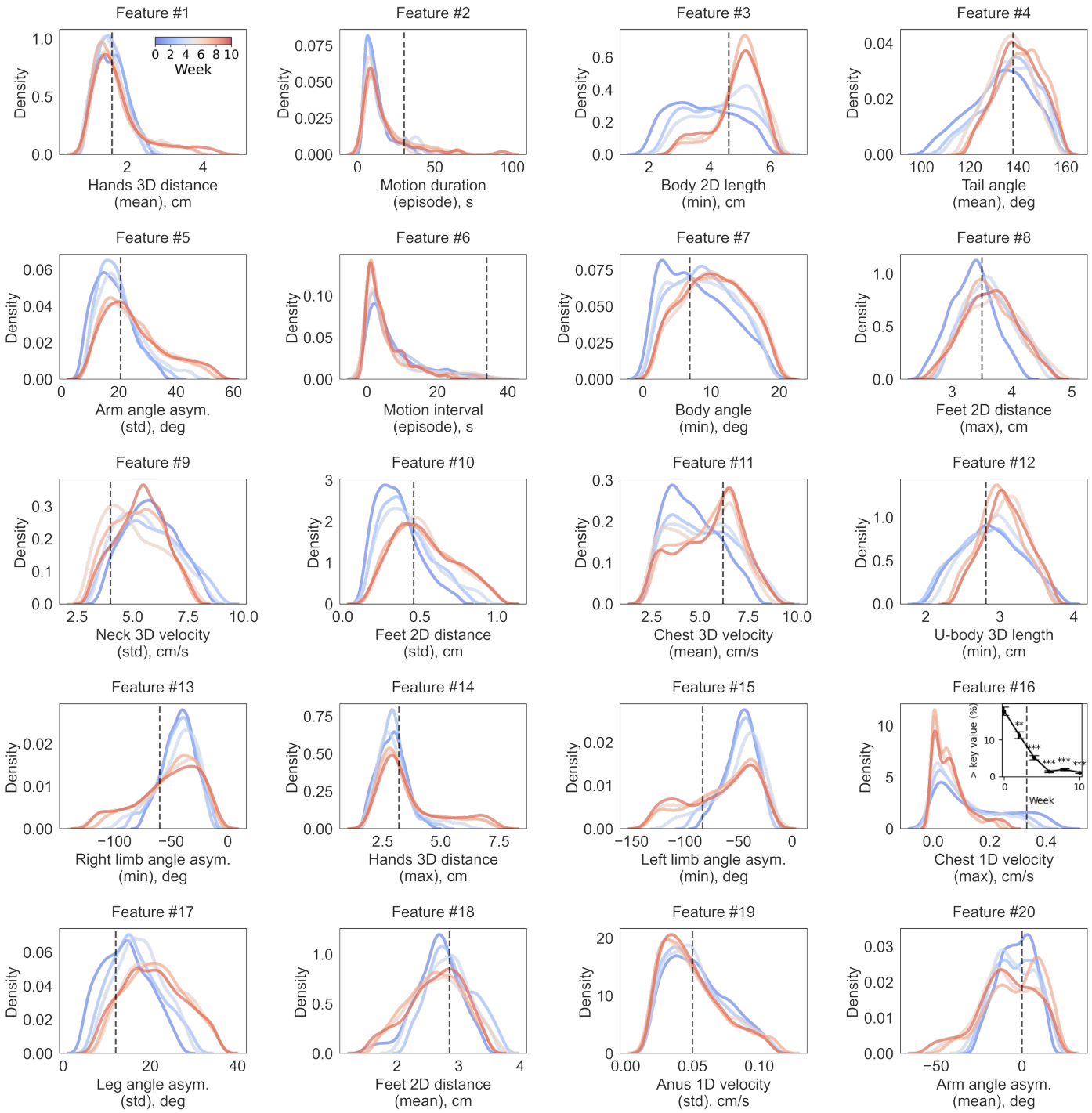

**Supplementary Figure 13. Comparison of body lengths across non-PD (NP) and PD groups.**

**(a)** Dot plots comparing body lengths (computed as the sum of 3D forebody [fbody; neck-chest] and hindbody [hbody; chest-anus] distances, averaged from frames with body angles within ±10°) across CT, A1, and A5 groups from both the raw pose and filtered move datasets at 0 and 10 wk post-injection. Please note that this measure differs from the 'body length (neck-anus distance)' presented in our original manuscript (see, Fig. 2a and Supplementary Fig. 5b). Pose dataset 0 wk: CT = 6.58 ± 0.02, A1 = 6.58 ± 0.04, A5 = 6.6 ± 0.04 cm; 10 wk: NP = 6.45 ± 0.04, A1 = 6.76 ± 0.07, A5 = 6.99 ± 0.06 cm; move dataset 0 wk: CT = 6.95 ± 0.05, A1: 6.99 ± 0.12, A5: 7.06 ± 0.05 cm; 10 wk: CT: 7.02 ± 0.06, A1: 7.28 ± 0.12, A5: 7.13 ± 0.21 cm. Two-way ANOVA tests were performed, and p-values were adjusted using Tukey's multiple comparisons method. In the raw pose dataset (left panel), significant differences in body lengths emerged at 10 wk, likely reflecting posture variations during non-moving (freeze) periods. In contrast, the move dataset (right panel) revealed no significant differences in body lengths between groups at either timepoint, indicating minimal confounds related to body size differences. **(b)** Table summarising the statistical results from two-way ANOVA tests comparing effects of group, time, and their interactions for both datasets. Significant effects were observed in the pose dataset whereas the move dataset showed no significant differences for group parameter, reinforcing the robustness of analyses based on this dataset. **(c)** Bar graphs depicting body lengths from the pose and move datasets for preliminary analyses of individual control (R1) and PD (A1) mice injected with virus at different ages (weeks indicated in parentheses). **(d)** APS measurements for the preliminary mice (R1[50], A1[10], A1[50]). Despite variations in body lengths related to age differences, APS remained robust and correctly reflected the expected PD status. APS remained normal in the R1 mouse despite larger body size, whereas APS increased to mild PD levels in A1 mice regardless of body length differences. Collectively, these results provide robust evidence that the distance-based features are unlikely to be confounded by body size (neck-chest-anus) differences, particularly within the move dataset used in current study. Statistical analysis was performed using two-way ANOVA followed by Tukey's post hoc correction for multiple comparisons.



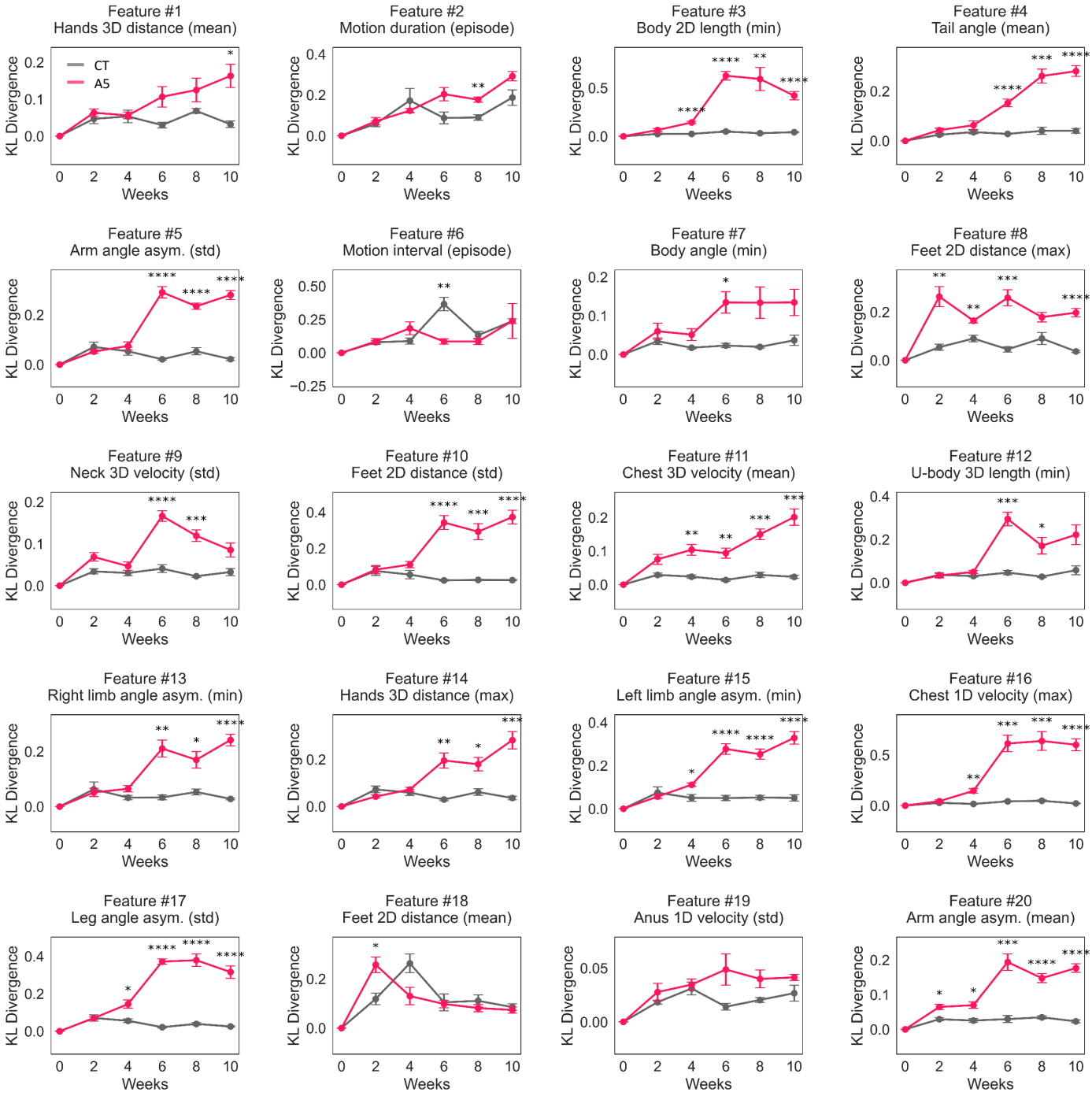

**Supplementary Figure 14. CT group's longitudinal analysis of the top 20 features (XGB model) in the KDE plots.**

For each feature, kernel density estimate (KDE) plots illustrate distribution shifts at distinct time points (0, 2, 4, 6, 8 and 10 wk). Vertical dashed lines indicate the key values.



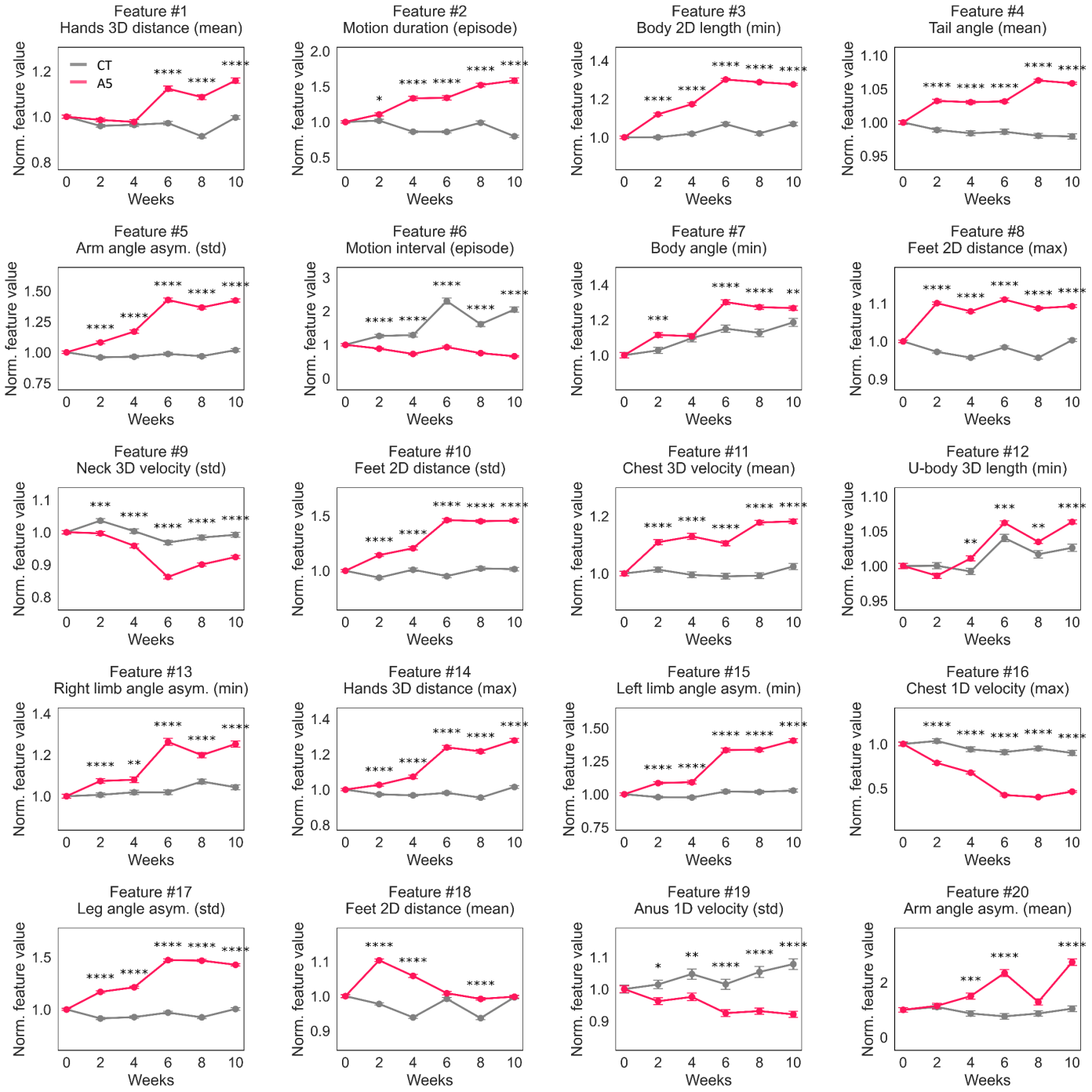

**Supplementary Figure 15. PD (A5) group's longitudinal analysis of the top 20 features (XGB model) in the KDE plots.**

For each feature, KDE plots illustrate distribution shifts at distinct time points (0, 2, 4, 6, 8 and 10 wk). Vertical dashed lines indicate the key values. For feature #16, a small line graph is shown above the KDE plot, representing the percentage of the data above the key value 0.33 cm (mean ± SEM, t-test compared to 0 wk) and source data are provided in the Source Data file.



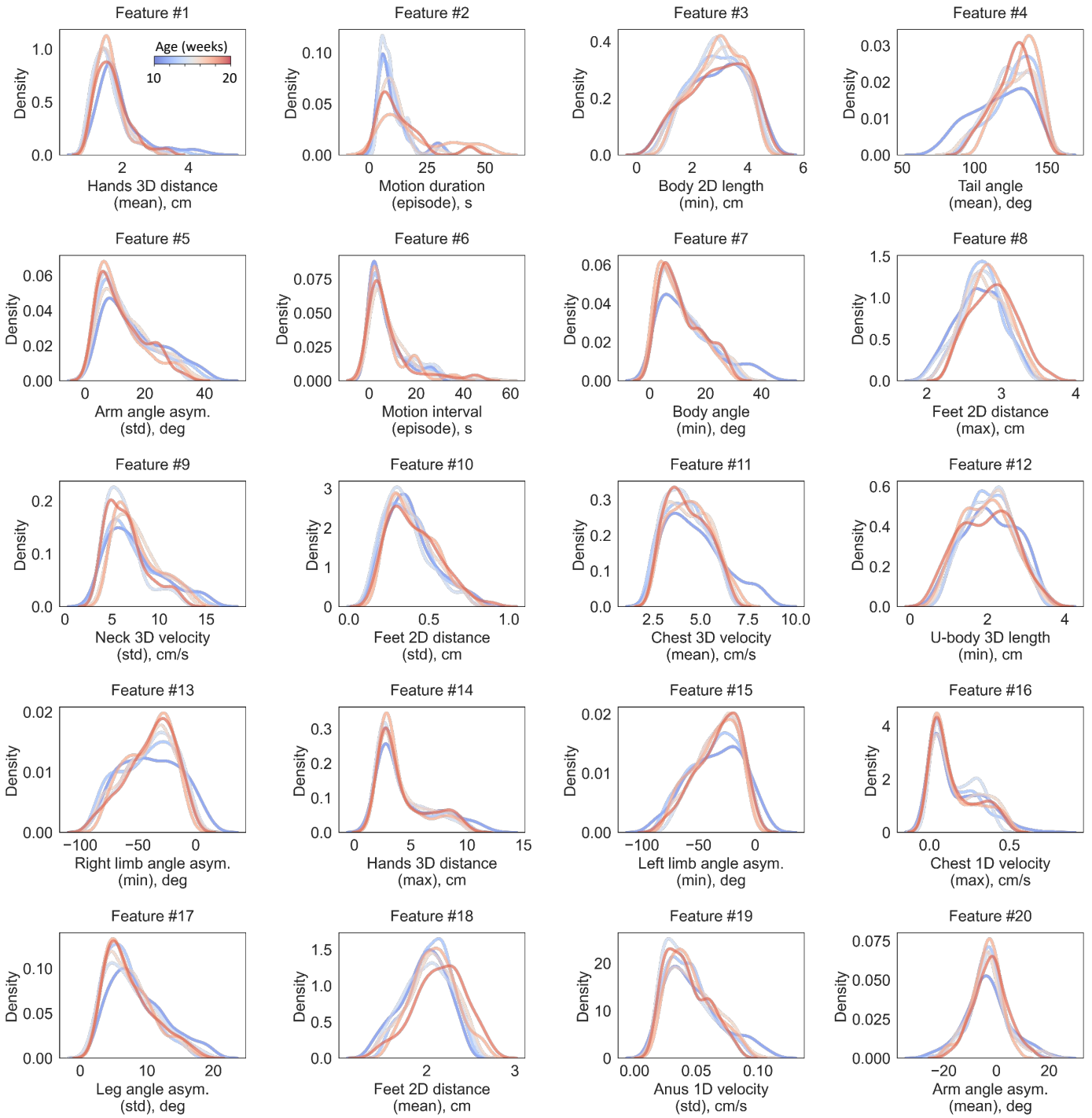

**Supplementary Figure 16. Longitudinal comparison of KL divergences (XGB model) between the CT and PD (A5) groups.**

For each group, the KL divergences of each feature from the respective baseline (0 wk) were computed over the experimental duration (0–10 wk) and plotted as line graphs (mean ± SEM. For each group, the KL divergence of each feature relative to its baseline value (0 wk) was computed across the experimental duration (0–10 wk). Each group consisted of 6 sampling sets, each containing 150 randomly selected clips. A two-way ANOVA (group × week) was performed for each feature, followed by weekly t-tests between groups (CT vs. A5). The resulting *p*-values from the weekly t-tests were corrected for multiple comparisons using the Bonferroni method. Detailed statistical results are provided in Supplementary Table 3. Source data are provided in the Source Data file.



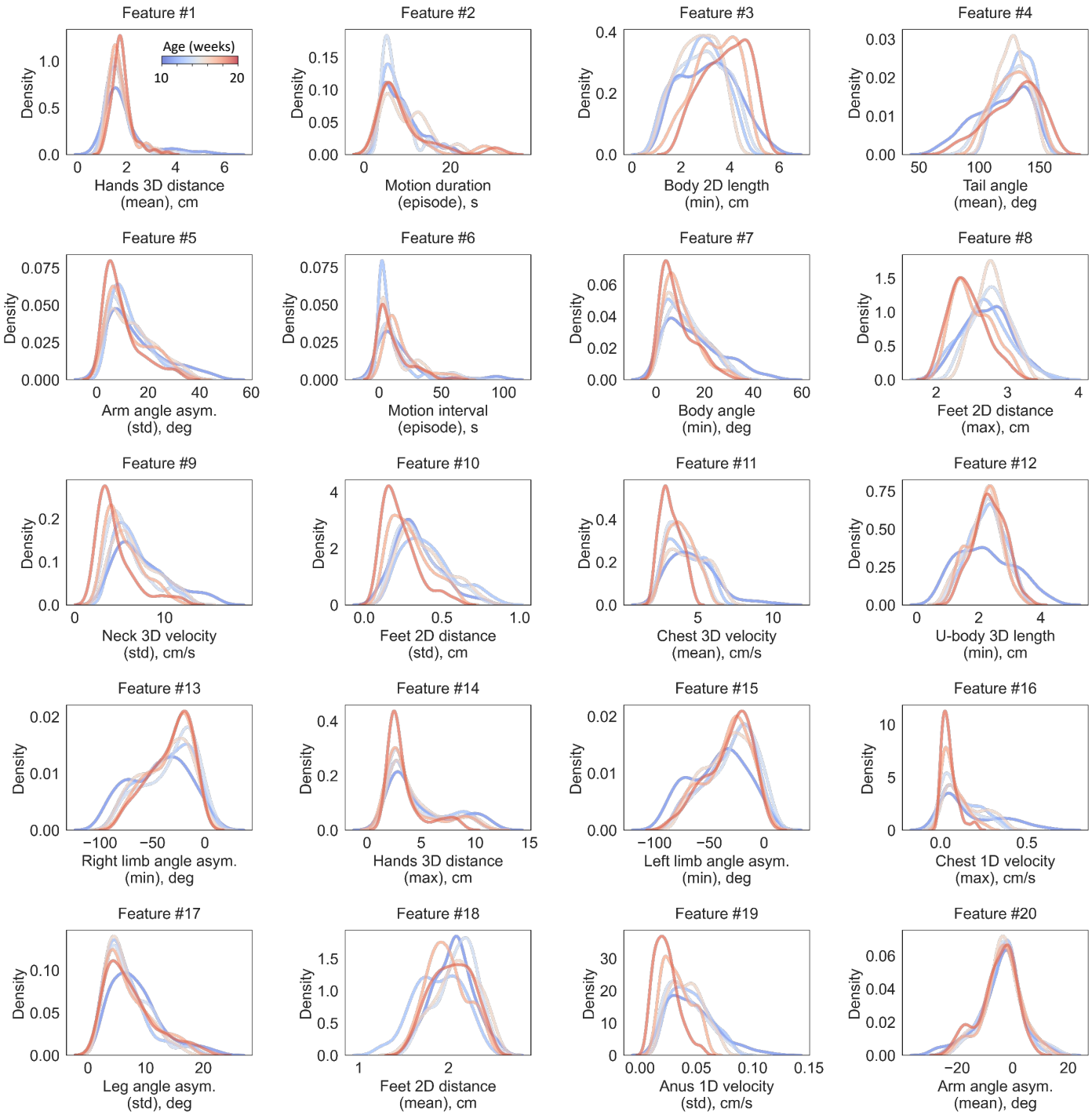

**Supplementary Figure 17. Longitudinal comparison of feature values (XGB model) between the CT and PD (A5) groups.**

**(a)** For each feature, the normalised feature values (mean ± SEM) were plotted over the experimental duration. For each feature, the values at each week were divided by the group's corresponding baseline (0 wk) mean value, and the normalised data were analysed over the experimental duration (0–10 wk). Each group consisted of 6 sampling sets, each containing 150 randomly selected clips. Two-way ANOVA (group × week) was performed for each feature on the normalised data, followed by weekly t-tests comparing the CT and A5 groups. *P*-values from weekly t-tests were corrected for multiple comparisons using the Bonferroni method. Detailed statistical results are provided in Supplementary Table 4. Source data are provided in the Source Data file.



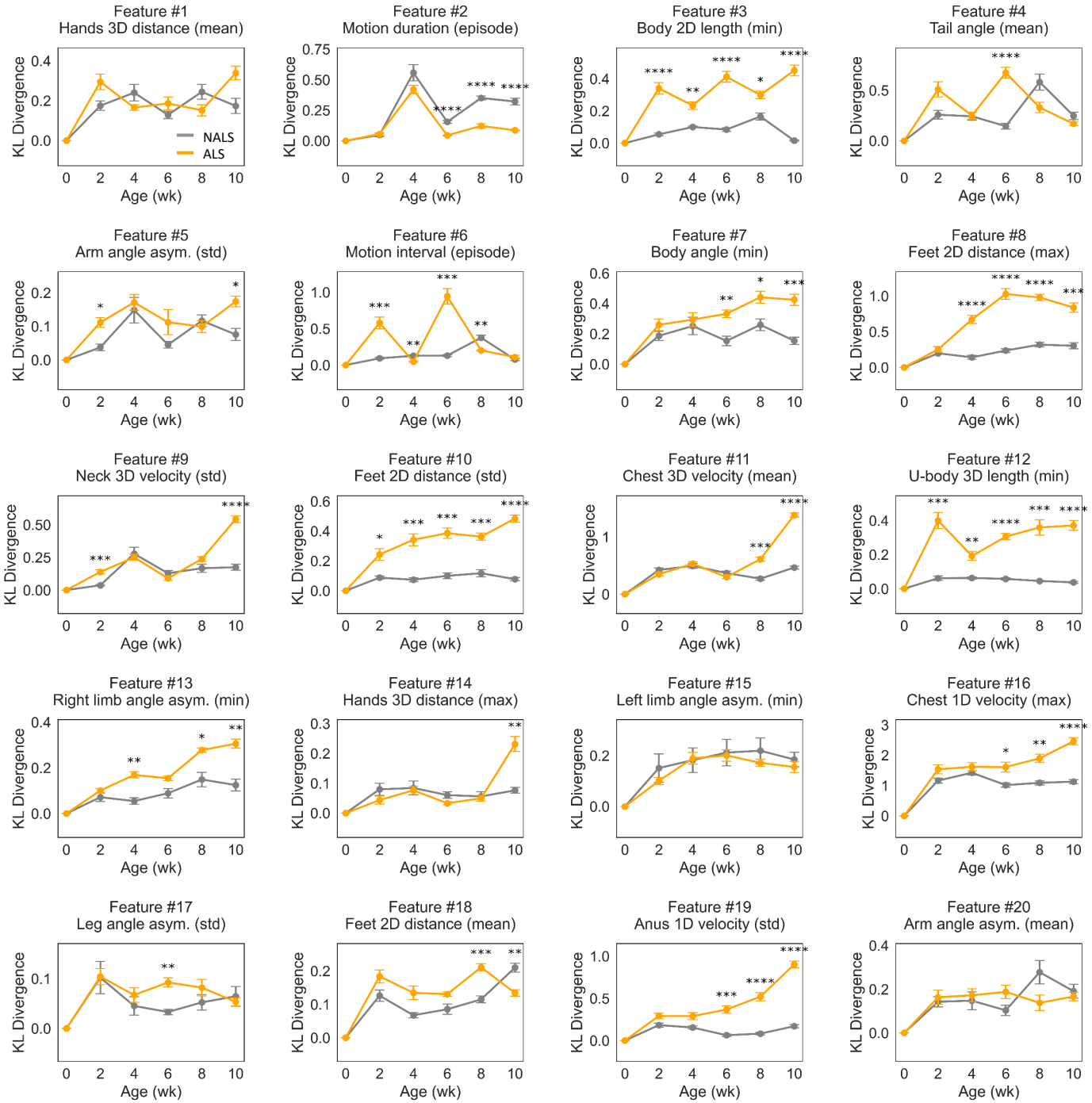

**Supplementary Figure 18. NALS group's longitudinal analysis of the top 20 features (XGB model) in the KDE plots.**

For each feature, KDE plots illustrate distribution shifts at distinct time points (10, 12, 14, 16, 18, and 20 wk [age]). Direct comparisons between CT (non-PD control in Supplementary Fig.14) and NALS (non-ALS control) groups are limited by age and gender differences.



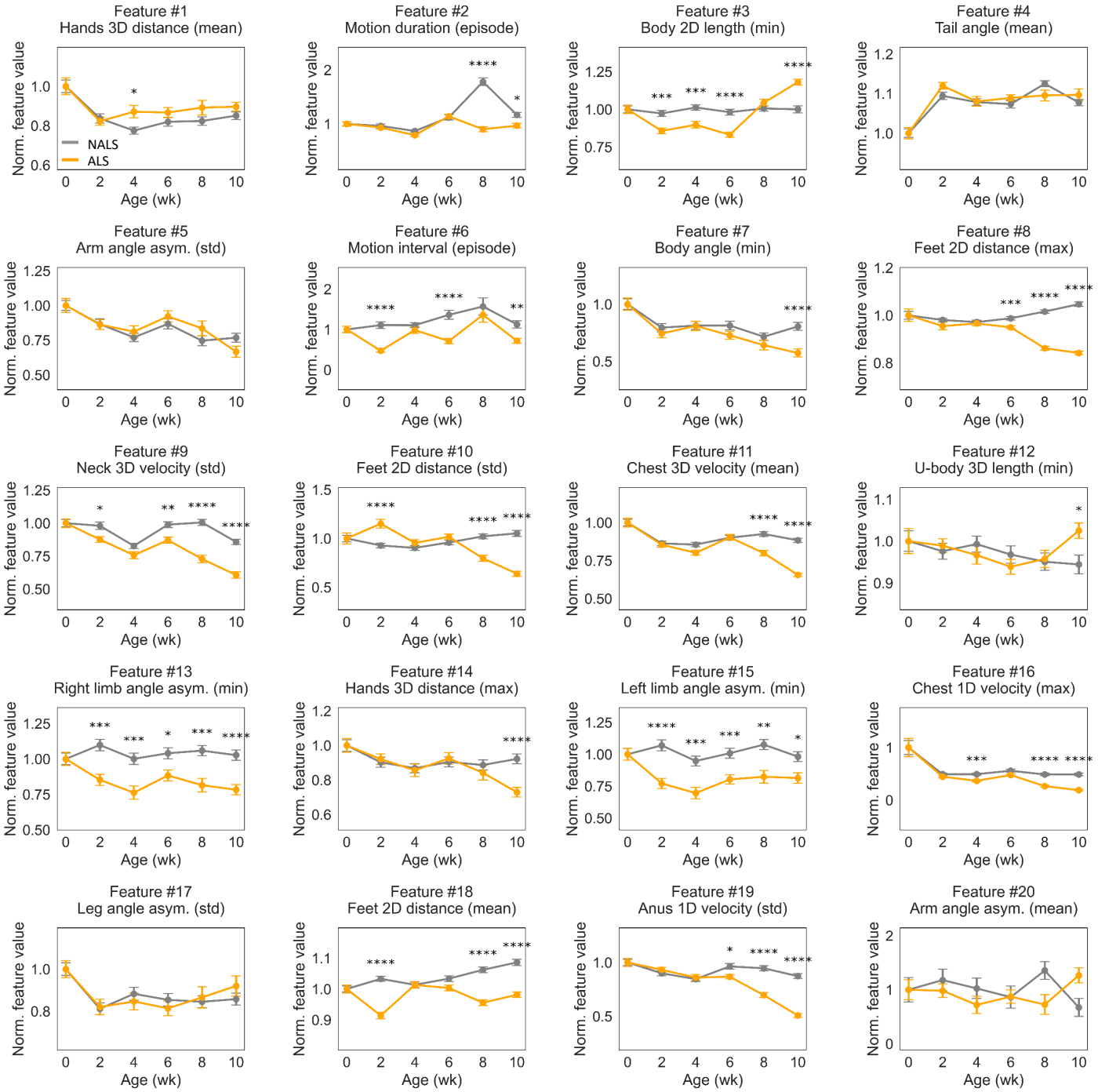

**Supplementary Figure 19. ALS group's longitudinal analysis of the top 20 features (XGB model) in the KDE plots.**

For each feature, KDE plots are shown at different time points (10, 12, 14, 16, 18, and 20 wk [age]). Direct comparisons between PD (A5 in Supplementary Fig.15) and ALS groups are limited by age and gender differences; however, the trends observed in the KDE plots are notable. For instance, limb asymmetry features appear less affected in ALS compared to PD mice, and generally, the feature distributions in ALS mice progressively exhibit increased positive kurtosis over time.



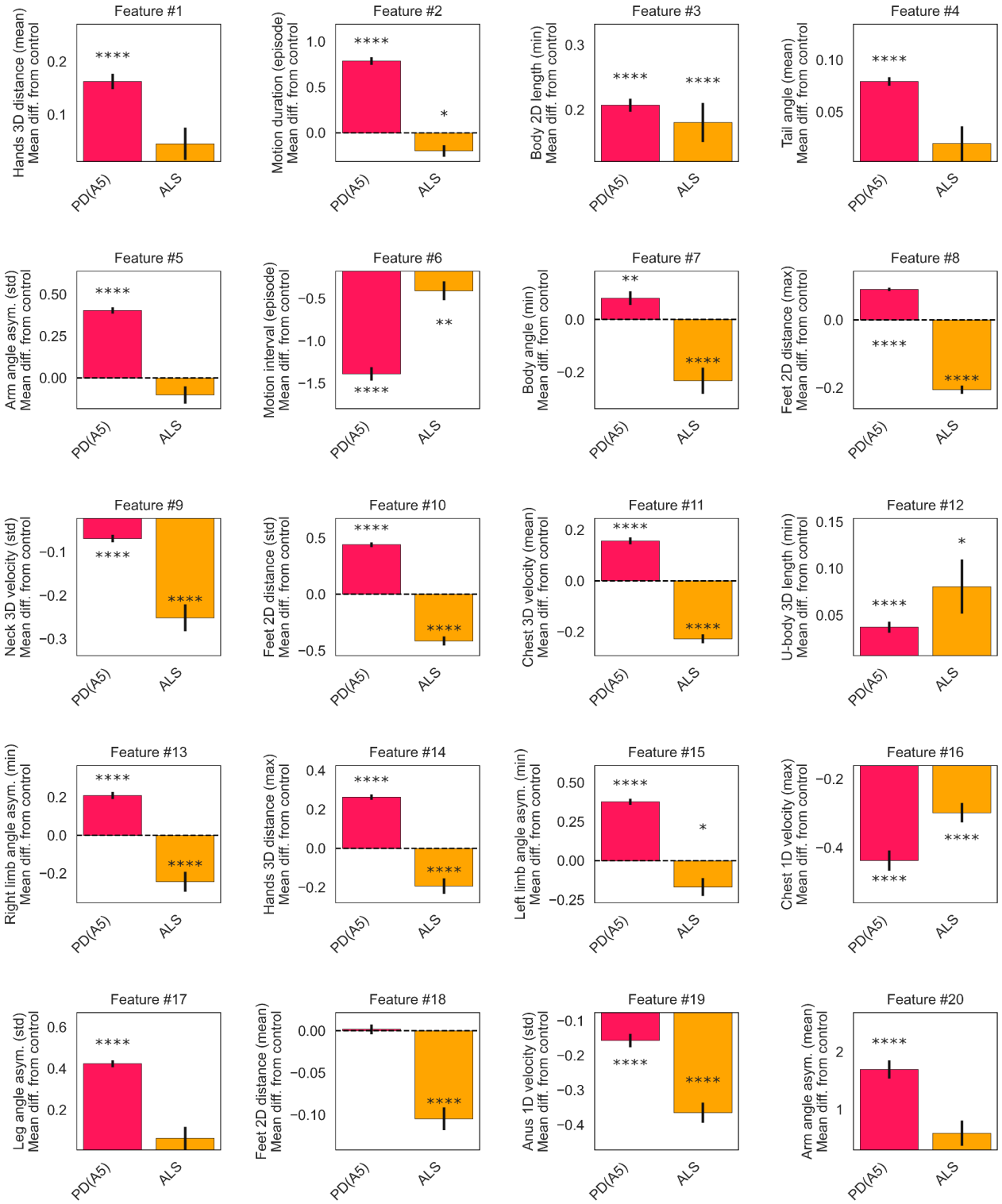

**Supplementary Figure 20. Longitudinal comparison of KL divergences (XGB model) between the NALS and ALS groups.**

For each group, the KL divergence of each feature relative to its baseline value (10 wk, non-symptomatic age) was computed across the experimental duration (10–20 wk [age]). Each group consisted of 6 sampling sets, each containing 150 randomly selected clips. A two-way ANOVA (group × week) was performed for each feature, followed by weekly t-tests between groups (NALS vs. ALS). The resulting p-values from the weekly t-tests were corrected for multiple comparisons using the Bonferroni method. Detailed statistical results are provided in Supplementary Table 5. Source data are provided in the Source Data file.



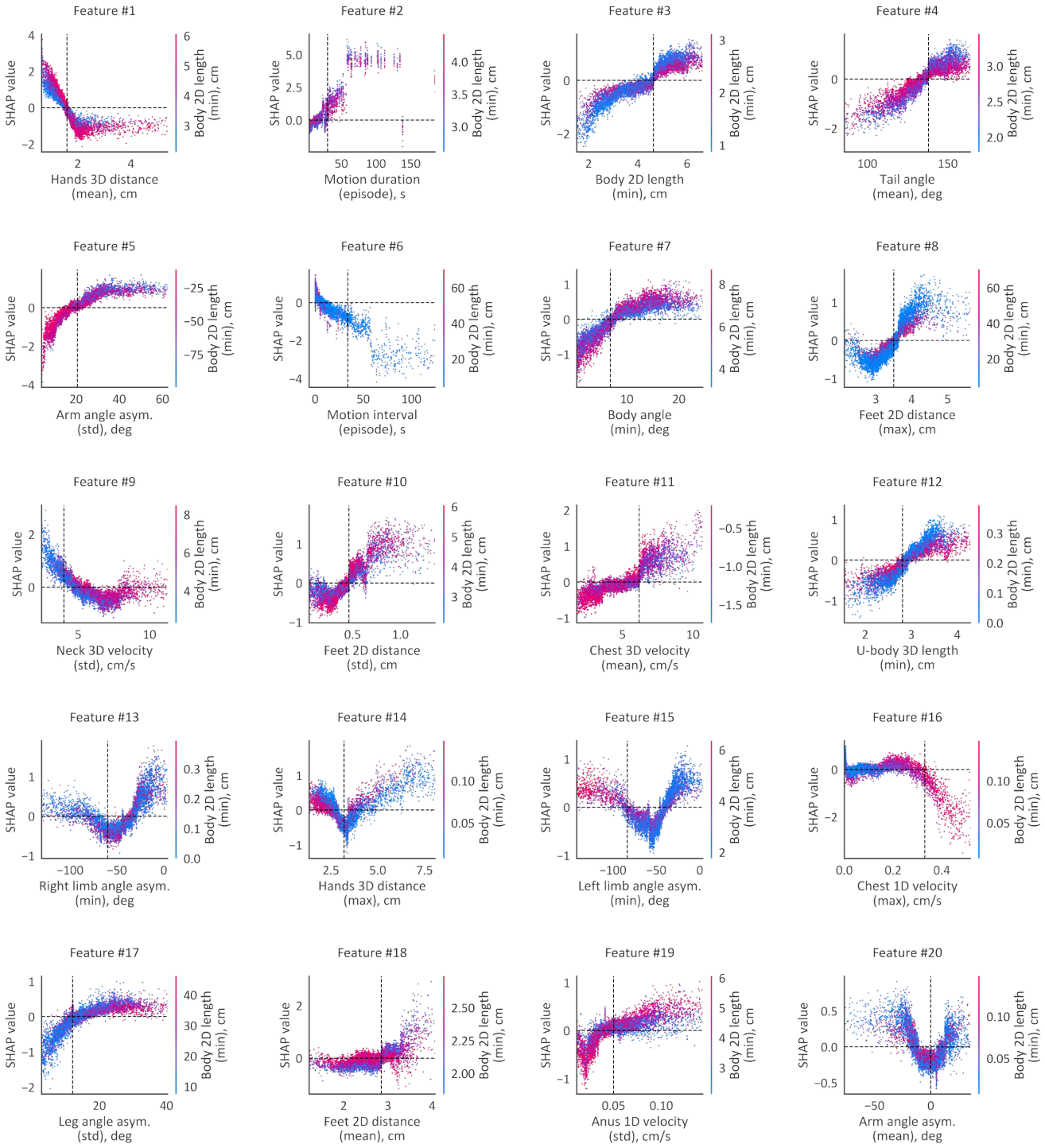

**Supplementary Figure 21. Longitudinal comparison of feature values (XGB model) between the NALS and ALS groups.**

For each feature, the normalised feature values (mean ± SEM) were plotted over the experimental duration. For each feature, the values at each week were divided by the group's corresponding baseline (10 wk, non-symptomatic age) mean value, and the normalised data were analysed over the experimental duration (10–20 wk [age]). Each group consisted of 6 sampling sets, each containing 150 randomly selected clips. Two-way ANOVA (group × week) was performed for each feature on the normalised data, followed by weekly t-tests comparing the NALS and ALS groups. P-values from weekly t-tests were corrected for multiple comparisons using the Bonferroni method. Detailed statistical results are provided in Supplementary Table 6. Source data are provided in the Source Data file.




**Supplementary Figure 22. Endpoint comparison of PD and ALS groups for the top 20 features identified by the XGB model.**

For each feature, differences between the non-disease control and experimental groups (PD: CT vs A5; MND: NALS vs ALS) were compared at their respective experimental endpoints (PD: 10 wk post-surgery; MND: 20 wk of age). Feature values for each group were normalised to their respective baseline means (PD: 0 wk post-surgery; ALS: 10 wk of age). The bar graphs show mean differences between experimental and control groups, with error bars representing SEM differences computed by error propagation. Notably, the direction of changes relative to controls varied significantly between PD and ALS groups in 40% of features (#2, 7, 8, 10, 11, 13, 14, and 15), reflecting distinct symptomatic manifestations between the two diseases. For example, Feature #11 illustrates that PD mice exhibited a more stooped posture compared to non-PD mice, whilst ALS mice displayed a more stretched posture compared to non-ALS mice. Furthermore, fewer features significantly differed from controls in ALS (75%) compared to PD (95%), suggesting that these behavioural features are more sensitive indicators of PD symptoms. Statistical significance between control/experimental pairs is indicated by asterisks, based on Bonferroni-corrected *p*-values. See Supplementary Table 7 for statistical details and the Methods section for further explanation. Source data are provided in Supplementary Tables 4 and 6. Note: This figure compares two distinct datasets; individual-level data points are therefore not available for display.

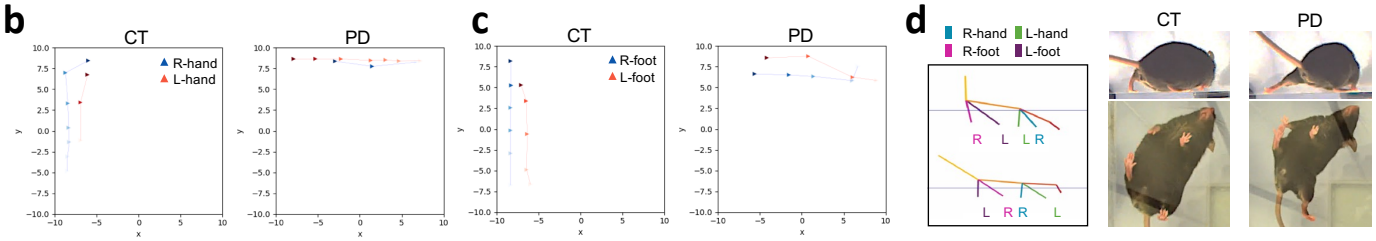



**Supplementary Figure 23. SHAP dependence plots of the top 20 features (XGB model).**

Each plot displays individual dots representing motion clips that contribute to the model's predictions. The x-axis shows the feature values, limited to the 1st–99th percentiles, whilst the y-axis indicates the SHAP value (log odds of PD likelihood), quantifying the feature's impact on model predictions as non-PD (negative SHAP values) or PD (positive SHAP values). The vertical dashed line intersects the SHAP value at zero, and the horizontal dashed line line intersects the key feature value. Dot colour indicates the value of the interacting feature for each plot is automatically determined by the SHAP library based on the highest correlation with the primary plotted feature's SHAP values. For instance, in subplot #1, the hands 3D distance dependence plot is color-coded by body 2D length (min), demonstrating that smaller hand distances have a greater impact on the prediction when the body length is longer. Similarly, subplot #8 shows that larger feet distance (max) more strongly influences the prediction during shorter motion durations. Linking the colour gradient to specific interacting features visually highlights that the primary feature's predictive influence is context-dependent rather than operating in isolation.

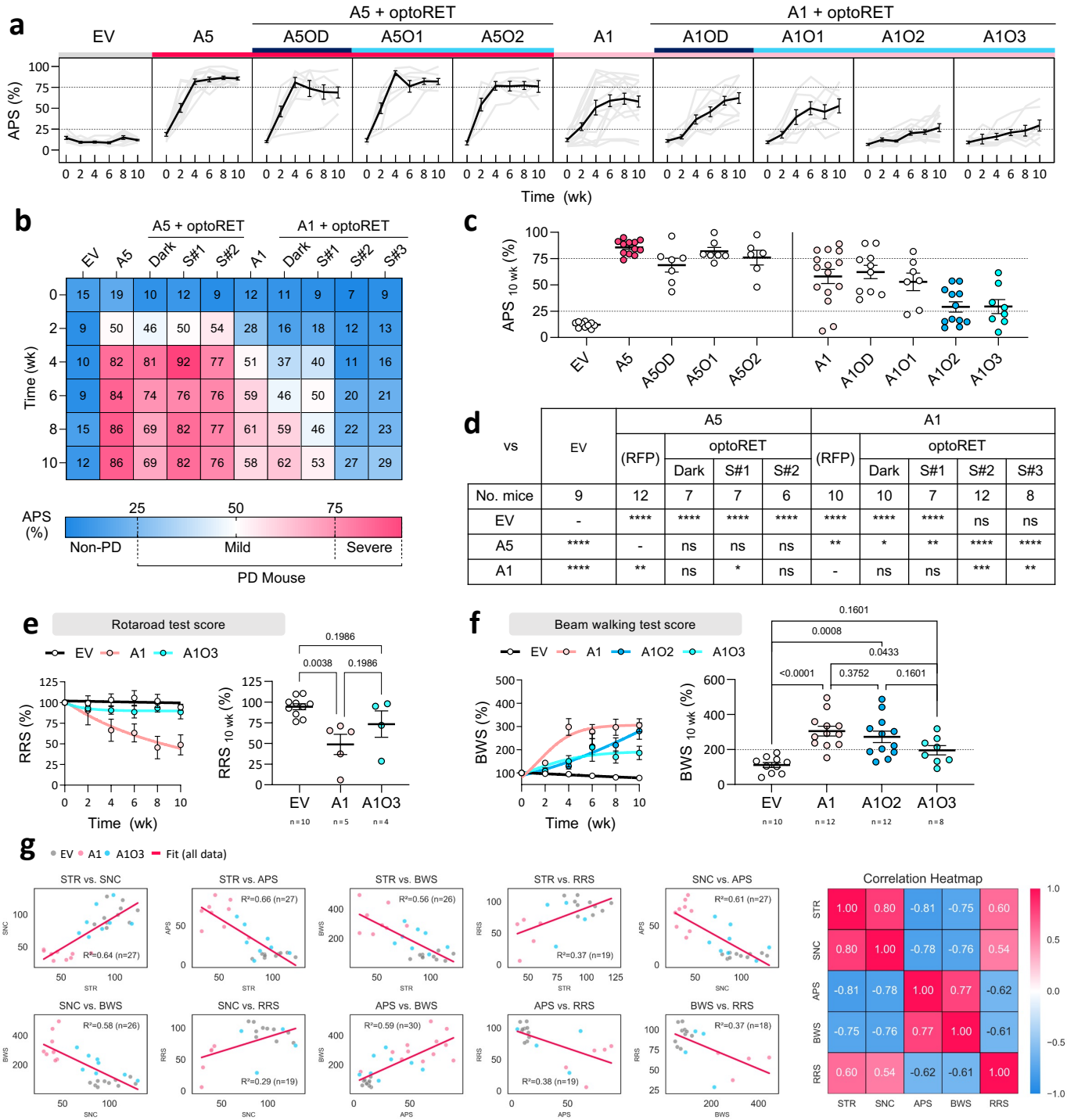
**a**

| | Feature | Unit | Key value | Major range | | | | Inflection range | | Minor range | | | |
|---|---|---|---|---|---|---|---|---|---|---|---|---|---|
| | | | | NP | | PD | | | | NP | | PD | |
| 1 | Hands 3D distance (mean) | cm | 1.60 | 2 | 3 | 0.5 | 1.7 | - | - | - | - | - | - |
| 2 | Motion duration | s | 30.10 | 0 | 22.65 | 23 | 23 | - | - | - | - | - | - |
| 3 | Body 2D distance (min) | cm | 4.63 | 1 | 3 | 4.63 | 6 | - | - | - | - | - | - |
| 4 | Tail angle (mean) | deg | 138.08 | 90 | 134 | 134 | 170 | - | - | - | - | - | - |
| 5 | Arm angle asymmetry (std) | deg | 20.63 | 0 | 10 | 30 | 60 | - | - | - | - | - | - |
| 6 | Motion interval | s | 33.95 | 0 | 150 | 4.9 | 34 | - | - | - | - | - | - |
| 7 | Body angle (min) | deg | 6.88 | 0 | 6 | 7.45 | 25 | - | - | - | - | - | - |
| 8 | Feet 2D distance (max) | cm | 3.50 | 2 | 3.62 | 3.62 | 5 | 2.5 | 3.5 | - | - | 1 | 2.5 |
| 9 | Neck 3D velocity (std) | cm/s | 4.00 | 4 | 11 | 2 | 4 | 6 | 8 | - | - | 8 | 12 |
| 10 | Feet 2D distance (std) | cm | 0.46 | 0 | 0.5 | 0.34 | 1.5 | 0.2 | 0.3 | - | - | 0 | 0.34 |
| 11 | Chest 3D velocity (mean) | cm/s | 6.19 | 1 | 6 | 6 | 10 | - | - | - | - | - | - |
| 12 | Nose-chest 3D distance (min) | cm | 2.81 | 1 | 3 | 3 | 5 | - | - | - | - | - | - |
| 13 | Right limb angle asymmetry (min) | deg | -60.00 | -90 | -30 | -30 | 30 | -90 | 30 | - | - | -140 | -90 |
| 14 | Hands 3D distance (max) | cm | 3.20 | 2 | 5 | 5 | 7 | 2.5 | 4 | - | - | 1 | 3 |
| 15 | Left limb angle asymmetry (min) | deg | -83.65 | -80 | -30 | -30 | 30 | -90 | -30 | - | - | -15 | -85 |
| 16 | Chest 1D velocity (max) | cm/s | 0.33 | 0.3 | 0.5 | 0.1 | 0.3 | 0.1 | 0.4 | 0 | 0.2 | 0 | 0.05 |
| 17 | Leg angle asymmetry (std) | deg | 12.03 | 0 | 11 | 17 | 34 | - | - | - | - | - | - |
| 18 | Feet 2D distance (mean) | cm | 2.85 | 3 | 4 | 3 | 4 | 3 | 3 | 1 | 3 | 1 | 3 |
| 19 | Anus 1D velocity (std) | cm/s | 0.05 | 0 | 0.05 | 0.05 | 0.15 | - | - | - | - | - | - |
| 20 | Arm angle asymmetry (mean) | deg | 0.00 | -5 | 20 | -20 | -40 | -20 | 20 | - | - | 10 | 40 |




**Supplementary Figure 24. Summary table of SHAP dependence plots for the top 20 features (XGB model).**

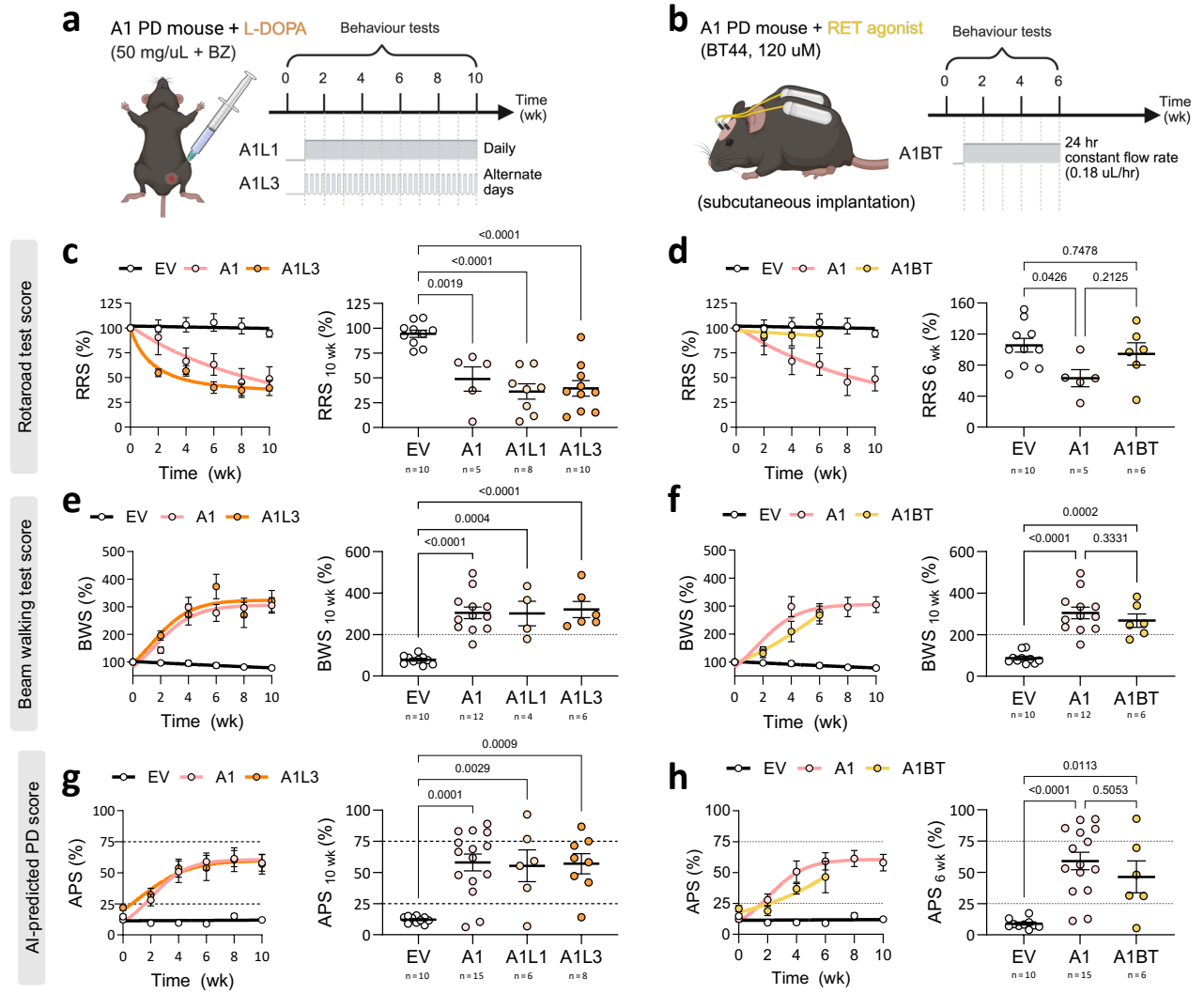
**(a)** Key feature values are identified by analysing feature dependence plots and node split conditions within the decision trees. Key values near a SHAP value of zero indicate points where the feature's impact on model predictions shifts direction. The major feature value range is defined by clusters of high data density or high magnitude of absolute SHAP values for the data. For some features, a minor range with an inflection point is revealed through SHAP analysis, which otherwise remains unveiled. **(b, c)** Representative trajectories of the hands and feet in CT and PD mice. **(d)** Example skeleton images highlighting extreme limb angle asymmetries (Feature #13, 15), alongside snapshot images from CT and PD mice.




| vs | EV | A5 | | | | A1 | | | | |
|---|---|---|---|---|---|---|---|---|---|---|
| | | (RFP) | optoRET | | | (RFP) | optoRET | | | |
| | | | Dark | S#1 | S#2 | | Dark | S#1 | S#2 | S#3 |
| No. mice | 9 | 12 | 7 | 7 | 6 | 10 | 10 | 7 | 12 | 8 |
| EV | - | **** | **** | **** | **** | **** | **** | **** | ns | ns |
| A5 | **** | - | ns | ns | ns | ** | * | ** | **** | **** |
| A1 | **** | ** | ns | * | ns | - | ns | ns | *** | ** |

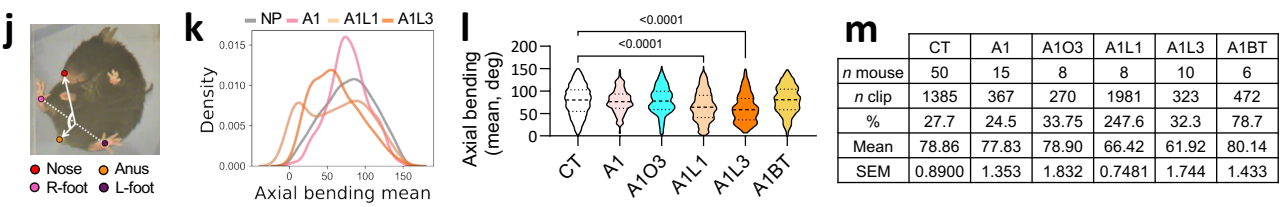
**Supplementary Figure 25. Behavioural assessments (RRS, BWS, and APS) in PD mice treated with optogenetic stimulation (optoRET).**

**(a)** Line graphs of APS for each mouse group over time. The black line represents mean ± SEM of the group, and the grey lines depict individual mice in the group. Groups with optoRET were unstimulated (dark) or stimulated with the pre-set long-term light schedules: daily (S#1), biweekly (S#2), or alternate days (S#3). Dashed lines on the graphs indicate *health status* categories: non-PD (0–25), mild PD (25–75), and severe PD (>75). **(b)** Heatmap visualization of panel (a) displays temporal trends in PD scores, showing the group mean at each time point. **(c)** Dot plots of APS for each group at 10 wk, detailed with mean ± SEM. **(d)** Statistical summary of multiple comparisons using one-way ANOVA followed by Bonferroni's multiple comparisons test. This analysis, based on the APS (XGB model-predicted PD scores) at 10 wk shown in panel (c), demonstrates the therapeutic efficacy of optoRET under various light schedules. Detailed statistical results are provided in Supplementary Table 8. **(e, f)** RRS and BWS comparisons between the EV, A1 and opto-treated groups, illustrated in line and dot graphs for the longitudinal (0-10 wk) and the endpoint (10 wk) analysis (RRS* [%]: EV = 94.40 ± 3.67, A1 = 48.84 ± 12.20, A1O3 = 73.42 ± 16.01; BWS [%]: EV = 78.12 ± 6.66, A1 = 305.0 ± 27.90, A1O2 = 272.1 ± 33.11, A1O3 = 195.4 ± 26.76). One-way ANOVA and post-hoc tests with Holm–Sidak multiple comparison corrections were performed. **(g)** Dot plots (with fitted regression lines in red) showing pairs of metrics and heatmap illustrating Pearson's correlation coefficients. For each correlation, datasets (CT and PD groups) were filtered based on each metric pair. Source data are provided in the Source Data file.




i

| Endpoint | Treatment | Group | Mean +/- SEM (n) | | | *P*-value (compared to EV) | | | *P*-value (compared to A1) | | |
|---|---|---|---|---|---|---|---|---|---|---|---|
| | | | RRS (%) | BWS (%) | APS (%) | RRS | BWS | APS | RRS | BWS | APS |
| 10 wk | - | EV | 94.40 ± 3.67 (10) | 78.12 ± 6.66 (10) | 12.11 ± 0.85 (10) | - | - | - | - | - | - |
| | - | A1 | 48.84 ± 12.20 (5) | 305.0 ± 27.90 (12) | 58.01 ± 6.69 (15) | 0.0019 | <0.0001 | <0.0001 | - | - | - |
| | optoRET | A1O2 | - | 272.1 ± 33.11 (12) | | - | 0.0008 | 0.1322 | - | 0.3752 | 0.0018 |
| | | A1O3 | 73.42 ± 16.01 (4) | 195.4 ± 26.76 (8) | | 0.1986 | 0.1601 | 0.1322 | 0.1986 | 0.0433 | 0.0062 |
| | L-DOPA | A1L1 | 36.31 ± 7.78 (8) | 301.8 ± 59.20 (4) | 55.38 ± 12.71 (6) | <0.0001 | 0.0004 | 0.0029 | 0.6679 | 0.9742 | 0.9643 |
| | | A1L3 | 39.44 ± 7.74 (10) | 320.9 ± 38.76 (6) | 56.98 ± 8.03 (8) | <0.0001 | <0.0001 | 0.0009 | 0.6679 | 0.9742 | 0.9643 |
| 6 wk | RET agonist (BT44) | EV | 105.5 ± 8.83 (10) | 87.46 ± 8.88 (10) | 8.95 ± 1.19 (10) | - | - | - | - | - | - |
| | | A1 | 63.14 ± 11.02 (5) | 305.0 ± 27.90 (12) | 59.04 ± 6.95 (15) | 0.0426 | <0.0001 | <0.0001 | - | - | - |
| | | A1BT | 94.42 ± 14.29 (6) | 267.9 ± 32.21 (6) | 46.38 ± 12.70 (6) | 0.7478 | 0.0002 | 0.0113 | 0.2125 | 0.3331 | 0.5053 |

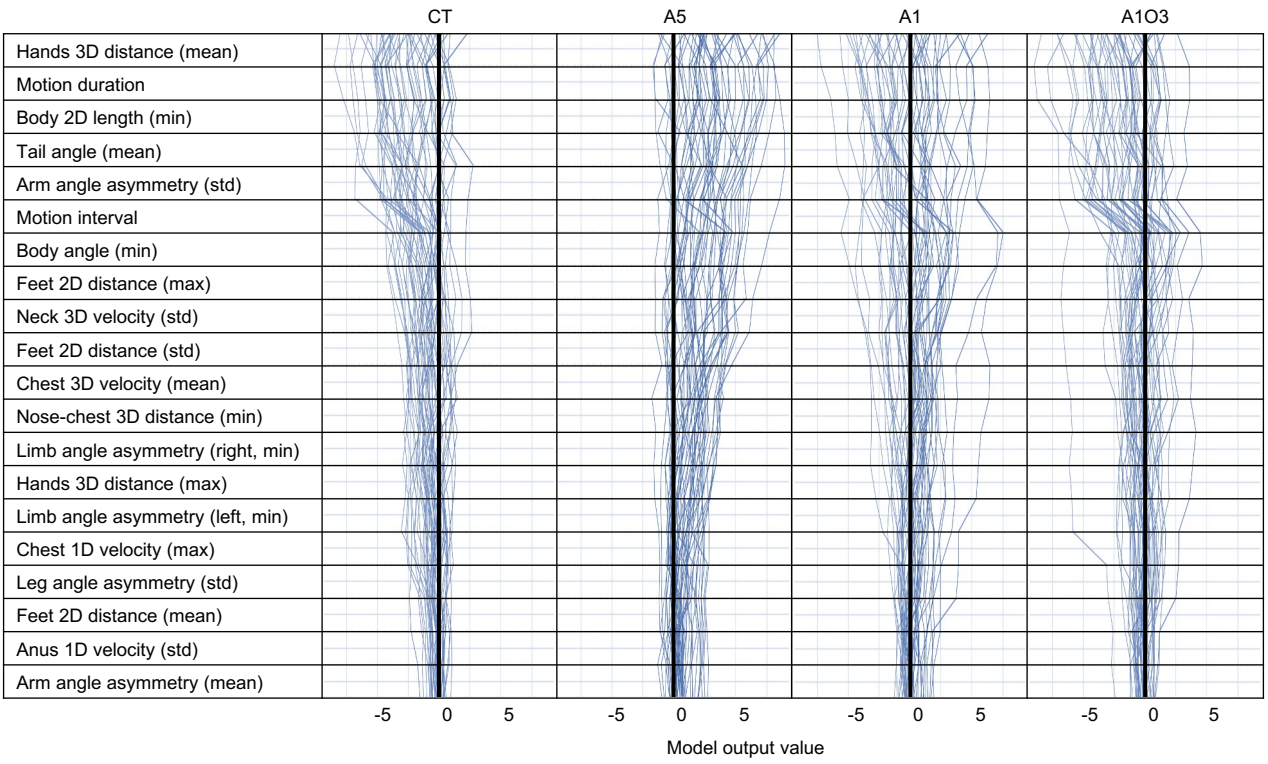



m

| | CT | A1 | A1O3 | A1L1 | A1L3 | A1BT |
|---|---|---|---|---|---|---|
| *n* mouse | 50 | 15 | 8 | 8 | 10 | 6 |
| *n* clip | 1385 | 367 | 270 | 1981 | 323 | 472 |
| % | 27.7 | 24.5 | 33.75 | 247.6 | 32.3 | 78.7 |
| Mean | 78.86 | 77.83 | 78.90 | 66.42 | 61.92 | 80.14 |
| SEM | 0.8900 | 1.353 | 1.832 | 0.7481 | 1.744 | 1.433 |

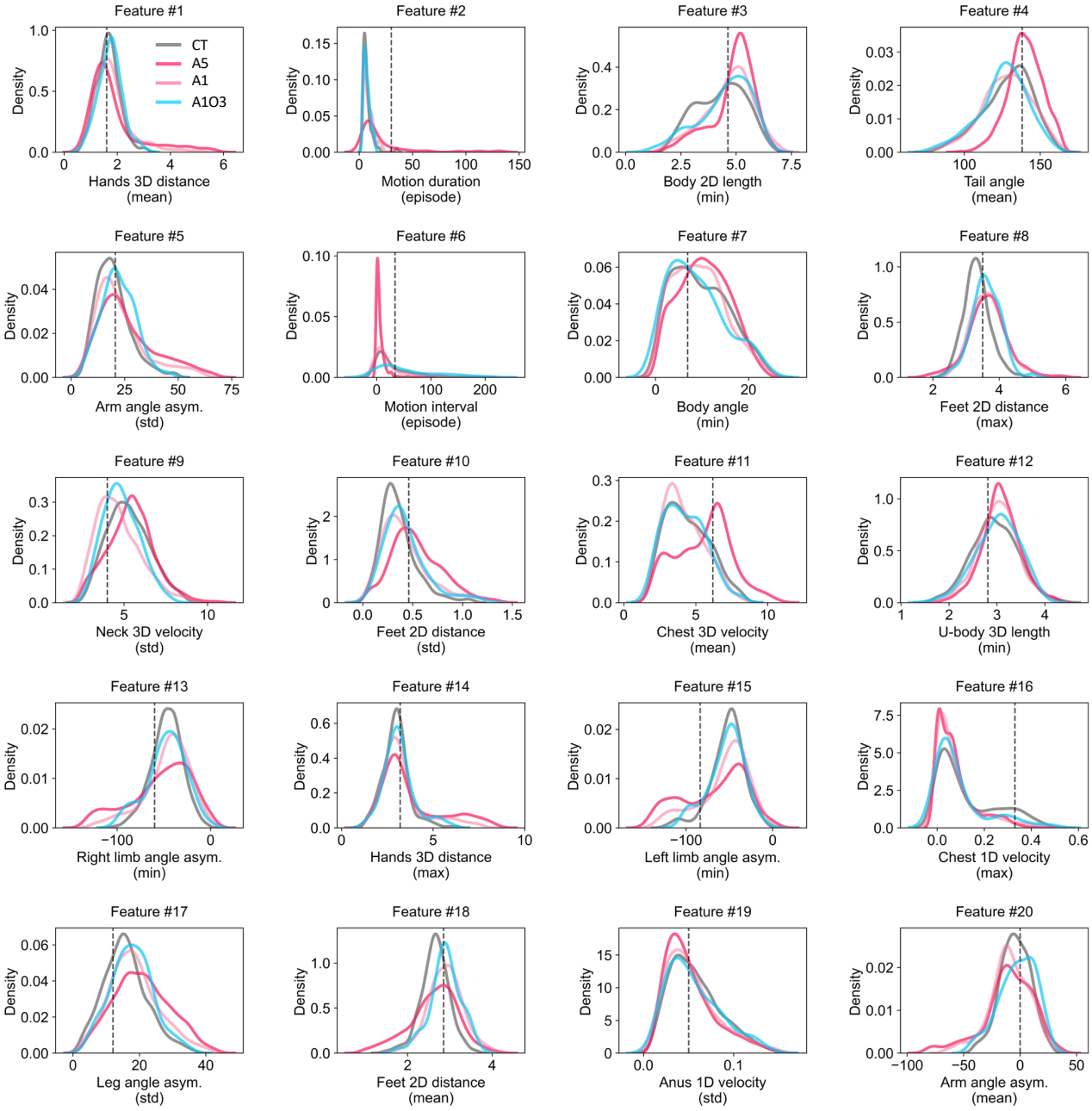
**Supplementary Figure 26. Behavioural assessments (RRS, BWS, and APS) in A1 PD mice treated with L-DOPA or RET agonist (BT44).**

**(a, b)** Schematic illustration of A1 mice treated with either L-DOPA or RET agonist (BT44). L-DOPA with Benserazide (BZ) was administered by intraperitoneal injection every day (A1L1) or alternate days (A1L3). BT44 was administered by direct brain infusion into the striatum at a constant flow rate (A1BT). In the latter group, the experimental endpoint was adjusted to 6 wk due to the limited volume of the osmotic pumps implanted. **(b-h)** Comparisons of behavioural assessments (RRS, BWS and APS) among A1 mice treated with L-DOPA or BT44, illustrated in line and dot graphs for the longitudinal and the endpoint. **(i)** Summary table of the behavioural assessments in A1 mice with optogenetic, L-DOPA or BT44 treatments. Significant *p*-values are highlighted. **(j)** Schematic illustration of axial bending angle measurement (the angle formed by the two vectors [arrows]). **(k)** KDE plots showing mean axial bending angles derived from threshold-filtered datasets (see Methods) for CT, A1, and L-DOPA groups. **(l, m)** Comparisons of axial bending angle across groups. Detailed interpretations of the BT44 and L-DOPA treatment groups are provided in Supplementary Notes 7 and 8, respectively. All statistics, one-way ANOVA and post-hoc tests with Holm–Sidak multiple comparison corrections were performed. Source data are provided in the Source Data file. Schematics were created in BioRender. Heo, W. (2025) https://BioRender.com/cykyauz.



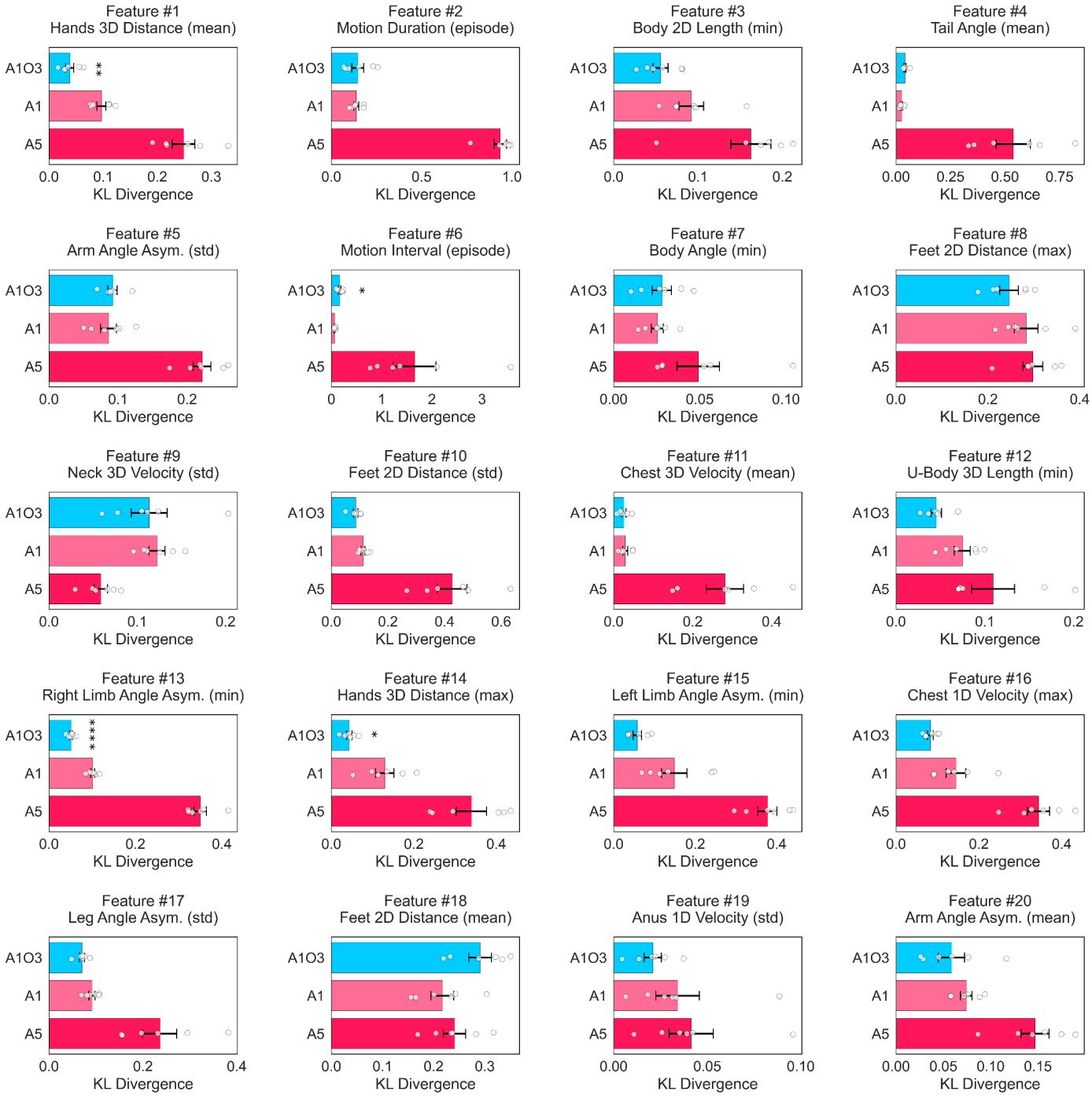

**Supplementary Figure 27. Group comparison of the decision tree plots (XGB model) at 10 wk.**

For the CT, A5, A1 and A1O3 groups, 50 clips from each group are randomly selected from the tested dataset at 10 wk and their decision plots are plotted. The top 20 features are only shown, in the order of the model's feature importance rank. The proportions of the sampled clips predicted as PD (model output value > 0) were 12% (6/50), 90% (5/50), 44% (22/50) and 16% (8/50) for the respective groups.



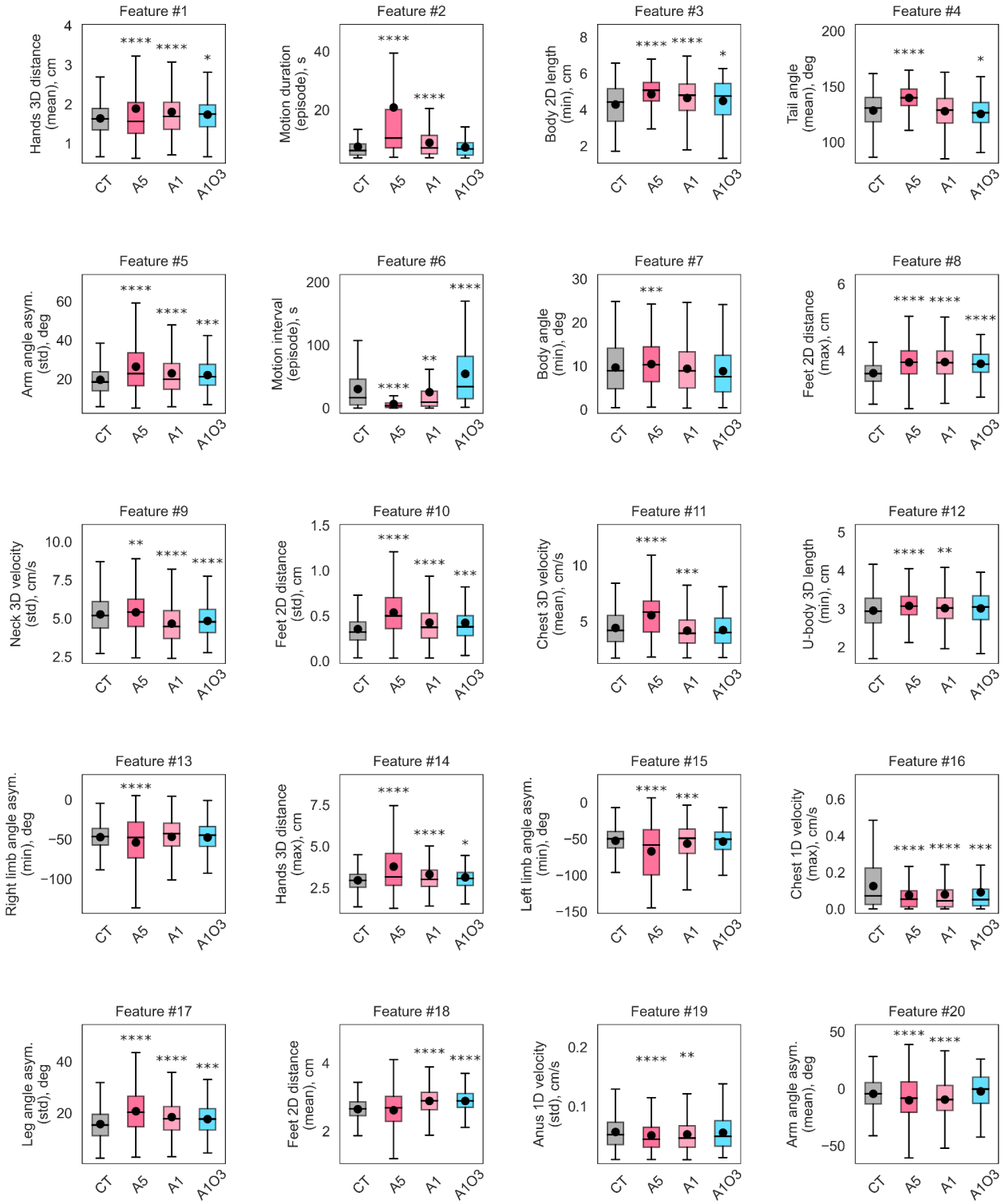

**Supplementary Figure 28. Group comparison of the top 20 features (XGB model) in the KDE plots at 10 wk.**

Kernel density estimate (KDE) plots for each feature compare distribution patterns across the CT, A5, A1, and A1O3 groups at 10 wk, with vertical dashed lines highlighting key feature values.



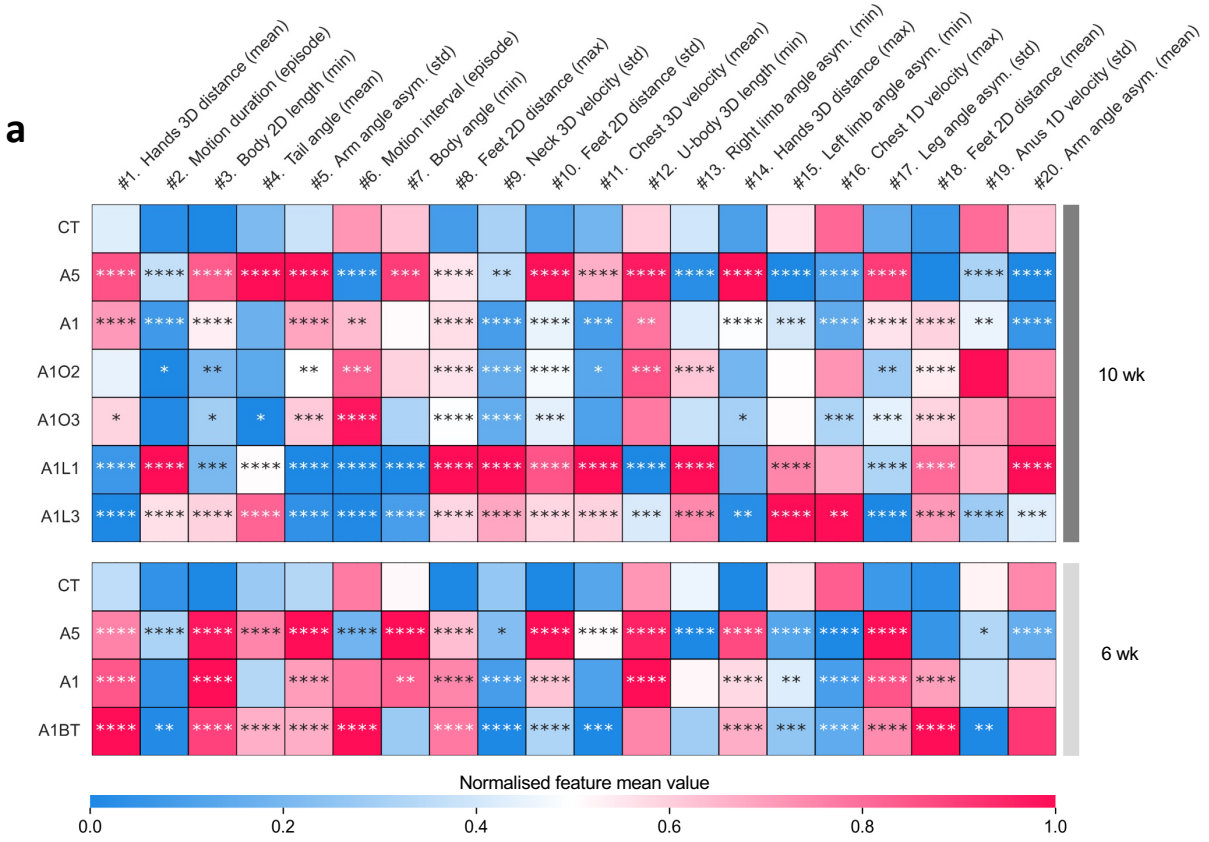

**Supplementary Figure 29. Comparison of KL divergences of the top 20 features (XGB model) between groups at 10 wk.**

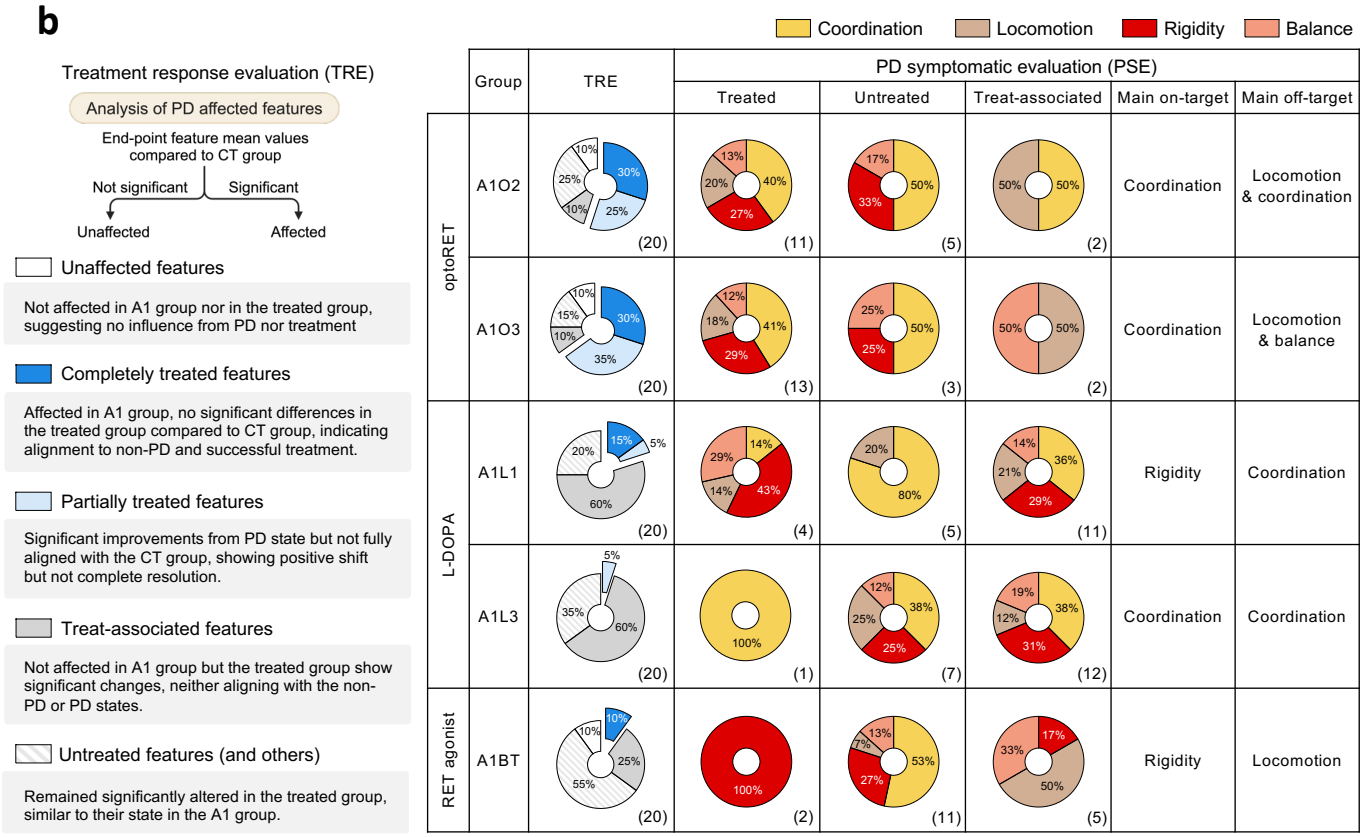
For each group, the KL divergence of each feature from the CT counterpart was computed at 10 wk, and the results are shown as bar graphs (mean ± SEM). Each group consists of 6 sets of the sampling datasets, each comprising 150 randomly selected clips. When comparing the magnitude of the differences to CT, the A1O3 group showed less significant differences for 7 features, more significant differences for 4 features, and similar differences for 9 features compared to the A1 group. In addition, for 4 features, the divergence in the A1O3 group differed significantly from that of the A1 group. See Supplementary Table 9 for detailed statistical results. All statistics, one-way ANOVA and post-hoc tests with Holm–Sidak multiple comparison corrections were performed. Source data are provided in the Source Data file.




**Supplementary Figure 30. Group comparisons of the feature values (XGB model) at 10 wk.**

Box plots show the median (black line), mean (black circle), and interquartile range (box). Whiskers extend to the most extreme data points within 1.5 × the interquartile range from the lower and upper quartiles (Tukey method). Individual outliers beyond this range are omitted from the plot for clarity but are retained in the dataset and included in the calculation of the mean and median. Statistical analysis was performed by one-way ANOVA followed by Holm–Sidak-corrected Welch's t-tests comparing each group to CT. Significant differences are indicated by asterisks. Exact p-values and sample sizes are provided in Supplementary Table 10. Source data are provided in the Source Data file.




**Supplementary Figure 31. Comparisons of treatment response and PD symptomatic evaluations in A1 PD mice with different treatments.**

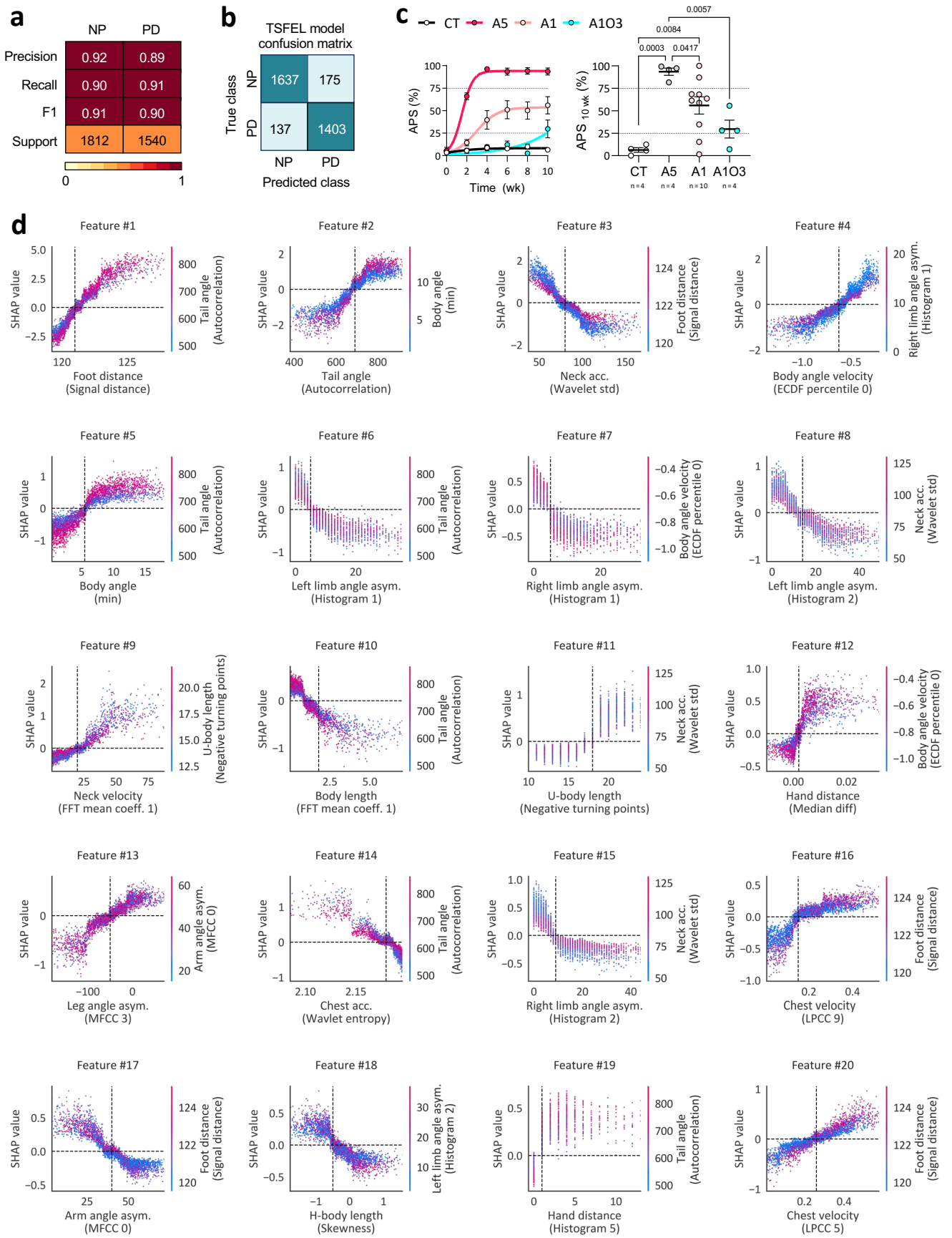
**(a)** Heatmaps of the mean feature values for each group at endpoint. Statistical analysis was performed using one-way ANOVA, followed by post-hoc comparisons using Welch's t-tests comparing each group to the reference (CT) group. Statistical significance is indicated by asterisks after Holm–Sidak correction for multiple comparisons. Detailed statistical results are provided in Supplementary Tables 10–15. **(b)** Comparisons of three treatment groups for the treatment response evaluation (TRE) and PD symptomatic evaluation (PSE) at 10 wk, except for the A1BT group (assessed at 6 wk). The descriptions of each TRE category are shown on the left, and the feature numbers included for each evaluation are indicated in brackets.

| Parent features from XGB model | | Node velocity (cm/s) | Pair distance (cm) | | Pair angle difference (rad) | |
|---|---|---|---|---|---|---|
| | | Neck | nose-chest | Body | | rleg-lleg |
| | | Anus | neck-anus | Tail | | rleg-rarm |
| | | Chest | chest-anus | | | rleg-larm |
| | | Tip | rfoot-lfoot | | | rarm-larm |
| | | | rhand-lhand | | | lleg-larm |
| | | | | | | lleg-rarm |
| Feature transform | Velocity (cm/s) | N/A | No | Yes | | No |
| | Acceleration (cm/s$^{-2}$) | Yes | No | No | | No |
| Sub-total (core features) | 23 features created | | | | | |

| TSFEL feature extraction | Statistical domain | Spectral domain | Temporal domain |
|---|---|---|---|
| | Absolute energy | FFT mean coefficient | Area under the curve |
| | Average power | Fundamental frequency | Autocorrelation |
| | ECDF | Human range energy | Centroid |
| | ECDF Percentile | LPCC | Mean absolute diff |
| | ECDF Percentile Count | MFCC | Mean diff |
| | Entropy | Max power spectrum | Median absolute diff |
| | Histogram | Maximum frequency | Median diff |
| | Interquartile range | Median frequency | Negative turning points |
| | Kurtosis | Power bandwidth | Peak to peak distance |
| | Max | Spectral centroid | Positive turning points |
| | Mean | Spectral decrease | Signal distance |
| | Mean absolute deviation | Spectral distance | Slope |
| | Median | Spectral entropy | Sum absolute diff |
| | Median absolute deviation | Spectral kurtosis | Zero crossing rate |
| | Min | Spectral positive turning points | Neighbourhood peaks |
| | Root mean square | Spectral roll-off | |
| | Skewness | Spectral roll-on | |
| | Standard deviation | Spectral skewness | |
| | Variance | Spectral slope | |
| | | Spectral spread | |
| | | Spectral variation | |
| | | Wavelet absolute mean | |
| | | Wavelet energy | |
| | | Wavelet standard deviation | |
| | | Wavelet entropy | |
| | | Wavelet variance | |
| Total | 4485 features created | | |
| AutoML feature selection | 332 features selected | | |

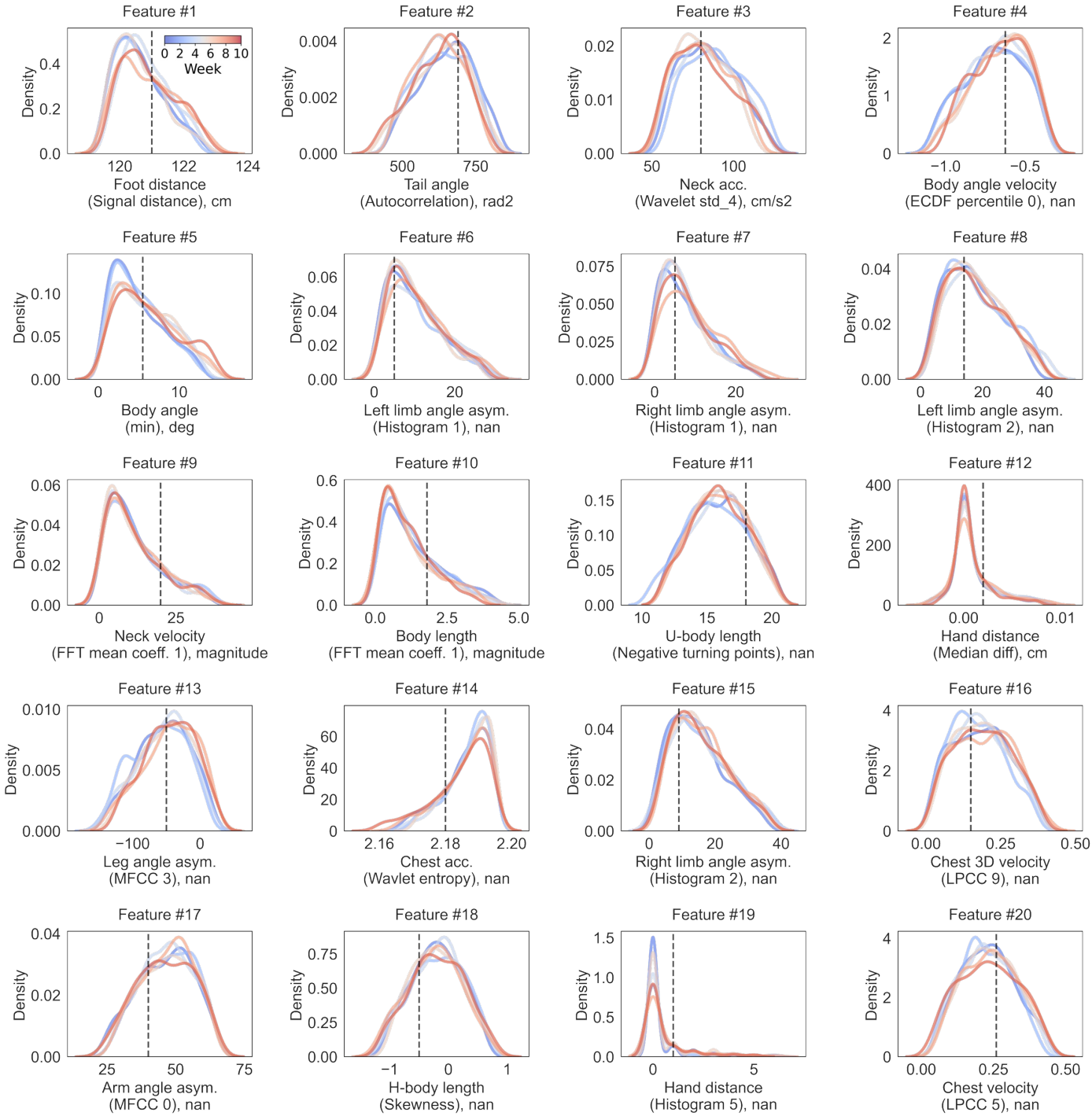
**Supplementary Figure 32. Summary table of the features engineered and extracted for the spectro-temporal analysis.**

Using the parent features from XGB model, total 23 kinematic features in 3D were created as a list of core features. By implementing TSFEL (Time Series Feature Extraction Library), total 4485 features from statistical, spectral and temporal domains, were created. Total 332 of them were selected through an automated ML processes using PyCaret library, as the key features for PD behaviour phenotyping.



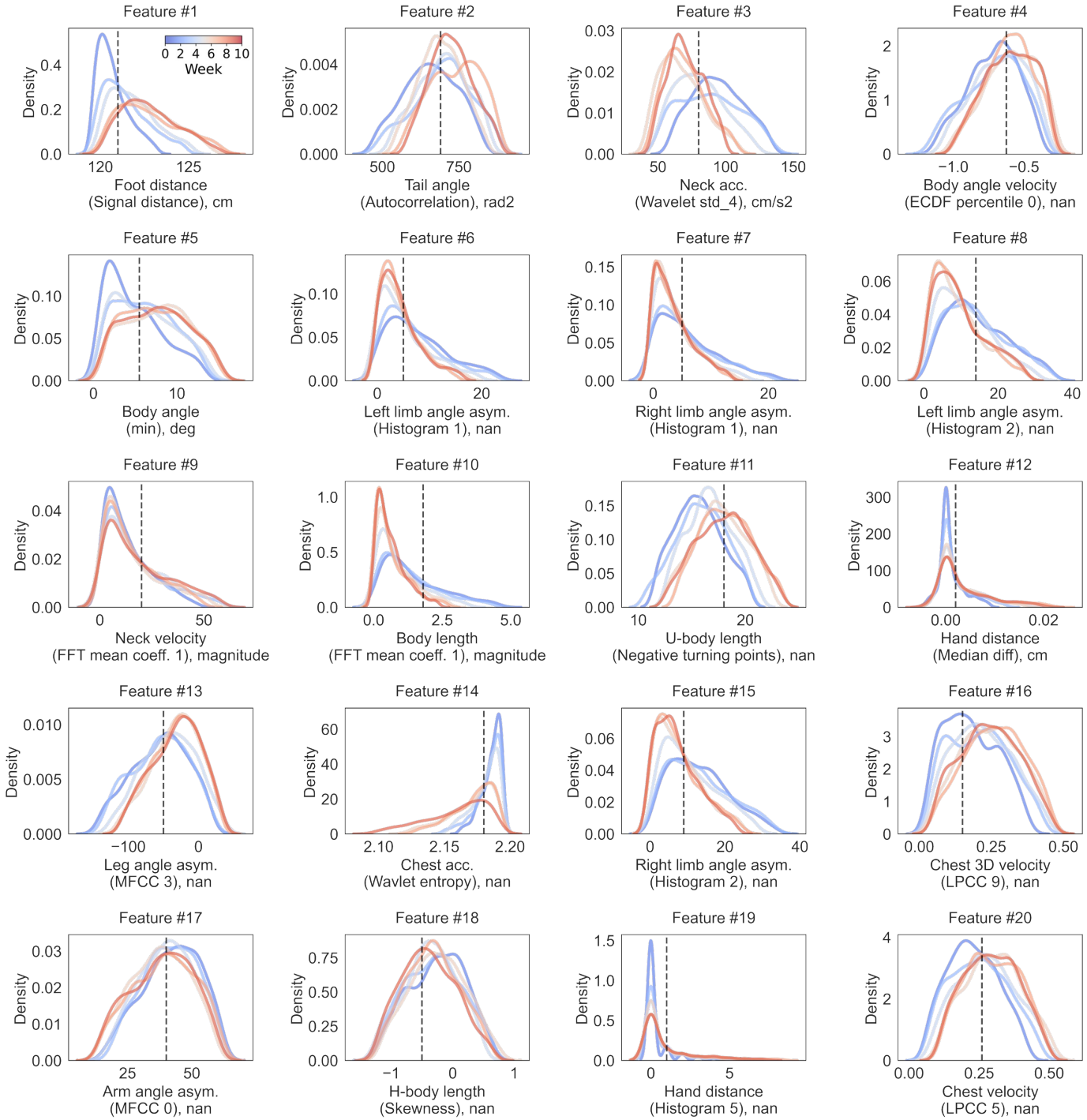

**Supplementary Figure 33. Model evaluation and SHAP dependence plots of top 20 features (TSFEL model).**

**(a)** Summary of the TSFEL model evaluation metrics. **(b)** Confusion matrix of the TSFEL model in the classification of validation dataset. **(c)** TSFEL model predicted PD scores for the CT, A5, A1 and A1O3 groups (n = 4, 4, 10 and 4, respectively). **(d)** SHAP dependence plots of the top 20 features (TSFEL model). See Supplementary Figure 23 legend for more detailed description on SHAP dependence plots. Statistical analyses was performed using one-way ANOVA followed by Holm–Sidak post hoc corrections for multiple comparisons. Source data are provided in the Source Data file.



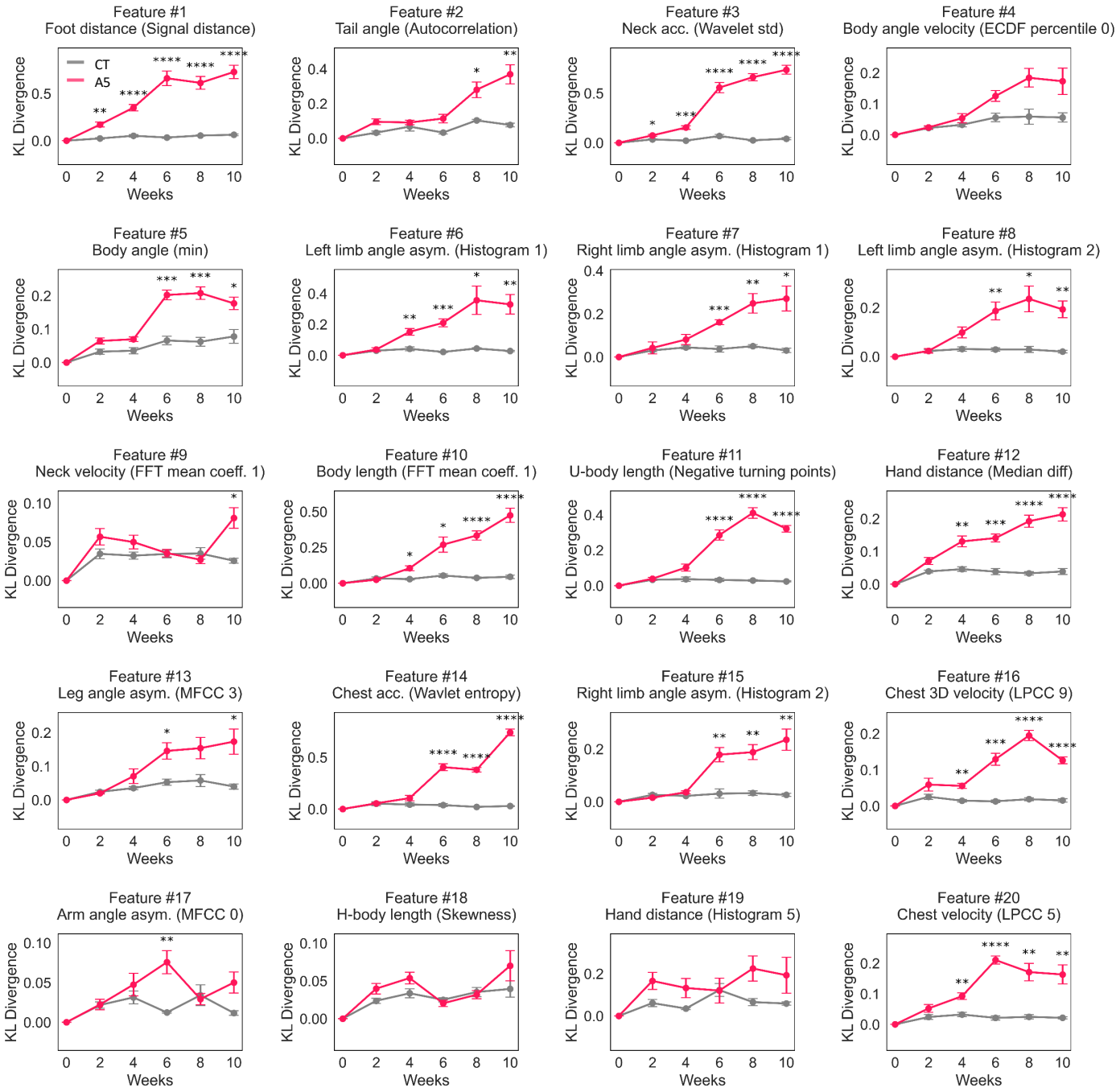

**Supplementary Figure 34. CT group's longitudinal analysis of the top 20 features (TSFEL model) in the KDE plots.**

For each feature, KDE plots of each week (0, 2, 4, 6, 8 and 10 wk) were plotted. Vertical dashed lines indicate the key values.



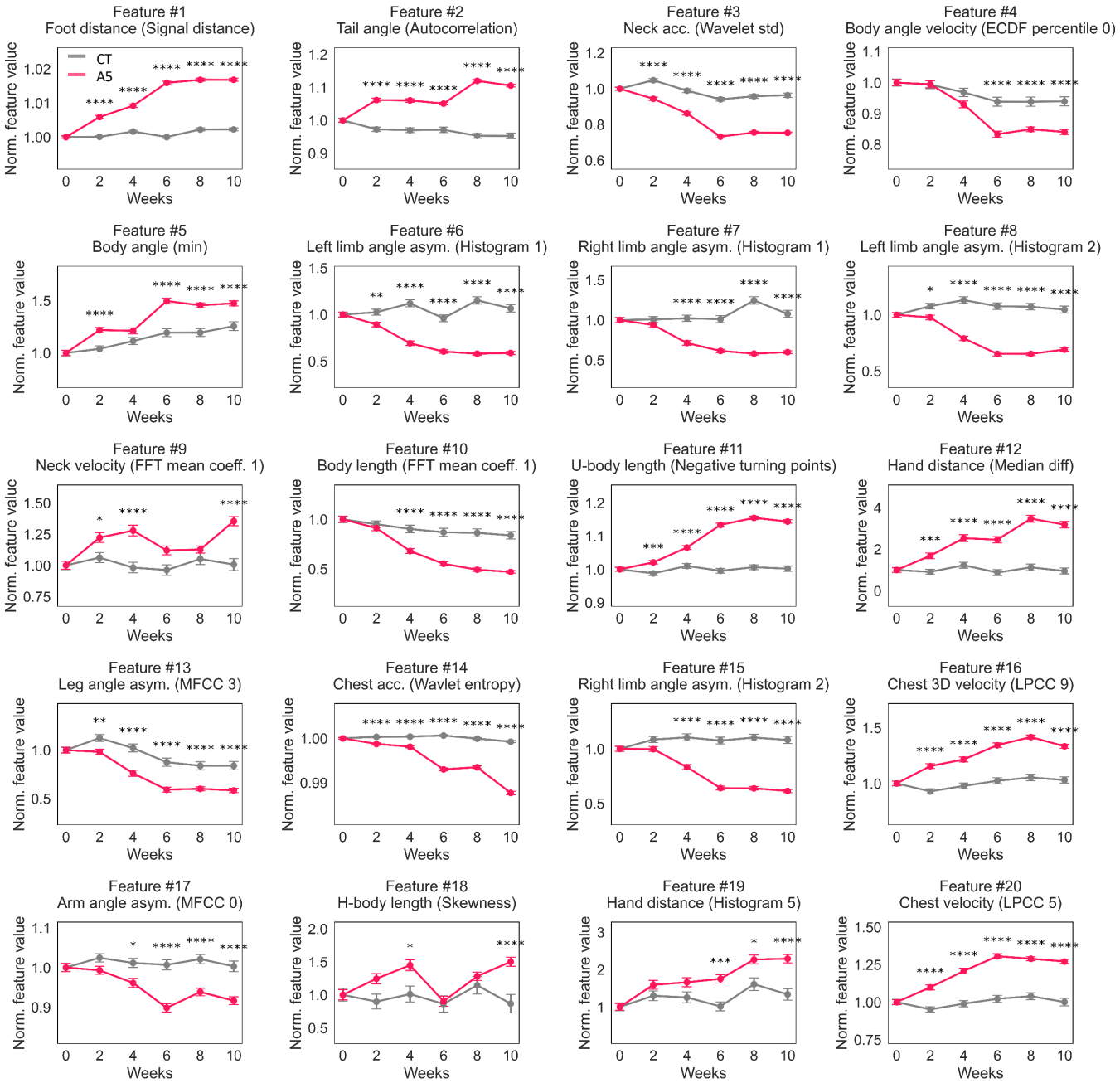

**Supplementary Figure 35. PD (A5) group's longitudinal analysis of the top 20 features (TSFEL model) in the KDE plots.**

For each feature, KDE plots of each week (0, 2, 4, 6, 8 and 10 wk) were plotted. Vertical dashed lines indicate the key values.



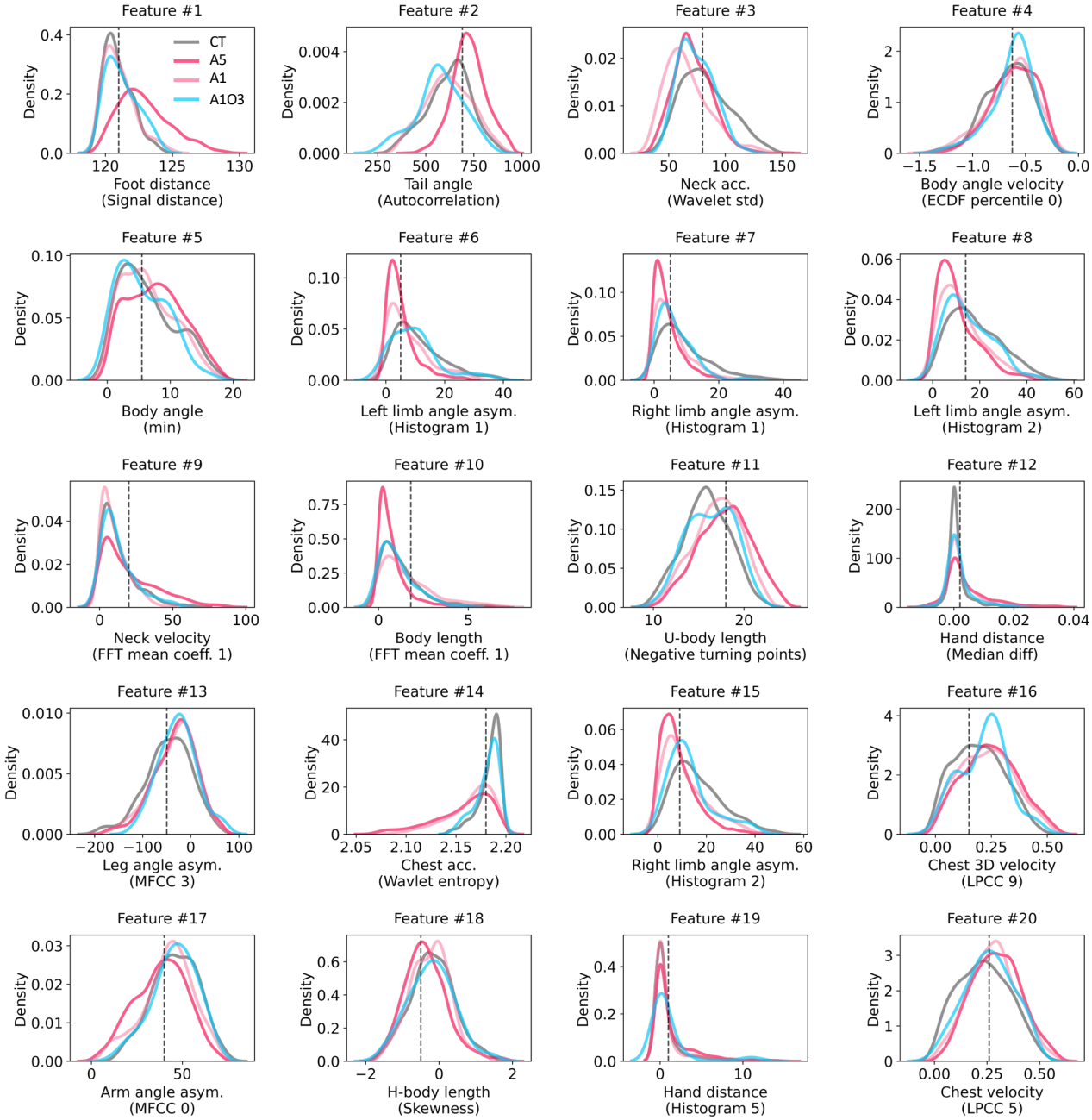

**Supplementary Figure 36. Longitudinal comparison of KL divergences (TSFEL model) between the CT and PD (A5) groups.**

For each group, the KL divergences of each feature from the respective baseline (0 wk) were computed over the experimental duration (0-10 wk) and plotted as line graphs (mean ± SEM. For each group, the KL divergence of each feature relative to its baseline value (0 wk) was computed across the experimental duration (0–10 wk). Each group consisted of 6 sampling sets, each containing 150 randomly selected clips. A two-way ANOVA (group × week) was performed for each feature, followed by weekly t-tests between groups (CT vs. A5). The resulting p-values from the weekly t-tests were corrected for multiple comparisons using the Bonferroni method. Detailed statistical results are provided in Supplementary Table 16. Source data are provided in the Source Data file.



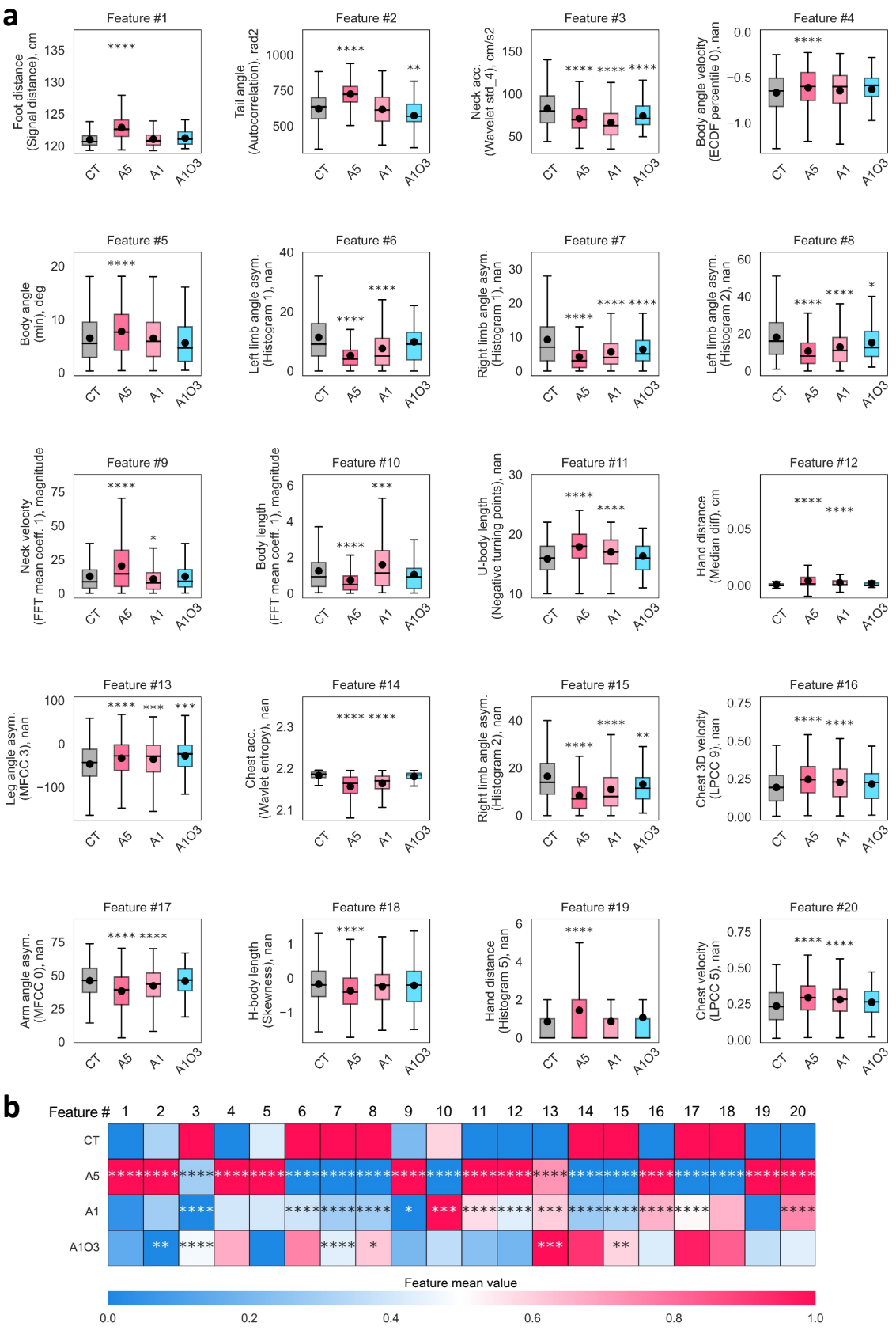

**Supplementary Figure 37. Longitudinal comparison of feature values (TSFEL model) between the CT and PD (A5) groups.**

For each group, the KL divergences of each feature from the respective baseline (0 wk) were computed over the experimental duration (0-10 wk) and plotted as line graphs (mean ± SEM) over time. For each feature, the values at each week were divided by the group's corresponding baseline (0 wk) mean value, and the normalised data were analysed over the experimental duration (0–10 wk). Each group consisted of 6 sampling sets, each containing 150 randomly selected clips. Two-way ANOVA (group × week) was performed for each feature on the normalised data, followed by weekly t-tests comparing the CT and A5 groups. P-values from weekly t-tests were corrected for multiple comparisons using the Bonferroni method. Detailed statistical results are provided in Supplementary Table 17. Source data are provided in the Source Data file.



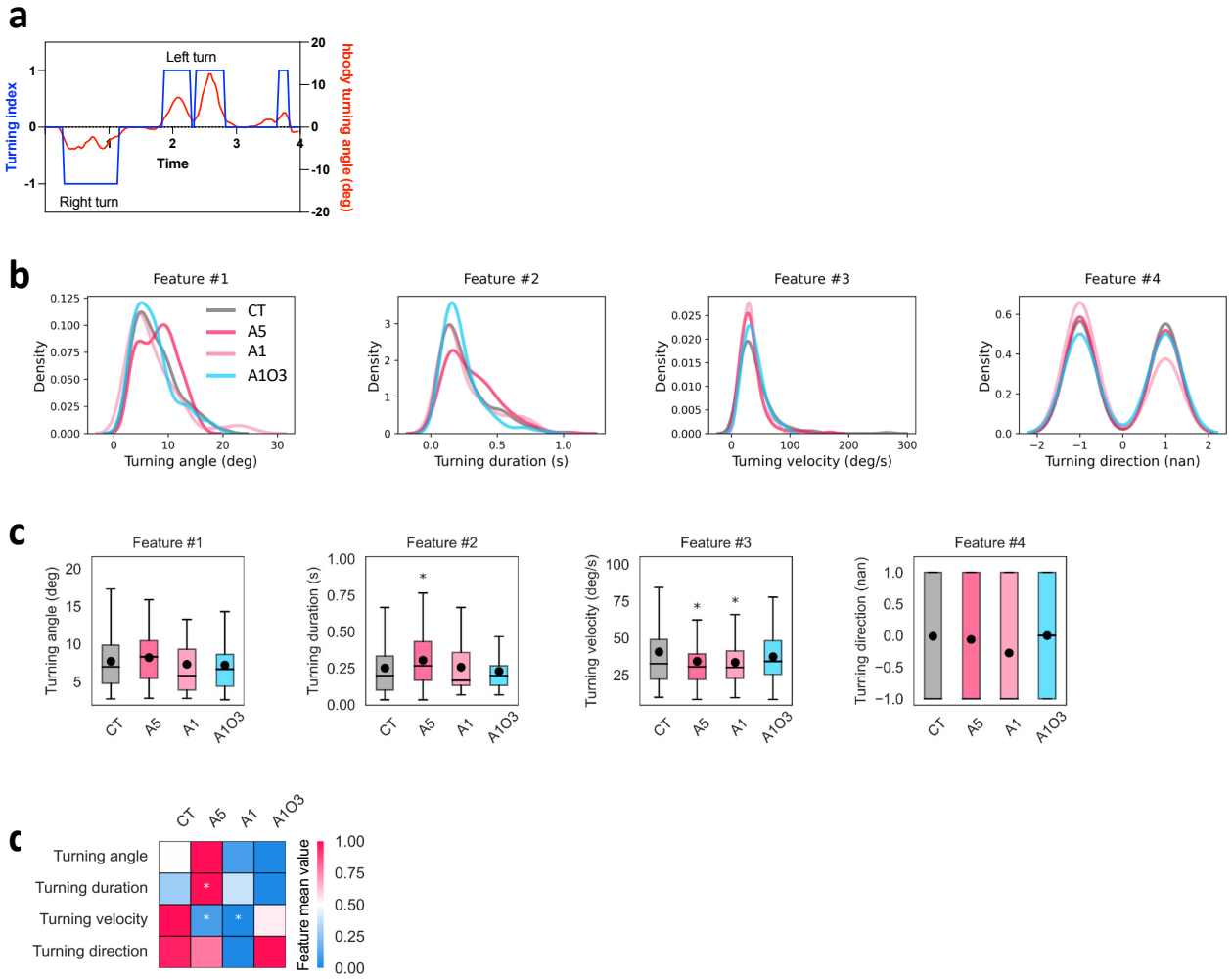

**Supplementary Figure 38. Group comparison of the KDE plots of the top 20 features (TSFEL model) at 10 wk.**

For each feature, KDE plots of the CT, A5, A1 and A1O3 groups were plotted. Vertical dashed lines indicate the key values.



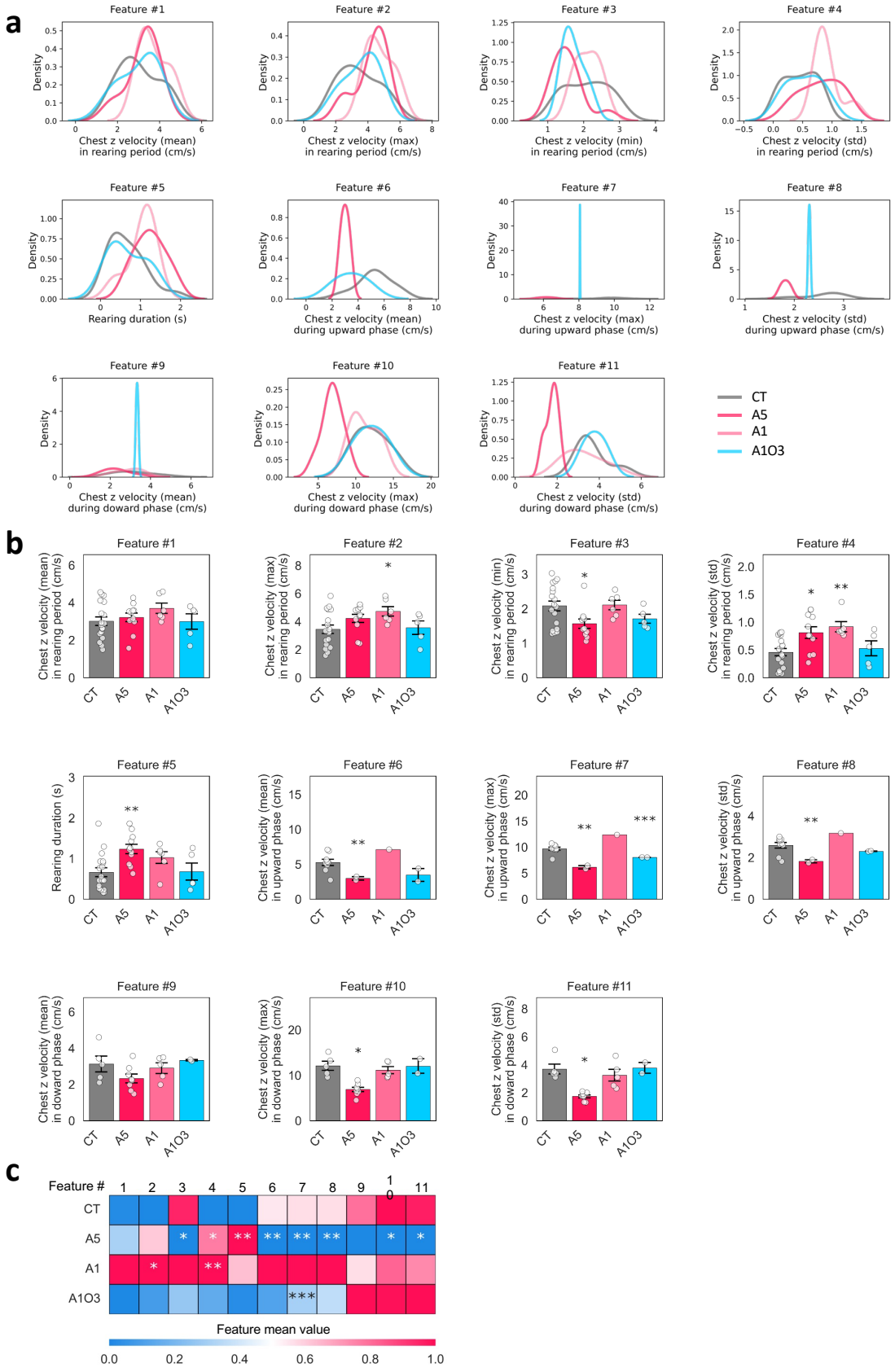

**Supplementary Figure 39. Group comparison of the top 20 features (TSFEL model) at 10 wk.**

**(a)** Box plots show the median (black line), mean (black circle), and interquartile range (box). Whiskers extend to the most extreme data points within 1.5 × the interquartile range from the lower and upper quartiles (Tukey method). Individual outliers beyond this range are omitted from the plot for clarity but are retained in the dataset and included in the calculation of the mean and median. The same data for Feature #14, #3 and #2 are also presented in panels e, h and k of Figure 4, respectively. **(b)** Heatmaps of the mean feature values for each group at 10 wk. Statistical analysis was performed by one-way ANOVA followed by Holm–Sidak-corrected Welch's t-tests comparing each group to CT. Significant differences are indicated by asterisks. Exact p-values and sample sizes are provided in Supplementary Table 18. Source data are provided in the Source Data file.



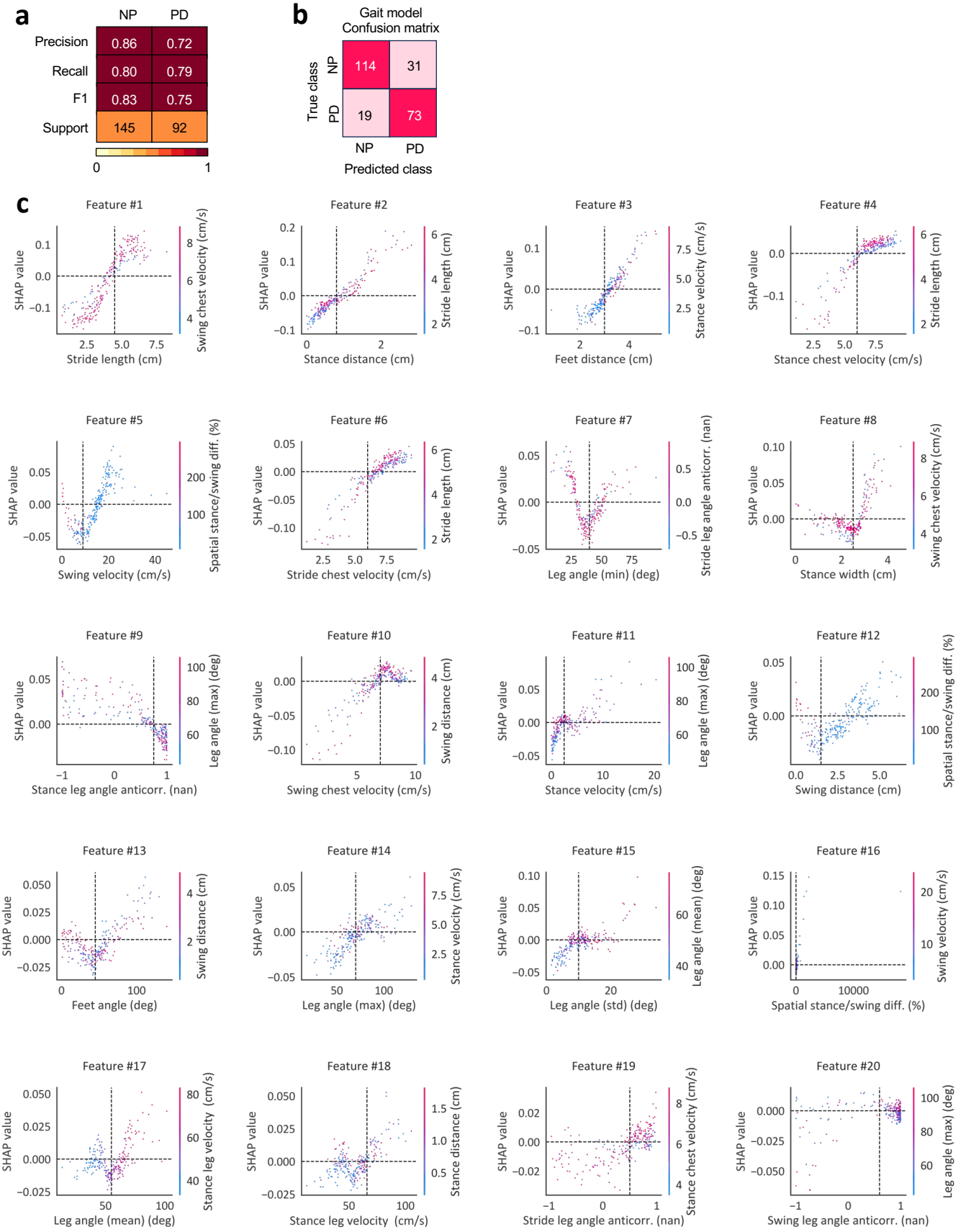

**Supplementary Figure 40. Group comparison of the turning features at 10 wk.**

**(a)** Detection of turning events based on the hind-body (hbody) angle. **(b)** For each feature, KDE plots of the CT, A5, A1 and A1O3 groups were plotted. **(c)** Box plots show the median (black line), mean (black circle), and interquartile range (box). Whiskers extend to the most extreme data points within 1.5 × the interquartile range from the lower and upper quartiles (Tukey method). Individual outliers beyond this range are omitted from the plot for clarity but are retained in the dataset and included in the calculation of the mean and median. The same data for Feature #2 and #3 are also presented in panels c and d of Figure 5, respectively. **(d)** Heatmaps of the mean feature values for each group at 10 wk. Statistical analysis was performed by one-way ANOVA followed by Benjamini–Hochberg corrected Welch's t-tests comparing to CT. Significant differences are indicated by asterisks. Exact p-values and sample sizes are provided in Supplementary Table 19. Source data are provided in the Source Data file.



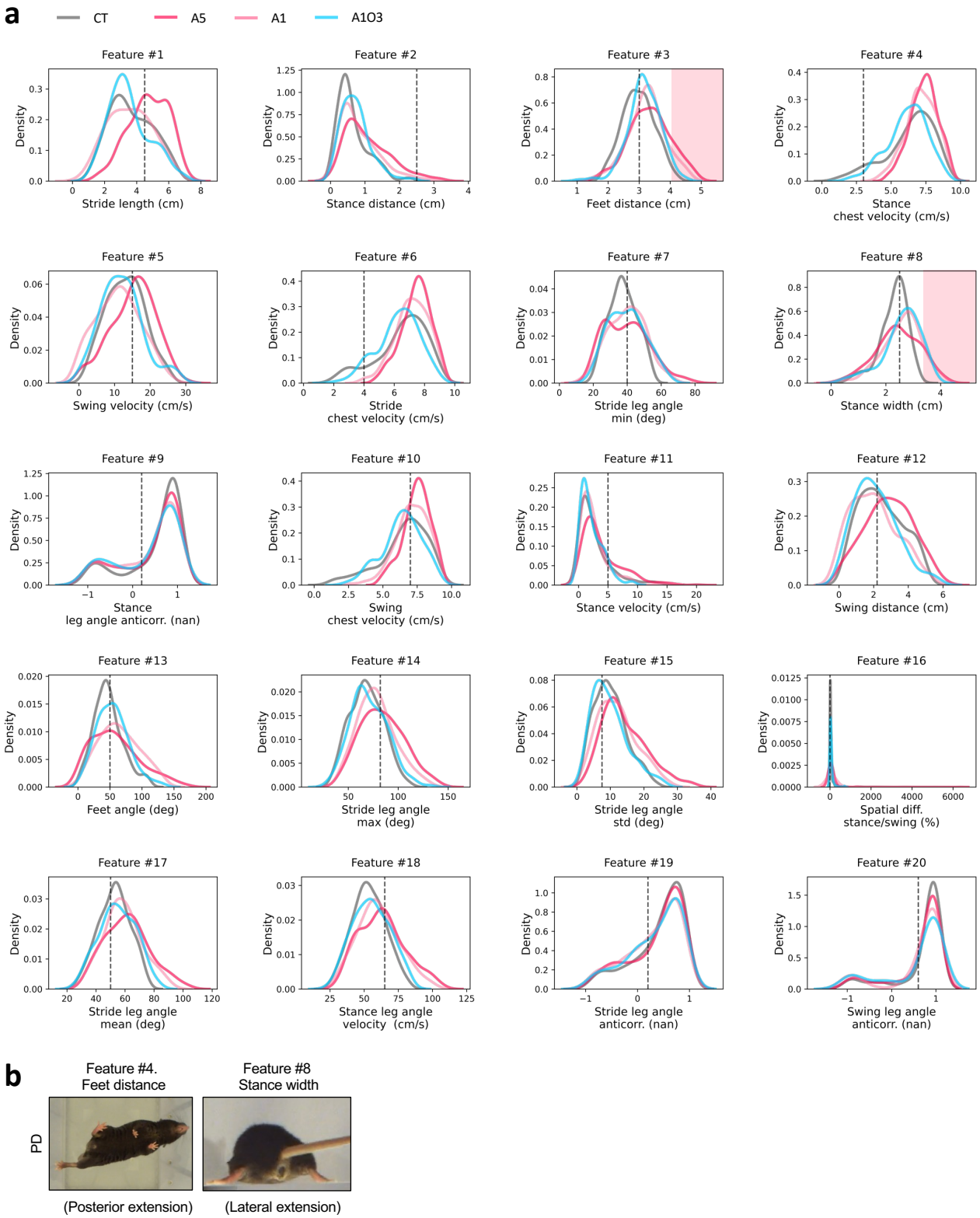

**Supplementary Figure 41. Group comparison of the rearing features at 10 wk.**

**(a)** For each feature, KDE plots of the Normal, A5X, A1X and A1X+S#3 groups were plotted. **(b)** Data for each feature are shown as bar graphs (mean ± SEM). The same data for Feature #4 is also presented in panel e of Figure 5.**(c)** Heatmaps of the mean feature values for each group at endpoint. Statistical analysis was performed using one-way ANOVA, followed by post-hoc comparisons using Welch's t-tests comparing each group to the reference (CT) group. Statistical significance is indicated by asterisks after Holm–Sidak correction for multiple comparisons. Detailed statistical results are provided in Supplementary Table 20. Source data are provided in the Source Data file.



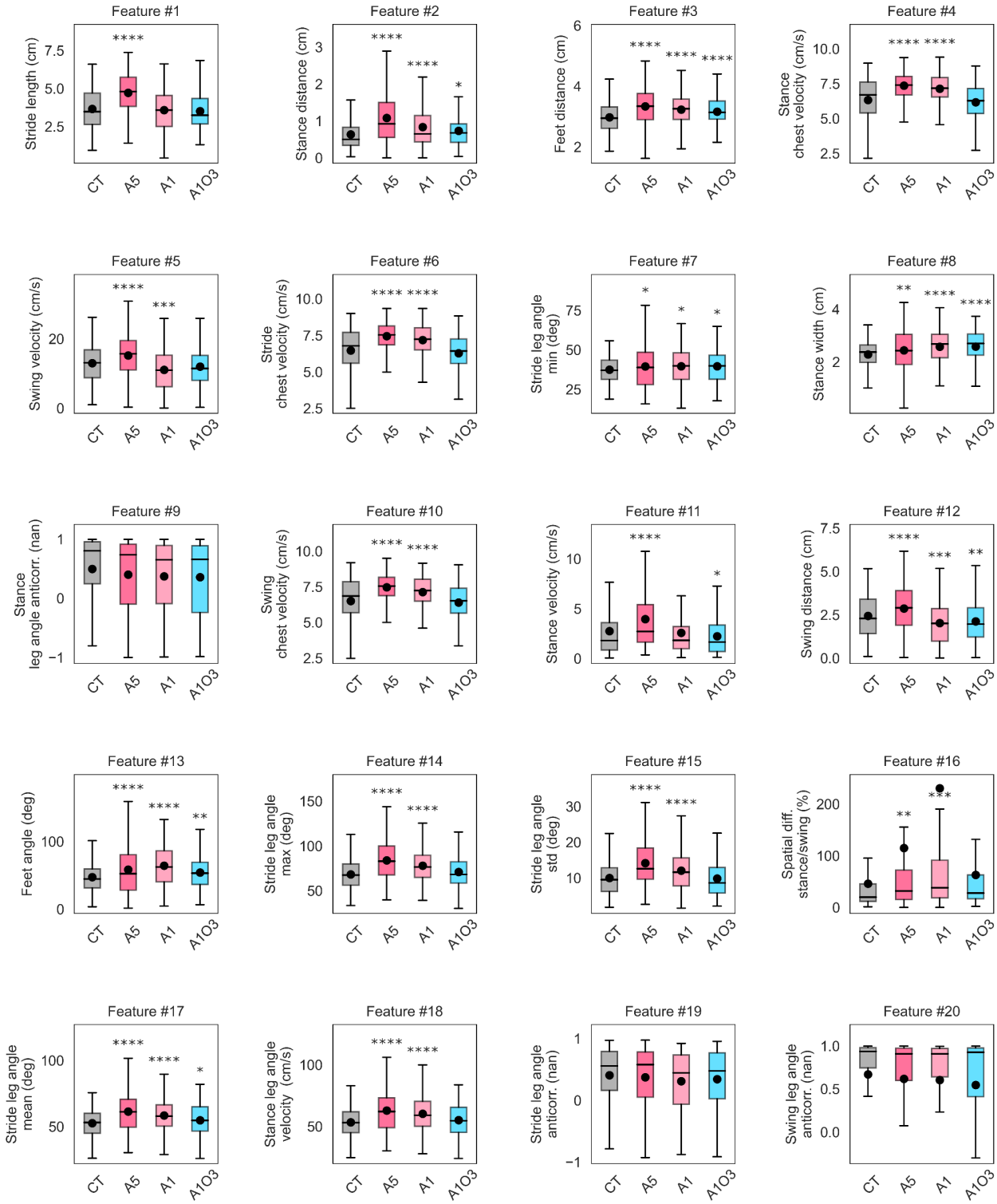

**Supplementary Figure 42. Model evaluation and SHAP dependence plots of top 20 features (Gait model).**

**(a)** Summary of the Gait model evaluation metrics. **(b)** Confusion matrix of the Gait model in the classification of validation dataset. **(c)** SHAP dependence plots of the top 20 features (Gait model). See Supplementary Figure 23 legend for more detailed description on SHAP dependence plots.



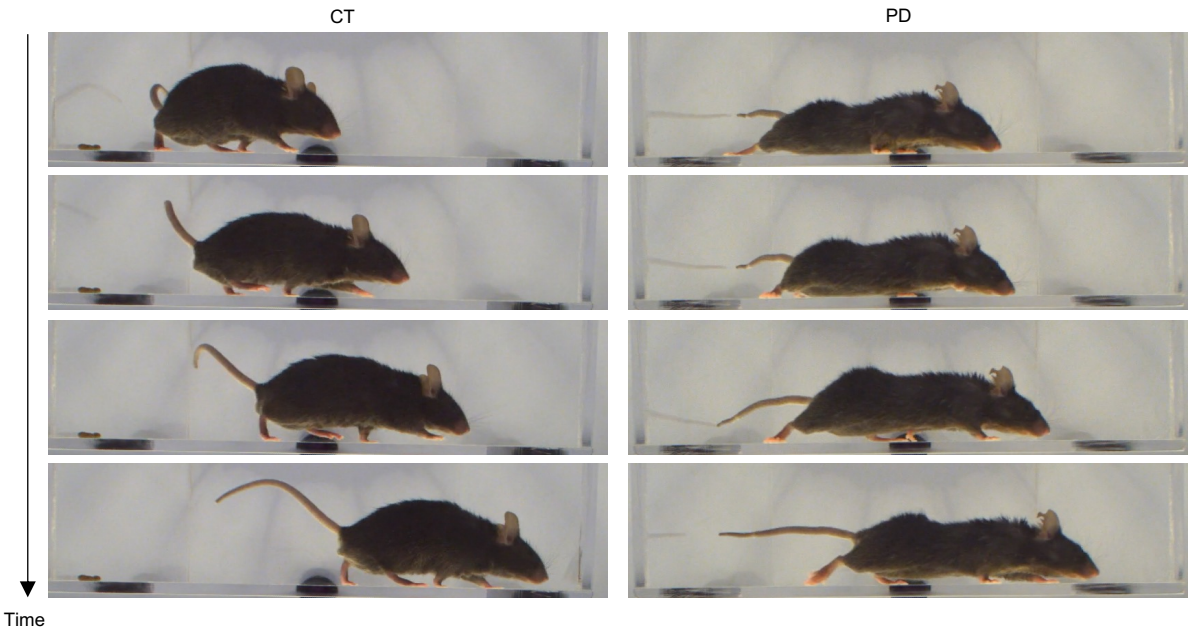

**Supplementary Figure 43. Group comparison of the top 20 features (Gait model) in KDE plots at 10 wk.**

(a) Kernel density estimate (KDE) plots for each feature compare distribution patterns across the CT, A5, A1, and A1O3 groups at 10 wk, with vertical dashed lines highlighting key feature values. The pink background in features #3 and #8 highlights the subpopulation of PD mice exhibiting abnormally high feet distance and stance width. **(b)** Snapshot video images capture instances of abnormally high feet distance and stance width observed in PD mice.




**Supplementary Figure 44. Group comparison of the top 20 features (Gait model) in bar plots at 10 wk.**

Box plots show the median (black line), mean (black circle), and interquartile range (box). Whiskers extend to the most extreme data points within 1.5 × the interquartile range from the lower and upper quartiles (Tukey method). Individual outliers beyond this range are omitted from the plot for clarity but are retained in the dataset and included in the calculation of the mean and median. Statistical analysis was performed by one-way ANOVA followed by Holm–Sidak-corrected Welch's t-tests comparing each group to CT. Significant differences are indicated by asterisks. Exact p-values and sample sizes are provided in Supplementary Table 22. Source data are provided in the Source Data file.




**Supplementary Figure 45. Snapshot video images of CT and PD mice in walking.**

Images were taken from OFT recordings at a manually decided cut-off to highlight differences in hindlimb positions between CT and PD mice during walking. For PD mice, images were captured during extreme hindlimb lagging/trailing (freezing gait). See Supplementary Movie 3.

# Supplementary Tables

List of Supplementary Tables:


1. Summary of details for the key experimental groups.
2. Classifier training parameter by PyCaret default setting.
3. Statistical summary of the KL divergences for the top 20 features identified by the XGB model comparing CT and PD (A5) groups.
4. Statistical summary of the feature values for the top 20 features identified by the XGB model, comparing the CT and PD (A5) groups.
5. Statistical summary of the KL divergences for the top 20 features identified by the XGB model comparing NALS and ALS groups.
6. Statistical summary of the feature values for the top 20 features identified by the XGB model, comparing the NALS and ALS groups.
7. Statistical comparisons of the top 20 features identified by the XGB model comparing PD (A5) and ALS groups.
8. Statistical summary of the APS (XGB model-predicted PD scores) at 10 wk across groups.
9. Statistical summary of the KL divergences for the top 20 features identified by the XGB model.
10. Statistical summary of group comparisons (A1O3) for the top 20 features (identified by the XGB model) at 10 wk.
11. Statistical summary of group comparisons (A1O2) for the top 20 features (identified by the XGB model) at 10 wk.
12. Statistical summary of group comparisons (A1L1) for the top 20 features (identified by the XGB model) at 10 wk.
13. Statistical summary of group comparisons (A1L1) for the top 20 features (identified by the XGB model) at 10 wk.
14. Statistical summary of group comparisons (A1BT) for the top 20 features (identified by the XGB model) at 6 wk.
15. Statistical summary of treatment group comparisons for the top 20 features (identified by the XGB model) at endpoints.
16. Statistical summary of the KL divergences for the top 20 features identified by the TSFEL model comparing CT and PD (A5) groups.
17. Statistical summary of the feature values for the top 20 features identified by the TSFEL model, comparing the CT and PD (A5) groups.
18. Statistical summary of group comparisons (A1O3) for the top 20 features (TSFEL model) at 10 wk.
19. Statistical summary of group comparisons (A1O3) for the turning features at 10 wk.
20. Statistical summary of group comparisons (A1O3) for the rearing features at 10 wk.
21. Definitions of the Gait model top 20 features.
22. Statistical summary of group comparisons (A1O3) for the top 20 features ( Gait model) at 10 wk.

**Supplementary Table 1. Summary of details for the key experimental groups.** Experimental groups are detailed by subgroup classification, description of experimental interventions, genetic backgrounds, gender, genotypes, experimental timelines, viral constructs (AAV-DJ/8-hSyn1; titres indicated), and the numbers of mice utilised for the total cohort, machine-learning (ML) dataset, unseen dataset for AI-predicted PD score (APS) analysis, and independent experimental replications. The total mouse n indicated in the table represents all mice included in this study; however, subsets of mice were variably involved across individual analyses, with specific numbers (n) described in the relevant text. Any groups not listed in this table or with amended details are described in the relevant text. DAT-CRE transgenic mice and SOD1-G93A transgenic mice were obtained from The Jackson Laboratory (strain #006302 and #002726, respectively).

| Group | # | Sub-group | Description | Genetic background | Gender | Genotype | Experimental timeline | AAV-DJ/8-hSyn1 vrius construct (titre, gp/mL) | Total mouse n | ML mouse n | Unseen mouse n | Experiment n |
|---|---|---|---|---|---|---|---|---|---|---|---|---|
| CT | 0 | NI | No virus injection | C57BL/6J | Male | WT | 20-30 wk old (10 wk) | - | 12 | 4 | 8 | 3 |
| | 1 | EV | Empty vector injection | C57BL/6J | Male | WT | | DIO-RFP (1E+11) | 10 | 0 | 10 | 2 |
| | 2 | R1 | low dose RFP expression | C57BL/6J | Male | WT | | RFP (1E+12) | 15 | 0 | 10 | 1 |
| | | | | B6SJL × C57BL/6J hybrid | Male | DAT-CRE | | DIO-RFP (1E+12) | | 4 | 1 | 2 |
| | 3 | R5 | high dose RFP expression | C57BL/6J | Male | WT | | RFP (5E+12) | 13 | 0 | 10 | 1 |
| | | | | B6SJL × C57BL/6J hybrid | Male | DAT-CRE | | DIO-RFP (5E+12) | | 2 | 1 | 1 |
| PD | 4 | A1 | low dose hA53T expression | C57BL/6J | Male | WT | | hA53T (1E+12) + RFP (1E+11) | 15 | 0 | 5 | 1 |
| | | | | B6SJL × C57BL/6J hybrid | Male | DAT-CRE | | hA53T (1E+12) + DIO-RFP (1E+11) | | 0 | 10 | 5 |
| | 5 | A5 | high dose hA53T expression | C57BL/6J | Male | WT | | hA53T (5E+12) + RFP (1E+11) | 22 | 0 | 8 | 2 |
| | | | | B6SJL × C57BL/6J hybrid | Male | DAT-CRE | | hA53T (5E+12) + DIO-RFP (1E+11) | | 11 | 3 | 5 |
| MND | 6 | NALS | ALS control | B6SJL × C57BL/6J hybrid | Female | WT | 10-20 wk old (10 wk) | - | 2 | | 2 | 1 |
| | 7 | ALS | ALS model | B6SJL × C57BL/6J hybrid | Female | SOD1-G93A | | - | 2 | | 2 | 1 |
| optoRET | 8 | A1OD | A1 + optoRET + dark | B6SJL × C57BL/6J hybrid | Male | DAT-CRE | 20-30 wk old (10 wk) | hA53T (1E+12) + DIO-optoRET (1E+11) | 10 | | 10 | 3 |
| | 9 | A1O1 | A1 + optoRET + light (daily schedule) | B6SJL × C57BL/6J hybrid | Male | DAT-CRE | | hA53T (1E+12) + DIO-optoRET (1E+11) | 7 | | 7 | 3 |
| | 10 | A1O2 | A1 + optoRET + light (biweekly schedule) | B6SJL × C57BL/6J hybrid | Male | DAT-CRE | | hA53T (1E+12) + DIO-optoRET (1E+11) | 12 | | 12 | 3 |
| | 11 | A1O3 | A1 + optoRET + light (alternate days schedule) | B6SJL × C57BL/6J hybrid | Male | DAT-CRE | | hA53T (1E+12) + DIO-optoRET (1E+11) | 8 | | 8 | 2 |
| | 12 | A5OD | A1 + optoRET + dark | B6SJL × C57BL/6J hybrid | Male | DAT-CRE | | hA53T (5E+12) + DIO-optoRET (1E+11) | 7 | | 7 | 2 |
| | 13 | A5O1 | A1 + optoRET + light (everyday schedule) | B6SJL × C57BL/6J hybrid | Male | DAT-CRE | | hA53T (5E+12) + DIO-optoRET (1E+11) | 7 | | 7 | 2 |
| | 14 | A5O2 | A1 + optoRET + light (biweekly schedule) | B6SJL × C57BL/6J hybrid | Male | DAT-CRE | | hA53T (5E+12) + DIO-optoRET (1E+11) | 6 | | 6 | 2 |
| L-DOPA | 15 | A1L1 | A1 + L-DOPA (daily schedule) | C57BL/6J | Male | WT | | hA53T (1E+12) + RFP (1E+11) | 10 | | 10 | 1 |
| | 16 | A1L3 | A1 + L-DOPA (alternate days schedule) | C57BL/6J | Male | WT | | hA53T (1E+12) + RFP (1E+11) | 10 | | 10 | 2 |
| RET agonist | 17 | A1BT | A1 + BT44 (direct brain infusion at a constant flow rate) | C57BL/6J | Male | WT | 20-26 wk old (6 wk) | hA53T (1E+12) + RFP (1E+11) | 6 | | 6 | 1 |

**Supplementary Table 2. Classifier training parameter by PyCaret default setting.** These defaults are derived from the underlying libraries (e.g. scikit-learn, XGBoost, LightGBM) as used by PyCaret. In this study, these default parameter settings are applied during model training using PyCaret. Values reflect the defaults used in PyCaret version 2.3.10. The default parameters have changed in more recent PyCaret versions. For the latest details or changes, please refer to the official documentation for PyCaret (https://pycaret.org/), Scikit-learn (https://scikit-learn.org/stable/modules/classes.html), XGB (https://xgboost.readthedocs.io/) and LightGBM (https://lightgbm.readthedocs.io/).

| Classifiers | Default parameters (PyCaret version 2.3.10) |
|---|---|
| Extreme Gradient Boosting (XGB) | 'objective': 'binary:logistic', 'use_label_encoder': None, 'base_score': 0.5, 'booster': 'gbtree', 'callbacks': None, 'colsample_bylevel': 1, 'colsample_bynode': 1, 'colsample_bytree': 1, 'early_stopping_rounds': None, 'enable_categorical': False, 'eval_metric': None, 'feature_types': None, 'gamma': 0, 'gpu_id': -1, 'grow_policy': 'depthwise', 'importance_type': None, 'interaction_constraints': '', 'learning_rate': 0.300000012, 'max_bin': 256, 'max_cat_threshold': 64, 'max_cat_to_onehot': 4, 'max_delta_step': 0, 'max_depth': 6, 'max_leaves': 0, 'min_child_weight': 1, 'missing': nan, 'monotone_constraints': '()', 'n_estimators': 100, 'n_jobs': -1, 'num_parallel_tree': 1, 'predictor': 'auto', 'random_state': 101, 'reg_alpha': 0, 'reg_lambda': 1, 'sampling_method': 'uniform', 'scale_pos_weight': 1, 'subsample': 1, 'tree_method': 'auto', 'validate_parameters': 1, 'verbosity': 0 |
| Extra Trees Classifier | 'bootstrap': False, 'ccp_alpha': 0.0, 'class_weight': None, 'criterion': 'gini', 'max_depth': None, 'max_features': 'auto', 'max_leaf_nodes': None, 'max_samples': None, 'min_impurity_decrease': 0.0, 'min_impurity_split': None, 'min_samples_leaf': 1, 'min_samples_split': 2, 'min_weight_fraction_leaf': 0.0, 'n_estimators': 100, 'n_jobs': -1, 'oob_score': False, 'random_state': 101, 'verbose': 0, 'warm_start': False |
| Random Forest Classifier | 'bootstrap': True, 'ccp_alpha': 0.0, 'class_weight': None, 'criterion': 'gini', 'max_depth': None, 'max_features': 'auto', 'max_leaf_nodes': None, 'max_samples': None, 'min_impurity_decrease': 0.0, 'min_impurity_split': None, 'min_samples_leaf': 1, 'min_samples_split': 2, 'min_weight_fraction_leaf': 0.0, 'n_estimators': 100, 'n_jobs': -1, 'oob_score': False, 'random_state': 101, 'verbose': 0, 'warm_start': False |
| LightGBM | 'boosting_type': 'gbdt', 'class_weight': None, 'colsample_bytree': 1.0, 'importance_type': 'split', 'learning_rate': 0.1, 'max_depth': -1, 'min_child_samples': 20, 'min_child_weight': 0.001, 'min_split_gain': 0.0, 'n_estimators': 100, 'n_jobs': -1, 'num_leaves': 31, 'objective': None, 'random_state': 101, 'reg_alpha': 0.0, 'reg_lambda': 0.0, 'silent': 'warn', 'subsample': 1.0, 'subsample_for_bin': 200000, 'subsample_freq': 0 |
| Gradient Boosting Classifier | ccp_alpha': 0.0, 'criterion': 'friedman_mse', 'init': None, 'learning_rate': 0.1, 'loss': 'deviance', 'max_depth': 3, 'max_features': None, 'max_leaf_nodes': None, 'min_impurity_decrease': 0.0, 'min_impurity_split': None, 'min_samples_leaf': 1, 'min_samples_split': 2, 'min_weight_fraction_leaf': 0.0, 'n_estimators': 100, 'n_iter_no_change': None, 'presort': 'deprecated', 'random_state': 101, 'subsample': 1.0, 'tol': 0.0001, 'validation_fraction': 0.1, 'verbose': 0, 'warm_start': False |
| AdaBoost Classifier | 'algorithm': 'SAMME.R', 'base_estimator': None, 'learning_rate': 1.0, 'n_estimators': 50, 'random_state': 101 |
| Decision Tree Classifier | 'ccp_alpha': 0.0, 'class_weight': None, 'criterion': 'gini', 'max_depth': None, 'max_features': None, 'max_leaf_nodes': None, 'min_impurity_decrease': 0.0, 'min_impurity_split': None, 'min_samples_leaf': 1, 'min_samples_split': 2, 'min_weight_fraction_leaf': 0.0, 'presort': 'deprecated', 'random_state': 101, 'splitter': 'best' |
| Logistic Regression | 'C': 1.0, 'class_weight': None, 'dual': False, 'fit_intercept': True, 'intercept_scaling': 1, 'l1_ratio': None, 'max_iter': 1000, 'multi_class': 'auto', 'n_jobs': None, 'penalty': 'l2', 'random_state': 101, 'solver': 'lbfgs', 'tol': 0.0001, 'verbose': 0, 'warm_start': False |
| Quadratic Discriminant Analysis (QDA) | 'priors': None, 'reg_param': 0.0, 'store_covariance': False, 'tol': 0.0001 |
| Linear Discriminant Analysis (LDA) | 'n_components': None, 'priors': None, 'shrinkage': None, 'solver': 'svd', 'store_covariance': False, 'tol': 0.0001 |
| Ridge Classifier | 'alpha': 1.0, 'class_weight': None, 'copy_X': True, 'fit_intercept': True, 'max_iter': None, 'normalize': False, 'random_state': 101, 'solver': 'auto', 'tol': 0.001 |
| K-Neighbors Classifier (KNN) | 'algorithm': 'auto', 'leaf_size': 30, 'metric': 'minkowski', 'metric_params': None, 'n_jobs': -1, 'n_neighbors': 5, 'p': 2, 'weights': 'uniform' |
| SVM – Linear Kernel | 'alpha': 0.0001, 'average': False, 'class_weight': None, 'early_stopping': False, 'epsilon': 0.1, 'eta0': 0.001, 'fit_intercept': True, 'l1_ratio': 0.15, 'learning_rate': 'optimal', 'loss': 'hinge', 'max_iter': 1000, 'n_iter_no_change': 5, 'n_jobs': -1, 'penalty': 'l2', 'power_t': 0.5, 'random_state': 101, 'shuffle': True, 'tol': 0.001, 'validation_fraction': 0.1, 'verbose': 0, 'warm_start': False |
| Naive Bayes (GaussianNB) | 'priors': None, 'var_smoothing': 1e-09 |
| Dummy Classifier | 'constant': None, 'random_state': 101, 'strategy': 'prior' |

**Supplementary Table 3. Statistical summary of the KL divergences for the top 20 features identified by the XGB model comparing CT and PD (A5) groups.** For each group, the KL divergence of each feature relative to its baseline value (0 wk) was computed across the experimental duration (0–10 wk). Each group consisted of 6 sampling sets, each containing 150 randomly selected clips. A two-way ANOVA (group × week) was performed for each feature, followed by weekly t-tests between groups (CT vs. A5). The resulting p-values from the weekly t-tests were corrected for multiple comparisons using the Bonferroni method. Source data are provided in the Source Data file (See S_Figure 16).

| Rank | Feature name | group | Week | n | Mean | SEM | raw_p | corrected_p | significant | ANOVA_p_Week | ANOVA_p_Group | ANOVA_p_Interaction |
|---|---|---|---|---|---|---|---|---|---|---|---|---|
| 1 | Hands 3D distance_mean | A5 | 0 | 6 | 0 | 0 | | 1 | ns | 3.70E-06 | 1.47E-05 | 0.001887869 |
| 1 | Hands 3D distance_mean | CT | 0 | 6 | 0 | 0 | | 1 | ns | 3.70E-06 | 1.47E-05 | 0.001887869 |
| 1 | Hands 3D distance_mean | A5 | 2 | 6 | 0.06326374 | 0.01014952 | 0.34822232 | 1 | ns | 3.70E-06 | 1.47E-05 | 0.001887869 |
| 1 | Hands 3D distance_mean | CT | 2 | 6 | 0.0467916 | 0.01330755 | 0.34822232 | 1 | ns | 3.70E-06 | 1.47E-05 | 0.001887869 |
| 1 | Hands 3D distance_mean | A5 | 4 | 6 | 0.0559817 | 0.0093035 | 0.89139966 | 1 | ns | 3.70E-06 | 1.47E-05 | 0.001887869 |
| 1 | Hands 3D distance_mean | CT | 4 | 6 | 0.05325403 | 0.01711037 | 0.89139966 | 1 | ns | 3.70E-06 | 1.47E-05 | 0.001887869 |
| 1 | Hands 3D distance_mean | A5 | 6 | 6 | 0.10657 | 0.02795522 | 0.02396557 | 0.14379344 | ns | 3.70E-06 | 1.47E-05 | 0.001887869 |
| 1 | Hands 3D distance_mean | CT | 6 | 6 | 0.02967787 | 0.00742458 | 0.02396557 | 0.14379344 | ns | 3.70E-06 | 1.47E-05 | 0.001887869 |
| 1 | Hands 3D distance_mean | A5 | 8 | 6 | 0.12496121 | 0.03171454 | 0.11088119 | 0.66528714 | ns | 3.70E-06 | 1.47E-05 | 0.001887869 |
| 1 | Hands 3D distance_mean | CT | 8 | 6 | 0.06820251 | 0.0068897 | 0.11088119 | 0.66528714 | ns | 3.70E-06 | 1.47E-05 | 0.001887869 |
| 1 | Hands 3D distance_mean | A5 | 10 | 6 | 0.1631368 | 0.03157142 | 0.00250439 | 0.01502632 | * | 3.70E-06 | 1.47E-05 | 0.001887869 |
| 1 | Hands 3D distance_mean | CT | 10 | 6 | 0.03208499 | 0.00864933 | 0.00250439 | 0.01502632 | * | 3.70E-06 | 1.47E-05 | 0.001887869 |
| 2 | Motion duration_episode | A5 | 0 | 6 | 0 | 0 | | 1 | ns | 2.12E-11 | 0.004076711 | 0.011551432 |
| 2 | Motion duration_episode | CT | 0 | 6 | 0 | 0 | | 1 | ns | 2.12E-11 | 0.004076711 | 0.011551432 |
| 2 | Motion duration_episode | A5 | 2 | 6 | 0.07111439 | 0.01795587 | 0.58579887 | 1 | ns | 2.12E-11 | 0.004076711 | 0.011551432 |
| 2 | Motion duration_episode | CT | 2 | 6 | 0.05821458 | 0.01422924 | 0.58579887 | 1 | ns | 2.12E-11 | 0.004076711 | 0.011551432 |
| 2 | Motion duration_episode | A5 | 4 | 6 | 0.12304998 | 0.01010413 | 0.42818587 | 1 | ns | 2.12E-11 | 0.004076711 | 0.011551432 |
| 2 | Motion duration_episode | CT | 4 | 6 | 0.17242783 | 0.05893497 | 0.42818587 | 1 | ns | 2.12E-11 | 0.004076711 | 0.011551432 |
| 2 | Motion duration_episode | A5 | 6 | 6 | 0.20369362 | 0.03261895 | 0.02274363 | 0.1364618 | ns | 2.12E-11 | 0.004076711 | 0.011551432 |
| 2 | Motion duration_episode | CT | 6 | 6 | 0.08710899 | 0.02856457 | 0.02274363 | 0.1364618 | ns | 2.12E-11 | 0.004076711 | 0.011551432 |
| 2 | Motion duration_episode | A5 | 8 | 6 | 0.1764069 | 0.01268369 | 0.00086766 | 0.00520593 | ** | 2.12E-11 | 0.004076711 | 0.011551432 |
| 2 | Motion duration_episode | CT | 8 | 6 | 0.08971392 | 0.01350124 | 0.00086766 | 0.00520593 | ** | 2.12E-11 | 0.004076711 | 0.011551432 |
| 2 | Motion duration_episode | A5 | 10 | 6 | 0.29149972 | 0.02340172 | 0.03876793 | 0.23260761 | ns | 2.12E-11 | 0.004076711 | 0.011551432 |
| 2 | Motion duration_episode | CT | 10 | 6 | 0.18678527 | 0.03730938 | 0.03876793 | 0.23260761 | ns | 2.12E-11 | 0.004076711 | 0.011551432 |
| 3 | Body 2D length_min | A5 | 0 | 6 | 0 | 0 | | 1 | ns | 4.48E-14 | 6.64E-18 | 2.68E-12 |
| 3 | Body 2D length_min | CT | 0 | 6 | 0 | 0 | | 1 | ns | 4.48E-14 | 6.64E-18 | 2.68E-12 |
| 3 | Body 2D length_min | A5 | 2 | 6 | 0.06409272 | 0.01500922 | 0.03932401 | 0.23594406 | ns | 4.48E-14 | 6.64E-18 | 2.68E-12 |
| 3 | Body 2D length_min | CT | 2 | 6 | 0.02358804 | 0.00818433 | 0.03932401 | 0.23594406 | ns | 4.48E-14 | 6.64E-18 | 2.68E-12 |
| 3 | Body 2D length_min | A5 | 4 | 6 | 0.14214055 | 0.01264605 | 6.05E-06 | 3.63E-05 | **** | 4.48E-14 | 6.64E-18 | 2.68E-12 |
| 3 | Body 2D length_min | CT | 4 | 6 | 0.02429108 | 0.00516854 | 6.05E-06 | 3.63E-05 | **** | 4.48E-14 | 6.64E-18 | 2.68E-12 |
| 3 | Body 2D length_min | A5 | 6 | 6 | 0.62480182 | 0.04535404 | 2.21E-07 | 1.33E-06 | **** | 4.48E-14 | 6.64E-18 | 2.68E-12 |
| 3 | Body 2D length_min | CT | 6 | 6 | 0.04946249 | 0.01046577 | 2.21E-07 | 1.33E-06 | **** | 4.48E-14 | 6.64E-18 | 2.68E-12 |
| 3 | Body 2D length_min | A5 | 8 | 6 | 0.59102622 | 0.11906223 | 0.00085374 | 0.00512247 | ** | 4.48E-14 | 6.64E-18 | 2.68E-12 |
| 3 | Body 2D length_min | CT | 8 | 6 | 0.03124369 | 0.00818214 | 0.00085374 | 0.00512247 | ** | 4.48E-14 | 6.64E-18 | 2.68E-12 |
| 3 | Body 2D length_min | A5 | 10 | 6 | 0.41894261 | 0.04233956 | 5.03E-06 | 3.02E-05 | **** | 4.48E-14 | 6.64E-18 | 2.68E-12 |
| 3 | Body 2D length_min | CT | 10 | 6 | 0.04253695 | 0.00583053 | 5.03E-06 | 3.02E-05 | **** | 4.48E-14 | 6.64E-18 | 2.68E-12 |
| 4 | Tail angle_mean | A5 | 0 | 6 | 0 | 0 | | 1 | ns | 4.66E-19 | 1.35E-19 | 3.23E-15 |
| 4 | Tail angle_mean | CT | 0 | 6 | 0 | 0 | | 1 | ns | 4.66E-19 | 1.35E-19 | 3.23E-15 |
| 4 | Tail angle_mean | A5 | 2 | 6 | 0.04282326 | 0.00789761 | 0.09239186 | 0.55435114 | ns | 4.66E-19 | 1.35E-19 | 3.23E-15 |
| 4 | Tail angle_mean | CT | 2 | 6 | 0.02446527 | 0.00591249 | 0.09239186 | 0.55435114 | ns | 4.66E-19 | 1.35E-19 | 3.23E-15 |
| 4 | Tail angle_mean | A5 | 4 | 6 | 0.0626721 | 0.01716293 | 0.1694277 | 1 | ns | 4.66E-19 | 1.35E-19 | 3.23E-15 |
| 4 | Tail angle_mean | CT | 4 | 6 | 0.03505663 | 0.0072906 | 0.1694277 | 1 | ns | 4.66E-19 | 1.35E-19 | 3.23E-15 |
| 4 | Tail angle_mean | A5 | 6 | 6 | 0.15211919 | 0.01546048 | 1.15E-05 | 6.91E-05 | **** | 4.66E-19 | 1.35E-19 | 3.23E-15 |
| 4 | Tail angle_mean | CT | 6 | 6 | 0.02763181 | 0.00138379 | 1.15E-05 | 6.91E-05 | **** | 4.66E-19 | 1.35E-19 | 3.23E-15 |
| 4 | Tail angle_mean | A5 | 8 | 6 | 0.26063073 | 0.0281452 | 3.90E-05 | 0.00023411 | *** | 4.66E-19 | 1.35E-19 | 3.23E-15 |
| 4 | Tail angle_mean | CT | 8 | 6 | 0.04007553 | 0.01456618 | 3.90E-05 | 0.00023411 | *** | 4.66E-19 | 1.35E-19 | 3.23E-15 |
| 4 | Tail angle_mean | A5 | 10 | 6 | 0.28013069 | 0.02141627 | 1.28E-06 | 7.67E-06 | **** | 4.66E-19 | 1.35E-19 | 3.23E-15 |
| 4 | Tail angle_mean | CT | 10 | 6 | 0.04024065 | 0.00949229 | 1.28E-06 | 7.67E-06 | **** | 4.66E-19 | 1.35E-19 | 3.23E-15 |
| 5 | Arm angle asym_std | A5 | 0 | 6 | 0 | 0 | | 1 | ns | 6.54E-19 | 3.24E-22 | 8.43E-20 |
| 5 | Arm angle asym_std | CT | 0 | 6 | 0 | 0 | | 1 | ns | 6.54E-19 | 3.24E-22 | 8.43E-20 |
| 5 | Arm angle asym_std | A5 | 2 | 6 | 0.05208557 | 0.00708974 | 0.38325495 | 1 | ns | 6.54E-19 | 3.24E-22 | 8.43E-20 |
| 5 | Arm angle asym_std | CT | 2 | 6 | 0.07087614 | 0.01934677 | 0.38325495 | 1 | ns | 6.54E-19 | 3.24E-22 | 8.43E-20 |
| 5 | Arm angle asym_std | A5 | 4 | 6 | 0.07478935 | 0.01584264 | 0.36289443 | 1 | ns | 6.54E-19 | 3.24E-22 | 8.43E-20 |
| 5 | Arm angle asym_std | CT | 4 | 6 | 0.05337683 | 0.01592131 | 0.36289443 | 1 | ns | 6.54E-19 | 3.24E-22 | 8.43E-20 |
| 5 | Arm angle asym_std | A5 | 6 | 6 | 0.29072932 | 0.02294471 | 3.95E-07 | 2.37E-06 | **** | 6.54E-19 | 3.24E-22 | 8.43E-20 |
| 5 | Arm angle asym_std | CT | 6 | 6 | 0.02104382 | 0.00347032 | 3.95E-07 | 2.37E-06 | **** | 6.54E-19 | 3.24E-22 | 8.43E-20 |
| 5 | Arm angle asym_std | A5 | 8 | 6 | 0.23458031 | 0.0127636 | 2.58E-06 | 1.55E-05 | **** | 6.54E-19 | 3.24E-22 | 8.43E-20 |
| 5 | Arm angle asym_std | CT | 8 | 6 | 0.05331553 | 0.01422925 | 2.58E-06 | 1.55E-05 | **** | 6.54E-19 | 3.24E-22 | 8.43E-20 |
| 5 | Arm angle asym_std | A5 | 10 | 6 | 0.28006733 | 0.01811415 | 9.58E-08 | 5.75E-07 | **** | 6.54E-19 | 3.24E-22 | 8.43E-20 |
| 5 | Arm angle asym_std | CT | 10 | 6 | 0.02166987 | 0.00618071 | 9.58E-08 | 5.75E-07 | **** | 6.54E-19 | 3.24E-22 | 8.43E-20 |
| 6 | Motion interval_episode | A5 | 0 | 6 | 0 | 0 | | 1 | ns | 1.28E-05 | 0.163170352 | 0.004161448 |
| 6 | Motion interval_episode | CT | 0 | 6 | 0 | 0 | | 1 | ns | 1.28E-05 | 0.163170352 | 0.004161448 |
| 6 | Motion interval_episode | A5 | 2 | 6 | 0.08445343 | 0.02221478 | 0.81834867 | 1 | ns | 1.28E-05 | 0.163170352 | 0.004161448 |
| 6 | Motion interval_episode | CT | 2 | 6 | 0.0785088 | 0.01191991 | 0.81834867 | 1 | ns | 1.28E-05 | 0.163170352 | 0.004161448 |
| 6 | Motion interval_episode | A5 | 4 | 6 | 0.18331525 | 0.04861667 | 0.10432924 | 0.62597546 | ns | 1.28E-05 | 0.163170352 | 0.004161448 |
| 6 | Motion interval_episode | CT | 4 | 6 | 0.08752678 | 0.02261625 | 0.10432924 | 0.62597546 | ns | 1.28E-05 | 0.163170352 | 0.004161448 |
| 6 | Motion interval_episode | A5 | 6 | 6 | 0.08466906 | 0.01909086 | 0.00040122 | 0.00240734 | ** | 1.28E-05 | 0.163170352 | 0.004161448 |
| 6 | Motion interval_episode | CT | 6 | 6 | 0.36514645 | 0.05044505 | 0.00040122 | 0.00240734 | ** | 1.28E-05 | 0.163170352 | 0.004161448 |
| 6 | Motion interval_episode | A5 | 8 | 6 | 0.08427983 | 0.02323727 | 0.23443366 | 1 | ns | 1.28E-05 | 0.163170352 | 0.004161448 |
| 6 | Motion interval_episode | CT | 8 | 6 | 0.13145645 | 0.02915619 | 0.23443366 | 1 | ns | 1.28E-05 | 0.163170352 | 0.004161448 |
| 6 | Motion interval_episode | A5 | 10 | 6 | 0.23841472 | 0.13105982 | 0.9924736 | 1 | ns | 1.28E-05 | 0.163170352 | 0.004161448 |
| 6 | Motion interval_episode | CT | 10 | 6 | 0.23713502 | 0.01819803 | 0.9924736 | 1 | ns | 1.28E-05 | 0.163170352 | 0.004161448 |
| 7 | Body angle_min | A5 | 0 | 6 | 0 | 0 | | 1 | ns | 0.000190308 | 3.80E-07 | 0.010806696 |
| 7 | Body angle_min | CT | 0 | 6 | 0 | 0 | | 1 | ns | 0.000190308 | 3.80E-07 | 0.010806696 |
| 7 | Body angle_min | A5 | 2 | 6 | 0.06000111 | 0.02059593 | 0.2758596 | 1 | ns | 0.000190308 | 3.80E-07 | 0.010806696 |
| 7 | Body angle_min | CT | 2 | 6 | 0.03426522 | 0.00862098 | 0.2758596 | 1 | ns | 0.000190308 | 3.80E-07 | 0.010806696 |
| 7 | Body angle_min | A5 | 4 | 6 | 0.05134669 | 0.01501236 | 0.0506779 | 0.3040674 | ns | 0.000190308 | 3.80E-07 | 0.010806696 |
| 7 | Body angle_min | CT | 4 | 6 | 0.01739716 | 0.00290707 | 0.0506779 | 0.3040674 | ns | 0.000190308 | 3.80E-07 | 0.010806696 |
| 7 | Body angle_min | A5 | 6 | 6 | 0.13442126 | 0.02768538 | 0.00277436 | 0.01664614 | * | 0.000190308 | 3.80E-07 | 0.010806696 |
| 7 | Body angle_min | CT | 6 | 6 | 0.02308279 | 0.00565822 | 0.00277436 | 0.01664614 | * | 0.000190308 | 3.80E-07 | 0.010806696 |
| 7 | Body angle_min | A5 | 8 | 6 | 0.13380843 | 0.04071754 | 0.01891012 | 0.11346075 | ns | 0.000190308 | 3.80E-07 | 0.010806696 |
| 7 | Body angle_min | CT | 8 | 6 | 0.01962039 | 0.00307588 | 0.01891012 | 0.11346075 | ns | 0.000190308 | 3.80E-07 | 0.010806696 |
| 7 | Body angle_min | A5 | 10 | 6 | 0.13454111 | 0.03367772 | 0.02218709 | 0.13312252 | ns | 0.000190308 | 3.80E-07 | 0.010806696 |
| 7 | Body angle_min | CT | 10 | 6 | 0.03655812 | 0.01339983 | 0.02218709 | 0.13312252 | ns | 0.000190308 | 3.80E-07 | 0.010806696 |
| 8 | Feet 2D distance_max | A5 | 0 | 6 | 0 | 0 | | 1 | ns | 1.48E-10 | 8.96E-16 | 1.72E-06 |
| 8 | Feet 2D distance_max | CT | 0 | 6 | 0 | 0 | | 1 | ns | 1.48E-10 | 8.96E-16 | 1.72E-06 |
| 8 | Feet 2D distance_max | A5 | 2 | 6 | 0.2644145 | 0.04157157 | 0.00067538 | 0.00405227 | ** | 1.48E-10 | 8.96E-16 | 1.72E-06 |
| 8 | Feet 2D distance_max | CT | 2 | 6 | 0.05402271 | 0.01251777 | 0.00067538 | 0.00405227 | ** | 1.48E-10 | 8.96E-16 | 1.72E-06 |
| 8 | Feet 2D distance_max | A5 | 4 | 6 | 0.16415819 | 0.02923678 | 0.00132575 | 0.00795447 | ** | 1.48E-10 | 8.96E-16 | 1.72E-06 |
| 8 | Feet 2D distance_max | CT | 4 | 6 | 0.0902789 | 0.01400128 | 0.00132575 | 0.00795447 | ** | 1.48E-10 | 8.96E-16 | 1.72E-06 |
| 8 | Feet 2D distance_max | A5 | 6 | 6 | 0.25957569 | 0.03346563 | 0.00012179 | 0.00073074 | *** | 1.48E-10 | 8.96E-16 | 1.72E-06 |
| 8 | Feet 2D distance_max | CT | 6 | 6 | 0.04521612 | 0.01143702 | 0.00012179 | 0.00073074 | *** | 1.48E-10 | 8.96E-16 | 1.72E-06 |
| 8 | Feet 2D distance_max | A5 | 8 | 6 | 0.17904429 | 0.02008271 | 0.01966929 | 0.11801574 | ns | 1.48E-10 | 8.96E-16 | 1.72E-06 |
| 8 | Feet 2D distance_max | CT | 8 | 6 | 0.09045323 | 0.02483918 | 0.01966929 | 0.11801574 | ns | 1.48E-10 | 8.96E-16 | 1.72E-06 |
| 8 | Feet 2D distance_max | A5 | 10 | 6 | 0.19775405 | 0.01728937 | 4.13E-06 | 2.48E-05 | **** | 1.48E-10 | 8.96E-16 | 1.72E-06 |
| 8 | Feet 2D distance_max | CT | 10 | 6 | 0.03676453 | 0.00456398 | 4.13E-06 | 2.48E-05 | **** | 1.48E-10 | 8.96E-16 | 1.72E-06 |
| 9 | Neck 3D velocity_std | A5 | 0 | 6 | 0 | 0 | | 1 | ns | 5.95E-14 | 3.17E-14 | 1.58E-08 |
| 9 | Neck 3D velocity_std | CT | 0 | 6 | 0 | 0 | | 1 | ns | 5.95E-14 | 3.17E-14 | 1.58E-08 |
| 9 | Neck 3D velocity_std | A5 | 2 | 6 | 0.06875228 | 0.01015042 | 0.01601466 | 0.09608796 | ns | 5.95E-14 | 3.17E-14 | 1.58E-08 |
| 9 | Neck 3D velocity_std | CT | 2 | 6 | 0.0341245 | 0.00634052 | 0.01601466 | 0.09608796 | ns | 5.95E-14 | 3.17E-14 | 1.58E-08 |
| 9 | Neck 3D velocity_std | A5 | 4 | 6 | 0.04656228 | 0.010095 | 0.20657647 | 1 | ns | 5.95E-14 | 3.17E-14 | 1.58E-08 |
| 9 | Neck 3D velocity_std | CT | 4 | 6 | 0.03024082 | 0.00664203 | 0.20657647 | 1 | ns | 5.95E-14 | 3.17E-14 | 1.58E-08 |
| 9 | Neck 3D velocity_std | A5 | 6 | 6 | 0.16645244 | 0.01251136 | 1.16E-05 | 6.98E-05 | **** | 5.95E-14 | 3.17E-14 | 1.58E-08 |
| 9 | Neck 3D velocity_std | CT | 6 | 6 | 0.04077018 | 0.00946668 | 1.16E-05 | 6.98E-05 | **** | 5.95E-14 | 3.17E-14 | 1.58E-08 |
| 9 | Neck 3D velocity_std | A5 | 8 | 6 | 0.11927038 | 0.01380192 | 4.31E-05 | 0.00025877 | *** | 5.95E-14 | 3.17E-14 | 1.58E-08 |
| 9 | Neck 3D velocity_std | CT | 8 | 6 | 0.02264524 | 0.00262936 | 4.31E-05 | 0.00025877 | *** | 5.95E-14 | 3.17E-14 | 1.58E-08 |
| 9 | Neck 3D velocity_std | A5 | 10 | 6 | 0.08531186 | 0.01671612 | 0.01846582 | 0.11079492 | ns | 5.95E-14 | 3.17E-14 | 1.58E-08 |
| 9 | Neck 3D velocity_std | CT | 10 | 6 | 0.0325462 | 0.00855018 | 0.01846582 | 0.11079492 | ns | 5.95E-14 | 3.17E-14 | 1.58E-08 |
| 10 | Feet 2D distance_std | A5 | 0 | 6 | 0 | 0 | | 1 | ns | 6.59E-12 | 1.10E-17 | 6.88E-13 |
| 10 | Feet 2D distance_std | CT | 0 | 6 | 0 | 0 | | 1 | ns | 6.59E-12 | 1.10E-17 | 6.88E-13 |
| 10 | Feet 2D distance_std | A5 | 2 | 6 | 0.0827779 | 0.02263045 | 0.82861064 | 1 | ns | 6.59E-12 | 1.10E-17 | 6.88E-13 |
| 10 | Feet 2D distance_std | CT | 2 | 6 | 0.07531385 | 0.02481912 | 0.82861064 | 1 | ns | 6.59E-12 | 1.10E-17 | 6.88E-13 |
| 10 | Feet 2D distance_std | A5 | 4 | 6 | 0.11034303 | 0.01777957 | 0.08564207 | 0.51385244 | ns | 6.59E-12 | 1.10E-17 | 6.88E-13 |
| 10 | Feet 2D distance_std | CT | 4 | 6 | 0.05549901 | 0.02260691 | 0.08564207 | 0.51385244 | ns | 6.59E-12 | 1.10E-17 | 6.88E-13 |
| 10 | Feet 2D distance_std | A5 | 6 | 6 | 0.34307724 | 0.03775398 | 7.62E-06 | 4.57E-05 | **** | 6.59E-12 | 1.10E-17 | 6.88E-13 |
| 10 | Feet 2D distance_std | CT | 6 | 6 | 0.02368241 | 0.00431611 | 7.62E-06 | 4.57E-05 | **** | 6.59E-12 | 1.10E-17 | 6.88E-13 |
| 10 | Feet 2D distance_std | A5 | 8 | 6 | 0.29224545 | 0.04431305 | 0.00013264 | 0.00079587 | *** | 6.59E-12 | 1.10E-17 | 6.88E-13 |
| 10 | Feet 2D distance_std | CT | 8 | 6 | 0.02603619 | 0.00262397 | 0.00013264 | 0.00079587 | *** | 6.59E-12 | 1.10E-17 | 6.88E-13 |
| 10 | Feet 2D distance_std | A5 | 10 | 6 | 0.37314355 | 0.03787602 | 3.55E-06 | 2.13E-05 | **** | 6.59E-12 | 1.10E-17 | 6.88E-13 |
| 10 | Feet 2D distance_std | CT | 10 | 6 | 0.02511744 | 0.00325392 | 3.55E-06 | 2.13E-05 | **** | 6.59E-12 | 1.10E-17 | 6.88E-13 |

| Rank | Feature name | group | Week | n | Mean | SEM | raw_p | corrected_p | significant | ANOVA_p_Week | ANOVA_p_Group | ANOVA_p_Interaction |
|---|---|---|---|---|---|---|---|---|---|---|---|---|
| 11 | Chest 3D velocity_mean | A5 | 0 | 6 | 0 | 0 | | 1 | ns | 6.58E-12 | 5.17E-18 | 1.06E-08 |
| 11 | Chest 3D velocity_mean | CT | 0 | 6 | 0 | 0 | | 1 | ns | 6.58E-12 | 5.17E-18 | 1.06E-08 |
| 11 | Chest 3D velocity_mean | A5 | 2 | 6 | 0.01533779 | 0.01507015 | 0.01594906 | 0.09569436 | ns | 6.58E-12 | 5.17E-18 | 1.06E-08 |
| 11 | Chest 3D velocity_mean | CT | 2 | 6 | 0.02896287 | 0.00541882 | 0.01594906 | 0.09569436 | ns | 6.58E-12 | 5.17E-18 | 1.06E-08 |
| 11 | Chest 3D velocity_mean | A5 | 4 | 6 | 0.10392427 | 0.01597309 | 0.00074429 | 0.00446577 | ** | 6.58E-12 | 5.17E-18 | 1.06E-08 |
| 11 | Chest 3D velocity_mean | CT | 4 | 6 | 0.02360413 | 0.00520217 | 0.00074429 | 0.00446577 | ** | 6.58E-12 | 5.17E-18 | 1.06E-08 |
| 11 | Chest 3D velocity_mean | A5 | 6 | 6 | 0.09390074 | 0.0149346 | 0.00041498 | 0.00248986 | ** | 6.58E-12 | 5.17E-18 | 1.06E-08 |
| 11 | Chest 3D velocity_mean | CT | 6 | 6 | 0.01377535 | 0.00406404 | 0.00041498 | 0.00248986 | ** | 6.58E-12 | 5.17E-18 | 1.06E-08 |
| 11 | Chest 3D velocity_mean | A5 | 8 | 6 | 0.15001469 | 0.01582964 | 4.55E-05 | 0.00027324 | *** | 6.58E-12 | 5.17E-18 | 1.06E-08 |
| 11 | Chest 3D velocity_mean | CT | 8 | 6 | 0.02898825 | 0.00794776 | 4.55E-05 | 0.00027324 | *** | 6.58E-12 | 5.17E-18 | 1.06E-08 |
| 11 | Chest 3D velocity_mean | A5 | 10 | 6 | 0.20136695 | 0.02414726 | 2.81E-05 | 0.00016876 | *** | 6.58E-12 | 5.17E-18 | 1.06E-08 |
| 11 | Chest 3D velocity_mean | CT | 10 | 6 | 0.02304223 | 0.00496618 | 2.81E-05 | 0.00016876 | *** | 6.58E-12 | 5.17E-18 | 1.06E-08 |
| 12 | U-body 3D length_min | A5 | 0 | 6 | 0 | 0 | | 1 | ns | 1.09E-11 | 1.00E-10 | 3.07E-08 |
| 12 | U-body 3D length_min | CT | 0 | 6 | 0 | 0 | | 1 | ns | 1.09E-11 | 1.00E-10 | 3.07E-08 |
| 12 | U-body 3D length_min | A5 | 2 | 6 | 0.03328983 | 0.01025936 | 0.82321345 | 1 | ns | 1.09E-11 | 1.00E-10 | 3.07E-08 |
| 12 | U-body 3D length_min | CT | 2 | 6 | 0.03644877 | 0.00918908 | 0.82321345 | 1 | ns | 1.09E-11 | 1.00E-10 | 3.07E-08 |
| 12 | U-body 3D length_min | A5 | 4 | 6 | 0.05008596 | 0.00738428 | 0.04874433 | 0.29246596 | ns | 1.09E-11 | 1.00E-10 | 3.07E-08 |
| 12 | U-body 3D length_min | CT | 4 | 6 | 0.03067043 | 0.00451562 | 0.04874433 | 0.29246596 | ns | 1.09E-11 | 1.00E-10 | 3.07E-08 |
| 12 | U-body 3D length_min | A5 | 6 | 6 | 0.29517801 | 0.03083891 | 1.68E-05 | 0.0001007 | *** | 1.09E-11 | 1.00E-10 | 3.07E-08 |
| 12 | U-body 3D length_min | CT | 6 | 6 | 0.04707094 | 0.00960665 | 1.68E-05 | 0.0001007 | *** | 1.09E-11 | 1.00E-10 | 3.07E-08 |
| 12 | U-body 3D length_min | A5 | 8 | 6 | 0.17123544 | 0.03852456 | 0.00422542 | 0.02535254 | * | 1.09E-11 | 1.00E-10 | 3.07E-08 |
| 12 | U-body 3D length_min | CT | 8 | 6 | 0.02830379 | 0.00646862 | 0.00422542 | 0.02535254 | * | 1.09E-11 | 1.00E-10 | 3.07E-08 |
| 12 | U-body 3D length_min | A5 | 10 | 6 | 0.22214934 | 0.04594141 | 0.00849319 | 0.05095913 | ns | 1.09E-11 | 1.00E-10 | 3.07E-08 |
| 12 | U-body 3D length_min | CT | 10 | 6 | 0.05787398 | 0.02049267 | 0.00849319 | 0.05095913 | ns | 1.09E-11 | 1.00E-10 | 3.07E-08 |
| 13 | Right limb angle asym_min | A5 | 0 | 6 | 0 | 0 | | 1 | ns | 8.24E-11 | 2.72E-12 | 1.73E-09 |
| 13 | Right limb angle asym_min | CT | 0 | 6 | 0 | 0 | | 1 | ns | 8.24E-11 | 2.72E-12 | 1.73E-09 |
| 13 | Right limb angle asym_min | A5 | 2 | 6 | 0.05127703 | 0.01470565 | 0.71429505 | 1 | ns | 8.24E-11 | 2.72E-12 | 1.73E-09 |
| 13 | Right limb angle asym_min | CT | 2 | 6 | 0.0627374 | 0.02663646 | 0.71429505 | 1 | ns | 8.24E-11 | 2.72E-12 | 1.73E-09 |
| 13 | Right limb angle asym_min | A5 | 4 | 6 | 0.06450111 | 0.01148595 | 0.04586696 | 0.27520178 | ns | 8.24E-11 | 2.72E-12 | 1.73E-09 |
| 13 | Right limb angle asym_min | CT | 4 | 6 | 0.03246968 | 0.00810089 | 0.04586696 | 0.27520178 | ns | 8.24E-11 | 2.72E-12 | 1.73E-09 |
| 13 | Right limb angle asym_min | A5 | 6 | 6 | 0.21055329 | 0.03104624 | 0.00026615 | 0.00159691 | ** | 8.24E-11 | 2.72E-12 | 1.73E-09 |
| 13 | Right limb angle asym_min | CT | 6 | 6 | 0.03301829 | 0.00908556 | 0.00026615 | 0.00159691 | ** | 8.24E-11 | 2.72E-12 | 1.73E-09 |
| 13 | Right limb angle asym_min | A5 | 8 | 6 | 0.16977854 | 0.0301356 | 0.00445325 | 0.02671951 | * | 8.24E-11 | 2.72E-12 | 1.73E-09 |
| 13 | Right limb angle asym_min | CT | 8 | 6 | 0.05286347 | 0.01082474 | 0.00445325 | 0.02671951 | * | 8.24E-11 | 2.72E-12 | 1.73E-09 |
| 13 | Right limb angle asym_min | A5 | 10 | 6 | 0.24157123 | 0.02126199 | 1.75E-06 | 1.05E-05 | **** | 8.24E-11 | 2.72E-12 | 1.73E-09 |
| 13 | Right limb angle asym_min | CT | 10 | 6 | 0.02779852 | 0.0037893 | 1.75E-06 | 1.05E-05 | **** | 8.24E-11 | 2.72E-12 | 1.73E-09 |
| 14 | Hands 3D distance_max | A5 | 0 | 6 | 0 | 0 | | 1 | ns | 3.43E-11 | 3.74E-11 | 1.07E-10 |
| 14 | Hands 3D distance_max | CT | 0 | 6 | 0 | 0 | | 1 | ns | 3.43E-11 | 3.74E-11 | 1.07E-10 |
| 14 | Hands 3D distance_max | A5 | 2 | 6 | 0.04182894 | 0.00636427 | 0.0801269 | 0.48076139 | ns | 3.43E-11 | 3.74E-11 | 1.07E-10 |
| 14 | Hands 3D distance_max | CT | 2 | 6 | 0.07217149 | 0.01422425 | 0.0801269 | 0.48076139 | ns | 3.43E-11 | 3.74E-11 | 1.07E-10 |
| 14 | Hands 3D distance_max | A5 | 4 | 6 | 0.07195629 | 0.01003378 | 0.4422395 | 1 | ns | 3.43E-11 | 3.74E-11 | 1.07E-10 |
| 14 | Hands 3D distance_max | CT | 4 | 6 | 0.05895477 | 0.01278182 | 0.4422395 | 1 | ns | 3.43E-11 | 3.74E-11 | 1.07E-10 |
| 14 | Hands 3D distance_max | A5 | 6 | 6 | 0.19562954 | 0.03237317 | 0.00049446 | 0.00296678 | ** | 3.43E-11 | 3.74E-11 | 1.07E-10 |
| 14 | Hands 3D distance_max | CT | 6 | 6 | 0.02931727 | 0.00580981 | 0.00049446 | 0.00296678 | ** | 3.43E-11 | 3.74E-11 | 1.07E-10 |
| 14 | Hands 3D distance_max | A5 | 8 | 6 | 0.17968456 | 0.02903418 | 0.00425971 | 0.02555824 | * | 3.43E-11 | 3.74E-11 | 1.07E-10 |
| 14 | Hands 3D distance_max | CT | 8 | 6 | 0.06117207 | 0.01397195 | 0.00425971 | 0.02555824 | * | 3.43E-11 | 3.74E-11 | 1.07E-10 |
| 14 | Hands 3D distance_max | A5 | 10 | 6 | 0.28237674 | 0.03700409 | 6.76E-05 | 0.00040571 | *** | 3.43E-11 | 3.74E-11 | 1.07E-10 |
| 14 | Hands 3D distance_max | CT | 10 | 6 | 0.03579513 | 0.00793728 | 6.76E-05 | 0.00040571 | *** | 3.43E-11 | 3.74E-11 | 1.07E-10 |
| 15 | Left limb angle asym_min | A5 | 0 | 6 | 0 | 0 | | 1 | ns | 2.10E-16 | 2.63E-18 | 4.69E-14 |
| 15 | Left limb angle asym_min | CT | 0 | 6 | 0 | 0 | | 1 | ns | 2.10E-16 | 2.63E-18 | 4.69E-14 |
| 15 | Left limb angle asym_min | A5 | 2 | 6 | 0.05611124 | 0.00880741 | 0.54556278 | 1 | ns | 2.10E-16 | 2.63E-18 | 4.69E-14 |
| 15 | Left limb angle asym_min | CT | 2 | 6 | 0.07426418 | 0.02764587 | 0.54556278 | 1 | ns | 2.10E-16 | 2.63E-18 | 4.69E-14 |
| 15 | Left limb angle asym_min | A5 | 4 | 6 | 0.11122671 | 0.00824466 | 0.0065996 | 0.03959762 | * | 2.10E-16 | 2.63E-18 | 4.69E-14 |
| 15 | Left limb angle asym_min | CT | 4 | 6 | 0.0502991 | 0.01582031 | 0.0065996 | 0.03959762 | * | 2.10E-16 | 2.63E-18 | 4.69E-14 |
| 15 | Left limb angle asym_min | A5 | 6 | 6 | 0.27698244 | 0.02435668 | 7.70E-06 | 4.62E-05 | **** | 2.10E-16 | 2.63E-18 | 4.69E-14 |
| 15 | Left limb angle asym_min | CT | 6 | 6 | 0.04962139 | 0.01183968 | 7.70E-06 | 4.62E-05 | **** | 2.10E-16 | 2.63E-18 | 4.69E-14 |
| 15 | Left limb angle asym_min | A5 | 8 | 6 | 0.25317066 | 0.02311507 | 1.23E-05 | 7.36E-05 | **** | 2.10E-16 | 2.63E-18 | 4.69E-14 |
| 15 | Left limb angle asym_min | CT | 8 | 6 | 0.05165149 | 0.01030345 | 1.23E-05 | 7.36E-05 | **** | 2.10E-16 | 2.63E-18 | 4.69E-14 |
| 15 | Left limb angle asym_min | A5 | 10 | 6 | 0.32885166 | 0.02961174 | 7.22E-06 | 4.33E-05 | **** | 2.10E-16 | 2.63E-18 | 4.69E-14 |
| 15 | Left limb angle asym_min | CT | 10 | 6 | 0.05017235 | 0.01446786 | 7.22E-06 | 4.33E-05 | **** | 2.10E-16 | 2.63E-18 | 4.69E-14 |
| 16 | Chest 1D velocity_max | A5 | 0 | 6 | 0 | 0 | | 1 | ns | 1.59E-15 | 9.37E-20 | 5.08E-14 |
| 16 | Chest 1D velocity_max | CT | 0 | 6 | 0

**Supplementary Table 4. Statistical summary of the feature values for the top 20 features identified by the XGB model, comparing the CT and PD (A5) groups.** For each feature, the values at each week were divided by the group's corresponding baseline (0 wk) mean value, and the normalised data were analysed over the experimental duration (0–10 wk). Each group consisted of 6 sampling sets, each containing 150 randomly selected clips. Two-way ANOVA (group × week) was performed for each feature on the normalised data, followed by weekly t-tests comparing the CT and A5 groups. P-values from weekly t-tests were corrected for multiple comparisons using the Bonferroni method. Source data are provided in the Source Data file (See S_Figure 17).

| Rank | Feature name | Week | group | n | Mean | SEM | raw_p | corrected_p | significant | ANOVA_p_Week | ANOVA_p_Group | ANOVA_p_Interaction |
|---|---|---|---|---|---|---|---|---|---|---|---|---|
| 1 | Hands 3D distance_mean | 0 | CT | 1766 | 1 | 0.00624222 | 1 | 1 | ns | 1.00E+00 | 1.00E+00 | 0.715666923 |
| 1 | Hands 3D distance_mean | 2 | CT | 1485 | 0.9597192 | 0.00627342 | 0.01207393 | 0.07244356 | ns | 1.00E+00 | 1.00E+00 | 0.715666923 |
| 1 | Hands 3D distance_mean | 4 | CT | 1173 | 0.96435594 | 0.00710173 | 0.33098172 | 1 | ns | 1.00E+00 | 1.00E+00 | 0.715666923 |
| 1 | Hands 3D distance_mean | 6 | CT | 1069 | 0.97191978 | 0.00778373 | 3.5459E-18 | 2.1275E-17 | **** | 1.00E+00 | 1.00E+00 | 0.715666923 |
| 1 | Hands 3D distance_mean | 8 | CT | 1056 | 0.91376941 | 0.0076422 | 5.3365E-22 | 3.2019E-21 | **** | 1.00E+00 | 1.00E+00 | 0.715666923 |
| 1 | Hands 3D distance_mean | 10 | CT | 1003 | 0.99652569 | 0.00823853 | 3.2893E-15 | 1.9736E-14 | **** | 1.00E+00 | 1.00E+00 | 0.715666923 |
| 1 | Hands 3D distance_mean | 0 | A5 | 2197 | 1 | 0.00769333 | 1 | 1 | ns | 1.00E+00 | 1.00E+00 | 0.715666923 |
| 1 | Hands 3D distance_mean | 2 | A5 | 2203 | 0.98595563 | 0.0074628 | 0.01207393 | 0.07244356 | ns | 1.00E+00 | 1.00E+00 | 0.715666923 |
| 1 | Hands 3D distance_mean | 4 | A5 | 1784 | 0.97718664 | 0.00962751 | 0.33098172 | 1 | ns | 1.00E+00 | 1.00E+00 | 0.715666923 |
| 1 | Hands 3D distance_mean | 6 | A5 | 2207 | 1.12362483 | 0.01147099 | 3.5459E-18 | 2.1275E-17 | **** | 1.00E+00 | 1.00E+00 | 0.715666923 |
| 1 | Hands 3D distance_mean | 8 | A5 | 2822 | 1.08641357 | 0.01050433 | 5.3365E-22 | 3.2019E-21 | **** | 1.00E+00 | 1.00E+00 | 0.715666923 |
| 1 | Hands 3D distance_mean | 10 | A5 | 2756 | 1.15921203 | 0.01203477 | 3.2893E-15 | 1.9736E-14 | **** | 1.00E+00 | 1.00E+00 | 0.715666923 |
| 2 | Motion duration_episode | 0 | CT | 1740 | 1 | 0.01440406 | 1 | 1 | ns | 1.00E+00 | 1 | 0.001190587 |
| 2 | Motion duration_episode | 2 | CT | 1469 | 1.01858632 | 0.01877639 | 0.00361896 | 0.02171373 | * | 1.00E+00 | 1 | 0.001190587 |
| 2 | Motion duration_episode | 4 | CT | 1178 | 0.86228792 | 0.01499087 | 1.5629E-36 | 9.3772E-36 | **** | 1.00E+00 | 1 | 0.001190587 |
| 2 | Motion duration_episode | 6 | CT | 1084 | 0.86079671 | 0.0154548 | 4.348E-23 | 2.6088E-22 | **** | 1.00E+00 | 1 | 0.001190587 |
| 2 | Motion duration_episode | 8 | CT | 1072 | 0.98943932 | 0.02322775 | 1.0772E-31 | 6.4635E-31 | **** | 1.00E+00 | 1 | 0.001190587 |
| 2 | Motion duration_episode | 10 | CT | 1028 | 0.79694783 | 0.01604723 | 7.1383E-34 | 4.283E-33 | **** | 1.00E+00 | 1 | 0.001190587 |
| 2 | Motion duration_episode | 0 | A5 | 2179 | 1 | 0.01731228 | 1 | 1 | ns | 1.00E+00 | 1 | 0.001190587 |
| 2 | Motion duration_episode | 2 | A5 | 2195 | 1.10730042 | 0.02152758 | 0.00361896 | 0.02171373 | * | 1.00E+00 | 1 | 0.001190587 |
| 2 | Motion duration_episode | 4 | A5 | 1795 | 1.33359301 | 0.02816807 | 1.5629E-36 | 9.3772E-36 | **** | 1.00E+00 | 1 | 0.001190587 |
| 2 | Motion duration_episode | 6 | A5 | 2250 | 1.34042835 | 0.03255006 | 4.348E-23 | 2.6088E-22 | **** | 1.00E+00 | 1 | 0.001190587 |
| 2 | Motion duration_episode | 8 | A5 | 2778 | 1.52159763 | 0.02649018 | 1.0772E-31 | 6.4635E-31 | **** | 1.00E+00 | 1 | 0.001190587 |
| 2 | Motion duration_episode | 10 | A5 | 2826 | 1.58415246 | 0.03831381 | 7.1383E-34 | 4.283E-33 | **** | 1.00E+00 | 1 | 0.001190587 |
| 3 | Body 2D length_min | 0 | CT | 1756 | 1 | 0.00692289 | 1 | 1 | ns | 1.00E+00 | 1.00E+00 | 4.39E-01 |
| 3 | Body 2D length_min | 2 | CT | 1480 | 1.00048019 | 0.00714572 | 4.8926E-32 | 2.9355E-31 | **** | 1.00E+00 | 1.00E+00 | 4.39E-01 |
| 3 | Body 2D length_min | 4 | CT | 1160 | 1.01918047 | 0.00815912 | 1.7392E-44 | 1.0435E-43 | **** | 1.00E+00 | 1.00E+00 | 4.39E-01 |
| 3 | Body 2D length_min | 6 | CT | 1076 | 1.06941962 | 0.00827668 | 3.318E-117 | 1.9911E-116 | **** | 1.00E+00 | 1.00E+00 | 4.39E-01 |
| 3 | Body 2D length_min | 8 | CT | 1067 | 1.02047984 | 0.00873362 | 2.30E-170 | 1.38E-169 | **** | 1.00E+00 | 1.00E+00 | 4.39E-01 |
| 3 | Body 2D length_min | 10 | CT | 1013 | 1.06986767 | 0.0086857 | 2.35E-96 | 1.41E-95 | **** | 1.00E+00 | 1.00E+00 | 4.39E-01 |
| 3 | Body 2D length_min | 0 | A5 | 2131 | 1 | 0.0067836 | 1.00E+00 | 1.00E+00 | ns | 1.00E+00 | 1.00E+00 | 4.39E-01 |
| 3 | Body 2D length_min | 2 | A5 | 2165 | 1.12039897 | 0.00675403 | 4.89E-32 | 2.94E-31 | **** | 1.00E+00 | 1.00E+00 | 4.39E-01 |
| 3 | Body 2D length_min | 4 | A5 | 1792 | 1.17337681 | 0.00693719 | 1.7392E-44 | 1.0435E-43 | **** | 1.00E+00 | 1.00E+00 | 4.39E-01 |
| 3 | Body 2D length_min | 6 | A5 | 2222 | 1.30199949 | 0.00543285 | 3.318E-117 | 1.9911E-116 | **** | 1.00E+00 | 1.00E+00 | 4.39E-01 |
| 3 | Body 2D length_min | 8 | A5 | 2862 | 1.28854701 | 0.00455023 | 2.30E-170 | 1.38E-169 | **** | 1.00E+00 | 1.00E+00 | 4.39E-01 |
| 3 | Body 2D length_min | 10 | A5 | 2797 | 1.2770145 | 0.00489067 | 2.35E-96 | 1.41E-95 | **** | 1.00E+00 | 1.00E+00 | 4.39E-01 |
| 4 | Tail angle_mean | 0 | CT | 1772 | 1 | 0.00295247 | 1 | 1 | ns | 1.00E+00 | 1.00E+00 | 1.83E-01 |
| 4 | Tail angle_mean | 2 | CT | 1479 | 0.98882041 | 0.00303378 | 4.4383E-29 | 2.663E-28 | **** | 1.00E+00 | 1.00E+00 | 1.83E-01 |
| 4 | Tail angle_mean | 4 | CT | 1162 | 0.98377041 | 0.0035668 | 1.6603E-28 | 9.9619E-28 | **** | 1.00E+00 | 1.00E+00 | 1.83E-01 |
| 4 | Tail angle_mean | 6 | CT | 1072 | 0.9860915 | 0.00389636 | 8.4212E-32 | 5.0527E-31 | **** | 1.00E+00 | 1.00E+00 | 1.83E-01 |
| 4 | Tail angle_mean | 8 | CT | 1057 | 0.98007574 | 0.00350151 | 1.251E-113 | 7.503E-113 | **** | 1.00E+00 | 1.00E+00 | 1.83E-01 |
| 4 | Tail angle_mean | 10 | CT | 1010 | 0.97906589 | 0.00385674 | 1.134E-102 | 6.805E-102 | **** | 1.00E+00 | 1.00E+00 | 1.83E-01 |
| 4 | Tail angle_mean | 0 | A5 | 2081 | 1 | 0.00225597 | 1.00E+00 | 1.00E+00 | ns | 1.00E+00 | 1.00E+00 | 1.83E-01 |
| 4 | Tail angle_mean | 2 | A5 | 2146 | 1.03217487 | 0.00240624 | 4.44E-29 | 2.66E-28 | **** | 1.00E+00 | 1.00E+00 | 1.83E-01 |
| 4 | Tail angle_mean | 4 | A5 | 1793 | 1.03029653 | 0.0024201 | 1.66E-28 | 9.9619E-28 | **** | 1.00E+00 | 1.00E+00 | 1.83E-01 |
| 4 | Tail angle_mean | 6 | A5 | 2243 | 1.03143814 | 0.00187641 | 8.42E-32 | 5.0527E-31 | **** | 1.00E+00 | 1.00E+00 | 1.83E-01 |
| 4 | Tail angle_mean | 8 | A5 | 2853 | 1.06272858 | 0.00171213 | 1.25E-113 | 7.50E-113 | **** | 1.00E+00 | 1.00E+00 | 1.83E-01 |
| 4 | Tail angle_mean | 10 | A5 | 2784 | 1.05851444 | 0.00164117 | 1.13E-102 | 6.81E-102 | **** | 1.00E+00 | 1.00E+00 | 1.83E-01 |
| 5 | Arm angle asym_std | 0 | CT | 1768 | 1 | 0.00981411 | 1 | 1 | ns | 1.00E+00 | 1.00E+00 | 8.03E-01 |
| 5 | Arm angle asym_std | 2 | CT | 1480 | 0.95869992 | 0.00941665 | 2.7947E-15 | 1.6768E-14 | **** | 1.00E+00 | 1.00E+00 | 8.03E-01 |
| 5 | Arm angle asym_std | 4 | CT | 1168 | 0.96406887 | 0.01067851 | 7.2531E-26 | 4.3518E-25 | **** | 1.00E+00 | 1.00E+00 | 8.03E-01 |
| 5 | Arm angle asym_std | 6 | CT | 1068 | 0.98690127 | 0.01213016 | 6.998E-74 | 4.1994E-73 | **** | 1.00E+00 | 1.00E+00 | 8.03E-01 |
| 5 | Arm angle asym_std | 8 | CT | 1064 | 0.96807004 | 0.01130133 | 3.78E-70 | 2.268E-69 | **** | 1.00E+00 | 1.00E+00 | 8.03E-01 |
| 5 | Arm angle asym_std | 10 | CT | 1004 | 1.01770638 | 0.01291671 | 9.4284E-60 | 5.657E-59 | **** | 1.00E+00 | 1.00E+00 | 8.03E-01 |
| 5 | Arm angle asym_std | 0 | A5 | 2061 | 1 | 0.01053231 | 1.00E+00 | 1.00E+00 | ns | 1.00E+00 | 1.00E+00 | 8.03E-01 |
| 5 | Arm angle asym_std | 2 | A5 | 2204 | 1.08014601 | 0.01083295 | 2.79E-15 | 1.68E-14 | **** | 1.00E+00 | 1.00E+00 | 8.03E-01 |
| 5 | Arm angle asym_std | 4 | A5 | 1794 | 1.16858984 | 0.01390237 | 7.25E-26 | 4.35E-25 | **** | 1.00E+00 | 1.00E+00 | 8.03E-01 |
| 5 | Arm angle asym_std | 6 | A5 | 2223 | 1.42655697 | 0.01526312 | 7.00E-74 | 4.20E-73 | **** | 1.00E+00 | 1.00E+00 | 8.03E-01 |
| 5 | Arm angle asym_std | 8 | A5 | 2847 | 1.36498588 | 0.01274748 | 3.78E-70 | 2.27E-69 | **** | 1.00E+00 | 1.00E+00 | 8.03E-01 |
| 5 | Arm angle asym_std | 10 | A5 | 2771 | 1.42209511 | 0.01390026 | 9.43E-60 | 5.66E-59 | **** | 1.00E+00 | 1.00E+00 | 8.03E-01 |
| 6 | Motion interval_episode | 0 | CT | 1735 | 1 | 0.03547019 | 1 | 1 | ns | 1.00E+00 | 1 | 0.980372693 |
| 6 | Motion interval_episode | 2 | CT | 1435 | 1.26091159 | 0.04861972 | 5.2843E-13 | 3.1706E-12 | **** | 1.00E+00 | 1 | 0.980372693 |
| 6 | Motion interval_episode | 4 | CT | 1141 | 1.28444409 | 0.05844416 | 1.1752E-20 | 7.0511E-20 | **** | 1.00E+00 | 1 | 0.980372693 |
| 6 | Motion interval_episode | 6 | CT | 1007 | 2.30032307 | 0.08927596 | 1.5985E-67 | 9.5909E-67 | **** | 1.00E+00 | 1 | 0.980372693 |
| 6 | Motion interval_episode | 8 | CT | 1019 | 1.61307697 | 0.07242427 | 1.3722E-45 | 8.2335E-45 | **** | 1.00E+00 | 1 | 0.980372693 |
| 6 | Motion interval_episode | 10 | CT | 951 | 2.04801625 | 0.07752967 | 1.373E-124 | 8.239E-124 | **** | 1.00E+00 | 1 | 0.980372693 |
| 6 | Motion interval_episode | 0 | A5 | 2088 | 1 | 0.03121839 | 1 | 1 | ns | 1.00E+00 | 1 | 0.980372693 |
| 6 | Motion interval_episode | 2 | A5 | 2099 | 0.88477145 | 0.02716546 | 5.2843E-13 | 3.1706E-12 | **** | 1.00E+00 | 1 | 0.980372693 |
| 6 | Motion interval_episode | 4 | A5 | 1730 | 0.72671304 | 0.02956831 | 1.1752E-20 | 7.0511E-20 | **** | 1.00E+00 | 1 | 0.980372693 |
| 6 | Motion interval_episode | 6 | A5 | 2169 | 0.93033157 | 0.03221267 | 1.5985E-67 | 9.5909E-67 | **** | 1.00E+00 | 1 | 0.980372693 |
| 6 | Motion interval_episode | 8 | A5 | 2752 | 0.7507241 | 0.02481409 | 1.3722E-45 | 8.2335E-45 | **** | 1.00E+00 | 1 | 0.980372693 |
| 6 | Motion interval_episode | 10 | A5 | 2790 | 0.65921153 | 0.01955832 | 1.373E-124 | 8.239E-124 | **** | 1.00E+00 | 1 | 0.980372693 |
| 7 | Body angle_min | 0 | CT | 1771 | 1 | 0.0159485 | 1 | 1 | ns | 0.999999999 | 1.00E+00 | 0.552339291 |
| 7 | Body angle_min | 2 | CT | 1467 | 1.02748744 | 0.01739344 | 6.0527E-05 | 0.00036316 | *** | 0.999999999 | 1.00E+00 | 0.552339291 |
| 7 | Body angle_min | 4 | CT | 1165 | 1.09639538 | 0.02027833 | 0.64362031 | 1 | ns | 0.999999999 | 1.00E+00 | 0.552339291 |
| 7 | Body angle_min | 6 | CT | 1078 | 1.15093813 | 0.02082651 | 1.072E-09 | 6.432E-09 | **** | 0.999999999 | 1.00E+00 | 0.552339291 |
| 7 | Body angle_min | 8 | CT | 1064 | 1.12687849 | 0.02172 | 1.2471E-09 | 7.4828E-09 | **** | 0.999999999 | 1.00E+00 | 0.552339291 |
| 7 | Body angle_min | 10 | CT | 1007 | 1.18660792 | 0.0228174 | 0.00098049 | 0.00588294 | ** | 0.999999999 | 1.00E+00 | 0.552339291 |
| 7 | Body angle_min | 0 | A5 | 2088 | 1 | 0.01480109 | 1 | 1 | ns | 0.999999999 | 1.00E+00 | 0.552339291 |
| 7 | Body angle_min | 2 | A5 | 2178 | 1.11152739 | 0.01360406 | 6.0527E-05 | 0.00036316 | *** | 0.999999999 | 1.00E+00 | 0.552339291 |
| 7 | Body angle_min | 4 | A5 | 1768 | 1.10801423 | 0.01539397 | 0.64362031 | 1 | ns | 0.999999999 | 1.00E+00 | 0.552339291 |
| 7 | Body angle_min | 6 | A5 | 2229 | 1.30197654 | 0.01389698 | 1.072E-09 | 6.4322E-09 | **** | 0.999999999 | 1.00E+00 | 0.552339291 |
| 7 | Body angle_min | 8 | A5 | 2841 | 1.27322637 | 0.01225533 | 1.2471E-09 | 7.4828E-09 | **** | 0.999999999 | 1.00E+00 | 0.552339291 |
| 7 | Body angle_min | 10 | A5 | 2796 | 1.267765 | 0.01226713 | 0.00098049 | 0.00588294 | ** | 0.999999999 | 1.00E+00 | 0.552339291 |
| 8 | Feet 2D distance_max | 0 | CT | 1776 | 1 | 0.00300905 | 1 | 1 | ns | 1.00E+00 | 1.00E+00 | 8.22E-02 |
| 8 | Feet 2D distance_max | 2 | CT | 1482 | 0.97220516 | 0.00294622 | 3.494E-137 | 2.096E-136 | **** | 1.00E+00 | 1.00E+00 | 8.22E-02 |
| 8 | Feet 2D distance_max | 4 | CT | 1173 | 0.95684935 | 0.00332436 | 2.109E-106 | 1.266E-105 | **** | 1.00E+00 | 1.00E+00 | 8.22E-02 |
| 8 | Feet 2D distance_max | 6 | CT | 1069 | 0.98434513 | 0.00353373 | 1.7398E-82 | 1.0439E-81 | **** | 1.00E+00 | 1.00E+00 | 8.22E-02 |
| 8 | Feet 2D distance_max | 8 | CT | 1043 | 0.9567551 | 0.00387451 | 6.697E-100 | 4.018E-99 | **** | 1.00E+00 | 1.00E+00 | 8.22E-02 |
| 8 | Feet 2D distance_max | 10 | CT | 1009 | 1.00382109 | 0.00374583 | 3.2811E-46 | 1.9687E-45 | **** | 1.00E+00 | 1.00E+00 | 8.22E-02 |
| 8 | Feet 2D distance_max | 0 | A5 | 2135 | 1 | 0.00344696 | 1 | 1 | ns | 1.00E+00 | 1.00E+00 | 8.22E-02 |
| 8 | Feet 2D distance_max | 2 | A5 | 2210 | 1.10112522 | 0.00354377 | 3.494E-137 | 2.096E-136 | **** | 1.00E+00 | 1.00E+00 | 8.22E-02 |
| 8 | Feet 2D distance_max | 4 | A5 | 1799 | 1.07949877 | 0.00375815 | 2.109E-106 | 1.266E-105 | **** | 1.00E+00 | 1.00E+00 | 8.22E-02 |
| 8 | Feet 2D distance_max | 6 | A5 | 2206 | 1.11057863 | 0.00409477 | 1.7398E-82 | 1.0439E-81 | **** | 1.00E+00 | 1.00E+00 | 8.22E-02 |
| 8 | Feet 2D distance_max | 8 | A5 | 2833 | 1.08754929 | 0.00334017 | 6.70E-100 | 4.02E-99 | **** | 1.00E+00 | 1.00E+00 | 8.22E-02 |
| 8 | Feet 2D distance_max | 10 | A5 | 2786 | 1.09306807 | 0.00349103 | 3.28E-46 | 1.97E-45 | **** | 1.00E+00 | 1.00E+00 | 8.22E-02 |
| 9 | Neck 3D velocity_std | 0 | CT | 1774 | 1 | 0.00553029 | 1 | 1 | ns | 1.00E+00 | 1.00E+00 | 9.06E-01 |
| 9 | Neck 3D velocity_std | 2 | CT | 1473 | 1.03567681 | 0.00615863 | 1.6742E-05 | 0.00010045 | *** | 1.00E+00 | 1.00E+00 | 9.06E-01 |
| 9 | Neck 3D velocity_std | 4 | CT | 1174 | 1.00319024 | 0.0068272 | 2.25E-06 | 1.3548E-05 | **** | 1.00E+00 | 1.00E+00 | 9.06E-01 |
| 9 | Neck 3D velocity_std | 6 | CT | 1071 | 0.96808526 | 0.00694727 | 7.2649E-29 | 4.359E-28 | **** | 1.00E+00 | 1.00E+00 | 9.06E-01 |
| 9 | Neck 3D velocity_std | 8 | CT | 1055 | 0.98359819 | 0.00731176 | 2.4899E-20 | 1.494E-19 | **** | 1.00E+00 | 1.00E+00 | 9.06E-01 |
| 9 | Neck 3D velocity_std | 10 | CT | 1005 | 0.9920473 | 0.00745398 | 4.7096E-15 | 2.8257E-14 | **** | 1.00E+00 | 1.00E+00 | 9.06E-01 |
| 9 | Neck 3D velocity_std | 0 | A5 | 2133 | 1 | 0.00526206 | 1.00E+00 | 1.00E+00 | ns | 1.00E+00 | 1.00E+00 | 9.06E-01 |
| 9 | Neck 3D velocity_std | 2 | A5 | 2172 | 0.99655732 | 0.00619829 | 1.67E-05 | 1.00E-04 | *** | 1.00E+00 | 1.00E+00 | 9.06E-01 |
| 9 | Neck 3D velocity_std | 4 | A5 | 1792 | 0.95815297 | 0.00625972 | 2.26E-06 | 1.3548E-05 | **** | 1.00E+00 | 1.00E+00 | 9.06E-01 |
| 9 | Neck 3D velocity_std | 6 | A5 | 2218 | 0.86175001 | 0.00564273 | 7.26E-29 | 4.359E-28 | **** | 1.00E+00 | 1.00E+00 | 9.06E-01 |
| 9 | Neck 3D velocity_std | 8 | A5 | 2806 | 0.90026014 | 0.00476374 | 2.4899E-20 | 1.494E-19 | **** | 1.00E+00 | 1.00E+00 | 9.06E-01 |
| 9 | Neck 3D velocity_std | 10 | A5 | 2779 | 0.92348689 | 0.00449456 | 4.7096E-15 | 2.8257E-14 | **** | 1.00E+00 | 1.00E+00 | 9.06E-01 |
| 10 | Feet 2D distance_std | 0 | CT | 1780 | 1 | 0.01177312 | 1 | 1 | ns | 1.00E+00 | 1.00E+00 | 8.34E-01 |
| 10 | Feet 2D distance_std | 2 | CT | 1480 | 0.93755416 | 0.01274896 | 2.8469E-29 | 1.7081E-28 | **** | 1.00E+00 | 1.00E+00 | 8.34E-01 |
| 10 | Feet 2D distance_std | 4 | CT | 1166 | 1.00968799 | 0.01431052 | 6.955E-19 | 4.173E-18 | **** | 1.00E+00 | 1.00E+00 | 8.34E-01 |
| 10 | Feet 2D distance_std | 6 | CT | 1072 | 0.95136255 | 0.01533082 | 3.964E-101 | 2.379E-100 | **** | 1.00E+00 | 1.00E+00 | 8.34E-01 |
| 10 | Feet 2D distance_std | 8 | CT | 1051 | 1.02095268 | 0.01627548 | 2.9108E-73 | 1.7465E-72 | **** | 1.00E+00 | 1.00E+00 | 8.34E-01 |
| 10 | Feet 2D distance_std | 10 | CT | 1003 | 1.01482686 | 0.01623753 | 5.8438E-73 | 3.5063E-72 | **** | 1.00E+00 | 1.00E+00 | 8.34E-01 |
| 10 | Feet 2D distance_std | 0 | A5 | 2144 | 1 | 0.01167641 | 1.00E+00 | 1.00E+00 | ns | 1.00E+00 | 1.00E+00 | 8.34E-01 |
| 10 | Feet 2D distance_std | 2 | A5 | 2196 | 1.14214503 | 0.01208058 | 2.85E-29 | 1.71E-28 | **** | 1.00E+00 | 1.00E+00 | 8.34E-01 |
| 10 | Feet 2D distance_std | 4 | A5 | 1788 | 1.20471555 | 0.01495089 | 6.955E-19 | 4.173E-18 | **** | 1.00E+00 | 1.00E+00 | 8.34E-01 |
| 10 | Feet 2D distance_std | 6 | A5 | 2215 | 1.46126515 | 0.01422182 | 3.964E-101 | 2.379E-100 | **** | 1.00E+00 | 1.00E+00 | 8.34E-01 |
| 10 | Feet 2D distance_std | 8 | A5 | 2842 | 1.45096258 | 0.01279393 | 2.91E-73 | 1.75E-72 | **** | 1.00E+00 | 1.00E+00 | 8.34E-01 |
| 10 | Feet 2D distance_std | 10 | A5 | 2784 | 1.45575897 | 0.01308489 | 5.84E-73 | 3.51E-72 | **** | 1.00E+00 | 1.00E+00 | 8.34E-01 |

| Rank | Feature name | Week | group | n | Mean | SEM | raw_p | corrected_p | significant | ANOVA_p_Week | ANOVA_p_Group | ANOVA_p_Interaction |
|---|---|---|---|---|---|---|---|---|---|---|---|---|
| 11 | Chest 3D velocity_mean | 0 | CT | 1771 | 1 | 0.00815669 | 1 | 1 | ns | 1.00E+00 | 1.00E+00 | 7.05E-01 |
| 11 | Chest 3D velocity_mean | 2 | CT | 1468 | 1.01362003 | 0.008637 | 2.3975E-13 | 1.4385E-12 | **** | 1.00E+00 | 1.00E+00 | 7.05E-01 |
| 11 | Chest 3D velocity_mean | 4 | CT | 1170 | 0.99500811 | 0.00994973 | 2.6263E-19 | 1.5758E-18 | **** | 1.00E+00 | 1.00E+00 | 7.05E-01 |
| 11 | Chest 3D velocity_mean | 6 | CT | 1060 | 0.99032271 | 0.010161 | 1.9524E-15 | 1.1714E-14 | **** | 1.00E+00 | 1.00E+00 | 7.05E-01 |
| 11 | Chest 3D velocity_mean | 8 | CT | 1066 | 0.9922996 | 0.01039418 | 4.673E-40 | 2.8038E-39 | **** | 1.00E+00 | 1.00E+00 | 7.05E-01 |
| 11 | Chest 3D velocity_mean | 10 | CT | 1017 | 1.02453013 | 0.01099013 | 6.4997E-27 | 3.8998E-26 | **** | 1.00E+00 | 1.00E+00 | 7.05E-01 |
| 11 | Chest 3D velocity_mean | 0 | A5 | 2130 | 1 | 0.00759552 | 1 | 1 | ns | 1.00E+00 | 1.00E+00 | 7.05E-01 |
| 11 | Chest 3D velocity_mean | 2 | A5 | 2189 | 1.10910899 | 0.00892063 | 2.3975E-13 | 1.4385E-12 | **** | 1.00E+00 | 1.00E+00 | 7.05E-01 |
| 11 | Chest 3D velocity_mean | 4 | A5 | 1752 | 1.12958932 | 0.01017169 | 2.63E-19 | 1.5758E-18 | **** | 1.00E+00 | 1.00E+00 | 7.05E-01 |
| 11 | Chest 3D velocity_mean | 6 | A5 | 2202 | 1.10513481 | 0.00869643 | 1.95E-15 | 1.1714E-14 | **** | 1.00E+00 | 1.00E+00 | 7.05E-01 |
| 11 | Chest 3D velocity_mean | 8 | A5 | 2820 | 1.17815184 | 0.00756858 | 4.67E-40 | 2.8038E-39 | **** | 1.00E+00 | 1.00E+00 | 7.05E-01 |
| 11 | Chest 3D velocity_mean | 10 | A5 | 2807 | 1.18191098 | 0.00779369 | 6.50E-27 | 3.8998E-26 | **** | 1.00E+00 | 1.00E+00 | 7.05E-01 |
| 12 | U-body 3D length_min | 0 | CT | 1788 | 1 | 0.00393496 | 1 | 1 | ns | 1.00E+00 | 1.00E+00 | 6.50E-01 |
| 12 | U-body 3D length_min | 2 | CT | 1459 | 1.00026364 | 0.00446982 | 0.01376045 | 0.08256269 | ns | 1.00E+00 | 1.00E+00 | 6.50E-01 |
| 12 | U-body 3D length_min | 4 | CT | 1164 | 0.99205008 | 0.00463483 | 0.00151058 | 0.00906347 | ** | 1.00E+00 | 1.00E+00 | 6.50E-01 |
| 12 | U-body 3D length_min | 6 | CT | 1075 | 1.04022876 | 0.00526272 | 6.6282E-05 | 0.00039769 | *** | 1.00E+00 | 1.00E+00 | 6.50E-01 |
| 12 | U-body 3D length_min | 8 | CT | 1056 | 1.01681389 | 0.00527785 | 0.00052487 | 0.0031492 | ** | 1.00E+00 | 1.00E+00 | 6.50E-01 |
| 12 | U-body 3D length_min | 10 | CT | 1010 | 1.02614662 | 0.00524594 | 3.8107E-12 | 2.2864E-11 | **** | 1.00E+00 | 1.00E+00 | 6.50E-01 |
| 12 | U-body 3D length_min | 0 | A5 | 2153 | 1 | 0.00376613 | 1.00E+00 | 1 | ns | 1.00E+00 | 1.00E+00 | 6.50E-01 |
| 12 | U-body 3D length_min | 2 | A5 | 2147 | 0.98590253 | 0.00372097 | 1.38E-02 | 0.08256269 | ns | 1.00E+00 | 1.00E+00 | 6.50E-01 |
| 12 | U-body 3D length_min | 4 | A5 | 1773 | 1.01092559 | 0.00373302 | 0.00151058 | 0.00906347 | ** | 1.00E+00 | 1.00E+00 | 6.50E-01 |
| 12 | U-body 3D length_min | 6 | A5 | 2249 | 1.06204212 | 0.0028157 | 6.6282E-05 | 0.00039769 | *** | 1.00E+00 | 1.00E+00 | 6.50E-01 |
| 12 | U-body 3D length_min | 8 | A5 | 2861 | 1.03476372 | 0.00246552 | 0.00052487 | 0.0031492 | ** | 1.00E+00 | 1.00E+00 | 6.50E-01 |
| 12 | U-body 3D length_min | 10 | A5 | 2786 | 1.06339181 | 0.00259722 | 3.8107E-12 | 2.2864E-11 | **** | 1.00E+00 | 1.00E+00 | 6.50E-01 |
| 13 | Right limb angle asym_min | 0 | CT | 1764 | 1 | 0.00884524 | 1 | 1 | ns | 1.00E+00 | 1.00E+00 | 6.12E-01 |
| 13 | Right limb angle asym_min | 2 | CT | 1469 | 1.00648601 | 0.00922726 | 8.614E-06 | 5.1684E-05 | **** | 1.00E+00 | 1.00E+00 | 6.12E-01 |
| 13 | Right limb angle asym_min | 4 | CT | 1167 | 1.01890137 | 0.01066097 | 0.00155494 | 0.00932963 | ** | 1.00E+00 | 1.00E+00 | 6.12E-01 |
| 13 | Right limb angle asym_min | 6 | CT | 1077 | 1.01870168 | 0.01152953 | 2.6333E-22 | 1.58E-21 | **** | 1.00E+00 | 1.00E+00 | 6.12E-01 |
| 13 | Right limb angle asym_min | 8 | CT | 1060 | 1.07109727 | 0.01167798 | 2.0637E-08 | 1.2382E-07 | **** | 1.00E+00 | 1.00E+00 | 6.12E-01 |
| 13 | Right limb angle asym_min | 10 | CT | 1015 | 1.0433047 | 0.01163656 | 2.3659E-16 | 1.4195E-15 | **** | 1.00E+00 | 1.00E+00 | 6.12E-01 |
| 13 | Right limb angle asym_min | 0 | A5 | 2124 | 1 | 0.00978322 | 1 | 1 | ns | 1.00E+00 | 1.00E+00 | 6.12E-01 |
| 13 | Right limb angle asym_min | 2 | A5 | 2203 | 1.07374352 | 0.01068062 | 8.614E-06 | 5.1684E-05 | **** | 1.00E+00 | 1.00E+00 | 6.12E-01 |
| 13 | Right limb angle asym_min | 4 | A5 | 1786 | 1.07955903 | 0.013825 | 0.00155494 | 0.00932963 | ** | 1.00E+00 | 1.00E+00 | 6.12E-01 |
| 13 | Right limb angle asym_min | 6 | A5 | 2195 | 1.26308244 | 0.01655332 | 2.6333E-22 | 1.58E-21 | **** | 1.00E+00 | 1.00E+00 | 6.12E-01 |
| 13 | Right limb angle asym_min | 8 | A5 | 2844 | 1.19873139 | 0.01316787 | 2.06E-08 | 1.24E-07 | **** | 1.00E+00 | 1.00E+00 | 6.12E-01 |
| 13 | Right limb angle asym_min | 10 | A5 | 2748 | 1.25278473 | 0.01484099 | 2.37E-16 | 1.42E-15 | **** | 1.00E+00 | 1.00E+00 | 6.12E-01 |
| 14 | Hands 3D distance_max | 0 | CT | 1762 | 1 | 0.00565675 | 1 | 1 | ns | 1.00E+00 | 1.00E+00 | 5.99E-01 |
| 14 | Hands 3D distance_max | 2 | CT | 1488 | 0.97309214 | 0.00575977 | 4.2981E-08 | 2.5788E-07 | **** | 1.00E+00 | 1.00E+00 | 5.99E-01 |
| 14 | Hands 3D distance_max | 4 | CT | 1175 | 0.96746171 | 0.00678629 | 1.3575E-14 | 8.1449E-14 | **** | 1.00E+00 | 1.00E+00 | 5.99E-01 |
| 14 | Hands 3D distance_max | 6 | CT | 1062 | 0.98168417 | 0.0074669 | 2.629E-49 | 1.5774E-48 | **** | 1.00E+00 | 1.00E+00 | 5.99E-01 |
| 14 | Hands 3D distance_max | 8 | CT | 1061 | 0.95453808 | 0.00757269 | 8.6345E-51 | 5.1807E-50 | **** | 1.00E+00 | 1.00E+00 | 5.99E-01 |
| 14 | Hands 3D distance_max | 10 | CT | 1004 | 1.01493284 | 0.00791276 | 5.0629E-44 | 3.0377E-43 | **** | 1.00E+00 | 1.00E+00 | 5.99E-01 |
| 14 | Hands 3D distance_max | 0 | A5 | 2169 | 1 | 0.00669862 | 1 | 1 | ns | 1.00E+00 | 1.00E+00 | 5.99E-01 |
| 14 | Hands 3D distance_max | 2 | A5 | 2203 | 1.02706347 | 0.00706815 | 4.2981E-08 | 2.5788E-07 | **** | 1.00E+00 | 1.00E+00 | 5.99E-01 |
| 14 | Hands 3D distance_max | 4 | A5 | 1781 | 1.07259569 | 0.01008358 | 1.3575E-14 | 8.1449E-14 | **** | 1.00E+00 | 1.00E+00 | 5.99E-01 |
| 14 | Hands 3D distance_max | 6 | A5 | 2217 | 1.23918795 | 0.01132086 | 2.629E-49 | 1.5774E-48 | **** | 1.00E+00 | 1.00E+00 | 5.99E-01 |
| 14 | Hands 3D distance_max | 8 | A5 | 2833 | 1.21670579 | 0.01015988 | 8.63E-51 | 5.1807E-50 | **** | 1.00E+00 | 1.00E+00 | 5.99E-01 |
| 14 | Hands 3D distance_max | 10 | A5 | 2766 | 1.27850028 | 0.01089068 | 5.06E-44 | 3.0377E-43 | **** | 1.00E+00 | 1.00E+00 | 5.99E-01 |
| 15 | Left limb angle asym_min | 0 | CT | 1759 | 1 | 0.00922314 | 1 | 1 | ns | 1.00E+00 | 1.00E+00 | 9.50E-02 |
| 15 | Left limb angle asym_min | 2 | CT | 1484 | 0.97761304 | 0.00850426 | 3.2633E-13 | 1.958E-12 | **** | 1.00E+00 | 1.00E+00 | 9.50E-02 |
| 15 | Left limb angle asym_min | 4 | CT | 1172 | 0.97520194 | 0.0099066 | 6.5084E-09 | 3.905E-08 | **** | 1.00E+00 | 1.00E+00 | 9.50E-02 |
| 15 | Left limb angle asym_min | 6 | CT | 1067 | 1.02019899 | 0.01165576 | 1.8627E-36 | 1.1176E-35 | **** | 1.00E+00 | 1.00E+00 | 9.50E-02 |
| 15 | Left limb angle asym_min | 8 | CT | 1057

**Supplementary Table 5. Statistical summary of the KL divergences for the top 20 features identified by the XGB model comparing NALS and ALS groups.** For each group, the KL divergence of each feature relative to its baseline value (10 wk, non-symptomatic age) was computed across the experimental duration (10–20 wk [age]). Each group consisted of 6 sampling sets, each containing 150 randomly selected clips. A two-way ANOVA (group × week) was performed for each feature, followed by weekly t-tests between groups (NALS vs. ALS). The resulting p-values from the weekly t-tests were corrected for multiple comparisons using the Bonferroni method. Source data are provided in the Source Data file (See S_Figure 20).

| Rank | Feature name | group | Week | n | Mean | SEM | raw_p | corrected_p | significant | ANOVA_p_Week | ANOVA_p_Group | ANOVA_p_Interaction |
|---|---|---|---|---|---|---|---|---|---|---|---|---|
| 1 | Hands 3D distance_mean | ALS | 0 | 6 | 0 | 0 | 1 | 1 | ns | 1.05E-11 | 8.78E-02 | 8.00166E-05 |
| 1 | Hands 3D distance_mean | NALS | 0 | 6 | 0 | 0 | 1 | 1 | ns | 1.05E-11 | 8.78E-02 | 8.00166E-05 |
| 1 | Hands 3D distance_mean | ALS | 2 | 6 | 0.29472718 | 0.03925967 | 0.02524964 | 0.15149783 | ns | 1.05E-11 | 8.78E-02 | 8.00166E-05 |
| 1 | Hands 3D distance_mean | NALS | 2 | 6 | 0.17497459 | 0.02316707 | 0.02524964 | 0.15149783 | ns | 1.05E-11 | 8.78E-02 | 8.00166E-05 |
| 1 | Hands 3D distance_mean | ALS | 4 | 6 | 0.16548393 | 0.01416023 | 0.11949613 | 0.71697676 | ns | 1.05E-11 | 8.78E-02 | 8.00166E-05 |
| 1 | Hands 3D distance_mean | NALS | 4 | 6 | 0.24049446 | 0.04172261 | 0.11949613 | 0.71697676 | ns | 1.05E-11 | 8.78E-02 | 8.00166E-05 |
| 1 | Hands 3D distance_mean | ALS | 6 | 6 | 0.18647739 | 0.03180216 | 0.14991381 | 0.89948286 | ns | 1.05E-11 | 8.78E-02 | 8.00166E-05 |
| 1 | Hands 3D distance_mean | NALS | 6 | 6 | 0.12891805 | 0.01872714 | 0.14991381 | 0.89948286 | ns | 1.05E-11 | 8.78E-02 | 8.00166E-05 |
| 1 | Hands 3D distance_mean | ALS | 8 | 6 | 0.15172574 | 0.02822428 | 0.07520344 | 0.45122066 | ns | 1.05E-11 | 8.78E-02 | 8.00166E-05 |
| 1 | Hands 3D distance_mean | NALS | 8 | 6 | 0.24456502 | 0.03728465 | 0.07520344 | 0.45122066 | ns | 1.05E-11 | 8.78E-02 | 8.00166E-05 |
| 1 | Hands 3D distance_mean | ALS | 10 | 6 | 0.33935222 | 0.03386703 | 0.00878057 | 0.05268339 | ns | 1.05E-11 | 8.78E-02 | 8.00166E-05 |
| 1 | Hands 3D distance_mean | NALS | 10 | 6 | 0.17390332 | 0.0380928 | 0.00878057 | 0.05268339 | ns | 1.05E-11 | 8.78E-02 | 8.00166E-05 |
| 2 | Motion duration_episode | ALS | 0 | 6 | 0 | 0 | 1 | 1 | ns | 6.82E-28 | 1.79724E-11 | 1.50823E-06 |
| 2 | Motion duration_episode | NALS | 0 | 6 | 0 | 0 | 1 | 1 | ns | 6.82E-28 | 1.79724E-11 | 1.50823E-06 |
| 2 | Motion duration_episode | ALS | 2 | 6 | 0.05523906 | 0.00871457 | 0.68030263 | 1 | ns | 6.82E-28 | 1.79724E-11 | 1.50823E-06 |
| 2 | Motion duration_episode | NALS | 2 | 6 | 0.04788315 | 0.01498523 | 0.68030263 | 1 | ns | 6.82E-28 | 1.79724E-11 | 1.50823E-06 |
| 2 | Motion duration_episode | ALS | 4 | 6 | 0.41884256 | 0.02404672 | 0.09208465 | 0.55250791 | ns | 6.82E-28 | 1.79724E-11 | 1.50823E-06 |
| 2 | Motion duration_episode | NALS | 4 | 6 | 0.55731567 | 0.06607893 | 0.09208465 | 0.55250791 | ns | 6.82E-28 | 1.79724E-11 | 1.50823E-06 |
| 2 | Motion duration_episode | ALS | 6 | 6 | 0.04392515 | 0.00428502 | 4.6008E-06 | 2.7605E-05 | **** | 6.82E-28 | 1.79724E-11 | 1.50823E-06 |
| 2 | Motion duration_episode | NALS | 6 | 6 | 0.15476994 | 0.01170247 | 4.6008E-06 | 2.7605E-05 | **** | 6.82E-28 | 1.79724E-11 | 1.50823E-06 |
| 2 | Motion duration_episode | ALS | 8 | 6 | 0.12163967 | 0.01731961 | 2.3526E-06 | 1.4116E-05 | **** | 6.82E-28 | 1.79724E-11 | 1.50823E-06 |
| 2 | Motion duration_episode | NALS | 8 | 6 | 0.35059822 | 0.01646972 | 2.3526E-06 | 1.4116E-05 | **** | 6.82E-28 | 1.79724E-11 | 1.50823E-06 |
| 2 | Motion duration_episode | ALS | 10 | 6 | 0.08611061 | 0.00327844 | 6.9736E-06 | 4.1842E-05 | **** | 6.82E-28 | 1.79724E-11 | 1.50823E-06 |
| 2 | Motion duration_episode | NALS | 10 | 6 | 0.32162771 | 0.02754786 | 6.9736E-06 | 4.1842E-05 | **** | 6.82E-28 | 1.79724E-11 | 1.50823E-06 |
| 3 | Body 2D length_min | ALS | 0 | 6 | 0 | 0 | 1 | 1 | ns | 2.06E-17 | 1.00E-25 | 1.71E-14 |
| 3 | Body 2D length_min | NALS | 0 | 6 | 0 | 0 | 1 | 1 | ns | 2.06E-17 | 1.00E-25 | 1.71E-14 |
| 3 | Body 2D length_min | ALS | 2 | 6 | 0.34081236 | 0.03584905 | 1.4861E-05 | 8.9167E-05 | **** | 2.06E-17 | 1.00E-25 | 1.71E-14 |
| 3 | Body 2D length_min | NALS | 2 | 6 | 0.05428077 | 0.00824195 | 1.4861E-05 | 8.9167E-05 | **** | 2.06E-17 | 1.00E-25 | 1.71E-14 |
| 3 | Body 2D length_min | ALS | 4 | 6 | 0.23385881 | 0.02358315 | 2.52E-04 | 1.51E-03 | ** | 2.06E-17 | 1.00E-25 | 1.71E-14 |
| 3 | Body 2D length_min | NALS | 4 | 6 | 0.10008738 | 0.00541491 | 2.52E-04 | 1.51E-03 | ** | 2.06E-17 | 1.00E-25 | 1.71E-14 |
| 3 | Body 2D length_min | ALS | 6 | 6 | 0.41289836 | 0.03427806 | 3.77E-06 | 2.26E-05 | **** | 2.06E-17 | 1.00E-25 | 1.71E-14 |
| 3 | Body 2D length_min | NALS | 6 | 6 | 0.08441036 | 0.01141276 | 3.77E-06 | 2.26E-05 | **** | 2.06E-17 | 1.00E-25 | 1.71E-14 |
| 3 | Body 2D length_min | ALS | 8 | 6 | 0.29927264 | 0.02345884 | 0.00207545 | 0.01245272 | * | 2.06E-17 | 1.00E-25 | 1.71E-14 |
| 3 | Body 2D length_min | NALS | 8 | 6 | 0.16576221 | 0.02235048 | 0.00207545 | 0.01245272 | * | 2.06E-17 | 1.00E-25 | 1.71E-14 |
| 3 | Body 2D length_min | ALS | 10 | 6 | 0.45229024 | 0.0336092 | 1.47E-07 | 8.82E-07 | **** | 2.06E-17 | 1.00E-25 | 1.71E-14 |
| 3 | Body 2D length_min | NALS | 10 | 6 | 0.01528039 | 0.0041456 | 1.47E-07 | 8.82E-07 | **** | 2.06E-17 | 1.00E-25 | 1.71E-14 |
| 4 | Tail angle_mean | ALS | 0 | 6 | 0 | 0 | 1 | 1 | ns | 1.67E-14 | 4.92E-03 | 4.60E-11 |
| 4 | Tail angle_mean | NALS | 0 | 6 | 0 | 0 | 1 | 1 | ns | 1.67E-14 | 4.92E-03 | 4.60E-11 |
| 4 | Tail angle_mean | ALS | 2 | 6 | 0.50944576 | 0.0749561 | 0.0154873 | 0.09292381 | ns | 1.67E-14 | 4.92E-03 | 4.60E-11 |
| 4 | Tail angle_mean | NALS | 2 | 6 | 0.2579788 | 0.04282723 | 0.0154873 | 0.09292381 | ns | 1.67E-14 | 4.92E-03 | 4.60E-11 |
| 4 | Tail angle_mean | ALS | 4 | 6 | 0.24943636 | 0.03421283 | 0.90517021 | 1 | ns | 1.67E-14 | 4.92E-03 | 4.60E-11 |
| 4 | Tail angle_mean | NALS | 4 | 6 | 0.24303598 | 0.03966443 | 0.90517021 | 1 | ns | 1.67E-14 | 4.92E-03 | 4.60E-11 |
| 4 | Tail angle_mean | ALS | 6 | 6 | 0.67456466 | 0.05470606 | 6.00E-06 | 3.60E-05 | **** | 1.67E-14 | 4.92E-03 | 4.60E-11 |
| 4 | Tail angle_mean | NALS | 6 | 6 | 0.1446031 | 0.02782626 | 6.00E-06 | 3.60E-05 | **** | 1.67E-14 | 4.92E-03 | 4.60E-11 |
| 4 | Tail angle_mean | ALS | 8 | 6 | 0.33051161 | 0.05161464 | 2.45E-02 | 0.14676044 | ns | 1.67E-14 | 4.92E-03 | 4.60E-11 |
| 4 | Tail angle_mean | NALS | 8 | 6 | 0.58206128 | 0.07981544 | 2.45E-02 | 0.14676044 | ns | 1.67E-14 | 4.92E-03 | 4.60E-11 |
| 4 | Tail angle_mean | ALS | 10 | 6 | 0.1690129 | 0.01679103 | 7.79E-02 | 4.67E-01 | ns | 1.67E-14 | 4.92E-03 | 4.60E-11 |
| 4 | Tail angle_mean | NALS | 10 | 6 | 0.24733419 | 0.03617091 | 7.79E-02 | 4.67E-01 | ns | 1.67E-14 | 4.92E-03 | 4.60E-11 |
| 5 | Arm angle asym_std | ALS | 0 | 6 | 0 | 0 | 1 | 1 | ns | 3.85E-09 | 1.01E-03 | 4.01E-02 |
| 5 | Arm angle asym_std | NALS | 0 | 6 | 0 | 0 | 1 | 1 | ns | 3.85E-09 | 1.01E-03 | 4.01E-02 |
| 5 | Arm angle asym_std | ALS | 2 | 6 | 0.11163662 | 0.01452356 | 0.00175145 | 0.01050868 | * | 3.85E-09 | 1.01E-03 | 4.01E-02 |
| 5 | Arm angle asym_std | NALS | 2 | 6 | 0.0372696 | 0.00992761 | 0.00175145 | 0.01050868 | * | 3.85E-09 | 1.01E-03 | 4.01E-02 |
| 5 | Arm angle asym_std | ALS | 4 | 6 | 0.17122284 | 0.02334808 | 0.61767012 | 1 | ns | 3.85E-09 | 1.01E-03 | 4.01E-02 |
| 5 | Arm angle asym_std | NALS | 4 | 6 | 0.14810527 | 0.03832734 | 0.61767012 | 1 | ns | 3.85E-09 | 1.01E-03 | 4.01E-02 |
| 5 | Arm angle asym_std | ALS | 6 | 6 | 0.11231627 | 0.03733435 | 1.13E-01 | 6.80E-01 | ns | 3.85E-09 | 1.01E-03 | 4.01E-02 |
| 5 | Arm angle asym_std | NALS | 6 | 6 | 0.04525491 | 0.00994064 | 1.13E-01 | 6.80E-01 | ns | 3.85E-09 | 1.01E-03 | 4.01E-02 |
| 5 | Arm angle asym_std | ALS | 8 | 6 | 0.09907821 | 0.01781828 | 5.03E-01 | 1.00E+00 | ns | 3.85E-09 | 1.01E-03 | 4.01E-02 |
| 5 | Arm angle asym_std | NALS | 8 | 6 | 0.11663689 | 0.01789293 | 5.03E-01 | 1.00E+00 | ns | 3.85E-09 | 1.01E-03 | 4.01E-02 |
| 5 | Arm angle asym_std | ALS | 10 | 6 | 0.17405952 | 0.01624253 | 2.25E-03 | 1.35E-02 | * | 3.85E-09 | 1.01E-03 | 4.01E-02 |
| 5 | Arm angle asym_std | NALS | 10 | 6 | 0.07578548 | 0.0178749 | 2.25E-03 | 1.35E-02 | * | 3.85E-09 | 1.01E-03 | 4.01E-02 |
| 6 | Motion interval_episode | ALS | 0 | 6 | 0 | 0 | 1 | 1 | ns | 1.89E-19 | 3.40904E-10 | 1.11048E-18 |
| 6 | Motion interval_episode | NALS | 0 | 6 | 0 | 0 | 1 | 1 | ns | 1.89E-19 | 3.40904E-10 | 1.11048E-18 |
| 6 | Motion interval_episode | ALS | 2 | 6 | 0.57866976 | 0.08120349 | 0.00015079 | 0.00090471 | *** | 1.89E-19 | 3.40904E-10 | 1.11048E-18 |
| 6 | Motion interval_episode | NALS | 2 | 6 | 0.09219923 | 0.0141898 | 0.00015079 | 0.00090471 | *** | 1.89E-19 | 3.40904E-10 | 1.11048E-18 |
| 6 | Motion interval_episode | ALS | 4 | 6 | 0.04614524 | 0.00953707 | 0.00043645 | 0.00261867 | ** | 1.89E-19 | 3.40904E-10 | 1.11048E-18 |
| 6 | Motion interval_episode | NALS | 4 | 6 | 0.12746286 | 0.01261477 | 0.00043645 | 0.00261867 | ** | 1.89E-19 | 3.40904E-10 | 1.11048E-18 |
| 6 | Motion interval_episode | ALS | 6 | 6 | 0.94316796 | 0.10627281 | 1.8714E-05 | 0.00011229 | *** | 1.89E-19 | 3.40904E-10 | 1.11048E-18 |
| 6 | Motion interval_episode | NALS | 6 | 6 | 0.12988464 | 0.01422652 | 1.8714E-05 | 0.00011229 | *** | 1.89E-19 | 3.40904E-10 | 1.11048E-18 |
| 6 | Motion interval_episode | ALS | 8 | 6 | 0.2007618 | 0.00852867 | 0.00053534 | 0.00321204 | ** | 1.89E-19 | 3.40904E-10 | 1.11048E-18 |
| 6 | Motion interval_episode | NALS | 8 | 6 | 0.37545146 | 0.03386281 | 0.00053534 | 0.00321204 | ** | 1.89E-19 | 3.40904E-10 | 1.11048E-18 |
| 6 | Motion interval_episode | ALS | 10 | 6 | 0.10931975 | 0.02404702 | 0.27446847 | 1 | ns | 1.89E-19 | 3.40904E-10 | 1.11048E-18 |
| 6 | Motion interval_episode | NALS | 10 | 6 | 0.0764879 | 0.01510203 | 0.27446847 | 1 | ns | 1.89E-19 | 3.40904E-10 | 1.11048E-18 |
| 7 | Body angle_min | ALS | 0 | 6 | 0 | 0 | 1 | 1 | ns | 2.08809E-13 | 4.39E-08 | 0.001652424 |
| 7 | Body angle_min | NALS | 0 | 6 | 0 | 0 | 1 | 1 | ns | 2.08809E-13 | 4.39E-08 | 0.001652424 |
| 7 | Body angle_min | ALS | 2 | 6 | 0.25973726 | 0.03805759 | 0.16137865 | 0.96827187 | ns | 2.08809E-13 | 4.39E-08 | 0.001652424 |
| 7 | Body angle_min | NALS | 2 | 6 | 0.18672403 | 0.02970353 | 0.16137865 | 0.96827187 | ns | 2.08809E-13 | 4.39E-08 | 0.001652424 |
| 7 | Body angle_min | ALS | 4 | 6 | 0.29383061 | 0.04461753 | 0.573776 | 1 | ns | 2.08809E-13 | 4.39E-08 | 0.001652424 |
| 7 | Body angle_min | NALS | 4 | 6 | 0.25166909 | 0.05715069 | 0.573776 | 1 | ns | 2.08809E-13 | 4.39E-08 | 0.001652424 |
| 7 | Body angle_min | ALS | 6 | 6 | 0.33273807 | 0.03733435 | 0.00174841 | 0.00747841 | ** | 2.08809E-13 | 4.39E-08 | 0.001652424 |
| 7 | Body angle_min | NALS | 6 | 6 | 0.15345771 | 0.0311605 | 0.0012464 | 0.00747841 | ** | 2.08809E-13 | 4.39E-08 | 0.001652424 |
| 7 | Body angle_min | ALS | 8 | 6 | 0.44141468 | 0.03884845 | 0.00806747 | 0.0484048 | * | 2.08809E-13 | 4.39E-08 | 0.001652424 |
| 7 | Body angle_min | NALS | 8 | 6 | 0.25958839 | 0.03916642 | 0.00806747 | 0.0484048 | * | 2.08809E-13 | 4.39E-08 | 0.001652424 |
| 7 | Body angle_min | ALS | 10 | 6 | 0.42481561 | 0.03683686 | 0.00011124 | 0.00066744 | *** | 2.08809E-13 | 4.39E-08 | 0.001652424 |
| 7 | Body angle_min | NALS | 10 | 6 | 0.15409785 | 0.02438254 | 0.00011124 | 0.00066744 | *** | 2.08809E-13 | 4.39E-08 | 0.001652424 |
| 8 | Feet 2D distance_max | ALS | 0 | 6 | 0 | 0 | 1 | 1 | ns | 1.99E-24 | 2.90E-25 | 5.26E-15 |
| 8 | Feet 2D distance_max | NALS | 0 | 6 | 0 | 0 | 1 | 1 | ns | 1.99E-24 | 2.90E-25 | 5.26E-15 |
| 8 | Feet 2D distance_max | ALS | 2 | 6 | 0.25192894 | 0.03920875 | 0.22656741 | 1 | ns | 1.99E-24 | 2.90E-25 | 5.26E-15 |
| 8 | Feet 2D distance_max | NALS | 2 | 6 | 0.19782187 | 0.01502965 | 0.22656741 | 1 | ns | 1.99E-24 | 2.90E-25 | 5.26E-15 |
| 8 | Feet 2D distance_max | ALS | 4 | 6 | 0.67097317 | 0.0582002 | 8.9696E-06 | 5.3818E-05 | **** | 1.99E-24 | 2.90E-25 | 5.26E-15 |
| 8 | Feet 2D distance_max | NALS | 4 | 6 | 0.14083052 | 0.02721313 | 8.9696E-06 | 5.3818E-05 | **** | 1.99E-24 | 2.90E-25 | 5.26E-15 |
| 8 | Feet 2D distance_max | ALS | 6 | 6 | 1.02687058 | 0.07539651 | 1.6682E-06 | 1.0009E-05 | **** | 1.99E-24 | 2.90E-25 | 5.26E-15 |
| 8 | Feet 2D distance_max | NALS | 6 | 6 | 0.23580453 | 0.02528969 | 1.6682E-06 | 1.0009E-05 | **** | 1.99E-24 | 2.90E-25 | 5.26E-15 |
| 8 | Feet 2D distance_max | ALS | 8 | 6 | 0.97866533 | 0.04464448 | 3.1515E-07 | 1.8909E-06 | **** | 1.99E-24 | 2.90E-25 | 5.26E-15 |
| 8 | Feet 2D distance_max | NALS | 8 | 6 | 0.31891464 | 0.0328442 | 3.1515E-07 | 1.8909E-06 | **** | 1.99E-24 | 2.90E-25 | 5.26E-15 |
| 8 | Feet 2D distance_max | ALS | 10 | 6 | 0.83741499 | 0.06686554 | 4.93E-05 | 2.96E-04 | *** | 1.99E-24 | 2.90E-25 | 5.26E-15 |
| 8 | Feet 2D distance_max | NALS | 10 | 6 | 0.30252347 | 0.0421235 | 4.93E-05 | 2.96E-04 | *** | 1.99E-24 | 2.90E-25 | 5.26E-15 |
| 9 | Neck 3D velocity_std | ALS | 0 | 6 | 0 | 0 | 1 | 1 | ns | 3.57E-22 | 2.78E-07 | 6.52E-12 |
| 9 | Neck 3D velocity_std | NALS | 0 | 6 | 0 | 0 | 1 | 1 | ns | 3.57E-22 | 2.78E-07 | 6.52E-12 |
| 9 | Neck 3D velocity_std | ALS | 2 | 6 | 0.13878081 | 0.01604262 | 0.00014306 | 0.00085838 | *** | 3.57E-22 | 2.78E-07 | 6.52E-12 |
| 9 | Neck 3D velocity_std | NALS | 2 | 6 | 0.03679226 | 0.00611491 | 0.00014306 | 0.00085838 | *** | 3.57E-22 | 2.78E-07 | 6.52E-12 |
| 9 | Neck 3D velocity_std | ALS | 4 | 6 | 0.25040807 | 0.02340489 | 0.63431936 | 1 | ns | 3.57E-22 | 2.78E-07 | 6.52E-12 |
| 9 | Neck 3D velocity_std | NALS | 4 | 6 | 0.27788926 | 0.0508958 | 0.63431936 | 1 | ns | 3.57E-22 | 2.78E-07 | 6.52E-12 |
| 9 | Neck 3D velocity_std | ALS | 6 | 6 | 0.09012832 | 0.01747463 | 2.01E-01 | 1.00E+00 | ns | 3.57E-22 | 2.78E-07 | 6.52E-12 |
| 9 | Neck 3D velocity_std | NALS | 6 | 6 | 0.12863375 | 0.02201317 | 2.01E-01 | 1.00E+00 | ns | 3.57E-22 | 2.78E-07 | 6.52E-12 |
| 9 | Neck 3D velocity_std | ALS | 8 | 6 | 0.23784279 | 0.01882023 | 8.00E-02 | 0.4801099 | ns | 3.57E-22 | 2.78E-07 | 6.52E-12 |
| 9 | Neck 3D velocity_std | NALS | 8 | 6 | 0.16710423 | 0.03105667 | 8.00E-02 | 0.4801099 | ns | 3.57E-22 | 2.78E-07 | 6.52E-12 |
| 9 | Neck 3D velocity_std | ALS | 10 | 6 | 0.54241326 | 0.02496469 | 8.4123E-07 | 5.0474E-06 | **** | 3.57E-22 | 2.78E-07 | 6.52E-12 |
| 9 | Neck 3D velocity_std | NALS | 10 | 6 | 0.17478212 | 0.02353654 | 8.4123E-07 | 5.0474E-06 | **** | 3.57E-22 | 2.78E-07 | 6.52E-12 |
| 10 | Feet 2D distance_std | ALS | 0 | 6 | 0 | 0 | 1 | 1 | ns | 1.71E-16 | 1.09E-23 | 4.42E-10 |
| 10 | Feet 2D distance_std | NALS | 0 | 6 | 0 | 0 | 1 | 1 | ns | 1.71E-16 | 1.09E-23 | 4.42E-10 |
| 10 | Feet 2D distance_std | ALS | 2 | 6 | 0.24325513 | 0.03993271 | 0.00359539 | 0.02157233 | * | 1.71E-16 | 1.09E-23 | 4.42E-10 |
| 10 | Feet 2D distance_std | NALS | 2 | 6 | 0.08769973 | 0.00989378 | 0.00359539 | 0.02157233 | * | 1.71E-16 | 1.09E-23 | 4.42E-10 |
| 10 | Feet 2D distance_std | ALS | 4 | 6 | 0.34191365 | 0.04048262 | 8.9958E-05 | 0.00053975 | *** | 1.71E-16 | 1.09E-23 | 4.42E-10 |
| 10 | Feet 2D distance_std | NALS | 4 | 6 | 0.07341867 | 0.01348445 | 8.9958E-05 | 0.00053975 | *** | 1.71E-16 | 1.09E-23 | 4.42E-10 |
| 10 | Feet 2D distance_std | ALS | 6 | 6 | 0.38620313 | 0.03456013 | 2.78E-05 | 1.67E-04 | *** | 1.71E-16 | 1.09E-23 | 4.42E-10 |
| 10 | Feet 2D distance_std | NALS | 6 | 6 | 0.10002792 | 0.01915252 | 2.78E-05 | 1.67E-04 | *** | 1.71E-16 | 1.09E-23 | 4.42E-10 |
| 10 | Feet 2D distance_std | ALS | 8 | 6 | 0.36304067 | 0.02471724 | 3.5348E-05 | 0.00021209 | *** | 1.71E-16 | 1.09E-23 | 4.42E-10 |
| 10 | Feet 2D distance_std | NALS | 8 | 6 | 0.11731451 | 0.02463476 | 3.5348E-05 | 0.00021209 | *** | 1.71E-16 | 1.09E-23 | 4.42E-10 |
| 10 | Feet 2D distance_std | ALS | 10 | 6 | 0.484339 | 0.02435 | 3.02E-08 | 1.81E-07 | **** | 1.71E-16 | 1.09E-23 | 4.42E-10 |
| 10 | Feet 2D distance_std | NALS | 10 | 6 | 0.07757371 | 0.01097559 | 3.02E-08 | 1.81E-07 | **** | 1.71E-16 | 1.09E-23 | 4.42E-10 |
| 11 | Chest 3D velocity_mean | ALS | 0 | 6 | 0 | 0 | 1 | 1 | ns | 3.15E-35 | 1.35E-15 | 5.76E-25 |
| 11 | Chest 3D velocity_mean | NALS | 0 | 6 | 0 | 0 | 1 | 1 | ns | 3.15E-35 | 1.35E-15 | 5.76E-25 |
| 11 | Chest 3D velocity_mean | ALS | 2 | 6 | 0.34926148 | 0.02886476 | 0.13304847 | 0.79829082 | ns | 3.15E-35 | 1.35E-15 | 5.76E-25 |
| 11 | Chest 3D velocity_mean | NALS | 2 | 6 | 0.42361624 | 0.03513436 | 0.13304847 | 0.79829082 | ns | 3.15E-35 | 1.35E-15 | 5.76E-25 |
| 11 | Chest 3D velocity_mean | ALS | 4 | 6 | 0.53293559 | 0.0337395 | 0.51587971 | 1 | ns | 3.15E-35 | 1.35E-15 | 5.76E-25 |
| 11 | Chest 3D velocity_mean | NALS | 4 | 6 | 0.495618 | 0.04394936 | 0.51587971 | 1 | ns | 3.15E-35 | 1.35E-15 | 5.76E-25 |
| 11 | Chest 3D velocity_mean | ALS | 6 | 6 | 0.30023675 | 0.02860105 | 0.15456207 | 0.9273724 | ns | 3.15E-35 | 1.35E-15 | 5.76E-25 |
| 11 | Chest 3D velocity_mean | NALS | 6 | 6 | 0.36984627 | 0.03499823 | 0.15456207 | 0.9273724 | ns | 3.15E-35 | 1.35E-15 | 5.76E-25 |
| 11 | Chest 3D velocity_mean | ALS | 8 | 6 | 0.61177163 | 0.03699785 | 2.87E-05 | 0.00017216 | *** | 3.15E-35 | 1.35E-15 | 5.76E-25 |
| 11 | Chest 3D velocity_mean | NALS | 8 | 6 | 0.271112 | 0.02931685 | 2.87E-05 | 0.00017216 | *** | 3.15E-35 | 1.35E-15 | 5.76E-25 |
| 11 | Chest 3D velocity_mean | ALS | 10 | 6 | 1.38322205 | 0.0372135 | 2.07E-09 | 1.2403E-08 | **** | 3.15E-35 | 1.35E-15 | 5.76E-25 |
| 11 | Chest 3D velocity_mean | NALS | 10 | 6 | 0.46590012 | 0.02651008 | 2.07E-09 | 1.2403E-08 | **** | 3.15E-35 | 1.35E-15 | 5.76E-25 |
| 12 | U-body 3D length_min | ALS | 0 | 6 | 0 | 0 | 1 | 1 | ns | 3.92E-14 | 1.19E-24 | 1.30E-10 |
| 12 | U-body 3D length_min | NALS | 0 | 6 | 0 | 0 | 1 | 1 | ns | 3.92E-14 | 1.19E-24 | 1.30E-10 |
| 12 | U-body 3D length_min | ALS | 2 | 6 | 0.39949173 | 0.04723854 | 4.0931E-05 | 0.00024559 | *** | 3.92E-14 | 1.19E-24 | 1.30E-10 |
| 12 | U-body 3D length_min | NALS | 2 | 6 | 0.06143787 | 0.01244805 | 4.0931E-05 | 0.00024559 | *** | 3.92E-14 | 1.19E-24 | 1.30E-10 |
| 12 | U-body 3D length_min | ALS | 4 | 6 | 0.19172142 | 0.02602317 | 0.000719 | 0.00431399 | ** | 3.92E-14 | 1.19E-24 | 1.30E-10 |
| 12 | U-body 3D length_min | NALS | 4 | 6 | 0.06293179 | 0.00643627 | 0.000719 | 0.00431399 | ** | 3.92E-14 | 1.19E-24 | 1.30E-10 |
| 12 | U-body 3D length_min | ALS | 6 | 6 | 0.30557049 | 0.01915858 | 2.59E-07 | 1.5523E-06 | **** | 3.92E-14 | 1.19E-24 | 1.30E-10 |
| 12 | U-body 3D length_min | NALS | 6 | 6 | 0.05746862 | 0.00703671 | 2.59E-07 | 1.5523E-06 | **** | 3.92E-14 | 1.19E-24 | 1.30E-10 |
| 12 | U-body 3D length_min | ALS | 8 | 6 | 0.35934816 | 0.04474645 | 3.6562E-05 | 0.00021937 | *** | 3.92E-14 | 1.19E-24 | 1.30E-10 |
| 12 | U-body 3D length_min | NALS | 8 | 6 | 0.04520711 | 0.00201223 | 3.6562E-05 | 0.00021937 | *** | 3.92E-14 | 1.19E-24 | 1.30E-10 |
| 12 | U-body 3D length_min | ALS | 10 | 6 | 0.37071898 | 0.02900213 | 5.3015E-07 | 3.1809E-06 | **** | 3.92E-14 | 1.19E-24 | 1.30E-10 |
| 12 | U-body 3D length_min | NALS | 10 | 6 | 0.03714926 | 0.00603463 | 5.3015E-07 | 3.1809E-06 | **** | 3.92E-14 | 1.19E-24 | 1.30E-10 |
| 13 | Right limb angle asym_.min | ALS | 0 | 6 | 0 | 0 | 1 | 1 | ns | 2.97E-19 | 2.09E-12 | 9.72E-06 |
| 13 | Right limb angle asym_.min | NALS | 0 | 6 | 0 | 0 | 1 | 1 | ns | 2.97E-19 | 2.09E-12 | 9.72E-06 |
| 13 | Right limb angle asym_.min | ALS | 2 | 6 | 0.10063516 | 0.00913912 | 0.18518961 | 1 | ns | 2.97E-19 | 2.09E-12 | 9.72E-06 |
| 13 | Right limb angle asym_.min | NALS | 2 | 6 | 0.07139725 | 0.01840303 | 0.18518961 | 1 | ns | 2.97E-19 | 2.09E-12 | 9.72E-06 |
| 13 | Right limb angle asym_.min | ALS | 4 | 6 | 0.16915763 | 0.01381195 | 0.0001848 | 0.00110882 | ** | 2.97E-19 | 2.09E-12 | 9.72E-06 |
| 13 | Right limb angle asym_.min | NALS | 4 | 6 | 0.05447599 | 0.01438122 | 0.0001848 | 0.00110882 | ** | 2.97E-19 | 2.09E-12 | 9.72E-06 |
| 13 | Right limb angle asym_.min | ALS | 6 | 6 | 0.15451532 | 0.01015566 | 0.01738824 | 0.10432941 | ns | 2.97E-19 | 2.09E-12 | 9.72E-06 |
| 13 | Right limb angle asym_.min | NALS | 6 | 6 | 0.08884962 | 0.02072363 | 0.01738824 | 0.10432941 | ns | 2.97E-19 | 2.09E-12 | 9.72E-06 |
| 13 | Right limb angle asym_.min | ALS | 8 | 6 | 0.27770197 | 0.00914972 | 0.00281342 | 0.01688051 | * | 2.97E-19 | 2.09E-12 | 9.72E-06 |
| 13 | Right limb angle asym_.min | NALS | 8 | 6 | 0.14894173 | 0.03144694 | 0.00281342 | 0.01688051 | * | 2.97E-19 | 2.09E-12 | 9.72E-06 |
| 13 | Right limb angle asym_.min | ALS | 10 | 6 | 0.30609512 | 0.01949928 | 2.35E-04 | 1.41E-03 | ** | 2.97E-19 | 2.09E-12 | 9.72E-06 |
| 13 | Right limb angle asym_.min | NALS | 10 | 6 | 0.12463794 | 0.02604565 | 2.35E-04 | 1.41E-03 | ** | 2.97E-19 | 2.09E-12 | 9.72E-06 |
| 14 | Hands 3D distance_max | ALS | 0 | 6 | 0 | 0 | 1 | 1 | ns | 2.82E-13 | 1.28E-01 | 4.98E-08 |
| 14 | Hands 3D distance_max | NALS | 0 | 6 | 0 | 0 | 1 | 1 | ns | 2.82E-13 | 1.28E-01 | 4.98E-08 |
| 14 | Hands 3D distance_max | ALS | 2 | 6 | 0.04373834 | 0.01360037 | 0.17406094 | 1 | ns | 2.82E-13 | 1.28E-01 | 4.98E-08 |
| 14 | Hands 3D distance_max | NALS | 2 | 6 | 0.07968728 | 0.02045635 | 0.17406094 | 1 | ns | 2.82E-13 | 1.28E-01 | 4.98E-08 |
| 14 | Hands 3D distance_max | ALS | 4 | 6 | 0.07638522 | 0.013219 | 0.77529513 | 1 | ns | 2.82E-13 | 1.28E-01 | 4.98E-08 |
| 14 | Hands 3D distance_max | NALS | 4 | 6 | 0.08425011 | 0.02333086 | 0.77529513 | 1 | ns | 2.82E-13 | 1.28E-01 | 4.98E-08 |
| 14 | Hands 3D distance_max | ALS | 6 | 6 | 0.03310328 | 0.00528623 | 0.04509476 | 0.27056858 | ns | 2.82E-13 | 1.28E-01 | 4.98E-08 |
| 14 | Hands 3D distance_max | NALS | 6 | 6 | 0.06045962 | 0.01071889 | 0.04509476 | 0.27056858 | ns | 2.82E-13 | 1.28E-01 | 4.98E-08 |
| 14 | Hands 3D distance_max | ALS | 8 | 6 | 0.04964546 | 0.00938545 | 0.73741659 | 1 | ns | 2.82E-13 | 1.28E-01 | 4.98E-08 |
| 14 | Hands 3D distance_max | NALS | 8 | 6 | 0.05600817 | 0.01558909 | 0.73741659 | 1 | ns | 2.82E-13 | 1.28E-01 | 4.98E-08 |
| 14 | Hands 3D distance_max | ALS | 10 | 6 | 0.23161635 | 0.0253208 | 1.92E-04 | 0.00114955 | ** | 2.82E-13 | 1.28E-01 | 4.98E-08 |
| 14 | Hands 3D distance_max | NALS | 10 | 6 | 0.07631753 | 0.00973014 | 1.92E-04 | 0.00114955 | ** | 2.82E-13 | 1.28E-01 | 4.98E-08 |
| 15 | Left limb angle asym_.min | ALS | 0 | 6 | 0 | 0 | 1 | 1 | ns | 2.27E-07 | 2.60E-01 | 9.31E-01 |
| 15 | Left limb angle asym_.min | NALS | 0 | 6 | 0 | 0 | 1 | 1 | ns | 2.27E-07 | 2.60E-01 | 9.31E-01 |
| 15 | Left limb angle asym_.min | ALS | 2 | 6 | 0.10053941 | 0.01368944 | 0.401017776 | 1 | ns | 2.27E-07 | 2.60E-01 | 9.31E-01 |
| 15 | Left limb angle asym_.min | NALS | 2 | 6 | 0.15100786 | 0.05588865 | 0.401017776 | 1 | ns | 2.27E-07 | 2.60E-01 | 9.31E-01 |
| 15 | Left limb angle asym_.min | ALS | 4 | 6 | 0.18932593 | 0.02288421 | 0.8995361 | 1 | ns | 2.27E-07 | 2.60E-01 | 9.31E-01 |
| 15 | Left limb angle asym_.min | NALS | 4 | 6 | 0.1823999 | 0.04834344 | 0.8995361 | 1 | ns | 2.27E-07 | 2.60E-01 | 9.31E-01 |
| 15 | Left limb angle asym_.min | ALS | 6 | 6 | 0.20083742 | 0.02264782 | 8.49E-01 | 1.00E+00 | ns | 2.27E-07 | 2.60E-01 | 9.31E-01 |
| 15 | Left limb angle asym_.min | NALS | 6 | 6 | 0.21200636 | 0.05257953 | 8.49E-01 | 1.00E+00 | ns | 2.27E-07 | 2.60E-01 | 9.31E-01 |
| 15 | Left limb angle asym_.min | ALS | 8 | 6 | 0.17166985 | 0.0138705 | 3.82E-01 | 1.00E+00 | ns | 2.27E-07 | 2.60E-01 | 9.31E-01 |
| 15 | Left limb angle

**Supplementary Table 6. Statistical summary of the feature values for the top 20 features identified by the XGB model, comparing the NALS and ALS groups.** For each feature, the values at each week were divided by the group's corresponding baseline (10 wk, non-symptomatic age) mean value, and the normalised data were analysed over the experimental duration (10–20 wk [age]). Each group consisted of 6 sampling sets, each containing 150 randomly selected clips. Two-way ANOVA (group × week) was performed for each feature on the normalised data, followed by weekly t-tests comparing the NALS and ALS groups. P-values from weekly t-tests were corrected for multiple comparisons using the Bonferroni method. Source data are provided in the Source Data file (See S_Figure 21).

| Rank | Feature name | Week | group | n | Mean | SEM | raw_p | corrected_p | significant | ANOVA_p_Week | ANOVA_p_Group | ANOVA_p_Interaction |
|---|---|---|---|---|---|---|---|---|---|---|---|---|
| 1 | Hands 3D distance_mean | 0 | NALS | 376 | 1 | 0.03244642 | 1 | 1 | ns | 1 | 1 | 0.968137519 |
| 1 | Hands 3D distance_mean | 2 | NALS | 357 | 0.83680607 | 0.02335603 | 0.65439048 | 1 | ns | 1 | 1 | 0.968137519 |
| 1 | Hands 3D distance_mean | 4 | NALS | 380 | 0.77498829 | 0.01780398 | 0.00436138 | 0.02616829 | * | 1 | 1 | 0.968137519 |
| 1 | Hands 3D distance_mean | 6 | NALS | 339 | 0.81967807 | 0.02229885 | 1.63E-01 | 9.78E-01 | ns | 1 | 1 | 0.968137519 |
| 1 | Hands 3D distance_mean | 8 | NALS | 368 | 0.82389444 | 0.02166143 | 9.07E-02 | 5.44E-01 | ns | 1 | 1 | 0.968137519 |
| 1 | Hands 3D distance_mean | 10 | NALS | 362 | 0.8508868 | 0.01970933 | 1.32E-01 | 7.94E-01 | ns | 1 | 1 | 0.968137519 |
| 1 | Hands 3D distance_mean | 0 | ALS | 273 | 1 | 0.04294197 | 1 | 1 | ns | 1 | 1 | 0.968137519 |
| 1 | Hands 3D distance_mean | 2 | ALS | 347 | 0.82275724 | 0.02085528 | 0.65439048 | 1 | ns | 1 | 1 | 0.968137519 |
| 1 | Hands 3D distance_mean | 4 | ALS | 235 | 0.87091932 | 0.0314506 | 0.00436138 | 0.02616829 | * | 1 | 1 | 0.968137519 |
| 1 | Hands 3D distance_mean | 6 | ALS | 312 | 0.86709779 | 0.02579818 | 1.63E-01 | 9.78E-01 | ns | 1 | 1 | 0.968137519 |
| 1 | Hands 3D distance_mean | 8 | ALS | 196 | 0.89195996 | 0.03709987 | 9.07E-02 | 5.44E-01 | ns | 1 | 1 | 0.968137519 |
| 1 | Hands 3D distance_mean | 10 | ALS | 277 | 0.89635502 | 0.02295216 | 1.32E-01 | 7.94E-01 | ns | 1 | 1 | 0.968137519 |
| 2 | Motion duration_episode | 0 | NALS | 380 | 1 | 0.03965498 | 1 | 1 | ns | 1 | 1 | 0.727162473 |
| 2 | Motion duration_episode | 2 | NALS | 361 | 0.96253592 | 0.03621998 | 0.53473706 | 1 | ns | 1 | 1 | 0.727162473 |
| 2 | Motion duration_episode | 4 | NALS | 385 | 0.86921368 | 0.02688005 | 2.37E-02 | 1.42E-01 | ns | 1 | 1 | 0.727162473 |
| 2 | Motion duration_episode | 6 | NALS | 343 | 1.12059009 | 0.05022001 | 7.50E-01 | 1.00E+00 | ns | 1 | 1 | 0.727162473 |
| 2 | Motion duration_episode | 8 | NALS | 372 | 1.78080841 | 0.07150477 | 1.99E-16 | 1.19E-15 | **** | 1 | 1 | 0.727162473 |
| 2 | Motion duration_episode | 10 | NALS | 366 | 1.16605373 | 0.04700521 | 2.47E-03 | 1.48E-02 | * | 1 | 1 | 0.727162473 |
| 2 | Motion duration_episode | 0 | ALS | 276 | 1 | 0.03733744 | 1 | 1 | ns | 1 | 1 | 0.727162473 |
| 2 | Motion duration_episode | 2 | ALS | 352 | 0.93307801 | 0.0304498 | 0.53473706 | 1 | ns | 1 | 1 | 0.727162473 |
| 2 | Motion duration_episode | 4 | ALS | 238 | 0.79188235 | 0.02261545 | 2.37E-02 | 1.42E-01 | ns | 1 | 1 | 0.727162473 |
| 2 | Motion duration_episode | 6 | ALS | 316 | 1.1411068 | 0.03920449 | 7.50E-01 | 1.00E+00 | ns | 1 | 1 | 0.727162473 |
| 2 | Motion duration_episode | 8 | ALS | 198 | 0.90223989 | 0.04603175 | 1.99E-16 | 1.19E-15 | **** | 1 | 1 | 0.727162473 |
| 2 | Motion duration_episode | 10 | ALS | 280 | 0.96794945 | 0.04217254 | 2.47E-03 | 1.48E-02 | * | 1 | 1 | 0.727162473 |
| 3 | Body 2D length_min | 0 | NALS | 376 | 1 | 0.02258652 | 1 | 1 | ns | 1 | 1 | 0.276711492 |
| 3 | Body 2D length_min | 2 | NALS | 357 | 0.97268405 | 0.02012385 | 2.03E-05 | 1.22E-04 | *** | 1 | 1 | 0.276711492 |
| 3 | Body 2D length_min | 4 | NALS | 380 | 1.01232621 | 0.01811582 | 8.65E-05 | 5.19E-04 | *** | 1 | 1 | 0.276711492 |
| 3 | Body 2D length_min | 6 | NALS | 339 | 0.98139319 | 0.02010888 | 2.64E-08 | 1.59E-07 | **** | 1 | 1 | 0.276711492 |
| 3 | Body 2D length_min | 8 | NALS | 368 | 1.00578691 | 0.01789499 | 2.07E-01 | 1.00E+00 | ns | 1 | 1 | 0.276711492 |
| 3 | Body 2D length_min | 10 | NALS | 362 | 1.00015527 | 0.02262361 | 1.14E-08 | 6.83E-08 | **** | 1 | 1 | 0.276711492 |
| 3 | Body 2D length_min | 0 | ALS | 273 | 1 | 0.02817325 | 1 | 1 | ns | 1 | 1 | 0.276711492 |
| 3 | Body 2D length_min | 2 | ALS | 347 | 0.85665768 | 0.01799253 | 2.03E-05 | 1.22E-04 | *** | 1 | 1 | 0.276711492 |
| 3 | Body 2D length_min | 4 | ALS | 235 | 0.89734101 | 0.02259957 | 8.65E-05 | 5.19E-04 | *** | 1 | 1 | 0.276711492 |
| 3 | Body 2D length_min | 6 | ALS | 312 | 0.83094541 | 0.01725386 | 2.64E-08 | 1.59E-07 | **** | 1 | 1 | 0.276711492 |
| 3 | Body 2D length_min | 8 | ALS | 196 | 1.04378928 | 0.02385434 | 2.07E-01 | 1.00E+00 | ns | 1 | 1 | 0.276711492 |
| 3 | Body 2D length_min | 10 | ALS | 277 | 1.18069167 | 0.01993549 | 1.14E-08 | 6.83E-08 | **** | 1 | 1 | 0.276711492 |
| 4 | Tail angle_mean | 0 | NALS | 376 | 1 | 0.0109366 | 1 | 1 | ns | 1 | 1 | 0.692804224 |
| 4 | Tail angle_mean | 2 | NALS | 304 | 1.09435775 | 0.00918885 | 4.28E-02 | 2.57E-01 | ns | 1 | 1 | 0.692804224 |
| 4 | Tail angle_mean | 4 | NALS | 307 | 1.07865344 | 0.00852557 | 9.05E-01 | 1.00E+00 | ns | 1 | 1 | 0.692804224 |
| 4 | Tail angle_mean | 6 | NALS | 307 | 1.07357361 | 0.00984775 | 2.24E-01 | 1.00E+00 | ns | 1 | 1 | 0.692804224 |
| 4 | Tail angle_mean | 8 | NALS | 302 | 1.12516718 | 0.00743296 | 3.89E-02 | 2.33E-01 | ns | 1 | 1 | 0.692804224 |
| 4 | Tail angle_mean | 10 | NALS | 334 | 1.07759346 | 0.00802525 | 2.14E-01 | 1.00E+00 | ns | 1 | 1 | 0.692804224 |
| 4 | Tail angle_mean | 0 | ALS | 273 | 1 | 0.0142652 | 1 | 1 | ns | 1 | 1 | 0.692804224 |
| 4 | Tail angle_mean | 2 | ALS | 293 | 1.11991162 | 0.00857101 | 4.28E-02 | 2.57E-01 | ns | 1 | 1 | 0.692804224 |
| 4 | Tail angle_mean | 4 | ALS | 196 | 1.08038329 | 0.0123048 | 9.05E-01 | 1.00E+00 | ns | 1 | 1 | 0.692804224 |
| 4 | Tail angle_mean | 6 | ALS | 266 | 1.08923781 | 0.00788964 | 2.24E-01 | 1.00E+00 | ns | 1 | 1 | 0.692804224 |
| 4 | Tail angle_mean | 8 | ALS | 145 | 1.09560953 | 0.0135814 | 3.89E-02 | 2.33E-01 | ns | 1 | 1 | 0.692804224 |
| 4 | Tail angle_mean | 10 | ALS | 229 | 1.09697981 | 0.01473739 | 2.14E-01 | 1.00E+00 | ns | 1 | 1 | 0.692804224 |
| 5 | Arm angle asym._std | 0 | NALS | 376 | 1 | 0.03583617 | 1 | 1 | ns | 1 | 1 | 0.640671948 |
| 5 | Arm angle asym._std | 2 | NALS | 304 | 0.86535339 | 0.03826868 | 9.60E-01 | 1.00E+00 | ns | 1 | 1 | 0.640671948 |
| 5 | Arm angle asym._std | 4 | NALS | 307 | 0.76991516 | 0.03031707 | 4.22E-01 | 1.00E+00 | ns | 1 | 1 | 0.640671948 |
| 5 | Arm angle asym._std | 6 | NALS | 307 | 0.86744395 | 0.03588383 | 3.13E-01 | 1.00E+00 | ns | 1 | 1 | 0.640671948 |
| 5 | Arm angle asym._std | 8 | NALS | 302 | 0.74627313 | 0.03546427 | 1.62E-01 | 9.72E-01 | ns | 1 | 1 | 0.640671948 |
| 5 | Arm angle asym._std | 10 | NALS | 334 | 0.76774354 | 0.03220352 | 4.94E-02 | 2.97E-01 | ns | 1 | 1 | 0.640671948 |
| 5 | Arm angle asym._std | 0 | ALS | 273 | 1 | 0.05030177 | 1 | 1 | ns | 1 | 1 | 0.640671948 |
| 5 | Arm angle asym._std | 2 | ALS | 293 | 0.86270835 | 0.03590763 | 9.60E-01 | 1.00E+00 | ns | 1 | 1 | 0.640671948 |
| 5 | Arm angle asym._std | 4 | ALS | 196 | 0.81104219 | 0.04303269 | 4.22E-01 | 1.00E+00 | ns | 1 | 1 | 0.640671948 |
| 5 | Arm angle asym._std | 6 | ALS | 266 | 0.92168109 | 0.04015202 | 3.13E-01 | 1.00E+00 | ns | 1 | 1 | 0.640671948 |
| 5 | Arm angle asym._std | 8 | ALS | 145 | 0.83496942 | 0.053821 | 1.62E-01 | 9.72E-01 | ns | 1 | 1 | 0.640671948 |
| 5 | Arm angle asym._std | 10 | ALS | 229 | 0.66682907 | 0.04030837 | 4.94E-02 | 2.97E-01 | ns | 1 | 1 | 0.640671948 |
| 6 | Motion interval_episode | 0 | NALS | 370 | 1 | 0.07751083 | 1 | 1 | ns | 1 | 0.016810024 | 0.883070872 |
| 6 | Motion interval_episode | 2 | NALS | 347 | 1.10731603 | 0.08191388 | 4.09E-12 | 2.46E-11 | **** | 1 | 0.016810024 | 0.883070872 |
| 6 | Motion interval_episode | 4 | NALS | 372 | 1.10504824 | 0.06181661 | 2.51E-01 | 1.00E+00 | ns | 1 | 0.016810024 | 0.883070872 |
| 6 | Motion interval_episode | 6 | NALS | 335 | 1.36149217 | 0.11241894 | 1.39E-06 | 8.35E-06 | **** | 1 | 0.016810024 | 0.883070872 |
| 6 | Motion interval_episode | 8 | NALS | 370 | 1.5689031 | 0.20997573 | 5.16E-01 | 1.00E+00 | ns | 1 | 0.016810024 | 0.883070872 |
| 6 | Motion interval_episode | 10 | NALS | 359 | 1.12550314 | 0.09137512 | 5.89E-04 | 3.53E-03 | ** | 1 | 0.016810024 | 0.883070872 |
| 6 | Motion interval_episode | 0 | ALS | 274 | 1 | 0.08221136 | 1 | 1 | ns | 1 | 0.016810024 | 0.883070872 |
| 6 | Motion interval_episode | 2 | ALS | 346 | 0.47406099 | 0.03638518 | 4.09E-12 | 2.46E-11 | **** | 1 | 0.016810024 | 0.883070872 |
| 6 | Motion interval_episode | 4 | ALS | 232 | 0.98582055 | 0.08622122 | 2.51E-01 | 1.00E+00 | ns | 1 | 0.016810024 | 0.883070872 |
| 6 | Motion interval_episode | 6 | ALS | 308 | 0.77146282 | 0.06638936 | 1.39E-06 | 8.35E-06 | **** | 1 | 0.016810024 | 0.883070872 |
| 6 | Motion interval_episode | 8 | ALS | 196 | 1.36242193 | 0.18236752 | 5.16E-01 | 1.00E+00 | ns | 1 | 0.016810024 | 0.883070872 |
| 6 | Motion interval_episode | 10 | ALS | 273 | 0.71813797 | 0.06201361 | 5.89E-04 | 3.53E-03 | ** | 1 | 0.016810024 | 0.883070872 |
| 7 | Body angle_min | 0 | NALS | 376 | 1 | 0.04596831 | 1 | 1 | ns | 1 | 1 | 0.304225285 |
| 7 | Body angle_min | 2 | NALS | 304 | 0.79508354 | 0.03619024 | 3.08E-01 | 1 | ns | 1 | 1 | 0.304225285 |
| 7 | Body angle_min | 4 | NALS | 307 | 0.81305217 | 0.03482307 | 0.9594559 | 1 | ns | 1 | 1 | 0.304225285 |
| 7 | Body angle_min | 6 | NALS | 307 | 0.81299036 | 0.03817422 | 1.01E-01 | 6.08E-01 | ns | 1 | 1 | 0.304225285 |
| 7 | Body angle_min | 8 | NALS | 302 | 0.71577534 | 0.03738867 | 1.9E-01 | 1.00E+00 | ns | 1 | 1 | 0.304225285 |
| 7 | Body angle_min | 10 | NALS | 334 | 0.80505419 | 0.03500197 | 7.4957E-06 | 4.4974E-05 | **** | 1 | 1 | 0.304225285 |
| 7 | Body angle_min | 0 | ALS | 273 | 1 | 0.05400547 | 1 | 1 | ns | 1 | 1 | 0.304225285 |
| 7 | Body angle_min | 2 | ALS | 293 | 0.74307857 | 0.03581768 | 3.08E-01 | 1 | ns | 1 | 1 | 0.304225285 |
| 7 | Body angle_min | 4 | ALS | 196 | 0.81028221 | 0.04086952 | 0.9594559 | 1 | ns | 1 | 1 | 0.304225285 |
| 7 | Body angle_min | 6 | ALS | 266 | 0.72754046 | 0.03444626 | 1.01E-01 | 6.08E-01 | ns | 1 | 1 | 0.304225285 |
| 7 | Body angle_min | 8 | ALS | 145 | 0.64179088 | 0.0427938 | 1.9E-01 | 1.00E+00 | ns | 1 | 1 | 0.304225285 |
| 7 | Body angle_min | 10 | ALS | 229 | 0.57309335 | 0.03509963 | 7.4957E-06 | 4.4974E-05 | **** | 1 | 1 | 0.304225285 |
| 8 | Feet 2D distance_max | 0 | NALS | 376 | 1 | 0.01657013 | 1 | 1 | ns | 1 | 1 | 0.516958231 |
| 8 | Feet 2D distance_max | 2 | NALS | 358 | 0.98026509 | 0.02707125 | 1.44E-01 | 8.43E-01 | ns | 1 | 1 | 0.516958231 |
| 8 | Feet 2D distance_max | 4 | NALS | 380 | 0.97145055 | 0.00793301 | 6.65E-01 | 1.00E+00 | ns | 1 | 1 | 0.516958231 |
| 8 | Feet 2D distance_max | 6 | NALS | 339 | 0.9875502 | 0.00701031 | 3.51E-05 | 2.10E-04 | *** | 1 | 1 | 0.516958231 |
| 8 | Feet 2D distance_max | 8 | NALS | 368 | 1.01592528 | 0.00735481 | 1.94E-35 | 1.17E-34 | **** | 1 | 1 | 0.516958231 |
| 8 | Feet 2D distance_max | 10 | NALS | 362 | 1.04690109 | 0.00993356 | 7.78E-48 | 4.67E-47 | **** | 1 | 1 | 0.516958231 |
| 8 | Feet 2D distance_max | 0 | ALS | 273 | 1 | 0.02588441 | 1 | 1 | ns | 1 | 1 | 0.516958231 |
| 8 | Feet 2D distance_max | 2 | ALS | 347 | 0.9546637 | 0.01611396 | 1.44E-01 | 8.43E-01 | ns | 1 | 1 | 0.516958231 |
| 8 | Feet 2D distance_max | 4 | ALS | 235 | 0.96579816 | 0.0105285 | 6.65E-01 | 1.00E+00 | ns | 1 | 1 | 0.516958231 |
| 8 | Feet 2D distance_max | 6 | ALS | 312 | 0.94955939 | 0.00568295 | 3.51E-05 | 2.10E-04 | *** | 1 | 1 | 0.516958231 |
| 8 | Feet 2D distance_max | 8 | ALS | 196 | 0.86166204 | 0.00778082 | 1.94E-35 | 1.17E-34 | **** | 1 | 1 | 0.516958231 |
| 8 | Feet 2D distance_max | 10 | ALS | 277 | 0.84152512 | 0.00717214 | 7.78E-48 | 4.67E-47 | **** | 1 | 1 | 0.516958231 |
| 9 | Neck 3D velocity_std | 0 | NALS | 376 | 1 | 0.0278789 | 1 | 1 | ns | 1 | 1 | 0.107653309 |
| 9 | Neck 3D velocity_std | 2 | NALS | 304 | 0.98031819 | 0.02743405 | 3.75E-03 | 0.02250378 | * | 1 | 1 | 0.107653309 |
| 9 | Neck 3D velocity_std | 4 | NALS | 307 | 0.82747987 | 0.01961831 | 2.73E-02 | 1.64E-01 | ns | 1 | 1 | 0.107653309 |
| 9 | Neck 3D velocity_std | 6 | NALS | 307 | 0.98887865 | 0.02191371 | 3.16E-04 | 1.89E-03 | ** | 1 | 1 | 0.107653309 |
| 9 | Neck 3D velocity_std | 8 | NALS | 302 | 1.00558224 | 0.02265851 | 2.62E-12 | 1.57E-11 | **** | 1 | 1 | 0.107653309 |
| 9 | Neck 3D velocity_std | 10 | NALS | 334 | 0.85795612 | 0.0195485 | 2.20E-15 | 1.32E-14 | **** | 1 | 1 | 0.107653309 |
| 9 | Neck 3D velocity_std | 0 | ALS | 273 | 1 | 0.03254331 | 1 | 1 | ns | 1 | 1 | 0.107653309 |
| 9 | Neck 3D velocity_std | 2 | ALS | 293 | 0.87661505 | 0.02252859 | 3.75E-03 | 0.02250378 | * | 1 | 1 | 0.107653309 |
| 9 | Neck 3D velocity_std | 4 | ALS | 196 | 0.7569271 | 0.02243006 | 2.73E-02 | 1.64E-01 | ns | 1 | 1 | 0.107653309 |
| 9 | Neck 3D velocity_std | 6 | ALS | 266 | 0.87139089 | 0.02394019 | 3.16E-04 | 1.89E-03 | ** | 1 | 1 | 0.107653309 |
| 9 | Neck 3D velocity_std | 8 | ALS | 145 | 0.72835876 | 0.02936129 | 2.62E-12 | 1.57E-11 | **** | 1 | 1 | 0.107653309 |
| 9 | Neck 3D velocity_std | 10 | ALS | 229 | 0.6064744 | 0.02391752 | 2.20E-15 | 1.32E-14 | **** | 1 | 1 | 0.107653309 |
| 10 | Feet 2D distance_std | 0 | NALS | 376 | 1 | 0.03356456 | 1 | 1 | ns | 1 | 1 | 0.811100356 |
| 10 | Feet 2D distance_std | 2 | NALS | 357 | 0.92799108 | 0.0240047 | 1.14E-05 | 6.85E-05 | **** | 1 | 1 | 0.811100356 |
| 10 | Feet 2D distance_std | 4 | NALS | 380 | 0.90313332 | 0.02483672 | 2.16E-01 | 1.00E+00 | ns | 1 | 1 | 0.811100356 |
| 10 | Feet 2D distance_std | 6 | NALS | 339 | 0.95895581 | 0.0233896 | 1.14E-01 | 6.84E-01 | ns | 1 | 1 | 0.811100356 |
| 10 | Feet 2D distance_std | 8 | NALS | 368 | 1.02144198 | 0.02553059 | 1.60E-07 | 9.59E-07 | **** | 1 | 1 | 0.811100356 |
| 10 | Feet 2D distance_std | 10 | NALS | 362 | 1.05243534 | 0.03074214 | 1.58E-21 | 9.49E-21 | **** | 1 | 1 | 0.811100356 |
| 10 | Feet 2D distance_std | 0 | ALS | 273 | 1 | 0.05668319 | 1 | 1 | ns | 1 | 1 | 0.811100356 |
| 10 | Feet 2D distance_std | 2 | ALS | 347 | 1.15120732 | 0.04486392 | 1.14E-05 | 6.85E-05 | **** | 1 | 1 | 0.811100356 |
| 10 | Feet 2D distance_std | 4 | ALS | 235 | 0.95455645 | 0.0342047 | 2.16E-01 | 1.00E+00 | ns | 1 | 1 | 0.811100356 |
| 10 | Feet 2D distance_std | 6 | ALS | 312 | 1.0165472 | 0.02816934 | 1.14E-01 | 6.84E-01 | ns | 1 | 1 | 0.811100356 |
| 10 | Feet 2D distance_std | 8 | ALS | 196 | 0.79733981 | 0.03238438 | 1.60E-07 | 9.59E-07 | **** | 1 | 1 | 0.811100356 |
| 10 | Feet 2D distance_std | 10 | ALS | 277 | 0.63849569 | 0.02603855 | 1.58E-21 | 9.49E-21 | **** | 1 | 1 | 0.811100356 |
| 11 | Chest 3D velocity_mean | 0 | NALS | 376 | 1 | 0.02156116 | 1 | 1 | ns | 1 | 1 | 0.620057799 |
| 11 | Chest 3D velocity_mean | 2 | NALS | 304 | 0.86298819 | 0.01509727 | 7.03E-01 | 1.00E+00 | ns | 1 | 1 | 0.620057799 |
| 11 | Chest 3D velocity_mean | 4 | NALS | 307 | 0.85507111 | 0.01421542 | 1.42E-02 | 8.51E-02 | ns | 1 | 1 | 0.620057799 |
| 11 | Chest 3D velocity_mean | 6 | NALS | 307 | 0.90054065 | 0.01518301 | 9.21E-01 | 1.00E+00 | ns | 1 | 1 | 0.620057799 |
| 11 | Chest 3D velocity_mean | 8 | NALS | 302 | 0.92496029 | 0.01572826 | 1.49E-06 | 8.94E-06 | **** | 1 | 1 | 0.620057799 |
| 11 | Chest 3D velocity_mean | 10 | NALS | 334 | 0.88339552 | 0.01398322 | 3.67E-29 | 2.20E-28 | **** | 1 | 1 | 0.620057799 |
| 11 | Chest 3D velocity_mean | 0 | ALS | 273 | 1 | 0.02915419 | 1 | 1 | ns | 1 | 1 | 0.620057799 |
| 11 | Chest 3D velocity_mean | 2 | ALS | 293 | 0.85456281 | 0.01613098 | 7.03E-01 | 1.00E+00 | ns | 1 | 1 | 0.620057799 |
| 11 | Chest 3D velocity_mean | 4 | ALS | 196 | 0.80111808 | 0.01602561 | 1.42E-02 | 8.51E-02 | ns | 1 | 1 | 0.620057799 |
| 11 | Chest 3D velocity_mean | 6 | ALS | 266 | 0.90287087 | 0.01825411 | 9.21E-01 | 1.00E+00 | ns | 1 | 1 | 0.620057799 |
| 11 | Chest 3D velocity_mean | 8 | ALS | 145 | 0.79891128 | 0.01779593 | 1.49E-06 | 8.94E-06 | **** | 1 | 1 | 0.620057799 |
| 11 | Chest 3D velocity_mean | 10 | ALS | 229 | 0.65620152 | 0.0108422 | 3.67E-29 | 2.20E-28 | **** | 1 | 1 | 0.620057799 |
| 12 | U-body 3D length_min | 0 | NALS | 376 | 1 | 0.02432119 | 1 | 1 | ns | 1 | 1 | 0.942228388 |
| 12 | U-body 3D length_min | 2 | NALS | 357 | 0.97598784 | 0.01935181 | 0.60294466 | 1 | ns | 1 | 1 | 0.942228388 |
| 12 | U-body 3D length_min | 4 | NALS | 380 | 0.9930572 | 0.01918147 | 0.37624872 | 1 | ns | 1 | 1 | 0.942228388 |
| 12 | U-body 3D length_min | 6 | NALS | 339 | 0.9680305 | 0.02083948 | 2.84E-01 | 1 | ns | 1 | 1 | 0.942228388 |
| 12 | U-body 3D length_min | 8 | NALS | 368 | 0.95079404 | 0.0209082 | 0.83490091 | 1 | ns | 1 | 1 | 0.942228388 |
| 12 | U-body 3D length_min | 10 | NALS | 362 | 0.94442628 | 0.02252607 | 8.02E-03 | 4.81E-02 | * | 1 | 1 | 0.942228388 |
| 12 | U-body 3D length_min | 0 | ALS | 273 | 1 | 0.02989751 | 1 | 1 | ns | 1 | 1 | 0.942228388 |
| 12 | U-body 3D length_min | 2 | ALS | 347 | 0.98925294 | 0.01649443 | 0.60294466 | 1 | ns | 1 | 1 | 0.942228388 |
| 12 | U-body 3D length_min | 4 | ALS | 235 | 0.96668502 | 0.0217299 | 0.37624872 | 1 | ns | 1 | 1 | 0.942228388 |
| 12 | U-body 3D length_min | 6 | ALS | 312 | 0.93877102 | 0.01759829 | 2.88E-01 | 1 | ns | 1 | 1 | 0.942228388 |
| 12 | U-body 3D length_min | 8 | ALS | 196 | 0.95756265 | 0.02089785 | 0.83490091 | 1 | ns | 1 | 1 | 0.942228388 |
| 12 | U-body 3D length_min | 10 | ALS | 277 | 1.02513554 | 0.01834954 | 8.02E-03 | 4.81E-02 | * | 1 | 1 | 0.942228388 |
| 13 | Right limb angle asym._min | 0 | NALS | 376 | 1 | 0.04110313 | 1 | 1 | ns | 1 | 1 | 0.80659571 |
| 13 | Right limb angle asym._min | 2 | NALS | 304 | 1.09850295 | 0.04049394 | 1.71E-05 | 1.02E-04 | *** | 1 | 1 | 0.80659571 |
| 13 | Right limb angle asym._min | 4 | NALS | 307 | 1.00080038 | 0.03934924 | 0.00012471 | 0.00074826 | *** | 1 | 1 | 0.80659571 |
| 13 | Right limb angle asym._min | 6 | NALS | 307 | 1.04028227 | 0.03878293 | 4.51E-03 | 2.70E-02 | * | 1 | 1 | 0.80659571 |
| 13 | Right limb angle asym._min | 8 | NALS | 302 | 1.0586897 | 0.03544283 | 7.16E-05 | 4.30E-04 | *** | 1 | 1 | 0.80659571 |
| 13 | Right limb angle asym._min | 10 | NALS | 334 | 1.02694719 | 0.03690332 | 7.91E-06 | 4.75E-05 | **** | 1 | 1 | 0.80659571 |
| 13 | Right limb angle asym._min | 0 | ALS | 273 | 1 | 0.04686535 | 1 | 1 | ns | 1 | 1 | 0.80659571 |
| 13 | Right limb angle asym._min | 2 | ALS | 293 | 0.85238325 | 0.03972518 | 1.71E-05 | 1.02E-04 | *** | 1 | 1 | 0.80659571 |
| 13 | Right limb angle asym._min | 4 | ALS | 196 | 0.76195857 | 0.04665055 | 0.00012471 | 0.00074826 | *** | 1 | 1 | 0.80659571 |
| 13 | Right limb angle asym._min | 6 | ALS | 266 | 0.88358906 | 0.0384852 | 4.51E-03 | 2.70E-02 | * | 1 | 1 | 0.80659571 |
| 13 | Right limb angle asym._min | 8 | ALS | 145 | 0.8147155 | 0.04759504 | 7.16E-05 | 4.30E-04 | *** | 1 | 1 | 0.80659571 |
| 13 | Right limb angle asym._min | 10 | ALS | 229 | 0.78298556 | 0.03702678 | 7.91E-06 | 4.75E-05 | **** | 1 | 1 | 0.80659571 |
| 14 | Hands 3D distance_max | 0 | NALS | 376 | 1 | 0.0335389 | 1 | 1 | ns | 1 | 1 | 0.609716905 |
| 14 | Hands 3D distance_max | 2 | NALS | 357 | 0.9024908 | 0.02903106 | 6.67E-01 | 1.00E+00 | ns | 1 | 1 | 0.609716905 |
| 14 | Hands 3D distance_max | 4 | NALS | 380 | 0.86823346 | 0.02665607 | 7.86E-01 | 1.00E+00 | ns | 1 | 1 | 0.609716905 |
| 14 | Hands 3D distance_max | 6 | NALS | 339 | 0.90443754 | 0.02888204 | 6.36E-01 | 1.00E+00 | ns | 1 | 1 | 0.609716905 |
| 14 | Hands 3D distance_max | 8 | NALS | 368 | 0.88684209 | 0.0290095 | 3.68E-01 | 1.00E+00 | ns | 1 | 1 | 0.609716905 |
| 14 | Hands 3D distance_max | 10 | NALS | 362 | 0.92213668 | 0.02888026 | 3.02E-06 | 1.81E-05 | **** | 1 | 1 | 0.609716905 |
| 14 | Hands 3D distance_max | 0 | ALS | 273 | 1 | 0.03987492 | 1 | 1 | ns | 1 | 1 | 0.609716905 |
| 14 | Hands 3D distance_max | 2 | ALS | 347 | 0.92077645 | 0.03100609 | 6.67E-01 | 1.00E+00 | ns | 1 | 1 | 0.609716905 |
| 14 | Hands 3D distance_max | 4 | ALS | 235 | 0.85620889 | 0.03615509 | 7.86E-01 | 1.00E+00 | ns | 1 | 1 | 0.609716905 |
| 14 | Hands 3D distance_max | 6 | ALS | 312 | 0.92509809 | 0.0329777 | 6.36E-01 | 1.00E+00 | ns | 1 | 1 | 0.609716905 |
| 14 | Hands 3D distance_max | 8 | ALS | 196 | 0.84181903 | 0.04150033 | 3.68E-01 | 1.00E+00 | ns | 1 | 1 | 0.609716905 |
| 14 | Hands 3D distance_max | 10 | ALS | 277 | 0.7290871 | 0.02774198 | 3.02E-06 | 1.81E-05 | **** | 1 | 1 | 0.609716905 |
| 15 | Left limb angle asym._min | 0 | NALS | 376 | 1 | 0.0467893 | 1 | 1 | ns | 1 | 1.00E+00 | 0.743280976 |
| 15 | Left limb angle asym._min | 2 | NALS | 304 | 1.06999864 | 0.04338117 | 5.74E-07 | 3.44E-06 | **** | 1 | 1.00E+00 | 0.743280976 |
| 15 | Left limb angle asym._min | 4 | NALS | 307 | 0.94778073 | 0.03882191 | 3.85E-05 | 2.31E-04 | *** | 1 | 1.00E+00 | 0.743280976 |
| 15 | Left limb angle asym._min | 6 | NALS | 307 | 1.00856294 | 0.03895553 | 1.51E-04 | 9.08E-04 | *** | 1 | 1.00E+00 | 0.743280976 |
| 15 | Left limb angle asym._min | 8 | NALS | 302 | 1.07605138 | 0.03977225 | 1.89E-04 | 1.13E-03 | ** | 1 | 1.00E+00 | 0.743280976 |
| 15 | Left limb angle asym._min | 10 | NALS | 334 | 0.98187107 | 0.03953998 | 4.39E-03 | 2.64E-02 | * | 1 | 1.00E+00 | 0.743280976 |
| 15 | Left limb angle asym._min | 0 | ALS | 273 | 1 | 0.04589296 | 1 | 1 | ns | 1 | 1.00E+00 | 0.743280976 |
| 15 | Left limb angle asym._min | 2 | ALS | 293 | 0.77185119 | 0.03979295 | 5.74E-07 | 3.44E-06 | **** | 1 | 1.00E+00 | 0.743280976 |
| 15 | Left limb angle asym._min | 4 | ALS | 196 | 0.69626255 | 0.04523548 | 3.85E-05 | 2.31E-04 | *** | 1 | 1.00E+00 | 0.743280976 |
| 15 | Left limb angle asym._min | 6 | ALS | 266 | 0.803321 | 0.03632565 | 1.51E-04 | 9.08E-04 | *** | 1 | 1.00E+00 | 0.743280976 |
| 15 | Left limb angle asym._min | 8 | ALS | 145 | 0.82398955 | 0.04969788 | 1.89E-04 | 1.13E-03 | ** | 1 | 1.00E+00 | 0.743280976 |
| 15 | Left limb angle asym._min | 10 | ALS | 229 | 0.81431364 | 0.04098797 | 4.39E-03 | 2.64E-02 | * | 1 | 1.00E+00 | 0.743280976 |
| 16 | Chest 1D velocity_max | 0 | NALS | 379 | 1 | 0.13463781 | 1 | 1 | ns | 1 | 1.00E+00 | 0.983022387 |
| 16 | Chest 1D velocity_max | 2 | NALS | 361 | 0.49198807 | 0.02526344 | 1.48E-01 | 8.87E-01 | ns | 1 | 1.00E+00 | 0.983022387 |
| 16 | Chest 1D velocity_max | 4 | NALS | 384 | 0.49331164 | 0.02152096 | 1.12E-04 | 6.73E-04 | *** | 1 | 1.00E+00 | 0.983022387 |
| 16 | Chest 1D velocity_max | 6 | NALS | 343 | 0.55845347 | 0.02828607 | 2.61E-02 | 1.57E-01 | ns | 1 | 1.00E+00 | 0.983022387 |
| 16 | Chest 1D velocity_max | 8 | NALS | 372 | 0.48715029 | 0.02632421 | 1.72E-08 | 1.03E-07 | **** | 1 | 1.00E+00 | 0.983022387 |
| 16 | Chest 1D velocity_max | 10 | NALS | 366 | 0.48723923 | 0.02551524 | 1.72E-20 | 1.03E-19 | **** | 1 | 1.00E+00 | 0.983022387 |
| 16 | Chest 1D velocity_max | 0 | ALS | 276 | 1 | 0.17665812 | 1 | 1 | ns | 1 | 1.00E+00 | 0.983022387 |
| 16 | Chest 1D velocity_max | 2 | ALS | 351 | 0.44513878 | 0.02001336 | 1.48E-01 | 8.87E-01 | ns | 1 | 1.00E+00 | 0.983022387 |
| 16 | Chest 1D velocity_max | 4 | ALS | 238 | 0.36632892 | 0.02270576 | 1.12E-04 | 6.73E-04 | *** | 1 | 1.00E+00 | 0.983022387 |
| 16 | Chest 1D velocity_max | 6 | ALS | 316 | 0.47752768 | 0.02208554 | 2.61E-02 | 1.57E-01 | ns | 1 | 1.00E+00 | 0.983022387 |
| 16 | Chest 1D velocity_max | 8 | ALS | 198 | 0.2651377 | 0.01954777 | 1.72E-08 | 1.03E-07 | **** | 1 | 1.00E+00 | 0.983022387 |
| 16 | Chest 1D velocity_max | 10 | ALS | 280 | 0.18914288 | 0.01213636 | 1.72E-20 | 1.03E-19 | **** | 1 | 1.00E+00 | 0.983022387 |
| 17 | Leg angle asym._std | 0 | NALS | 376 | 1 | 0.03027278 | 1 | 1 | ns | 1 | 0.741834603 | 0.816010316 |
| 17 | Leg angle asym._std | 2 | NALS | 304 | 0.81165023 | 0.02808353 | 8.51E-01 | 1.00E+00 | ns | 1 | 0.741834603 | 0.816010316 |
| 17 | Leg angle asym._std | 4 | NALS | 307 | 0.88268709 | 0.03102684 | 4.71E-01 | 1.00E+00 | ns | 1 | 0.741834603 | 0.816010316 |
| 17 | Leg angle asym._std | 6 | NALS | 307 | 0.85416432 | 0.03016555 | 3.79E-01 | 1.00E+00 | ns | 1 | 0.741834603 | 0.816010316 |
| 17 | Leg angle asym._std | 8 | NALS | 302 | 0.84502092 | 0.03116537 | 7.07E-01 |

**Supplementary Table 7. Statistical comparisons of the top 20 features identified by the XGB model comparing PD (A5) and ALS groups.** For each feature, values from PD (at 10 wk post-surgery) and ALS (at 20 wk of age) groups were normalised relative to their matched control group means (CT for PD, WT for ALS). Statistical significance was assessed using Welch's t-test (unequal variances) comparing each disease group to their respective control group. Source data are provided in Supplementary Tables 4 and 6.

| Rank | Parameter | Group | n | Mean_diff | SEM_diff | corrected_p | Significance |
|---|---|---|---|---|---|---|---|
| 1 | Hands 3D distance_mean | PD(A5) | 2756 | 0.162686334 | 0.014584544 | 1.97E-14 | **** |
| 1 | Hands 3D distance_mean | ALS | 277 | 0.045468225 | 0.03025326 | 0.794408044 | ns |
| 2 | Motion duration_episode | PD(A5) | 2826 | 0.787204636 | 0.041538671 | 4.28E-33 | **** |
| 2 | Motion duration_episode | ALS | 280 | -0.198104276 | 0.063150715 | 1.48E-02 | * |
| 3 | Body 2D length_min | PD(A5) | 2797 | 0.207146827 | 0.009967946 | 1.41E-95 | **** |
| 3 | Body 2D length_min | ALS | 277 | 0.180536399 | 0.030164893 | 6.83E-08 | **** |
| 4 | Tail angle_mean | PD(A5) | 2784 | 0.079448551 | 0.004191403 | 6.81E-102 | **** |
| 4 | Tail angle_mean | ALS | 229 | 0.01938635 | 0.016780802 | 1 | ns |
| 5 | Arm angle asym._std | PD(A5) | 2771 | 0.404388738 | 0.01897521 | 5.66E-59 | **** |
| 5 | Arm angle asym._std | ALS | 229 | -0.100914471 | 0.051592941 | 0.296609597 | ns |
| 6 | Motion interval_episode | PD(A5) | 2790 | -1.388804715 | 0.079958603 | 8.24E-124 | **** |
| 6 | Motion interval_episode | ALS | 273 | -0.407365168 | 0.110431428 | 0.003531384 | ** |
| 7 | Body angle_min | PD(A5) | 2796 | 0.081157082 | 0.025905914 | 0.005882938 | ** |
| 7 | Body angle_min | ALS | 229 | -0.231960833 | 0.04956936 | 4.49743E-05 | **** |
| 8 | Feet 2D distance_max | PD(A5) | 2786 | 0.09003698 | 0.005120403 | 1.97E-45 | **** |
| 8 | Feet 2D distance_max | ALS | 277 | -0.205375963 | 0.01225215 | 4.67E-47 | **** |
| 9 | Neck 3D velocity_std | PD(A5) | 2779 | -0.068560416 | 0.008704187 | 2.82575E-14 | **** |
| 9 | Neck 3D velocity_std | ALS | 229 | -0.251481717 | 0.030889996 | 1.32E-14 | **** |
| 10 | Feet 2D distance_std | PD(A5) | 2784 | 0.44093211 | 0.020853577 | 3.51E-72 | **** |
| 10 | Feet 2D distance_std | ALS | 277 | -0.413939657 | 0.040287533 | 9.49E-21 | **** |
| 11 | Chest 3D velocity_mean | PD(A5) | 2807 | 0.157380852 | 0.013473108 | 3.90E-26 | **** |
| 11 | Chest 3D velocity_mean | ALS | 229 | -0.227108 | 0.017694173 | 2.20E-28 | **** |
| 12 | U-body 3D length_min | PD(A5) | 2786 | 0.03724519 | 0.00585367 | 2.29E-11 | **** |
| 12 | U-body 3D length_min | ALS | 277 | 0.08070926 | 0.029053906 | 4.81E-02 | * |
| 13 | Right limb angle asym._min | PD(A5) | 2748 | 0.209480031 | 0.01885907 | 1.42E-15 | **** |
| 13 | Right limb angle asym._min | ALS | 229 | -0.243961629 | 0.05227655 | 4.74756E-05 | **** |
| 14 | Hands 3D distance_max | PD(A5) | 2766 | 0.263567435 | 0.013461755 | 3.04E-43 | **** |
| 14 | Hands 3D distance_max | ALS | 277 | -0.193049579 | 0.040046059 | 1.81E-05 | **** |
| 15 | Left limb angle asym._min | PD(A5) | 2750 | 0.377645194 | 0.019315189 | 4.19E-47 | **** |
| 15 | Left limb angle asym._min | ALS | 229 | -0.167557435 | 0.056951063 | 0.026367472 | * |
| 16 | Chest 1D velocity_max | PD(A5) | 2798 | -0.437640672 | 0.029897602 | 4.33E-75 | **** |
| 16 | Chest 1D velocity_max | ALS | 280 | -0.298096347 | 0.028254535 | 1.03E-19 | **** |
| 17 | Leg angle asym._std | PD(A5) | 2793 | 0.422838958 | 0.017048476 | 2.57E-94 | **** |
| 17 | Leg angle asym._std | ALS | 229 | 0.062658523 | 0.055313579 | 1 | ns |
| 18 | Feet 2D distance_mean | PD(A5) | 2782 | 0.001800359 | 0.005788474 | 1 | ns |
| 18 | Feet 2D distance_mean | ALS | 277 | -0.104519653 | 0.013523291 | 2.14302E-12 | **** |
| 19 | Anus 1D velocity_std | PD(A5) | 2790 | -0.156951379 | 0.019093362 | 1.28E-16 | **** |
| 19 | Anus 1D velocity_std | ALS | 277 | -0.365009519 | 0.029104378 | 1.69E-29 | **** |
| 20 | Arm angle asym._mean | PD(A5) | 2746 | 1.694347026 | 0.157733005 | 1.05E-15 | **** |
| 20 | Arm angle asym._mean | ALS | 229 | 0.593278188 | 0.217554004 | 0.06476644 | ns |

**Supplementary Table 8. Statistical summary of the APS (XGB model-predicted PD scores) at 10 wk across groups.** Statistical analysis was performed using one-way ANOVA, followed by Bonferroni's correction for multiple comparisons. Source data are provided in the Source Data file (See S_Figure 25).

| Group | Number of values | Mean | Std. Deviation | Std. Error of Mean |
|---|---|---|---|---|
| EV | 10 | 12.11 | 2.698 | 0.8531 |
| A5 | 12 | 85.61 | 6.729 | 1.942 |
| A5OD | 7 | 68.77 | 17.54 | 6.628 |
| A5O1 | 7 | 82 | 9.655 | 3.649 |
| A5O2 | 6 | 75.93 | 17.14 | 6.998 |
| A1 | 15 | 58.01 | 25.9 | 6.688 |
| A1OD | 10 | 62.26 | 20.21 | 6.392 |
| A1O1 | 7 | 52.88 | 22.27 | 8.415 |
| A1O2 | 12 | 29.06 | 17.11 | 4.94 |
| A1O3 | 8 | 29.41 | 18.97 | 6.708 |

| ANOVA summary | |
|---|---|
| F | 18.74 |
| P value | <0.0001 |
| P value summary | **** |
| Significant diff. among means (P < 0.05)? | Yes |
| R squared | 0.6676 |

| Bonferroni's multiple comparisons test | Mean Diff. | 95.00% CI of diff. | Summary | Adjusted P Value |
|---|---|---|---|---|
| EV vs. A5 | -73.5 | -95.03 to -51.96 | **** | <0.0001 |
| EV vs. A5OD | -56.66 | -81.44 to -31.88 | **** | <0.0001 |
| EV vs. A5O1 | -69.89 | -94.67 to -45.10 | **** | <0.0001 |
| EV vs. A5O2 | -63.82 | -89.79 to -37.85 | **** | <0.0001 |
| EV vs. A1 | -45.9 | -66.43 to -25.37 | **** | <0.0001 |
| EV vs. A1OD | -50.15 | -72.64 to -27.66 | **** | <0.0001 |
| EV vs. A1O1 | -40.77 | -65.55 to -15.98 | **** | <0.0001 |
| EV vs. A1O2 | -16.95 | -38.48 to 4.583 | ns | 0.2492 |
| EV vs. A1O3 | -17.3 | -41.15 to 6.559 | ns | 0.3791 |
| A5 vs. EV | 73.5 | 51.96 to 95.03 | **** | <0.0001 |
| A5 vs. A5OD | 16.84 | -7.082 to 40.76 | ns | 0.435 |
| A5 vs. A5O1 | 3.607 | -20.31 to 27.53 | ns | >0.9999 |
| A5 vs. A5O2 | 9.673 | -15.47 to 34.82 | ns | >0.9999 |
| A5 vs. A1 | 27.6 | 8.119 to 47.07 | ** | 0.0011 |
| A5 vs. A1OD | 23.35 | 1.812 to 44.88 | * | 0.0247 |
| A5 vs. A1O1 | 32.73 | 8.809 to 56.65 | ** | 0.0018 |
| A5 vs. A1O2 | 56.55 | 36.01 to 77.08 | **** | <0.0001 |
| A5 vs. A1O3 | 56.2 | 33.24 to 79.15 | **** | <0.0001 |
| A1 vs. EV | 45.9 | 25.37 to 66.43 | **** | <0.0001 |
| A1 vs. A5 | -27.6 | -47.07 to -8.119 | ** | 0.0011 |
| A1 vs. A5OD | -10.76 | -33.78 to 12.26 | ns | >0.9999 |
| A1 vs. A5O1 | -23.99 | -47.01 to -0.9689 | * | 0.0353 |
| A1 vs. A5O2 | -17.92 | -42.22 to 6.369 | ns | 0.3485 |
| A1 vs. A1OD | -4.251 | -24.78 to 16.28 | ns | >0.9999 |
| A1 vs. A1O1 | 5.131 | -17.89 to 28.15 | ns | >0.9999 |
| A1 vs. A1O2 | 28.95 | 9.470 to 48.43 | *** | 0.0005 |
| A1 vs. A1O3 | 28.6 | 6.585 to 50.62 | ** | 0.0035 |

**Supplementary Table 9. Statistical summary of the KL divergences for the top 20 features identified by the XGB model.** For each group, the KL divergence of each feature compared to the CT counterpart was computed at 10 wk. Each group consists of 6 sampling sets, each containing 150 randomly selected clips. A one-way ANOVA was performed across groups, followed by pairwise comparisons using t-tests against the reference groups (CT or A1). The p-values from pairwise comparisons were corrected for multiple comparisons using the Holm–Sidak method. Source data are provided in the Source Data file (See S_Figure 29).

| Rank | Parameter | Group | n | Mean | SEM | ANOVA p-value | Reference | Raw Post-hoc p-value | Corrected Post-hoc p-value | Significance | Reference | Raw Post-hoc p-value | Corrected Post-hoc p-value | Significance |
|---|---|---|---|---|---|---|---|---|---|---|---|---|---|---|
| 1 | Hands 3D distance (mean) | CT | 6 | 0 | 0 | 1.4657E-11 | CT | | | | A1 | 8.5978E-05 | 0.00034387 | *** |
| 1 | Hands 3D distance (mean) | A5 | 6 | 0.24853803 | 0.02091022 | 1.4657E-11 | CT | 7.4259E-05 | 0.000297 | *** | A1 | 0.00035378 | 0.00106097 | ** |
| 1 | Hands 3D distance (mean) | A1 | 6 | 0.09672699 | 0.0083876 | 1.4657E-11 | CT | 8.5978E-05 | 0.000297 | *** | A1 | | | |
| 1 | Hands 3D distance (mean) | A1O3 | 6 | 0.03812882 | 0.00734181 | 1.4657E-11 | CT | 0.00348621 | 0.00696026 | ** | A1 | 0.00039152 | 0.00106097 | ** |
| 2 | Motion duration (episode) | CT | 6 | 0 | 0 | 1.0213E-16 | CT | | | | A1 | 0.00016279 | 0.0004883 | *** |
| 2 | Motion duration (episode) | A5 | 6 | 0.93621279 | 0.03433908 | 1.0213E-16 | CT | 1.242E-06 | 4.9681E-06 | **** | A1 | 2.4896E-07 | 9.9584E-07 | **** |
| 2 | Motion duration (episode) | A1 | 6 | 0.13810015 | 0.01367004 | 1.0213E-16 | CT | 0.00016279 | 0.0004883 | *** | A1 | | | |
| 2 | Motion duration (episode) | A1O3 | 6 | 0.14644016 | 0.03310061 | 1.0213E-16 | CT | 0.00686575 | 0.01368435 | * | A1 | 0.82285053 | 0.96861806 | |
| 3 | Body 2D length (min) | CT | 6 | 0 | 0 | 1.7628E-06 | CT | | | | A1 | 0.00151666 | 0.00605287 | ** |
| 3 | Body 2D length (min) | A5 | 6 | 0.1625595 | 0.02377397 | 1.7628E-06 | CT | 0.00102104 | 0.00407792 | ** | A1 | 0.03412213 | 0.09891317 | |
| 3 | Body 2D length (min) | A1 | 6 | 0.09186109 | 0.01465504 | 1.7628E-06 | CT | 0.00151666 | 0.00454309 | ** | A1 | | | |
| 3 | Body 2D length (min) | A1O3 | 6 | 0.05542202 | 0.00901598 | 1.7628E-06 | CT | 0.00165607 | 0.00454309 | ** | A1 | 0.06577993 | 0.12723287 | |
| 4 | Tail angle (mean) | CT | 6 | 0 | 0 | 6.2023E-09 | CT | | | | A1 | 0.00202415 | 0.00606017 | ** |
| 4 | Tail angle (mean) | A5 | 6 | 0.53773734 | 0.07829356 | 6.2023E-09 | CT | 0.00100041 | 0.00299822 | ** | A1 | 0.00122854 | 0.00490512 | ** |
| 4 | Tail angle (mean) | A1 | 6 | 0.02546974 | 0.00433337 | 6.2023E-09 | CT | 0.00202415 | 0.0040442 | ** | A1 | | | |
| 4 | Tail angle (mean) | A1O3 | 6 | 0.04029791 | 0.00467342 | 6.2023E-09 | CT | 0.00034628 | 0.00138442 | ** | A1 | 0.04243136 | 0.08306231 | |
| 5 | Arm angle asym. (std) | CT | 6 | 0 | 0 | 3.9614E-12 | CT | | | | A1 | 0.00065626 | 0.00196748 | ** |
| 5 | Arm angle asym. (std) | A5 | 6 | 0.22156443 | 0.01282172 | 3.9614E-12 | CT | 1.1887E-05 | 4.7548E-05 | **** | A1 | 1.4311E-05 | 5.7244E-05 | **** |
| 5 | Arm angle asym. (std) | A1 | 6 | 0.08598877 | 0.01142796 | 3.9614E-12 | CT | 0.00065626 | 0.00131208 | ** | A1 | | | |
| 5 | Arm angle asym. (std) | A1O3 | 6 | 0.09182841 | 0.00676987 | 3.9614E-12 | CT | 3.9026E-05 | 0.00011707 | *** | A1 | 0.67165539 | 0.89218982 | |
| 6 | Motion interval (episode) | CT | 6 | 0 | 0 | 4.3377E-05 | CT | | | | A1 | 0.00023606 | 0.0009439 | *** |
| 6 | Motion interval (episode) | A5 | 6 | 1.65484272 | 0.42703004 | 4.3377E-05 | CT | 0.01169811 | 0.02325937 | * | A1 | 0.01358664 | 0.03424944 | * |
| 6 | Motion interval (episode) | A1 | 6 | 0.06267018 | 0.00670456 | 4.3377E-05 | CT | 0.00023606 | 0.0009439 | *** | A1 | | | |
| 6 | Motion interval (episode) | A1O3 | 6 | 0.16419783 | 0.02674113 | 4.3377E-05 | CT | 0.00166435 | 0.00498473 | ** | A1 | 0.01154936 | 0.03424944 | * |
| 7 | Body angle (min) | CT | 6 | 0 | 0 | 0.00088124 | CT | | | | A1 | 0.00080964 | 0.00323464 | ** |
| 7 | Body angle (min) | A5 | 6 | 0.04903378 | 0.01228417 | 0.00088124 | CT | 0.01040966 | 0.02071095 | * | A1 | 0.11349299 | 0.30329885 | |
| 7 | Body angle (min) | A1 | 6 | 0.02524431 | 0.00351047 | 0.00088124 | CT | 0.00080964 | 0.00323464 | ** | A1 | | | |
| 7 | Body angle (min) | A1O3 | 6 | 0.02791496 | 0.00559586 | 0.00088124 | CT | 0.00414537 | 0.01238462 | * | A1 | 0.69609165 | 0.90763971 | |
| 8 | Feet 2D distance (max) | CT | 6 | 0 | 0 | 1.8123E-09 | CT | | | | A1 | 0.00011377 | 0.000455 | *** |
| 8 | Feet 2D distance (max) | A5 | 6 | 0.29763162 | 0.02183963 | 1.8123E-09 | CT | 3.8142E-05 | 0.00015256 | *** | A1 | 0.67686725 | 0.89558523 | |
| 8 | Feet 2D distance (max) | A1 | 6 | 0.28304216 | 0.02600732 | 1.8123E-09 | CT | 0.00011377 | 0.00022752 | *** | A1 | | | |
| 8 | Feet 2D distance (max) | A1O3 | 6 | 0.24577454 | 0.02015415 | 1.8123E-09 | CT | 6.5562E-05 | 0.00019667 | *** | A1 | 0.28537722 | 0.63505235 | |
| 9 | Neck 3D velocity (std) | CT | 6 | 0 | 0 | 1.019E-06 | CT | | | | A1 | 3.8947E-05 | 0.00015578 | *** |
| 9 | Neck 3D velocity (std) | A5 | 6 | 0.05858997 | 0.00767981 | 1.019E-06 | CT | 0.00061538 | 0.001845 | ** | A1 | 0.00033888 | 0.00101629 | ** |
| 9 | Neck 3D velocity (std) | A1 | 6 | 0.12224279 | 0.00900838 | 1.019E-06 | CT | 3.8947E-05 | 0.00015578 | *** | A1 | | | |
| 9 | Neck 3D velocity (std) | A1O3 | 6 | 0.11340837 | 0.02028614 | 1.019E-06 | CT | 0.00252717 | 0.00504796 | ** | A1 | 0.70265108 | 0.91158362 | |
| 10 | Feet 2D distance (std) | CT | 6 | 0 | 0 | 2.4805E-09 | CT | | | | A1 | 1.4963E-05 | 5.9849E-05 | **** |
| 10 | Feet 2D distance (std) | A5 | 6 | 0.42658563 | 0.05275707 | 2.4805E-09 | CT | 0.00046883 | 0.00093744 | *** | A1 | 0.00175341 | 0.00525101 | ** |
| 10 | Feet 2D distance (std) | A1 | 6 | 0.11166519 | 0.00677095 | 2.4805E-09 | CT | 1.4963E-05 | 5.9849E-05 | **** | A1 | | | |
| 10 | Feet 2D distance (std) | A1O3 | 6 | 0.08581155 | 0.00802658 | 2.4805E-09 | CT | 0.00012398 | 0.0003719 | *** | A1 | 0.03419018 | 0.06721139 | |
| 11 | Chest 3D velocity (mean) | CT | 6 | 0 | 0 | 1.2431E-07 | CT | | | | A1 | 0.00606837 | 0.01809487 | * |
| 11 | Chest 3D velocity (mean) | A5 | 6 | 0.28126673 | 0.04730435 | 1.2431E-07 | CT | 0.00192244 | 0.00766762 | ** | A1 | 0.00291013 | 0.01158979 | * |
| 11 | Chest 3D velocity (mean) | A1 | 6 | 0.02911746 | 0.00638831 | 1.2431E-07 | CT | 0.00606837 | 0.01809487 | * | A1 | | | |
| 11 | Chest 3D velocity (mean) | A1O3 | 6 | 0.02531245 | 0.00558812 | 1.2431E-07 | CT | 0.00622727 | 0.01809487 | * | A1 | 0.66365413 | 0.88687146 | |
| 12 | U-body 3D length (min) | CT | 6 | 0 | 0 | 8.9539E-05 | CT | | | | A1 | 0.00040001 | 0.00159909 | ** |
| 12 | U-body 3D length (min) | A5 | 6 | 0.10925164 | 0.02419242 | 8.9539E-05 | CT | 0.00630634 | 0.0125729 | * | A1 | 0.22456437 | 0.39869959 | |
| 12 | U-body 3D length (min) | A1 | 6 | 0.07455505 | 0.00891448 | 8.9539E-05 | CT | 0.00040001 | 0.00159909 | ** | A1 | | | |
| 12 | U-body 3D length (min) | A1O3 | 6 | 0.04529496 | 0.00580946 | 8.9539E-05 | CT | 0.00055601 | 0.0016671 | ** | A1 | 0.02343544 | 0.06867154 | |
| 13 | Right limb angle asym. (min) | CT | 6 | 0 | 0 | 4.3876E-18 | CT | | | | A1 | 3.5095E-06 | 1.2372E-05 | **** |
| 13 | Right limb angle asym. (min) | A5 | 6 | 0.34962419 | 0.01432611 | 4.3876E-18 | CT | 2.1536E-06 | 8.6142E-06 | **** | A1 | 3.0931E-06 | 1.2372E-05 | **** |
| 13 | Right limb angle asym. (min) | A1 | 6 | 0.100987 | 0.00456612 | 4.3876E-18 | CT | 3.5095E-06 | 1.0528E-05 | **** | A1 | | | |
| 13 | Right limb angle asym. (min) | A1O3 | 6 | 0.05092985 | 0.0032422 | 4.3876E-18 | CT | 1.9009E-05 | 3.8018E-05 | **** | A1 | 8.8969E-06 | 1.7794E-05 | **** |
| 14 | Hands 3D distance (max) | CT | 6 | 0 | 0 | 2.6677E-09 | CT | | | | A1 | 0.00220934 | 0.0066134 | ** |
| 14 | Hands 3D distance (max) | A5 | 6 | 0.33935577 | 0.03681653 | 2.6677E-09 | CT | 0.00025233 | 0.00100896 | ** | A1 | 0.00113205 | 0.00452054 | ** |
| 14 | Hands 3D distance (max) | A1 | 6 | 0.12945619 | 0.02246339 | 2.6677E-09 | CT | 0.00220934 | 0.00441381 | ** | A1 | | | |
| 14 | Hands 3D distance (max) | A1O3 | 6 | 0.04340557 | 0.00675169 | 2.6677E-09 | CT | 0.00135259 | 0.00405227 | ** | A1 | 0.01080096 | 0.02148527 | * |
| 15 | Left limb angle asym. (min) | CT | 6 | 0 | 0 | 1.2285E-10 | CT | | | | A1 | 0.00504408 | 0.01505603 | * |
| 15 | Left limb angle asym. (min) | A5 | 6 | 0.37697644 | 0.0234627 | 1.2285E-10 | CT | 1.7012E-05 | 6.8048E-05 | **** | A1 | 0.00021312 | 0.00085221 | *** |
| 15 | Left limb angle asym. (min) | A1 | 6 | 0.14843977 | 0.03116238 | 1.2285E-10 | CT | 0.00504408 | 0.01006271 | * | A1 | | | |
| 15 | Left limb angle asym. (min) | A1O3 | 6 | 0.05771553 | 0.01041517 | 1.2285E-10 | CT | 0.00262692 | 0.00786007 | ** | A1 | 0.0322279 | 0.06341716 | |
| 16 | Chest 1D velocity (max) | CT | 6 | 0 | 0 | 1.847E-10 | CT | | | | A1 | 0.00183718 | 0.00550141 | ** |
| 16 | Chest 1D velocity (max) | A5 | 6 | 0.34418727 | 0.02662771 | 1.847E-10 | CT | 4.9379E-05 | 0.0001975 | *** | A1 | 0.00024995 | 0.00099943 | *** |
| 16 | Chest 1D velocity (max) | A1 | 6 | 0.1446222 | 0.02407751 | 1.847E-10 | CT | 0.00183718 | 0.00367098 | ** | A1 | | | |
| 16 | Chest 1D velocity (max) | A1O3 | 6 | 0.08281255 | 0.0067853 | 1.847E-10 | CT | 6.5302E-05 | 0.0001975 | *** | A1 | 0.04985402 | 0.09722262 | |
| 17 | Leg angle asym. (std) | CT | 6 | 0 | 0 | 2.1019E-07 | CT | | | | A1 | 2.6731E-05 | 0.00010692 | *** |
| 17 | Leg angle asym. (std) | A5 | 6 | 0.23570965 | 0.03626673 | 2.1019E-07 | CT | 0.00128725 | 0.00257285 | ** | A1 | 0.00998463 | 0.02965581 | * |
| 17 | Leg angle asym. (std) | A1 | 6 | 0.09144966 | 0.00624036 | 2.1019E-07 | CT | 2.6731E-05 | 0.00010692 | *** | A1 | | | |
| 17 | Leg angle asym. (std) | A1O3 | 6 | 0.06996137 | 0.00527154 | 2.1019E-07 | CT | 4.3415E-05 | 0.00013024 | *** | A1 | 0.02568758 | 0.05071531 | |
| 18 | Feet 2D distance (mean) | CT | 6 | 0 | 0 | 4.6966E-09 | CT | | | | A1 | 0.00020305 | 0.00081194 | *** |
| 18 | Feet 2D distance (mean) | A5 | 6 | 0.24056345 | 0.02176779 | 4.6966E-09 | CT | 0.00010565 | 0.00031691 | *** | A1 | 0.46583436 | 0.71466707 | |
| 18 | Feet 2D distance (mean) | A1 | 6 | 0.21683894 | 0.0224773 | 4.6966E-09 | CT | 0.00020305 | 0.00040605 | *** | A1 | | | |
| 18 | Feet 2D distance (mean) | A1O3 | 6 | 0.29076692 | 0.02228808 | 4.6966E-09 | CT | 4.7205E-05 | 0.0001888 | *** | A1 | 0.04166043 | 0.11984682 | |
| 19 | Anus 1D velocity (std) | CT | 6 | 0 | 0 | 0.01465619 | CT | | | | A1 | 0.03231505 | 0.1231285 | |
| 19 | Anus 1D velocity (std) | A5 | 6 | 0.04147672 | 0.01181899 | 0.01465619 | CT | 0.01711293 | 0.05046525 | | A1 | 0.66708455 | 0.8891673 | |
| 19 | Anus 1D velocity (std) | A1 | 6 | 0.0341328 | 0.01161596 | 0.01465619 | CT | 0.03231505 | 0.06358583 | | A1 | | | |
| 19 | Anus 1D velocity (std) | A1O3 | 6 | 0.02087004 | 0.00462345 | 0.01465619 | CT | 0.00631789 | 0.02503308 | * | A1 | 0.32633501 | 0.69427431 | |
| 20 | Arm angle asym. (mean) | CT | 6 | 0 | 0 | 7.664E-08 | CT | | | | A1 | 7.0033E-05 | 0.0002801 | *** |
| 20 | Arm angle asym. (mean) | A5 | 6 | 0.14679412 | 0.01491311 | 7.664E-08 | CT | 0.00018439 | 0.00055307 | *** | A1 | 0.00315564 | 0.00943709 | ** |
| 20 | Arm angle asym. (mean) | A1 | 6 | 0.07411869 | 0.00616103 | 7.664E-08 | CT | 7.0033E-05 | 0.0002801 | *** | A1 | | | |
| 20 | Arm angle asym. (mean) | A1O3 | 6 | 0.05854297 | 0.0139324 | 7.664E-08 | CT | 0.00847379 | 0.01687578 | * | A1 | 0.34115461 | 0.56592276 | |

**Supplementary Table 10. Statistical summary of group comparisons (A1O3) for the top 20 features (identified by the XGB model) at 10 wk.** One-way ANOVA was performed, followed by post-hoc comparisons using Welch's t-tests comparing each group to the reference (CT) group. Statistical significance is indicated by asterisks after Holm–Sidak correction for multiple comparisons. This PDF table displays only the top 20 features in ascending rank order for concise presentation. Additional features are included in the full version of the table, available in the Source Data file (see S_Table 10). The underlying source data for this table is provided in the same Source Data file (see S_Figure 30).

| Rank | Parameter | Group | n | Mean | SEM | ANOVA p-value | Raw Post-hoc p-value | Corrected Post-hoc p-value | Significance |
|---|---|---|---|---|---|---|---|---|---|
| 1 | Hands 3D distance (mean) | CT | 1003 | 1.644375387 | 0.013594462 | 2.57E-13 | | | |
| 1 | Hands 3D distance (mean) | A5 | 2756 | 1.890718315 | 0.019629156 | 2.57E-13 | 1.27E-24 | 3.81E-24 | **** |
| 1 | Hands 3D distance (mean) | A1 | 954 | 1.806494177 | 0.02270016 | 2.57E-13 | 1.13E-09 | 2.26E-09 | **** |
| 1 | Hands 3D distance (mean) | A1O3 | 164 | 1.737294412 | 0.034592914 | 2.57E-13 | 0.01316317 | 0.01316317 | * |
| 2 | Motion duration (episode) | CT | 1028 | 7.456485084 | 0.150142723 | 3.90E-100 | | | |
| 2 | Motion duration (episode) | A5 | 2826 | 20.90206416 | 0.505530649 | 3.90E-100 | 5.87E-131 | 1.76E-130 | **** |
| 2 | Motion duration (episode) | A1 | 968 | 8.811329201 | 0.166990617 | 3.90E-100 | 1.92E-09 | 3.83E-09 | **** |
| 2 | Motion duration (episode) | A1O3 | 170 | 7.267058823 | 0.230052177 | 3.90E-100 | 0.49096013 | 0.49096013 | ns |
| 3 | Body 2D length (min) | CT | 1013 | 4.29673504 | 0.034882946 | 1.77E-47 | | | |
| 3 | Body 2D length (min) | A5 | 2797 | 4.858024465 | 0.018605098 | 1.77E-47 | 3.28E-43 | 9.85E-43 | **** |
| 3 | Body 2D length (min) | A1 | 959 | 4.654991922 | 0.035344274 | 1.77E-47 | 7.70E-13 | 1.54E-12 | **** |
| 3 | Body 2D length (min) | A1O3 | 165 | 4.492609563 | 0.090605563 | 1.77E-47 | 0.044885489 | 0.044885489 | * |
| 4 | Tail angle (mean) | CT | 1010 | 128.5831328 | 0.506514546 | 5.91E-183 | | | |
| 4 | Tail angle (mean) | A5 | 2784 | 139.994748 | 0.217054871 | 5.91E-183 | 2.72E-83 | 8.16E-83 | **** |
| 4 | Tail angle (mean) | A1 | 961 | 128.0040494 | 0.524420471 | 5.91E-183 | 0.427143685 | 0.427143685 | ns |
| 4 | Tail angle (mean) | A1O3 | 166 | 125.5143003 | 1.226791969 | 5.91E-183 | 0.021671597 | 0.042873535 | * |
| 5 | Arm angle asym. (std) | CT | 1004 | 19.70322 | 0.250072961 | 5.85E-52 | | | |
| 5 | Arm angle asym. (std) | A5 | 2771 | 26.45002002 | 0.258535473 | 5.85E-52 | 2.30E-74 | 6.91E-74 | **** |
| 5 | Arm angle asym. (std) | A1 | 952 | 23.02053518 | 0.382920041 | 5.85E-52 | 6.22E-13 | 1.24E-12 | **** |
| 5 | Arm angle asym. (std) | A1O3 | 165 | 22.17509838 | 0.606602649 | 5.85E-52 | 0.000211064 | 0.000211064 | *** |
| 6 | Motion interval (episode) | CT | 951 | 30.3361374 | 1.148404362 | 2.95E-208 | | | |
| 6 | Motion interval (episode) | A5 | 2790 | 6.540011947 | 0.194037366 | 2.95E-208 | 7.20E-78 | 2.16E-77 | **** |
| 6 | Motion interval (episode) | A1 | 938 | 25.30167022 | 1.303416925 | 2.95E-208 | 0.003798395 | 0.003798395 | ** |
| 6 | Motion interval (episode) | A1O3 | 151 | 54.45871965 | 4.293563319 | 2.95E-208 | 1.92E-07 | 3.84E-07 | **** |
| 7 | Body angle (min) | CT | 1007 | 9.707072693 | 0.186658265 | 1.09E-08 | | | |
| 7 | Body angle (min) | A5 | 2796 | 10.47089411 | 0.101318344 | 1.09E-08 | 0.000332208 | 0.000996294 | *** |
| 7 | Body angle (min) | A1 | 960 | 9.410668841 | 0.179847705 | 1.09E-08 | 0.252963102 | 0.252963102 | ns |
| 7 | Body angle (min) | A1O3 | 165 | 8.879004786 | 0.470058488 | 1.09E-08 | 0.103011896 | 0.195412342 | ns |
| 8 | Feet 2D distance (max) | CT | 1009 | 3.32565192 | 0.012419669 | 1.08E-58 | | | |
| 8 | Feet 2D distance (max) | A5 | 2786 | 3.648510809 | 0.01165259 | 1.08E-58 | 1.78E-75 | 5.33E-75 | **** |
| 8 | Feet 2D distance (max) | A1 | 952 | 3.661384728 | 0.016485325 | 1.08E-58 | 1.35E-55 | 2.70E-55 | **** |
| 8 | Feet 2D distance (max) | A1O3 | 165 | 3.607997611 | 0.033290847 | 1.08E-58 | 1.12E-13 | 1.12E-13 | **** |
| 9 | Neck 3D velocity (std) | CT | 1005 | 5.274273039 | 0.039629475 | 5.07E-49 | | | |
| 9 | Neck 3D velocity (std) | A5 | 2779 | 5.409820275 | 0.026329312 | 5.07E-49 | 0.004433004 | 0.004433004 | ** |
| 9 | Neck 3D velocity (std) | A1 | 960 | 4.672596162 | 0.041934851 | 5.07E-49 | 8.18E-25 | 2.45E-24 | **** |
| 9 | Neck 3D velocity (std) | A1O3 | 169 | 4.8462384 | 0.080766051 | 5.07E-49 | 3.27E-06 | 6.55E-06 | **** |
| 10 | Feet 2D distance (std) | CT | 1003 | 0.354993408 | 0.005679999 | 5.64E-102 | | | |
| 10 | Feet 2D distance (std) | A5 | 2784 | 0.538039994 | 0.004836098 | 5.64E-102 | 2.42E-119 | 7.26E-119 | **** |
| 10 | Feet 2D distance (std) | A1 | 962 | 0.4260558 | 0.007958734 | 5.64E-102 | 5.48E-13 | 1.10E-12 | **** |
| 10 | Feet 2D distance (std) | A1O3 | 163 | 0.423828528 | 0.016975625 | 5.64E-102 | 0.000161749 | 0.000161749 | *** |
| 11 | Chest 3D velocity (mean) | CT | 1017 | 4.436367595 | 0.047588901 | 2.00E-129 | | | |
| 11 | Chest 3D velocity (mean) | A5 | 2807 | 5.569819495 | 0.036728201 | 2.00E-129 | 7.74E-74 | 2.32E-73 | **** |
| 11 | Chest 3D velocity (mean) | A1 | 967 | 4.19557509 | 0.045325613 | 2.00E-129 | 0.000254915 | 0.000509765 | *** |
| 11 | Chest 3D velocity (mean) | A1O3 | 169 | 4.239961771 | 0.110176932 | 2.00E-129 | 0.103070936 | 0.103070936 | ns |
| 12 | U-body 3D length (min) | CT | 1010 | 2.955434212 | 0.015108979 | 3.00E-15 | | | |
| 12 | U-body 3D length (min) | A5 | 2786 | 3.081868406 | 0.007527144 | 3.00E-15 | 1.15E-13 | 3.46E-13 | **** |
| 12 | U-body 3D length (min) | A1 | 970 | 3.019004064 | 0.013368844 | 3.00E-15 | 0.001651656 | 0.003300585 | ** |
| 12 | U-body 3D length (min) | A1O3 | 165 | 3.01549293 | 0.034959859 | 3.00E-15 | 0.116180555 | 0.116180555 | ns |
| 13 | Right limb angle asym. (min) | CT | 1015 | -47.02516898 | 0.524497915 | 1.86E-14 | | | |
| 13 | Right limb angle asym. (min) | A5 | 2748 | -53.62158509 | 0.635222849 | 1.86E-14 | 1.59E-15 | 4.76E-15 | **** |
| 13 | Right limb angle asym. (min) | A1 | 952 | -46.56664432 | 0.809033294 | 1.86E-14 | 0.634449719 | 0.866372992 | ns |
| 13 | Right limb angle asym. (min) | A1O3 | 165 | -47.35712743 | 1.630669541 | 1.86E-14 | 0.846534536 | 0.866372992 | ns |
| 14 | Hands 3D distance (max) | CT | 1004 | 2.964436455 | 0.023111761 | 6.78E-58 | | | |
| 14 | Hands 3D distance (max) | A5 | 2766 | 3.788195691 | 0.032269093 | 6.78E-58 | 1.49E-90 | 4.48E-90 | **** |
| 14 | Hands 3D distance (max) | A1 | 952 | 3.319962597 | 0.04014604 | 6.78E-58 | 2.94E-14 | 5.87E-14 | **** |
| 14 | Hands 3D distance (max) | A1O3 | 168 | 3.144696741 | 0.067151447 | 6.78E-58 | 0.011871222 | 0.011871222 | * |
| 15 | Left limb angle asym. (min) | CT | 1013 | -52.23488367 | 0.627043819 | 4.69E-42 | | | |
| 15 | Left limb angle asym. (min) | A5 | 2750 | -67.02386119 | 0.709026864 | 4.69E-42 | 3.89E-53 | 1.17E-52 | **** |
| 15 | Left limb angle asym. (min) | A1 | 957 | -56.24930235 | 0.949519257 | 4.69E-42 | 0.000430064 | 0.000859944 | *** |
| 15 | Left limb angle asym. (min) | A1O3 | 165 | -53.41421194 | 1.614316424 | 4.69E-42 | 0.496614541 | 0.496614541 | ns |
| 16 | Chest 1D velocity (max) | CT | 1023 | 0.126115621 | 0.003979424 | 7.13E-44 | | | |
| 16 | Chest 1D velocity (max) | A5 | 2798 | 0.075819707 | 0.001556038 | 7.13E-44 | 1.62E-30 | 4.87E-30 | **** |
| 16 | Chest 1D velocity (max) | A1 | 967 | 0.080005088 | 0.003143136 | 7.13E-44 | 2.35E-19 | 4.70E-19 | **** |
| 16 | Chest 1D velocity (max) | A1O3 | 171 | 0.091935497 | 0.00854018 | 7.13E-44 | 0.000346566 | 0.000346566 | *** |
| 17 | Leg angle asym. (std) | CT | 1011 | 15.78164918 | 0.204935769 | 7.65E-67 | | | |
| 17 | Leg angle asym. (std) | A5 | 2793 | 20.78733556 | 0.159883993 | 7.65E-67 | 9.39E-77 | 2.82E-76 | **** |
| 17 | Leg angle asym. (std) | A1 | 951 | 18.4948376 | 0.244881491 | 7.65E-67 | 3.91E-17 | 7.81E-17 | **** |
| 17 | Leg angle asym. (std) | A1O3 | 168 | 17.71926441 | 0.484264242 | 7.65E-67 | 0.000285215 | 0.000285215 | *** |
| 18 | Feet 2D distance (mean) | CT | 1012 | 2.649405946 | 0.010592168 | 5.20E-50 | | | |
| 18 | Feet 2D distance (mean) | A5 | 2782 | 2.621668976 | 0.011022254 | 5.20E-50 | 0.069706236 | 0.069706236 | ns |
| 18 | Feet 2D distance (mean) | A1 | 951 | 2.892390144 | 0.013639202 | 5.20E-50 | 9.23E-43 | 2.77E-42 | **** |
| 18 | Feet 2D distance (mean) | A1O3 | 164 | 2.891877867 | 0.02886733 | 5.20E-50 | 1.71E-13 | 3.42E-13 | **** |
| 19 | Anus 1D velocity (std) | CT | 1017 | 0.057159963 | 0.000883982 | 1.28E-07 | | | |
| 19 | Anus 1D velocity (std) | A5 | 2790 | 0.051265951 | 0.000517814 | 1.28E-07 | 1.03E-08 | 3.09E-08 | **** |
| 19 | Anus 1D velocity (std) | A1 | 958 | 0.052957039 | 0.000930699 | 1.28E-07 | 0.001077572 | 0.002153982 | ** |
| 19 | Anus 1D velocity (std) | A1O3 | 166 | 0.055731648 | 0.002280738 | 1.28E-07 | 0.559875466 | 0.559875466 | ns |
| 20 | Arm angle asym. (mean) | CT | 1000 | -4.197482711 | 0.423907327 | 1.63E-17 | | | |
| 20 | Arm angle asym. (mean) | A5 | 2746 | -10.00596094 | 0.429355191 | 1.63E-17 | 1.27E-21 | 3.81E-21 | **** |
| 20 | Arm angle asym. (mean) | A1 | 949 | -9.427281326 | 0.573753871 | 1.63E-17 | 3.46E-13 | 6.92E-13 | **** |
| 20 | Arm angle asym. (mean) | A1O3 | 166 | -2.168320228 | 1.243866831 | 1.63E-17 | 0.12409917 | 0.12409917 | ns |

**Supplementary Table 11. Statistical summary of group comparisons (A1O2) for the top 20 features (identified by the XGB model) at 10 wk.** One-way ANOVA was performed, followed by post-hoc comparisons using Welch's t-tests comparing each group to the reference (CT) group. Statistical significance is indicated by asterisks after Holm–Sidak correction for multiple comparisons. This PDF table displays only the top 20 features in ascending rank order for concise presentation. Additional features are included in the full version of the table, available in the Source Data file (see S_Table 11).

| Rank | Parameter | Group | n | Mean | SEM | ANOVA p-value | Raw Post-hoc p-value | Corrected Post-hoc p-value | Significance |
|---|---|---|---|---|---|---|---|---|---|
| 1 | Hands 3D distance (mean) | CT | 1003 | 1.644375387 | 0.013594462 | 1.59E-19 | | | |
| 1 | Hands 3D distance (mean) | A5 | 2756 | 1.890718315 | 0.019629156 | 1.59E-19 | 1.27E-24 | 3.81E-24 | **** |
| 1 | Hands 3D distance (mean) | A1 | 954 | 1.806494177 | 0.02270016 | 1.59E-19 | 1.13E-09 | 2.26E-09 | **** |
| 1 | Hands 3D distance (mean) | A1O2 | 779 | 1.655849422 | 0.018771137 | 1.59E-19 | 0.620627182 | 0.620627182 | ns |
| 2 | Motion duration (episode) | CT | 1028 | 7.456485084 | 0.150142723 | 2.71E-132 | | | |
| 2 | Motion duration (episode) | A5 | 2826 | 20.90206416 | 0.505530649 | 2.71E-132 | 5.87E-131 | 1.76E-130 | **** |
| 2 | Motion duration (episode) | A1 | 968 | 8.811329201 | 0.166990617 | 2.71E-132 | 1.92E-09 | 3.83E-09 | **** |
| 2 | Motion duration (episode) | A1O2 | 788 | 7.037817259 | 0.115963501 | 2.71E-132 | 0.027449947 | 0.027449947 | * |
| 3 | Body 2D length (min) | CT | 1013 | 4.29673504 | 0.034882946 | 3.27E-54 | | | |
| 3 | Body 2D length (min) | A5 | 2797 | 4.858024465 | 0.018605098 | 3.27E-54 | 3.28E-43 | 9.85E-43 | **** |
| 3 | Body 2D length (min) | A1 | 959 | 4.654991922 | 0.035344274 | 3.27E-54 | 7.70E-13 | 1.54E-12 | **** |
| 3 | Body 2D length (min) | A1O2 | 779 | 4.435511094 | 0.04043941 | 3.27E-54 | 0.009445368 | 0.009445368 | ** |
| 4 | Tail angle (mean) | CT | 1010 | 128.5831328 | 0.506514546 | 3.11E-202 | | | |
| 4 | Tail angle (mean) | A5 | 2784 | 139.994748 | 0.217054871 | 3.11E-202 | 2.72E-83 | 8.16E-83 | **** |
| 4 | Tail angle (mean) | A1 | 961 | 128.0040494 | 0.524420471 | 3.11E-202 | 0.427143685 | 0.427143685 | ns |
| 4 | Tail angle (mean) | A1O2 | 779 | 127.4945559 | 0.561466995 | 3.11E-202 | 0.150170582 | 0.277789961 | ns |
| 5 | Arm angle asym. (std) | CT | 1004 | 19.70322 | 0.250072961 | 1.05E-63 | | | |
| 5 | Arm angle asym. (std) | A5 | 2771 | 26.45002002 | 0.258535473 | 1.05E-63 | 2.30E-74 | 6.91E-74 | **** |
| 5 | Arm angle asym. (std) | A1 | 952 | 23.02053518 | 0.382920041 | 1.05E-63 | 6.22E-13 | 1.24E-12 | **** |
| 5 | Arm angle asym. (std) | A1O2 | 779 | 20.93645444 | 0.354171363 | 1.05E-63 | 0.004510786 | 0.004510786 | ** |
| 6 | Motion interval (episode) | CT | 951 | 30.3361374 | 1.148404362 | 3.60E-200 | | | |
| 6 | Motion interval (episode) | A5 | 2790 | 6.540011947 | 0.194037366 | 3.60E-200 | 7.20E-78 | 2.16E-77 | **** |
| 6 | Motion interval (episode) | A1 | 938 | 25.30167022 | 1.303416925 | 3.60E-200 | 0.003798395 | 0.003798395 | ** |
| 6 | Motion interval (episode) | A1O2 | 742 | 38.38773585 | 1.753517876 | 3.60E-200 | 1.28E-04 | 2.56E-04 | *** |
| 7 | Body angle (min) | CT | 1007 | 9.707072693 | 0.186658265 | 5.16E-08 | | | |
| 7 | Body angle (min) | A5 | 2796 | 10.47089411 | 0.101318344 | 5.16E-08 | 0.000332208 | 0.000996294 | *** |
| 7 | Body angle (min) | A1 | 960 | 9.410668841 | 0.179847705 | 5.16E-08 | 0.252963102 | 0.441935874 | ns |
| 7 | Body angle (min) | A1O2 | 779 | 9.6330119 | 0.206341107 | 5.16E-08 | 0.790136707 | 0.790136707 | ns |
| 8 | Feet 2D distance (max) | CT | 1009 | 3.32565192 | 0.012419669 | 2.15E-57 | | | |
| 8 | Feet 2D distance (max) | A5 | 2786 | 3.648510809 | 0.01165259 | 2.15E-57 | 1.78E-75 | 5.33E-75 | **** |
| 8 | Feet 2D distance (max) | A1 | 952 | 3.661384728 | 0.016485325 | 2.15E-57 | 1.35E-55 | 2.70E-55 | **** |
| 8 | Feet 2D distance (max) | A1O2 | 779 | 3.652808896 | 0.023155866 | 2.15E-57 | 1.42E-33 | 1.42E-33 | **** |
| 9 | Neck 3D velocity (std) | CT | 1005 | 5.274273039 | 0.039629475 | 2.96E-57 | | | |
| 9 | Neck 3D velocity (std) | A5 | 2779 | 5.409820275 | 0.026329312 | 2.96E-57 | 0.004433004 | 0.004433004 | ** |
| 9 | Neck 3D velocity (std) | A1 | 960 | 4.672596162 | 0.041934851 | 2.96E-57 | 8.18E-25 | 2.45E-24 | **** |
| 9 | Neck 3D velocity (std) | A1O2 | 779 | 4.862038942 | 0.044861347 | 2.96E-57 | 8.04E-12 | 1.61E-11 | **** |
| 10 | Feet 2D distance (std) | CT | 1003 | 0.354993408 | 0.005679999 | 1.77E-101 | | | |
| 10 | Feet 2D distance (std) | A5 | 2784 | 0.538039994 | 0.004836098 | 1.77E-101 | 2.42E-119 | 7.26E-119 | **** |
| 10 | Feet 2D distance (std) | A1 | 962 | 0.4260558 | 0.007958734 | 1.77E-101 | 5.48E-13 | 1.10E-12 | **** |
| 10 | Feet 2D distance (std) | A1O2 | 779 | 0.431952051 | 0.009628263 | 1.77E-101 | 9.03E-12 | 9.03E-12 | **** |
| 11 | Chest 3D velocity (mean) | CT | 1017 | 4.436367595 | 0.047588901 | 3.80E-153 | | | |
| 11 | Chest 3D velocity (mean) | A5 | 2807 | 5.569819495 | 0.036728201 | 3.80E-153 | 7.74E-74 | 2.32E-73 | **** |
| 11 | Chest 3D velocity (mean) | A1 | 967 | 4.19557509 | 0.045325613 | 3.80E-153 | 0.000254915 | 0.000509765 | *** |
| 11 | Chest 3D velocity (mean) | A1O2 | 779 | 4.289104347 | 0.051534031 | 3.80E-153 | 0.035929001 | 0.035929001 | * |
| 12 | U-body 3D length (min) | CT | 1010 | 2.955434212 | 0.015108979 | 1.99E-14 | | | |
| 12 | U-body 3D length (min) | A5 | 2786 | 3.081868406 | 0.007527144 | 1.99E-14 | 1.15E-13 | 3.46E-13 | **** |
| 12 | U-body 3D length (min) | A1 | 970 | 3.019004064 | 0.013368844 | 1.99E-14 | 0.001651656 | 0.001651656 | ** |
| 12 | U-body 3D length (min) | A1O2 | 779 | 3.042145861 | 0.017706144 | 1.99E-14 | 0.000201646 | 0.000403251 | *** |
| 13 | Right limb angle asym. (min) | CT | 1015 | -47.02516898 | 0.524497915 | 9.54E-26 | | | |
| 13 | Right limb angle asym. (min) | A5 | 2748 | -53.62158509 | 0.635222849 | 9.54E-26 | 1.59E-15 | 4.76E-15 | **** |
| 13 | Right limb angle asym. (min) | A1 | 952 | -46.56664432 | 0.809033294 | 9.54E-26 | 0.634449719 | 0.634449719 | ns |
| 13 | Right limb angle asym. (min) | A1O2 | 779 | -43.14845347 | 0.6684922 | 9.54E-26 | 0.00000545 | 0.0000109 | **** |
| 14 | Hands 3D distance (max) | CT | 1004 | 2.964436455 | 0.023111761 | 1.14E-74 | | | |
| 14 | Hands 3D distance (max) | A5 | 2766 | 3.788195691 | 0.032269093 | 1.14E-74 | 1.49E-90 | 4.48E-90 | **** |
| 14 | Hands 3D distance (max) | A1 | 952 | 3.319962597 | 0.04014604 | 1.14E-74 | 2.94E-14 | 5.87E-14 | **** |
| 14 | Hands 3D distance (max) | A1O2 | 779 | 3.044716828 | 0.035709177 | 1.14E-74 | 0.059322122 | 0.059322122 | ns |
| 15 | Left limb angle asym. (min) | CT | 1013 | -52.23488367 | 0.627043819 | 2.00E-50 | | | |
| 15 | Left limb angle asym. (min) | A5 | 2750 | -67.02386119 | 0.709026864 | 2.00E-50 | 3.89E-53 | 1.17E-52 | **** |
| 15 | Left limb angle asym. (min) | A1 | 957 | -56.24930235 | 0.949519257 | 2.00E-50 | 0.000430064 | 0.000859944 | *** |
| 15 | Left limb angle asym. (min) | A1O2 | 779 | -53.56420096 | 0.921594576 | 2.00E-50 | 0.233243273 | 0.233243273 | ns |
| 16 | Chest 1D velocity (max) | CT | 1023 | 0.126115621 | 0.003979424 | 1.28E-54 | | | |
| 16 | Chest 1D velocity (max) | A5 | 2798 | 0.075819707 | 0.001556038 | 1.28E-54 | 1.62E-30 | 4.87E-30 | **** |
| 16 | Chest 1D velocity (max) | A1 | 967 | 0.080005088 | 0.003143136 | 1.28E-54 | 2.35E-19 | 4.70E-19 | **** |
| 16 | Chest 1D velocity (max) | A1O2 | 782 | 0.119880588 | 0.004546597 | 1.28E-54 | 0.302255233 | 0.302255233 | ns |
| 17 | Leg angle asym. (std) | CT | 1011 | 15.78164918 | 0.204935769 | 1.13E-80 | | | |
| 17 | Leg angle asym. (std) | A5 | 2793 | 20.78733556 | 0.159883993 | 1.13E-80 | 9.39E-77 | 2.82E-76 | **** |
| 17 | Leg angle asym. (std) | A1 | 951 | 18.4948376 | 0.244881491 | 1.13E-80 | 3.91E-17 | 7.81E-17 | **** |
| 17 | Leg angle asym. (std) | A1O2 | 779 | 16.68298693 | 0.268227366 | 1.13E-80 | 0.007660495 | 0.007660495 | ** |
| 18 | Feet 2D distance (mean) | CT | 1012 | 2.649405946 | 0.010592168 | 2.82E-64 | | | |
| 18 | Feet 2D distance (mean) | A5 | 2782 | 2.621668976 | 0.011022254 | 2.82E-64 | 0.069706236 | 0.069706236 | ns |
| 18 | Feet 2D distance (mean) | A1 | 951 | 2.892390144 | 0.013639202 | 2.82E-64 | 9.23E-43 | 2.77E-42 | **** |
| 18 | Feet 2D distance (mean) | A1O2 | 779 | 2.867606207 | 0.015985991 | 2.82E-64 | 9.34E-29 | 1.87E-28 | **** |
| 19 | Anus 1D velocity (std) | CT | 1017 | 0.057159963 | 0.000883982 | 3.21E-15 | | | |
| 19 | Anus 1D velocity (std) | A5 | 2790 | 0.051265951 | 0.000517814 | 3.21E-15 | 1.03E-08 | 3.09E-08 | **** |
| 19 | Anus 1D velocity (std) | A1 | 958 | 0.052957039 | 0.000930699 | 3.21E-15 | 0.001077572 | 0.002153982 | ** |
| 19 | Anus 1D velocity (std) | A1O2 | 779 | 0.059545626 | 0.001046782 | 3.21E-15 | 0.081830035 | 0.081830035 | ns |
| 20 | Arm angle asym. (mean) | CT | 1000 | -4.197482711 | 0.423907327 | 5.39E-26 | | | |
| 20 | Arm angle asym. (mean) | A5 | 2746 | -10.00596094 | 0.429355191 | 5.39E-26 | 1.27E-21 | 3.81E-21 | **** |
| 20 | Arm angle asym. (mean) | A1 | 949 | -9.427281326 | 0.573753871 | 5.39E-26 | 3.46E-13 | 6.92E-13 | **** |
| 20 | Arm angle asym. (mean) | A1O2 | 779 | -3.117740307 | 0.56320718 | 5.39E-26 | 0.125793063 | 0.125793063 | ns |

**Supplementary Table 12. Statistical summary of group comparisons (A1L1) for the top 20 features (identified by the XGB model) at 10 wk.** One-way ANOVA was performed, followed by post-hoc comparisons using Welch's t-tests comparing each group to the reference (CT) group. Statistical significance is indicated by asterisks after Holm–Sidak correction for multiple comparisons. This PDF table displays only the top 20 features in ascending rank order for concise presentation. Additional features are included in the full version of the table, available in the Source Data file (see S_Table 12).

| Rank | Parameter | Group | n | Mean | SEM | ANOVA p-value | Raw Post-hoc p-value | Corrected Post-hoc p-value | Significance |
|---|---|---|---|---|---|---|---|---|---|
| 1 | Hands 3D distance (mean) | CT | 1003 | 1.644375387 | 0.013594462 | 3.42E-81 | | | |
| 1 | Hands 3D distance (mean) | A5 | 2756 | 1.890718315 | 0.019629156 | 3.42E-81 | 1.27E-24 | 2.54E-24 | **** |
| 1 | Hands 3D distance (mean) | A1 | 954 | 1.806494177 | 0.02270016 | 3.42E-81 | 1.13E-09 | 1.13E-09 | **** |
| 1 | Hands 3D distance (mean) | A1L1 | 1685 | 1.437116406 | 0.008075352 | 3.42E-81 | 1.80E-37 | 5.39E-37 | **** |
| 2 | Motion duration (episode) | CT | 1028 | 7.456485084 | 0.150142723 | 0 | | | |
| 2 | Motion duration (episode) | A5 | 2826 | 20.90206416 | 0.505530649 | 0 | 5.87E-131 | 1.17E-130 | **** |
| 2 | Motion duration (episode) | A1 | 968 | 8.811329201 | 0.166990617 | 0 | 1.92E-09 | 1.92E-09 | **** |
| 2 | Motion duration (episode) | A1L1 | 1703 | 133.7172245 | 4.522502884 | 0 | 1.86E-141 | 5.57E-141 | **** |
| 3 | Body 2D length (min) | CT | 1013 | 4.29673504 | 0.034882946 | 8.07E-68 | | | |
| 3 | Body 2D length (min) | A5 | 2797 | 4.858024465 | 0.018605098 | 8.07E-68 | 3.28E-43 | 9.85E-43 | **** |
| 3 | Body 2D length (min) | A1 | 959 | 4.654991922 | 0.035344274 | 8.07E-68 | 7.70E-13 | 1.54E-12 | **** |
| 3 | Body 2D length (min) | A1L1 | 1685 | 4.433456128 | 0.022049669 | 8.07E-68 | 0.000941068 | 0.000941068 | *** |
| 4 | Tail angle (mean) | CT | 1010 | 128.5831328 | 0.506514546 | 1.30E-142 | | | |
| 4 | Tail angle (mean) | A5 | 2784 | 139.994748 | 0.217054871 | 1.30E-142 | 2.72E-83 | 8.16E-83 | **** |
| 4 | Tail angle (mean) | A1 | 961 | 128.0040494 | 0.524420471 | 1.30E-142 | 0.427143685 | 0.427143685 | ns |
| 4 | Tail angle (mean) | A1L1 | 1685 | 132.8484258 | 0.476769255 | 1.30E-142 | 1.01E-09 | 2.02E-09 | **** |
| 5 | Arm angle asym. (std) | CT | 1004 | 19.70322 | 0.250072961 | 7.78E-230 | | | |
| 5 | Arm angle asym. (std) | A5 | 2771 | 26.45002002 | 0.258535473 | 7.78E-230 | 2.30E-74 | 6.91E-74 | **** |
| 5 | Arm angle asym. (std) | A1 | 952 | 23.02053518 | 0.382920041 | 7.78E-230 | 6.22E-13 | 6.22E-13 | **** |
| 5 | Arm angle asym. (std) | A1L1 | 1685 | 15.41288987 | 0.11340252 | 7.78E-230 | 6.55E-51 | 1.31E-50 | **** |
| 6 | Motion interval (episode) | CT | 951 | 30.3361374 | 1.148404362 | 5.04E-246 | | | |
| 6 | Motion interval (episode) | A5 | 2790 | 6.540011947 | 0.194037366 | 5.04E-246 | 7.20E-78 | 1.44E-77 | **** |
| 6 | Motion interval (episode) | A1 | 938 | 25.30167022 | 1.303416925 | 5.04E-246 | 0.003798395 | 0.003798395 | ** |
| 6 | Motion interval (episode) | A1L1 | 1685 | 6.081226508 | 0.275210103 | 5.04E-246 | 3.50E-79 | 1.05E-78 | **** |
| 7 | Body angle (min) | CT | 1007 | 9.707072693 | 0.186658265 | 1.53E-45 | | | |
| 7 | Body angle (min) | A5 | 2796 | 10.47089411 | 0.101318344 | 1.53E-45 | 0.000332208 | 0.000664306 | *** |
| 7 | Body angle (min) | A1 | 960 | 9.410668841 | 0.179847705 | 1.53E-45 | 0.252963102 | 0.252963102 | ns |
| 7 | Body angle (min) | A1L1 | 1685 | 8.010351972 | 0.128681039 | 1.53E-45 | 1.09E-13 | 3.27E-13 | **** |
| 8 | Feet 2D distance (max) | CT | 1009 | 3.32565192 | 0.012419669 | 2.69E-183 | | | |
| 8 | Feet 2D distance (max) | A5 | 2786 | 3.648510809 | 0.01165259 | 2.69E-183 | 1.78E-75 | 3.55E-75 | **** |
| 8 | Feet 2D distance (max) | A1 | 952 | 3.661384728 | 0.016485325 | 2.69E-183 | 1.35E-55 | 1.35E-55 | **** |
| 8 | Feet 2D distance (max) | A1L1 | 1685 | 3.961677239 | 0.012080672 | 2.69E-183 | 4.20E-236 | 1.26E-235 | **** |
| 9 | Neck 3D velocity (std) | CT | 1005 | 5.274273039 | 0.039629475 | 0 | | | |
| 9 | Neck 3D velocity (std) | A5 | 2779 | 5.409820275 | 0.026329312 | 0 | 0.004433004 | 0.004433004 | ** |
| 9 | Neck 3D velocity (std) | A1 | 960 | 4.672596162 | 0.041934851 | 0 | 8.18E-25 | 1.64E-24 | **** |
| 9 | Neck 3D velocity (std) | A1L1 | 1685 | 7.181732064 | 0.057008177 | 0 | 1.67E-146 | 5.01E-146 | **** |
| 10 | Feet 2D distance (std) | CT | 1003 | 0.354993408 | 0.005679999 | 3.40E-120 | | | |
| 10 | Feet 2D distance (std) | A5 | 2784 | 0.538039994 | 0.004836098 | 3.40E-120 | 2.42E-119 | 7.26E-119 | **** |
| 10 | Feet 2D distance (std) | A1 | 962 | 0.4260558 | 0.007958734 | 3.40E-120 | 5.48E-13 | 5.48E-13 | **** |
| 10 | Feet 2D distance (std) | A1L1 | 1685 | 0.509152707 | 0.004202374 | 3.40E-120 | 5.19E-95 | 1.04E-94 | **** |
| 11 | Chest 3D velocity (mean) | CT | 1017 | 4.436367595 | 0.047588901 | 3.56E-194 | | | |
| 11 | Chest 3D velocity (mean) | A5 | 2807 | 5.569819495 | 0.036728201 | 3.56E-194 | 7.74E-74 | 1.55E-73 | **** |
| 11 | Chest 3D velocity (mean) | A1 | 967 | 4.19557509 | 0.045325613 | 3.56E-194 | 0.000254915 | 0.000254915 | *** |
| 11 | Chest 3D velocity (mean) | A1L1 | 1685 | 6.38420457 | 0.066167905 | 3.56E-194 | 1.30E-114 | 3.91E-114 | **** |
| 12 | U-body 3D length (min) | CT | 1010 | 2.955434212 | 0.015108979 | 1.28E-139 | | | |
| 12 | U-body 3D length (min) | A5 | 2786 | 3.081868406 | 0.007527144 | 1.28E-139 | 1.15E-13 | 2.31E-13 | **** |
| 12 | U-body 3D length (min) | A1 | 970 | 3.019004064 | 0.013368844 | 1.28E-139 | 0.001651656 | 0.001651656 | ** |
| 12 | U-body 3D length (min) | A1L1 | 1685 | 2.749324103 | 0.010160157 | 1.28E-139 | 8.57E-29 | 2.57E-28 | **** |
| 13 | Right limb angle asym. (min) | CT | 1015 | -47.02516898 | 0.524497915 | 7.42E-96 | | | |
| 13 | Right limb angle asym. (min) | A5 | 2748 | -53.62158509 | 0.635222849 | 7.42E-96 | 1.59E-15 | 3.17E-15 | **** |
| 13 | Right limb angle asym. (min) | A1 | 952 | -46.56664432 | 0.809033294 | 7.42E-96 | 0.634449719 | 0.634449719 | ns |
| 13 | Right limb angle asym. (min) | A1L1 | 1685 | -36.30625571 | 0.393958787 | 7.42E-96 | 1.45E-56 | 4.34E-56 | **** |
| 14 | Hands 3D distance (max) | CT | 1004 | 2.964436455 | 0.023111761 | 2.54E-108 | | | |
| 14 | Hands 3D distance (max) | A5 | 2766 | 3.788195691 | 0.032269093 | 2.54E-108 | 1.49E-90 | 4.48E-90 | **** |
| 14 | Hands 3D distance (max) | A1 | 952 | 3.319962597 | 0.04014604 | 2.54E-108 | 2.94E-14 | 5.87E-14 | **** |
| 14 | Hands 3D distance (max) | A1L1 | 1685 | 3.015527435 | 0.014741477 | 2.54E-108 | 0.062517516 | 0.062517516 | ns |
| 15 | Left limb angle asym. (min) | CT | 1013 | -52.23488367 | 0.627043819 | 9.83E-107 | | | |
| 15 | Left limb angle asym. (min) | A5 | 2750 | -67.02386119 | 0.709026864 | 9.83E-107 | 3.89E-53 | 1.17E-52 | **** |
| 15 | Left limb angle asym. (min) | A1 | 957 | -56.24930235 | 0.949519257 | 9.83E-107 | 0.000430064 | 0.000430064 | *** |
| 15 | Left limb angle asym. (min) | A1L1 | 1685 | -46.9563005 | 0.523711021 | 9.83E-107 | 1.27E-10 | 2.54E-10 | **** |
| 16 | Chest 1D velocity (max) | CT | 1023 | 0.126115621 | 0.003979424 | 7.16E-64 | | | |
| 16 | Chest 1D velocity (max) | A5 | 2798 | 0.075819707 | 0.001556038 | 7.16E-64 | 1.62E-30 | 4.87E-30 | **** |
| 16 | Chest 1D velocity (max) | A1 | 967 | 0.080005088 | 0.003143136 | 7.16E-64 | 2.35E-19 | 4.70E-19 | **** |
| 16 | Chest 1D velocity (max) | A1L1 | 1702 | 0.117193161 | 0.002701002 | 7.16E-64 | 0.063723091 | 0.063723091 | ns |
| 17 | Leg angle asym. (std) | CT | 1011 | 15.78164918 | 0.204935769 | 1.43E-105 | | | |
| 17 | Leg angle asym. (std) | A5 | 2793 | 20.78733556 | 0.159883993 | 1.43E-105 | 9.39E-77 | 2.82E-76 | **** |
| 17 | Leg angle asym. (std) | A1 | 951 | 18.4948376 | 0.244881491 | 1.43E-105 | 3.91E-17 | 7.81E-17 | **** |
| 17 | Leg angle asym. (std) | A1L1 | 1685 | 16.91582212 | 0.111715179 | 1.43E-105 | 1.29E-06 | 1.29E-06 | **** |
| 18 | Feet 2D distance (mean) | CT | 1012 | 2.649405946 | 0.010592168 | 2.69E-138 | | | |
| 18 | Feet 2D distance (mean) | A5 | 2782 | 2.621668976 | 0.011022254 | 2.69E-138 | 0.069706236 | 0.069706236 | ns |
| 18 | Feet 2D distance (mean) | A1 | 951 | 2.892390144 | 0.013639202 | 2.69E-138 | 9.23E-43 | 1.85E-42 | **** |
| 18 | Feet 2D distance (mean) | A1L1 | 1685 | 2.991827443 | 0.012287399 | 2.69E-138 | 1.41E-91 | 4.23E-91 | **** |
| 19 | Anus 1D velocity (std) | CT | 1017 | 0.057159963 | 0.000883982 | 7.12E-10 | | | |
| 19 | Anus 1D velocity (std) | A5 | 2790 | 0.051265951 | 0.000517814 | 7.12E-10 | 1.03E-08 | 3.09E-08 | **** |
| 19 | Anus 1D velocity (std) | A1 | 958 | 0.052957039 | 0.000930699 | 7.12E-10 | 0.001077572 | 0.002153982 | ** |
| 19 | Anus 1D velocity (std) | A1L1 | 1685 | 0.055414916 | 0.000625152 | 7.12E-10 | 0.107174168 | 0.107174168 | ns |
| 20 | Arm angle asym. (mean) | CT | 1000 | -4.197482711 | 0.423907327 | 2.24E-69 | | | |
| 20 | Arm angle asym. (mean) | A5 | 2746 | -10.00596094 | 0.429355191 | 2.24E-69 | 1.27E-21 | 3.81E-21 | **** |
| 20 | Arm angle asym. (mean) | A1 | 949 | -9.427281326 | 0.573753871 | 2.24E-69 | 3.46E-13 | 6.92E-13 | **** |
| 20 | Arm angle asym. (mean) | A1L1 | 1685 | -0.679603656 | 0.230715523 | 2.24E-69 | 4.89E-13 | 6.92E-13 | **** |

**Supplementary Table 13. Statistical summary of group comparisons (A1L3) for the top 20 features (identified by the XGB model) at 10 wk.** One-way ANOVA was performed, followed by post-hoc comparisons using Welch's t-tests comparing each group to the reference (CT) group. Statistical significance is indicated by asterisks after Holm–Sidak correction for multiple comparisons. This PDF table displays only the top 20 features in ascending rank order for concise presentation. Additional features are included in the full version of the table, available in the Source Data file (see S_Table 13).

| Rank | Parameter | Group | n | Mean | SEM | ANOVA p-value | Raw Post-hoc p-value | Corrected Post-hoc p-value | Significance |
|---|---|---|---|---|---|---|---|---|---|
| 1 | Hands 3D distance (mean) | CT | 1003 | 1.644375387 | 0.013594462 | 6.47E-96 | | | |
| 1 | Hands 3D distance (mean) | A5 | 2756 | 1.890718315 | 0.019629156 | 6.47E-96 | 1.27E-24 | 2.54E-24 | **** |
| 1 | Hands 3D distance (mean) | A1 | 954 | 1.806494177 | 0.02270016 | 6.47E-96 | 1.13E-09 | 1.13E-09 | **** |
| 1 | Hands 3D distance (mean) | A1L3 | 1726 | 1.397125157 | 0.008789913 | 6.47E-96 | 1.17E-49 | 3.51E-49 | **** |
| 2 | Motion duration (episode) | CT | 1028 | 7.456485084 | 0.150142723 | 2.05E-201 | | | |
| 2 | Motion duration (episode) | A5 | 2826 | 20.90206416 | 0.505530649 | 2.05E-201 | 5.87E-131 | 1.17E-130 | **** |
| 2 | Motion duration (episode) | A1 | 968 | 8.811329201 | 0.166990617 | 2.05E-201 | 1.92E-09 | 1.92E-09 | **** |
| 2 | Motion duration (episode) | A1L3 | 1745 | 36.90492837 | 0.990676374 | 2.05E-201 | 9.44E-156 | 2.83E-155 | **** |
| 3 | Body 2D length (min) | CT | 1013 | 4.29673504 | 0.034882946 | 2.01E-51 | | | |
| 3 | Body 2D length (min) | A5 | 2797 | 4.858024465 | 0.018605098 | 2.01E-51 | 3.28E-43 | 9.85E-43 | **** |
| 3 | Body 2D length (min) | A1 | 959 | 4.654991922 | 0.035344274 | 2.01E-51 | 7.70E-13 | 7.70E-13 | **** |
| 3 | Body 2D length (min) | A1L3 | 1726 | 4.692933611 | 0.020230415 | 2.01E-51 | 3.39E-22 | 6.78E-22 | **** |
| 4 | Tail angle (mean) | CT | 1010 | 128.5831328 | 0.506514546 | 1.53E-202 | | | |
| 4 | Tail angle (mean) | A5 | 2784 | 139.994748 | 0.217054871 | 1.53E-202 | 2.72E-83 | 8.16E-83 | **** |
| 4 | Tail angle (mean) | A1 | 961 | 128.0040494 | 0.524420471 | 1.53E-202 | 0.427143685 | 0.427143685 | ns |
| 4 | Tail angle (mean) | A1L3 | 1726 | 137.3590979 | 0.243169267 | 1.53E-202 | 4.99E-51 | 9.97E-51 | **** |
| 5 | Arm angle asym. (std) | CT | 1004 | 19.70322 | 0.250072961 | 1.11E-212 | | | |
| 5 | Arm angle asym. (std) | A5 | 2771 | 26.45002002 | 0.258535473 | 1.11E-212 | 2.30E-74 | 6.91E-74 | **** |
| 5 | Arm angle asym. (std) | A1 | 952 | 23.02053518 | 0.382920041 | 1.11E-212 | 6.22E-13 | 6.22E-13 | **** |
| 5 | Arm angle asym. (std) | A1L3 | 1726 | 15.86987761 | 0.138220477 | 1.11E-212 | 5.39E-39 | 1.08E-38 | **** |
| 6 | Motion interval (episode) | CT | 951 | 30.3361374 | 1.148404362 | 1.54E-243 | | | |
| 6 | Motion interval (episode) | A5 | 2790 | 6.540011947 | 0.194037366 | 1.54E-243 | 7.20E-78 | 1.56E-77 | **** |
| 6 | Motion interval (episode) | A1 | 938 | 25.30167022 | 1.303416925 | 1.54E-243 | 0.003798395 | 0.003798395 | ** |
| 6 | Motion interval (episode) | A1L3 | 1719 | 6.2277293 | 0.296629255 | 1.54E-243 | 5.18E-78 | 1.56E-77 | **** |
| 7 | Body angle (min) | CT | 1007 | 9.707072693 | 0.186658265 | 3.86E-37 | | | |
| 7 | Body angle (min) | A5 | 2796 | 10.47089411 | 0.101318344 | 3.86E-37 | 0.000332208 | 0.000664306 | *** |
| 7 | Body angle (min) | A1 | 960 | 9.410668841 | 0.179847705 | 3.86E-37 | 0.252963102 | 0.252963102 | ns |
| 7 | Body angle (min) | A1L3 | 1726 | 8.27069997 | 0.127397957 | 3.86E-37 | 2.58E-10 | 7.75E-10 | **** |
| 8 | Feet 2D distance (max) | CT | 1009 | 3.32565192 | 0.012419669 | 1.17E-74 | | | |
| 8 | Feet 2D distance (max) | A5 | 2786 | 3.648510809 | 0.01165259 | 1.17E-74 | 1.78E-75 | 3.55E-75 | **** |
| 8 | Feet 2D distance (max) | A1 | 952 | 3.661384728 | 0.016485325 | 1.17E-74 | 1.35E-55 | 1.35E-55 | **** |
| 8 | Feet 2D distance (max) | A1L3 | 1726 | 3.671642588 | 0.00948565 | 1.17E-74 | 8.01E-98 | 2.40E-97 | **** |
| 9 | Neck 3D velocity (std) | CT | 1005 | 5.274273039 | 0.039629475 | 4.50E-171 | | | |
| 9 | Neck 3D velocity (std) | A5 | 2779 | 5.409820275 | 0.026329312 | 4.50E-171 | 0.004433004 | 0.004433004 | ** |
| 9 | Neck 3D velocity (std) | A1 | 960 | 4.672596162 | 0.041934851 | 4.50E-171 | 8.18E-25 | 1.64E-24 | **** |
| 9 | Neck 3D velocity (std) | A1L3 | 1726 | 6.301795622 | 0.043295624 | 4.50E-171 | 5.22E-65 | 1.57E-64 | **** |
| 10 | Feet 2D distance (std) | CT | 1003 | 0.354993408 | 0.005679999 | 1.29E-116 | | | |
| 10 | Feet 2D distance (std) | A5 | 2784 | 0.538039994 | 0.004836098 | 1.29E-116 | 2.42E-119 | 7.26E-119 | **** |
| 10 | Feet 2D distance (std) | A1 | 962 | 0.4260558 | 0.007958734 | 1.29E-116 | 5.48E-13 | 5.48E-13 | **** |
| 10 | Feet 2D distance (std) | A1L3 | 1726 | 0.452737241 | 0.004333191 | 1.29E-116 | 7.06E-41 | 1.41E-40 | **** |
| 11 | Chest 3D velocity (mean) | CT | 1017 | 4.436367595 | 0.047588901 | 4.21E-126 | | | |
| 11 | Chest 3D velocity (mean) | A5 | 2807 | 5.569819495 | 0.036728201 | 4.21E-126 | 7.74E-74 | 2.32E-73 | **** |
| 11 | Chest 3D velocity (mean) | A1 | 967 | 4.19557509 | 0.045325613 | 4.21E-126 | 0.000254915 | 0.000254915 | *** |
| 11 | Chest 3D velocity (mean) | A1L3 | 1726 | 5.402486167 | 0.046724558 | 4.21E-126 | 9.5E-46 | 1.9E-45 | **** |
| 12 | U-body 3D length (min) | CT | 1010 | 2.955434212 | 0.015108979 | 1.43E-49 | | | |
| 12 | U-body 3D length (min) | A5 | 2786 | 3.081868406 | 0.007527144 | 1.43E-49 | 1.15E-13 | 3.46E-13 | **** |
| 12 | U-body 3D length (min) | A1 | 970 | 3.019004064 | 0.013368844 | 1.43E-49 | 0.001651656 | 0.001651656 | ** |
| 12 | U-body 3D length (min) | A1L3 | 1726 | 2.891692038 | 0.010089688 | 1.43E-49 | 0.000461271 | 0.00092233 | *** |
| 13 | Right limb angle asym. (min) | CT | 1015 | -47.02516898 | 0.524497915 | 2.95E-52 | | | |
| 13 | Right limb angle asym. (min) | A5 | 2748 | -53.62158509 | 0.635222849 | 2.95E-52 | 1.59E-15 | 3.17E-15 | **** |
| 13 | Right limb angle asym. (min) | A1 | 952 | -46.56664432 | 0.809033294 | 2.95E-52 | 0.634449719 | 0.634449719 | ns |
| 13 | Right limb angle asym. (min) | A1L3 | 1726 | -40.95320292 | 0.466750166 | 2.95E-52 | 9.45E-18 | 2.83E-17 | **** |
| 14 | Hands 3D distance (max) | CT | 1004 | 2.964436455 | 0.023111761 | 5.11E-129 | | | |
| 14 | Hands 3D distance (max) | A5 | 2766 | 3.788195691 | 0.032269093 | 5.11E-129 | 1.49E-90 | 4.48E-90 | **** |
| 14 | Hands 3D distance (max) | A1 | 952 | 3.319962597 | 0.04014604 | 5.11E-129 | 2.94E-14 | 5.87E-14 | **** |
| 14 | Hands 3D distance (max) | A1L3 | 1726 | 2.889187878 | 0.016779638 | 5.11E-129 | 0.008485821 | 0.008485821 | ** |
| 15 | Left limb angle asym. (min) | CT | 1013 | -52.23488367 | 0.627043819 | 3.88E-186 | | | |
| 15 | Left limb angle asym. (min) | A5 | 2750 | -67.02386119 | 0.709026864 | 3.88E-186 | 3.89E-53 | 7.79E-53 | **** |
| 15 | Left limb angle asym. (min) | A1 | 957 | -56.24930235 | 0.949519257 | 3.88E-186 | 0.000430064 | 0.000430064 | *** |
| 15 | Left limb angle asym. (min) | A1L3 | 1726 | -40.25531735 | 0.369997218 | 3.88E-186 | 1.33E-56 | 4E-56 | **** |
| 16 | Chest 1D velocity (max) | CT | 1023 | 0.126115621 | 0.003979424 | 1.12E-108 | | | |
| 16 | Chest 1D velocity (max) | A5 | 2798 | 0.075819707 | 0.001556038 | 1.12E-108 | 1.62E-30 | 4.87E-30 | **** |
| 16 | Chest 1D velocity (max) | A1 | 967 | 0.080005088 | 0.003143136 | 1.12E-108 | 2.35E-19 | 4.7E-19 | **** |
| 16 | Chest 1D velocity (max) | A1L3 | 1738 | 0.139301375 | 0.002734419 | 1.12E-108 | 0.006372626 | 0.006372626 | ** |
| 17 | Leg angle asym. (std) | CT | 1011 | 15.78164918 | 0.204935769 | 3.40E-177 | | | |
| 17 | Leg angle asym. (std) | A5 | 2793 | 20.78733556 | 0.159883993 | 3.40E-177 | 9.39E-77 | 2.82E-76 | **** |
| 17 | Leg angle asym. (std) | A1 | 951 | 18.4948376 | 0.244881491 | 3.40E-177 | 3.91E-17 | 7.81E-17 | **** |
| 17 | Leg angle asym. (std) | A1L3 | 1726 | 14.77006225 | 0.110950367 | 3.40E-177 | 0.0000151 | 0.0000151 | **** |
| 18 | Feet 2D distance (mean) | CT | 1012 | 2.649405946 | 0.010592168 | 4.40E-130 | | | |
| 18 | Feet 2D distance (mean) | A5 | 2782 | 2.621668976 | 0.011022254 | 4.40E-130 | 0.069706236 | 0.069706236 | ns |
| 18 | Feet 2D distance (mean) | A1 | 951 | 2.892390144 | 0.013639202 | 4.40E-130 | 9.23E-43 | 1.85E-42 | **** |
| 18 | Feet 2D distance (mean) | A1L3 | 1726 | 2.947580946 | 0.008989402 | 4.40E-130 | 2.83E-93 | 8.48E-93 | **** |
| 19 | Anus 1D velocity (std) | CT | 1017 | 0.057159963 | 0.000883982 | 1.62E-09 | | | |
| 19 | Anus 1D velocity (std) | A5 | 2790 | 0.051265951 | 0.000517814 | 1.62E-09 | 1.03E-08 | 2.06E-08 | **** |
| 19 | Anus 1D velocity (std) | A1 | 958 | 0.052957039 | 0.000930699 | 1.62E-09 | 0.001077572 | 0.001077572 | ** |
| 19 | Anus 1D velocity (std) | A1L3 | 1726 | 0.050914761 | 0.00053126 | 1.62E-09 | 1.71E-09 | 5.13E-09 | **** |
| 20 | Arm angle asym. (mean) | CT | 1000 | -4.197482711 | 0.423907327 | 1.20E-22 | | | |
| 20 | Arm angle asym. (mean) | A5 | 2746 | -10.00596094 | 0.429355191 | 1.20E-22 | 1.27E-21 | 3.81E-21 | **** |
| 20 | Arm angle asym. (mean) | A1 | 949 | -9.427281326 | 0.573753871 | 1.20E-22 | 3.46E-13 | 6.92E-13 | **** |
| 20 | Arm angle asym. (mean) | A1L3 | 1726 | -5.971498727 | 0.274008937 | 1.20E-22 | 0.000451161 | 0.000451161 | *** |

**Supplementary Table 14. Statistical summary of group comparisons (A1BT) for the top 20 features (identified by the XGB model) at 6 wk.** One-way ANOVA was performed, followed by post-hoc comparisons using Welch's t-tests comparing each group to the reference (CT) group. Statistical significance is indicated by asterisks after Holm–Sidak correction for multiple comparisons. This PDF table displays only the top 20 features in ascending rank order for concise presentation. Additional features are included in the full version of the table, available in the Source Data file (see S_Table 14).

| Rank | Parameter | Group | n | Mean | SEM | ANOVA p-value | Raw Post-hoc p-value | Corrected Post-hoc p-value | Significance |
|---|---|---|---|---|---|---|---|---|---|
| 1 | Hands 3D distance (mean) | CT | 1069 | 1.603772965 | 0.012843997 | 1.92E-21 | | | |
| 1 | Hands 3D distance (mean) | A5 | 2207 | 1.83267426 | 0.01870961 | 1.92E-21 | 1.40E-23 | 4.19E-23 | **** |
| 1 | Hands 3D distance (mean) | A1 | 672 | 1.884179871 | 0.026054661 | 1.92E-21 | 3.86E-21 | 7.71E-21 | **** |
| 1 | Hands 3D distance (mean) | A1BT | 275 | 1.974157067 | 0.046282984 | 1.92E-21 | 1.62E-13 | 1.62E-13 | **** |
| 2 | Motion duration (episode) | CT | 1084 | 8.053874539 | 0.144599774 | 4.38E-93 | | | |
| 2 | Motion duration (episode) | A5 | 2250 | 17.68625185 | 0.429481008 | 4.38E-93 | 7.19E-93 | 2.16E-92 | **** |
| 2 | Motion duration (episode) | A1 | 690 | 7.938550725 | 0.157098354 | 4.38E-93 | 5.89E-01 | 5.89E-01 | ns |
| 2 | Motion duration (episode) | A1BT | 278 | 7.345923261 | 0.171456564 | 4.38E-93 | 0.001664058 | 0.003325347 | ** |
| 3 | Body 2D length (min) | CT | 1076 | 4.294935601 | 0.033240268 | 1.04E-68 | | | |
| 3 | Body 2D length (min) | A5 | 2222 | 4.953072469 | 0.020667685 | 1.04E-68 | 2.62E-59 | 7.86E-59 | **** |
| 3 | Body 2D length (min) | A1 | 677 | 4.969226882 | 0.041398275 | 1.04E-68 | 4.05E-35 | 8.09E-35 | **** |
| 3 | Body 2D length (min) | A1BT | 275 | 4.893389703 | 0.062184591 | 1.04E-68 | 3.2E-16 | 3.2E-16 | **** |
| 4 | Tail angle (mean) | CT | 1072 | 129.5058236 | 0.511718267 | 3.76E-45 | | | |
| 4 | Tail angle (mean) | A5 | 2243 | 136.4137491 | 0.248165627 | 3.76E-45 | 1.57E-32 | 4.7E-32 | **** |
| 4 | Tail angle (mean) | A1 | 680 | 130.3714011 | 0.632460453 | 3.76E-45 | 0.287525885 | 0.287525885 | ns |
| 4 | Tail angle (mean) | A1BT | 275 | 135.0937194 | 0.948876105 | 3.76E-45 | 0.000000331 | 0.000000662 | **** |
| 5 | Arm angle asym. (std) | CT | 1068 | 19.1068203 | 0.234844945 | 3.01E-61 | | | |
| 5 | Arm angle asym. (std) | A5 | 2223 | 26.53300752 | 0.283883771 | 3.01E-61 | 3.82E-85 | 1.15E-84 | **** |
| 5 | Arm angle asym. (std) | A1 | 670 | 23.20498188 | 0.427951381 | 3.01E-61 | 1.46E-16 | 2.91E-16 | **** |
| 5 | Arm angle asym. (std) | A1BT | 275 | 22.80722024 | 0.74808557 | 3.01E-61 | 0.0000035 | 0.0000035 | **** |
| 6 | Motion interval (episode) | CT | 1007 | 34.0734194 | 1.322395702 | 3.93E-145 | | | |
| 6 | Motion interval (episode) | A5 | 2169 | 9.22978331 | 0.319580596 | 3.93E-145 | 1.89E-65 | 5.66E-65 | **** |
| 6 | Motion interval (episode) | A1 | 635 | 34.77790026 | 1.860769164 | 3.93E-145 | 0.757675216 | 0.757675216 | ns |
| 6 | Motion interval (episode) | A1BT | 262 | 56.98498728 | 4.697384412 | 3.93E-145 | 4.04E-06 | 8.08E-06 | **** |
| 7 | Body angle (min) | CT | 1078 | 9.415275187 | 0.17069152 | 2.43E-13 | | | |
| 7 | Body angle (min) | A5 | 2229 | 10.75345865 | 0.114779784 | 2.43E-13 | 9.67E-11 | 2.9E-10 | **** |
| 7 | Body angle (min) | A1 | 687 | 10.27424513 | 0.220561713 | 2.43E-13 | 0.002110284 | 0.004216115 | ** |
| 7 | Body angle (min) | A1BT | 275 | 8.7722321 | 0.340493681 | 2.43E-13 | 0.092092518 | 0.092092518 | ns |
| 8 | Feet 2D distance (max) | CT | 1069 | 3.263696693 | 0.011716439 | 5.27E-114 | | | |
| 8 | Feet 2D distance (max) | A5 | 2206 | 3.706958636 | 0.013667765 | 5.27E-114 | 1.53E-122 | 4.58E-122 | **** |
| 8 | Feet 2D distance (max) | A1 | 682 | 3.786898764 | 0.021444245 | 5.27E-114 | 3.94E-85 | 7.88E-85 | **** |
| 8 | Feet 2D distance (max) | A1BT | 275 | 3.805269456 | 0.032791501 | 5.27E-114 | 9.34E-42 | 9.34E-42 | **** |
| 9 | Neck 3D velocity (std) | CT | 1071 | 5.146877547 | 0.036935531 | 1.12E-20 | | | |
| 9 | Neck 3D velocity (std) | A5 | 2218 | 5.048163364 | 0.033055341 | 1.12E-20 | 0.046525177 | 0.046525177 | * |
| 9 | Neck 3D velocity (std) | A1 | 679 | 4.676584494 | 0.045768185 | 1.12E-20 | 2.59E-15 | 5.17E-15 | **** |
| 9 | Neck 3D velocity (std) | A1BT | 275 | 4.424208859 | 0.061006811 | 1.12E-20 | 4.70E-22 | 1.41E-21 | **** |
| 10 | Feet 2D distance (std) | CT | 1072 | 0.332793154 | 0.005362826 | 8.64E-123 | | | |
| 10 | Feet 2D distance (std) | A5 | 2215 | 0.540075046 | 0.005256303 | 8.64E-123 | 7.99E-149 | 2.4E-148 | **** |
| 10 | Feet 2D distance (std) | A1 | 681 | 0.460898905 | 0.009876088 | 8.64E-123 | 1.67E-28 | 3.33E-28 | **** |
| 10 | Feet 2D distance (std) | A1BT | 275 | 0.399309764 | 0.012838422 | 8.64E-123 | 0.00000251 | 0.00000251 | **** |
| 11 | Chest 3D velocity (mean) | CT | 1060 | 4.288244385 | 0.043998618 | 4.16E-75 | | | |
| 11 | Chest 3D velocity (mean) | A5 | 2202 | 5.20800762 | 0.040982385 | 4.16E-75 | 9.94E-51 | 2.98E-50 | **** |
| 11 | Chest 3D velocity (mean) | A1 | 689 | 4.236451651 | 0.05336434 | 4.16E-75 | 0.454070605 | 0.454070605 | ns |
| 11 | Chest 3D velocity (mean) | A1BT | 275 | 3.978245064 | 0.069353899 | 4.16E-75 | 0.000179005 | 0.000357977 | *** |
| 12 | U-body 3D length (min) | CT | 1075 | 2.995992593 | 0.015157316 | 1.23E-07 | | | |
| 12 | U-body 3D length (min) | A5 | 2249 | 3.077956794 | 0.008160331 | 1.23E-07 | 2.08E-06 | 6.25E-06 | **** |
| 12 | U-body 3D length (min) | A1 | 683 | 3.092802131 | 0.017993564 | 1.23E-07 | 0.0000408 | 0.0000817 | **** |
| 12 | U-body 3D length (min) | A1BT | 275 | 3.006077724 | 0.024868417 | 1.23E-07 | 0.729272916 | 0.729272916 | ns |
| 13 | Right limb angle asym. (min) | CT | 1077 | -45.91622977 | 0.519673947 | 8.79E-20 | | | |
| 13 | Right limb angle asym. (min) | A5 | 2195 | -54.0623466 | 0.708513616 | 8.79E-20 | 3.26E-20 | 9.77E-20 | **** |
| 13 | Right limb angle asym. (min) | A1 | 674 | -44.90232162 | 0.897592754 | 8.79E-20 | 0.32849979 | 0.32849979 | ns |
| 13 | Right limb angle asym. (min) | A1BT | 275 | -48.91168209 | 1.497266446 | 8.79E-20 | 0.059600277 | 0.115648361 | ns |
| 14 | Hands 3D distance (max) | CT | 1062 | 2.86732305 | 0.021809472 | 4.87E-55 | | | |
| 14 | Hands 3D distance (max) | A5 | 2217 | 3.671713291 | 0.0335437 | 4.87E-55 | 7.48E-85 | 2.24E-84 | **** |
| 14 | Hands 3D distance (max) | A1 | 674 | 3.397134449 | 0.045412025 | 4.87E-55 | 1.37E-24 | 2.74E-24 | **** |
| 14 | Hands 3D distance (max) | A1BT | 275 | 3.480316605 | 0.08015186 | 4.87E-55 | 1.42E-12 | 1.42E-12 | **** |
| 15 | Left limb angle asym. (min) | CT | 1067 | -51.86531218 | 0.592560605 | 1.16E-23 | | | |
| 15 | Left limb angle asym. (min) | A5 | 2216 | -63.59344492 | 0.766107819 | 1.16E-23 | 4.82E-33 | 1.45E-32 | **** |
| 15 | Left limb angle asym. (min) | A1 | 671 | -55.6889893 | 1.112611708 | 1.16E-23 | 0.002478385 | 0.002478385 | ** |
| 15 | Left limb angle asym. (min) | A1BT | 275 | -60.093686 | 1.953142593 | 1.16E-23 | 0.0000691 | 0.000138132 | *** |
| 16 | Chest 1D velocity (max) | CT | 1089 | 0.127478457 | 0.003795931 | 1.59E-56 | | | |
| 16 | Chest 1D velocity (max) | A5 | 2227 | 0.069521559 | 0.001725213 | 1.59E-56 | 1.74E-41 | 5.23E-41 | **** |
| 16 | Chest 1D velocity (max) | A1 | 690 | 0.076083333 | 0.003555781 | 1.59E-56 | 1.94E-22 | 3.89E-22 | **** |
| 16 | Chest 1D velocity (max) | A1BT | 278 | 0.079627518 | 0.005883213 | 1.59E-56 | 2.26E-11 | 2.26E-11 | **** |
| 17 | Leg angle asym. (std) | CT | 1071 | 15.23515896 | 0.210870799 | 6.02E-93 | | | |
| 17 | Leg angle asym. (std) | A5 | 2196 | 21.44957666 | 0.173589443 | 6.02E-93 | 3.65E-104 | 1.1E-103 | **** |
| 17 | Leg angle asym. (std) | A1 | 676 | 20.44932951 | 0.312169298 | 6.02E-93 | 1.13E-40 | 2.26E-40 | **** |
| 17 | Leg angle asym. (std) | A1BT | 275 | 19.67860716 | 0.559403365 | 6.02E-93 | 8.01E-13 | 8.01E-13 | **** |
| 18 | Feet 2D distance (mean) | CT | 1073 | 2.63770504 | 0.009408228 | 1.37E-68 | | | |
| 18 | Feet 2D distance (mean) | A5 | 2196 | 2.647969824 | 0.012871051 | 1.37E-68 | 0.519722261 | 0.519722261 | ns |
| 18 | Feet 2D distance (mean) | A1 | 674 | 2.941242674 | 0.018097523 | 1.37E-68 | 1.51E-45 | 4.53E-45 | **** |
| 18 | Feet 2D distance (mean) | A1BT | 275 | 3.080237852 | 0.029609185 | 1.37E-68 | 3.03E-36 | 6.07E-36 | **** |
| 19 | Anus 1D velocity (std) | CT | 1073 | 0.053830455 | 0.000839097 | 6.01E-03 | | | |
| 19 | Anus 1D velocity (std) | A5 | 2219 | 0.051477174 | 0.00059768 | 6.01E-03 | 2.25E-02 | 4.44E-02 | * |
| 19 | Anus 1D velocity (std) | A1 | 677 | 0.051945639 | 0.001111663 | 6.01E-03 | 0.176193576 | 0.176193576 | ns |
| 19 | Anus 1D velocity (std) | A1BT | 275 | 0.047472379 | 0.001618195 | 6.01E-03 | 0.000536297 | 0.001608027 | ** |
| 20 | Arm angle asym. (mean) | CT | 1072 | -3.074188838 | 0.401693733 | 3.03E-18 | | | |
| 20 | Arm angle asym. (mean) | A5 | 2187 | -8.545298082 | 0.459235766 | 3.03E-18 | 5.14E-19 | 1.54E-18 | **** |
| 20 | Arm angle asym. (mean) | A1 | 669 | -4.538058081 | 0.674366965 | 3.03E-18 | 6.24E-02 | 1.21E-01 | ns |
| 20 | Arm angle asym. (mean) | A1BT | 275 | -1.488877625 | 1.115096387 | 3.03E-18 | 0.181918513 | 0.181918513 | ns |

**Supplementary Table 15. Statistical summary of treatment group comparisons for the top 20 features (identified by the XGB model) at endpoints.** One-way ANOVA was performed, followed by post-hoc comparisons using Welch's t-tests comparing each group to the reference (CT) group. Statistical significance is indicated by asterisks after Holm–Sidak correction for multiple comparisons. The top 20 features are listed in ascending rank order, with additional features appended afterwards.

| Rank | Parameter | Group | Global_name | Souce_Table# | Week | n | Mean | SEM | Significance | norm_value | norm_log |
|---|---|---|---|---|---|---|---|---|---|---|---|
| 1 | Hands 3D distance (mean) | CT | A1O3_CT | 9 | 10 | 1003 | 1.64 | 0.01 | | 0.43 | 0.47 |
| 1 | Hands 3D distance (mean) | A5 | A1O3_A5 | 9 | 10 | 2756 | 1.89 | 0.02 | **** | 0.86 | 0.88 |
| 1 | Hands 3D distance (mean) | A1 | A1O3_A1 | 9 | 10 | 954 | 1.81 | 0.02 | **** | 0.71 | 0.74 |
| 1 | Hands 3D distance (mean) | A1O2 | A1O2 | 10 | 10 | 779 | 1.66 | 0.02 | ns | 0.45 | 0.49 |
| 1 | Hands 3D distance (mean) | A1O3 | A1O3 | 9 | 10 | 164 | 1.74 | 0.03 | * | 0.59 | 0.63 |
| 1 | Hands 3D distance (mean) | A1L1 | A1L1 | 11 | 10 | 1685 | 1.44 | 0.01 | **** | 0.07 | 0.08 |
| 1 | Hands 3D distance (mean) | A1L3 | A1L3 | 12 | 10 | 1726 | 1.40 | 0.01 | **** | 0.00 | 0.00 |
| 1 | Hands 3D distance (mean) | CT | A1BT_CT | 13 | 6 | 1069 | 1.60 | 0.01 | | 0.36 | 0.40 |
| 1 | Hands 3D distance (mean) | A5 | A1BT_A5 | 13 | 6 | 2207 | 1.83 | 0.02 | **** | 0.75 | 0.78 |
| 1 | Hands 3D distance (mean) | A1 | A1BT_A1 | 13 | 6 | 672 | 1.88 | 0.03 | **** | 0.84 | 0.87 |
| 1 | Hands 3D distance (mean) | A1BT | A1BT | 13 | 6 | 275 | 1.97 | 0.05 | **** | 1.00 | 1.00 |
| 2 | Motion duration (episode) | CT | A1O3_CT | 9 | 10 | 1028 | 7.46 | 0.15 | | 0.00 | 0.02 |
| 2 | Motion duration (episode) | A5 | A1O3_A5 | 9 | 10 | 2826 | 20.90 | 0.51 | **** | 0.11 | 0.37 |
| 2 | Motion duration (episode) | A1 | A1O3_A1 | 9 | 10 | 968 | 8.81 | 0.17 | **** | 0.01 | 0.08 |
| 2 | Motion duration (episode) | A1O2 | A1O2 | 10 | 10 | 788 | 7.04 | 0.12 | * | 0.00 | 0.00 |
| 2 | Motion duration (episode) | A1O3 | A1O3 | 9 | 10 | 170 | 7.27 | 0.23 | ns | 0.00 | 0.01 |
| 2 | Motion duration (episode) | A1L1 | A1L1 | 11 | 10 | 1703 | 133.72 | 4.52 | **** | 1.00 | 1.00 |
| 2 | Motion duration (episode) | A1L3 | A1L3 | 12 | 10 | 1745 | 36.90 | 0.99 | **** | 0.24 | 0.56 |
| 2 | Motion duration (episode) | CT | A1BT_CT | 13 | 6 | 1084 | 8.05 | 0.14 | | 0.01 | 0.05 |
| 2 | Motion duration (episode) | A5 | A1BT_A5 | 13 | 6 | 2250 | 17.69 | 0.43 | **** | 0.08 | 0.31 |
| 2 | Motion duration (episode) | A1 | A1BT_A1 | 13 | 6 | 690 | 7.94 | 0.16 | ns | 0.01 | 0.04 |
| 2 | Motion duration (episode) | A1BT | A1BT | 13 | 6 | 278 | 7.35 | 0.17 | ** | 0.00 | 0.01 |
| 3 | Body 2D length (min) | CT | A1O3_CT | 9 | 10 | 1013 | 4.30 | 0.03 | | 0.00 | 0.00 |
| 3 | Body 2D length (min) | A5 | A1O3_A5 | 9 | 10 | 2797 | 4.86 | 0.02 | **** | 0.84 | 0.84 |
| 3 | Body 2D length (min) | A1 | A1O3_A1 | 9 | 10 | 959 | 4.65 | 0.04 | **** | 0.53 | 0.55 |
| 3 | Body 2D length (min) | A1O2 | A1O2 | 10 | 10 | 779 | 4.44 | 0.04 | ** | 0.21 | 0.22 |
| 3 | Body 2D length (min) | A1O3 | A1O3 | 9 | 10 | 165 | 4.49 | 0.09 | * | 0.29 | 0.31 |
| 3 | Body 2D length (min) | A1L1 | A1L1 | 11 | 10 | 1685 | 4.43 | 0.02 | *** | 0.21 | 0.22 |
| 3 | Body 2D length (min) | A1L3 | A1L3 | 12 | 10 | 1726 | 4.69 | 0.02 | **** | 0.59 | 0.61 |
| 3 | Body 2D length (min) | CT | A1BT_CT | 13 | 6 | 1076 | 4.29 | 0.03 | | 0.00 | 0.00 |
| 3 | Body 2D length (min) | A5 | A1BT_A5 | 13 | 6 | 2222 | 4.95 | 0.02 | **** | 0.98 | 0.98 |
| 3 | Body 2D length (min) | A1 | A1BT_A1 | 13 | 6 | 677 | 4.97 | 0.04 | **** | 1.00 | 1.00 |
| 3 | Body 2D length (min) | A1BT | A1BT | 13 | 6 | 275 | 4.89 | 0.06 | **** | 0.89 | 0.89 |
| 4 | Tail angle (mean) | CT | A1O3_CT | 9 | 10 | 1010 | 128.58 | 0.51 | | 0.21 | 0.22 |
| 4 | Tail angle (mean) | A5 | A1O3_A5 | 9 | 10 | 2784 | 139.99 | 0.22 | **** | 1.00 | 1.00 |
| 4 | Tail angle (mean) | A1 | A1O3_A1 | 9 | 10 | 961 | 128.00 | 0.52 | ns | 0.17 | 0.18 |
| 4 | Tail angle (mean) | A1O2 | A1O2 | 10 | 10 | 779 | 127.49 | 0.56 | ns | 0.14 | 0.14 |
| 4 | Tail angle (mean) | A1O3 | A1O3 | 9 | 10 | 166 | 125.51 | 1.23 | * | 0.00 | 0.00 |
| 4 | Tail angle (mean) | A1L1 | A1L1 | 11 | 10 | 1685 | 132.85 | 0.48 | **** | 0.51 | 0.52 |
| 4 | Tail angle (mean) | A1L3 | A1L3 | 12 | 10 | 1726 | 137.36 | 0.24 | **** | 0.82 | 0.83 |
| 4 | Tail angle (mean) | CT | A1BT_CT | 13 | 6 | 1072 | 129.51 | 0.51 | | 0.28 | 0.29 |
| 4 | Tail angle (mean) | A5 | A1BT_A5 | 13 | 6 | 2243 | 136.41 | 0.25 | **** | 0.75 | 0.76 |
| 4 | Tail angle (mean) | A1 | A1BT_A1 | 13 | 6 | 680 | 130.37 | 0.63 | ns | 0.34 | 0.35 |
| 4 | Tail angle (mean) | A1BT | A1BT | 13 | 6 | 275 | 135.09 | 0.95 | **** | 0.66 | 0.67 |
| 5 | Arm angle asym. (std) | CT | A1O3_CT | 9 | 10 | 1004 | 19.70 | 0.25 | | 0.39 | 0.45 |
| 5 | Arm angle asym. (std) | A5 | A1O3_A5 | 9 | 10 | 2771 | 26.45 | 0.26 | **** | 0.99 | 0.99 |
| 5 | Arm angle asym. (std) | A1 | A1O3_A1 | 9 | 10 | 952 | 23.02 | 0.38 | **** | 0.68 | 0.74 |
| 5 | Arm angle asym. (std) | A1O2 | A1O2 | 10 | 10 | 779 | 20.94 | 0.35 | ** | 0.50 | 0.56 |
| 5 | Arm angle asym. (std) | A1O3 | A1O3 | 9 | 10 | 165 | 22.18 | 0.61 | *** | 0.61 | 0.67 |
| 5 | Arm angle asym. (std) | A1L1 | A1L1 | 11 | 10 | 1685 | 15.41 | 0.11 | **** | 0.00 | 0.00 |
| 5 | Arm angle asym. (std) | A1L3 | A1L3 | 12 | 10 | 1726 | 15.87 | 0.14 | **** | 0.04 | 0.05 |
| 5 | Arm angle asym. (std) | CT | A1BT_CT | 13 | 6 | 1068 | 19.11 | 0.23 | | 0.33 | 0.40 |
| 5 | Arm angle asym. (std) | A5 | A1BT_A5 | 13 | 6 | 2223 | 26.53 | 0.28 | **** | 1.00 | 1.00 |
| 5 | Arm angle asym. (std) | A1 | A1BT_A1 | 13 | 6 | 670 | 23.20 | 0.43 | **** | 0.70 | 0.75 |
| 5 | Arm angle asym. (std) | A1BT | A1BT | 13 | 6 | 275 | 22.81 | 0.75 | **** | 0.66 | 0.72 |
| 6 | Motion interval (episode) | CT | A1O3_CT | 9 | 10 | 951 | 30.34 | 1.15 | | 0.48 | 0.72 |
| 6 | Motion interval (episode) | A5 | A1O3_A5 | 9 | 10 | 2790 | 6.54 | 0.19 | **** | 0.01 | 0.03 |
| 6 | Motion interval (episode) | A1 | A1O3_A1 | 9 | 10 | 938 | 25.30 | 1.30 | ** | 0.38 | 0.64 |
| 6 | Motion interval (episode) | A1O2 | A1O2 | 10 | 10 | 742 | 38.39 | 1.75 | *** | 0.63 | 0.82 |
| 6 | Motion interval (episode) | A1O3 | A1O3 | 9 | 10 | 151 | 54.46 | 4.29 | **** | 0.95 | 0.98 |
| 6 | Motion interval (episode) | A1L1 | A1L1 | 11 | 10 | 1685 | 6.08 | 0.28 | **** | 0.00 | 0.00 |
| 6 | Motion interval (episode) | A1L3 | A1L3 | 12 | 10 | 1719 | 6.23 | 0.30 | **** | 0.00 | 0.01 |
| 6 | Motion interval (episode) | CT | A1BT_CT | 13 | 6 | 1007 | 34.07 | 1.32 | | 0.55 | 0.77 |
| 6 | Motion interval (episode) | A5 | A1BT_A5 | 13 | 6 | 2169 | 9.23 | 0.32 | **** | 0.06 | 0.19 |
| 6 | Motion interval (episode) | A1 | A1BT_A1 | 13 | 6 | 635 | 34.78 | 1.86 | ns | 0.56 | 0.78 |
| 6 | Motion interval (episode) | A1BT | A1BT | 13 | 6 | 262 | 56.98 | 4.70 | **** | 1.00 | 1.00 |
| 7 | Body angle (min) | CT | A1O3_CT | 9 | 10 | 1007 | 9.71 | 0.19 | | 0.62 | 0.65 |
| 7 | Body angle (min) | A5 | A1O3_A5 | 9 | 10 | 2796 | 10.47 | 0.10 | *** | 0.90 | 0.91 |
| 7 | Body angle (min) | A1 | A1O3_A1 | 9 | 10 | 960 | 9.41 | 0.18 | ns | 0.51 | 0.55 |
| 7 | Body angle (min) | A1O2 | A1O2 | 10 | 10 | 779 | 9.63 | 0.21 | ns | 0.59 | 0.63 |
| 7 | Body angle (min) | A1O3 | A1O3 | 9 | 10 | 165 | 8.88 | 0.47 | ns | 0.32 | 0.35 |
| 7 | Body angle (min) | A1L1 | A1L1 | 11 | 10 | 1685 | 8.01 | 0.13 | **** | 0.00 | 0.00 |
| 7 | Body angle (min) | A1L3 | A1L3 | 12 | 10 | 1726 | 8.27 | 0.13 | **** | 0.09 | 0.11 |
| 7 | Body angle (min) | CT | A1BT_CT | 13 | 6 | 1078 | 9.42 | 0.17 | | 0.51 | 0.55 |
| 7 | Body angle (min) | A5 | A1BT_A5 | 13 | 6 | 2229 | 10.75 | 0.11 | **** | 1.00 | 1.00 |
| 7 | Body angle (min) | A1 | A1BT_A1 | 13 | 6 | 687 | 10.27 | 0.22 | ** | 0.83 | 0.85 |
| 7 | Body angle (min) | A1BT | A1BT | 13 | 6 | 275 | 8.77 | 0.34 | ns | 0.28 | 0.31 |
| 8 | Feet 2D distance (max) | CT | A1O3_CT | 9 | 10 | 1009 | 3.33 | 0.01 | | 0.09 | 0.10 |
| 8 | Feet 2D distance (max) | A5 | A1O3_A5 | 9 | 10 | 2786 | 3.65 | 0.01 | **** | 0.55 | 0.58 |
| 8 | Feet 2D distance (max) | A1 | A1O3_A1 | 9 | 10 | 952 | 3.66 | 0.02 | **** | 0.57 | 0.59 |
| 8 | Feet 2D distance (max) | A1O2 | A1O2 | 10 | 10 | 779 | 3.65 | 0.02 | **** | 0.56 | 0.58 |
| 8 | Feet 2D distance (max) | A1O3 | A1O3 | 9 | 10 | 165 | 3.61 | 0.03 | **** | 0.49 | 0.52 |
| 8 | Feet 2D distance (max) | A1L1 | A1L1 | 11 | 10 | 1685 | 3.96 | 0.01 | **** | 1.00 | 1.00 |
| 8 | Feet 2D distance (max) | A1L3 | A1L3 | 12 | 10 | 1726 | 3.67 | 0.01 | **** | 0.58 | 0.61 |
| 8 | Feet 2D distance (max) | CT | A1BT_CT | 13 | 6 | 1069 | 3.26 | 0.01 | | 0.00 | 0.00 |
| 8 | Feet 2D distance (max) | A5 | A1BT_A5 | 13 | 6 | 2206 | 3.71 | 0.01 | **** | 0.64 | 0.66 |
| 8 | Feet 2D distance (max) | A1 | A1BT_A1 | 13 | 6 | 682 | 3.79 | 0.02 | **** | 0.75 | 0.77 |
| 8 | Feet 2D distance (max) | A1BT | A1BT | 13 | 6 | 275 | 3.81 | 0.03 | **** | 0.78 | 0.79 |
| 9 | Neck 3D velocity (std) | CT | A1O3_CT | 9 | 10 | 1005 | 5.27 | 0.04 | | 0.31 | 0.36 |
| 9 | Neck 3D velocity (std) | A5 | A1O3_A5 | 9 | 10 | 2779 | 5.41 | 0.03 | ** | 0.36 | 0.42 |
| 9 | Neck 3D velocity (std) | A1 | A1O3_A1 | 9 | 10 | 960 | 4.67 | 0.04 | **** | 0.09 | 0.11 |
| 9 | Neck 3D velocity (std) | A1O2 | A1O2 | 10 | 10 | 779 | 4.86 | 0.04 | **** | 0.16 | 0.19 |
| 9 | Neck 3D velocity (std) | A1O3 | A1O3 | 9 | 10 | 169 | 4.85 | 0.08 | **** | 0.15 | 0.19 |
| 9 | Neck 3D velocity (std) | A1L1 | A1L1 | 11 | 10 | 1685 | 7.18 | 0.06 | **** | 1.00 | 1.00 |
| 9 | Neck 3D velocity (std) | A1L3 | A1L3 | 12 | 10 | 1726 | 6.30 | 0.04 | **** | 0.68 | 0.73 |
| 9 | Neck 3D velocity (std) | CT | A1BT_CT | 13 | 6 | 1071 | 5.15 | 0.04 | | 0.26 | 0.31 |
| 9 | Neck 3D velocity (std) | A5 | A1BT_A5 | 13 | 6 | 2218 | 5.05 | 0.03 | * | 0.23 | 0.27 |
| 9 | Neck 3D velocity (std) | A1 | A1BT_A1 | 13 | 6 | 679 | 4.68 | 0.05 | **** | 0.09 | 0.11 |
| 9 | Neck 3D velocity (std) | A1BT | A1BT | 13 | 6 | 275 | 4.42 | 0.06 | **** | 0.00 | 0.00 |
| 10 | Feet 2D distance (std) | CT | A1O3_CT | 9 | 10 | 1003 | 0.35 | 0.01 | | 0.11 | 0.13 |
| 10 | Feet 2D distance (std) | A5 | A1O3_A5 | 9 | 10 | 2784 | 0.54 | 0.00 | **** | 0.99 | 0.99 |
| 10 | Feet 2D distance (std) | A1 | A1O3_A1 | 9 | 10 | 962 | 0.43 | 0.01 | **** | 0.45 | 0.51 |
| 10 | Feet 2D distance (std) | A1O2 | A1O2 | 10 | 10 | 779 | 0.43 | 0.01 | **** | 0.48 | 0.54 |
| 10 | Feet 2D distance (std) | A1O3 | A1O3 | 9 | 10 | 163 | 0.42 | 0.02 | *** | 0.44 | 0.50 |
| 10 | Feet 2D distance (std) | A1L1 | A1L1 | 11 | 10 | 1685 | 0.51 | 0.00 | **** | 0.85 | 0.88 |
| 10 | Feet 2D distance (std) | A1L3 | A1L3 | 12 | 10 | 1726 | 0.45 | 0.00 | **** | 0.58 | 0.64 |
| 10 | Feet 2D distance (std) | CT | A1BT_CT | 13 | 6 | 1072 | 0.33 | 0.01 | | 0.00 | 0.00 |
| 10 | Feet 2D distance (std) | A5 | A1BT_A5 | 13 | 6 | 2215 | 0.54 | 0.01 | **** | 1.00 | 1.00 |
| 10 | Feet 2D distance (std) | A1 | A1BT_A1 | 13 | 6 | 681 | 0.46 | 0.01 | **** | 0.62 | 0.67 |
| 10 | Feet 2D distance (std) | A1BT | A1BT | 13 | 6 | 275 | 0.40 | 0.01 | **** | 0.32 | 0.38 |
| 11 | Chest 3D velocity (mean) | CT | A1O3_CT | 9 | 10 | 1017 | 4.44 | 0.05 | | 0.19 | 0.23 |
| 11 | Chest 3D velocity (mean) | A5 | A1O3_A5 | 9 | 10 | 2807 | 5.57 | 0.04 | **** | 0.66 | 0.71 |
| 11 | Chest 3D velocity (mean) | A1 | A1O3_A1 | 9 | 10 | 967 | 4.20 | 0.05 | *** | 0.09 | 0.11 |
| 11 | Chest 3D velocity (mean) | A1O2 | A1O2 | 10 | 10 | 779 | 4.29 | 0.05 | * | 0.13 | 0.16 |
| 11 | Chest 3D velocity (mean) | A1O3 | A1O3 | 9 | 10 | 169 | 4.24 | 0.11 | ns | 0.11 | 0.13 |
| 11 | Chest 3D velocity (mean) | A1L1 | A1L1 | 11 | 10 | 1685 | 6.38 | 0.07 | **** | 1.00 | 1.00 |
| 11 | Chest 3D velocity (mean) | A1L3 | A1L3 | 12 | 10 | 1726 | 5.40 | 0.05 | **** | 0.59 | 0.65 |
| 11 | Chest 3D velocity (mean) | CT | A1BT_CT | 13 | 6 | 1060 | 4.29 | 0.04 | | 0.13 | 0.16 |
| 11 | Chest 3D velocity (mean) | A5 | A1BT_A5 | 13 | 6 | 2202 | 5.21 | 0.04 | **** | 0.51 | 0.57 |
| 11 | Chest 3D velocity (mean) | A1 | A1BT_A1 | 13 | 6 | 689 | 4.24 | 0.05 | ns | 0.11 | 0.13 |
| 11 | Chest 3D velocity (mean) | A1BT | A1BT | 13 | 6 | 275 | 3.98 | 0.07 | *** | 0.00 | 0.00 |
| 12 | U-body 3D length (min) | CT | A1O3_CT | 9 | 10 | 1010 | 2.96 | 0.02 | | 0.60 | 0.61 |
| 12 | U-body 3D length (min) | A5 | A1O3_A5 | 9 | 10 | 2786 | 3.08 | 0.01 | **** | 0.97 | 0.97 |
| 12 | U-body 3D length (min) | A1 | A1O3_A1 | 9 | 10 | 970 | 3.02 | 0.01 | ** | 0.79 | 0.79 |
| 12 | U-body 3D length (min) | A1O2 | A1O2 | 10 | 10 | 779 | 3.04 | 0.02 | *** | 0.85 | 0.86 |
| 12 | U-body 3D length (min) | A1O3 | A1O3 | 9 | 10 | 165 | 3.02 | 0.03 | ns | 0.77 | 0.78 |
| 12 | U-body 3D length (min) | A1L1 | A1L1 | 11 | 10 | 1685 | 2.75 | 0.01 | **** | 0.00 | 0.00 |
| 12 | U-body 3D length (min) | A1L3 | A1L3 | 12 | 10 | 1726 | 2.89 | 0.01 | *** | 0.41 | 0.43 |
| 12 | U-body 3D length (min) | CT | A1BT_CT | 13 | 6 | 1075 | 3.00 | 0.02 | | 0.72 | 0.73 |
| 12 | U-body 3D length (min) | A5 | A1BT_A5 | 13 | 6 | 2249 | 3.08 | 0.01 | **** | 0.96 | 0.96 |
| 12 | U-body 3D length (min) | A1 | A1BT_A1 | 13 | 6 | 683 | 3.09 | 0.02 | **** | 1.00 | 1.00 |
| 12 | U-body 3D length (min) | A1BT | A1BT | 13 | 6 | 275 | 3.01 | 0.02 | ns | 0.75 | 0.76 |
| 13 | Right limb angle asym. (min) | CT | A1O3_CT | 9 | 10 | 1015 | -47.03 | 0.52 | | 0.40 | |
| 13 | Right limb angle asym. (min) | A5 | A1O3_A5 | 9 | 10 | 2748 | -53.62 | 0.64 | **** | 0.02 | |
| 13 | Right limb angle asym. (min) | A1 | A1O3_A1 | 9 | 10 | 952 | -46.57 | 0.81 | ns | 0.42 | |
| 13 | Right limb angle asym. (min) | A1O2 | A1O2 | 10 | 10 | 779 | -43.15 | 0.67 | **** | 0.61 | |
| 13 | Right limb angle asym. (min) | A1O3 | A1O3 | 9 | 10 | 165 | -47.36 | 1.63 | ns | 0.38 | |
| 13 | Right limb angle asym. (min) | A1L1 | A1L1 | 11 | 10 | 1685 | -36.31 | 0.39 | **** | 1.00 | |
| 13 | Right limb angle asym. (min) | A1L3 | A1L3 | 12 | 10 | 1726 | -40.95 | 0.47 | **** | 0.74 | |
| 13 | Right limb angle asym. (min) | CT | A1BT_CT | 13 | 6 | 1077 | -45.92 | 0.52 | | 0.46 | |
| 13 | Right limb angle asym. (min) | A5 | A1BT_A5 | 13 | 6 | 2195 | -54.06 | 0.71 | **** | 0.00 | |
| 13 | Right limb angle asym. (min) | A1 | A1BT_A1 | 13 | 6 | 674 | -44.90 | 0.90 | ns | 0.52 | |
| 13 | Right limb angle asym. (min) | A1BT | A1BT | 13 | 6 | 275 | -48.91 | 1.50 | ns | 0.29 | |
| 14 | Hands 3D distance (max) | CT | A1O3_CT | 9 | 10 | 1004 | 2.96 | 0.02 | | 0.11 | 0.12 |
| 14 | Hands 3D distance (max) | A5 | A1O3_A5 | 9 | 10 | 2766 | 3.79 | 0.03 | **** | 1.00 | 1.00 |
| 14 | Hands 3D distance (max) | A1 | A1O3_A1 | 9 | 10 | 952 | 3.32 | 0.04 | **** | 0.49 | 0.53 |
| 14 | Hands 3D distance (max) | A1O2 | A1O2 | 10 | 10 | 779 | 3.04 | 0.04 | ns | 0.19 | 0.22 |
| 14 | Hands 3D distance (max) | A1O3 | A1O3 | 9 | 10 | 168 | 3.14 | 0.07 | * | 0.30 | 0.33 |
| 14 | Hands 3D distance (max) | A1L1 | A1L1 | 11 | 10 | 1685 | 3.02 | 0.01 | ns | 0.16 | 0.18 |
| 14 | Hands 3D distance (max) | A1L3 | A1L3 | 12 | 10 | 1726 | 2.89 | 0.02 | ** | 0.02 | 0.03 |
| 14 | Hands 3D distance (max) | CT | A1BT_CT | 13 | 6 | 1062 | 2.87 | 0.02 | | 0.00 | 0.00 |
| 14 | Hands 3D distance (max) | A5 | A1BT_A5 | 13 | 6 | 2217 | 3.67 | 0.03 | **** | 0.87 | 0.89 |
| 14 | Hands 3D distance (max) | A1 | A1BT_A1 | 13 | 6 | 674 | 3.40 | 0.05 | **** | 0.58 | 0.61 |
| 14 | Hands 3D distance (max) | A1BT | A1BT | 13 | 6 | 275 | 3.48 | 0.08 | **** | 0.67 | 0.70 |
| 15 | Left limb angle asym. (min) | CT | A1O3_CT | 9 | 10 | 1013 | -52.23 | 0.63 | | 0.55 | |
| 15 | Left limb angle asym. (min) | A5 | A1O3_A5 | 9 | 10 | 2750 | -67.02 | 0.71 | **** | 0.00 | |
| 15 | Left limb angle asym. (min) | A1 | A1O3_A1 | 9 | 10 | 957 | -56.25 | 0.95 | *** | 0.40 | |
| 15 | Left limb angle asym. (min) | A1O2 | A1O2 | 10 | 10 | 779 | -53.56 | 0.92 | ns | 0.50 | |
| 15 | Left limb angle asym. (min) | A1O3 | A1O3 | 9 | 10 | 165 | -53.41 | 1.61 | ns | 0.51 | |
| 15 | Left limb angle asym. (min) | A1L1 | A1L1 | 11 | 10 | 1685 | -46.96 | 0.52 | **** | 0.75 | |
| 15 | Left limb angle asym. (min) | A1L3 | A1L3 | 12 | 10 | 1726 | -40.26 | 0.37 | **** | 1.00 | |
| 15 | Left limb angle asym. (min) | CT | A1BT_CT | 13 | 6 | 1067 | -51.87 | 0.59 | | 0.57 | |
| 15 | Left limb angle asym. (min) | A5 | A1BT_A5 | 13 | 6 | 2216 | -63.59 | 0.77 | **** | 0.13 | |
| 15 | Left limb angle asym. (min) | A1 | A1BT_A1 | 13 | 6 | 671 | -55.69 | 1.11 | ** | 0.42 | |
| 15 | Left limb angle asym. (min) | A1BT | A1BT | 13 | 6 | 275 | -60.09 | 1.95 | *** | 0.26 | |
| 16 | Chest 1D velocity (max) | CT | A1O3_CT | 9 | 10 | 1023 | 0.13 | 0.00 | | 0.81 | 0.86 |
| 16 | Chest 1D velocity (max) | A5 | A1O3_A5 | 9 | 10 | 2798 | 0.08 | 0.00 | **** | 0.09 | 0.12 |
| 16 | Chest 1D velocity (max) | A1 | A1O3_A1 | 9 | 10 | 967 | 0.08 | 0.00 | **** | 0.15 | 0.20 |
| 16 | Chest 1D velocity (max) | A1O2 | A1O2 | 10 | 10 | 782 | 0.12 | 0.00 | ns | 0.72 | 0.78 |
| 16 | Chest 1D velocity (max) | A1O3 | A1O3 | 9 | 10 | 171 | 0.09 | 0.01 | *** | 0.32 | 0.40 |
| 16 | Chest 1D velocity (max) | A1L1 | A1L1 | 11 | 10 | 1702 | 0.12 | 0.00 | ns | 0.68 | 0.75 |
| 16 | Chest 1D velocity (max) | A1L3 | A1L3 | 12 | 10 | 1738 | 0.14 | 0.00 | ** | 1.00 | 1.00 |
| 16 | Chest 1D velocity (max) | CT | A1BT_CT | 13 | 6 | 1089 | 0.13 | 0.00 | | 0.83 | 0.87 |
| 16 | Chest 1D velocity (max) | A5 | A1BT_A5 | 13 | 6 | 2227 | 0.07 | 0.00 | **** | 0.00 | 0.00 |
| 16 | Chest 1D velocity (max) | A1 | A1BT_A1 | 13 | 6 | 690 | 0.08 | 0.00 | **** | 0.09 | 0.13 |
| 16 | Chest 1D velocity (max) | A1BT | A1BT | 13 | 6 | 278 | 0.08 | 0.01 | **** | 0.14 | 0.20 |
| 17 | Leg angle asym. (std) | CT | A1O3_CT | 9 | 10 | 1011 | 15.78 | 0.20 | | 0.15 | 0.18 |
| 17 | Leg angle asym. (std) | A5 | A1O3_A5 | 9 | 10 | 2793 | 20.79 | 0.16 | **** | 0.90 | 0.92 |
| 17 | Leg angle asym. (std) | A1 | A1O3_A1 | 9 | 10 | 951 | 18.49 | 0.24 | **** | 0.56 | 0.60 |
| 17 | Leg angle asym. (std) | A1O2 | A1O2 | 10 | 10 | 779 | 16.68 | 0.27 | ** | 0.29 | 0.33 |
| 17 | Leg angle asym. (std) | A1O3 | A1O3 | 9 | 10 | 168 | 17.72 | 0.48 | *** | 0.44 | 0.49 |
| 17 | Leg angle asym. (std) | A1L1 | A1L1 | 11 | 10 | 1685 | 16.92 | 0.11 | **** | 0.32 | 0.36 |
| 17 | Leg angle asym. (std) | A1L3 | A1L3 | 12 | 10 | 1726 | 14.77 | 0.11 | **** | 0.00 | 0.00 |
| 17 | Leg angle asym. (std) | CT | A1BT_CT | 13 | 6 | 1071 | 15.24 | 0.21 | | 0.07 | 0.08 |
| 17 | Leg angle asym. (std) | A5 | A1BT_A5 | 13 | 6 | 2196 | 21.45 | 0.17 | **** | 1.00 | 1.00 |
| 17 | Leg angle asym. (std) | A1 | A1BT_A1 | 13 | 6 | 676 | 20.45 | 0.31 | **** | 0.85 | 0.87 |
| 17 | Leg angle asym. (std) | A1BT | A1BT | 13 | 6 | 275 | 19.68 | 0.56 | **** | 0.73 | 0.77 |
| 18 | Feet 2D distance (mean) | CT | A1O3_CT | 9 | 10 | 1012 | 2.65 | 0.01 | | 0.06 | 0.07 |
| 18 | Feet 2D distance (mean) | A5 | A1O3_A5 | 9 | 10 | 2782 | 2.62 | 0.01 | ns | 0.00 | 0.00 |
| 18 | Feet 2D distance (mean) | A1 | A1O3_A1 | 9 | 10 | 951 | 2.89 | 0.01 | **** | 0.59 | 0.61 |
| 18 | Feet 2D distance (mean) | A1O2 | A1O2 | 10 | 10 | 779 | 2.87 | 0.02 | **** | 0.54 | 0.56 |
| 18 | Feet 2D distance (mean) | A1O3 | A1O3 | 9 | 10 | 164 | 2.89 | 0.03 | **** | 0.59 | 0.61 |
| 18 | Feet 2D distance (mean) | A1L1 | A1L1 | 11 | 10 | 1685 | 2.99 | 0.01 | **** | 0.81 | 0.82 |
| 18 | Feet 2D distance (mean) | A1L3 | A1L3 | 12 | 10 | 1726 | 2.95 | 0.01 | **** | 0.71 | 0.73 |
| 18 | Feet 2D distance (mean) | CT | A1BT_CT | 13 | 6 | 1073 | 2.64 | 0.01 | | 0.03 | 0.04 |
| 18 | Feet 2D distance (mean) | A5 | A1BT_A5 | 13 | 6 | 2196 | 2.65 | 0.01 | ns | 0.06 | 0.06 |
| 18 | Feet 2D distance (mean) | A1 | A1BT_A1 | 13 | 6 | 674 | 2.94 | 0.02 | **** | 0.70 | 0.71 |
| 18 | Feet 2D distance (mean) | A1BT | A1BT | 13 | 6 | 275 | 3.08 | 0.03 | **** | 1.00 | 1.00 |
| 19 | Anus 1D velocity (std) | CT | A1O3_CT | 9 | 10 | 1017 | 0.06 | 0.00 | | 0.80 | 0.82 |
| 19 | Anus 1D velocity (std) | A5 | A1O3_A5 | 9 | 10 | 2790 | 0.05 | 0.00 | **** | 0.31 | 0.34 |
| 19 | Anus 1D velocity (std) | A1 | A1O3_A1 | 9 | 10 | 958 | 0.05 | 0.00 | ** | 0.45 | 0.48 |
| 19 | Anus 1D velocity (std) | A1O2 | A1O2 | 10 | 10 | 779 | 0.06 | 0.00 | ns | 1.00 | 1.00 |
| 19 | Anus 1D velocity (std) | A1O3 | A1O3 | 9 | 10 | 166 | 0.06 | 0.00 | ns | 0.68 | 0.71 |
| 19 | Anus 1D velocity (std) | A1L1 | A1L1 | 11 | 10 | 1685 | 0.06 | 0.00 | ns | 0.66 | 0.68 |
| 19 | Anus 1D velocity (std) | A1L3 | A1L3 | 12 | 10 | 1726 | 0.05 | 0.00 | **** | 0.29 | 0.31 |
| 19 | Anus 1D velocity (std) | CT | A1BT_CT | 13 | 6 | 1073 | 0.05 | 0.00 | | 0.53 | 0.55 |
| 19 | Anus 1D velocity (std) | A5 | A1BT_A5 | 13 | 6 | 2219 | 0.05 | 0.00 | * | 0.33 | 0.36 |
| 19 | Anus 1D velocity (std) | A1 | A1BT_A1 | 13 | 6 | 677 | 0.05 | 0.00 | ns | 0.37 | 0.40 |
| 19 | Anus 1D velocity (std) | A1BT | A1BT | 13 | 6 | 275 | 0.05 | 0.00 | ** | 0.00 | 0.00 |
| 20 | Arm angle asym. (mean) | CT | A1O3_CT | 9 | 10 | 1000 | -4.20 | 0.42 | | 0.62 | |
| 20 | Arm angle asym. (mean) | A5 | A1O3_A5 | 9 | 10 | 2746 | -10.01 | 0.43 | **** | 0.00 | |
| 20 | Arm angle asym. (mean) | A1 | A1O3_A1 | 9 | 10 | 949 | -9.43 | 0.57 | **** | 0.06 | |
| 20 | Arm angle asym. (mean) | A1O2 | A1O2 | 10 | 10 | 779 | -3.12 | 0.56 | ns | 0.74 | |
| 20 | Arm angle asym. (mean) | A1O3 | A1O3 | 9 | 10 | 166 | -2.17 | 1.24 | ns | 0.84 | |
| 20 | Arm angle asym. (mean) | A1L1 | A1L1 | 11 | 10 | 1685 | -0.68 | 0.23 | **** | 1.00 | |
| 20 | Arm angle asym. (mean) | A1L3 | A1L3 | 12 | 10 | 1726 | -5.97 | 0.27 | *** | 0.43 | |
| 20 | Arm angle asym. (mean) | CT | A1BT_CT | 13 | 6 | 1072 | -3.07 | 0.40 | | 0.74 | |
| 20 | Arm angle asym. (mean) | A5 | A1BT_A5 | 13 | 6 | 2187 | -8.55 | 0.46 | **** | 0.16 | |
| 20 | Arm angle asym. (mean) | A1 | A1BT_A1 | 13 | 6 | 669 | -4.54 | 0.67 | ns | 0.59 | |
| 20 | Arm angle asym. (mean) | A1BT | A1BT | 13 | 6 | 275 | -1.49 | 1.12 | ns | 0.91 | |

**Supplementary Table 16. Statistical summary of the KL divergences for the top 20 features identified by the TSFEL model comparing CT and PD (A5) groups.** For each group, the KL divergence of each feature relative to its baseline value (0 wk) was computed across the experimental duration (0–10 wk). Each group consisted of 6 sampling sets, each containing 150 randomly selected clips. A two-way ANOVA (group × week) was performed for each feature, followed by weekly t-tests between groups (CT vs. A5). The resulting p-values from the weekly t-tests were corrected for multiple comparisons using the Bonferroni method. Source data are provided in the Source Data file (See S_Figure 36).

| Rank | Feature name | group | Week | n | Mean | SEM | raw_p | corrected_p | significant | ANOVA_p_ Week | ANOVA_p_ Group | ANOVA_p_ Interaction |
|---|---|---|---|---|---|---|---|---|---|---|---|---|
| 1 | Foot distance_Signal distance | A5 | 0 | 6 | 0 | 0 | | 1 | ns | 3.93E-16 | 6.16E-25 | 8.67E-14 |
| 1 | Foot distance_Signal distance | CT | 0 | 6 | 0 | 0 | | 1 | ns | 3.93E-16 | 6.16E-25 | 8.67E-14 |
| 1 | Foot distance_Signal distance | A5 | 2 | 6 | 0.17037522 | 0.02646104 | 0.000321265 | 0.001927588 | ** | 3.93E-16 | 6.16E-25 | 8.67E-14 |
| 1 | Foot distance_Signal distance | CT | 2 | 6 | 0.023515 | 0.00720487 | 0.000321265 | 0.001927588 | ** | 3.93E-16 | 6.16E-25 | 8.67E-14 |
| 1 | Foot distance_Signal distance | A5 | 4 | 6 | 0.35026564 | 0.03390482 | 8.80242E-06 | 5.28145E-05 | **** | 3.93E-16 | 6.16E-25 | 8.67E-14 |
| 1 | Foot distance_Signal distance | CT | 4 | 6 | 0.05185242 | 0.01236075 | 8.80242E-06 | 5.28145E-05 | **** | 3.93E-16 | 6.16E-25 | 8.67E-14 |
| 1 | Foot distance_Signal distance | A5 | 6 | 6 | 0.66230744 | 0.07718672 | 1.06087E-05 | 6.36519E-05 | **** | 3.93E-16 | 6.16E-25 | 8.67E-14 |
| 1 | Foot distance_Signal distance | CT | 6 | 6 | 0.03341345 | 0.00876266 | 1.06087E-05 | 6.36519E-05 | **** | 3.93E-16 | 6.16E-25 | 8.67E-14 |
| 1 | Foot distance_Signal distance | A5 | 8 | 6 | 0.61365844 | 0.06685874 | 8.21868E-06 | 4.93121E-05 | **** | 3.93E-16 | 6.16E-25 | 8.67E-14 |
| 1 | Foot distance_Signal distance | CT | 8 | 6 | 0.05446035 | 0.00570742 | 8.21868E-06 | 4.93121E-05 | **** | 3.93E-16 | 6.16E-25 | 8.67E-14 |
| 1 | Foot distance_Signal distance | A5 | 10 | 6 | 0.72959533 | 0.07149887 | 3.19215E-06 | 1.91529E-05 | **** | 3.93E-16 | 6.16E-25 | 8.67E-14 |
| 1 | Foot distance_Signal distance | CT | 10 | 6 | 0.06219027 | 0.0089115 | 3.19215E-06 | 1.91529E-05 | **** | 3.93E-16 | 6.16E-25 | 8.67E-14 |
| 2 | Tail angle_Autocorrelation | A5 | 0 | 6 | 0 | 0 | | 1 | ns | 3.45E-13 | 3.14E-10 | 4.79E-07 |
| 2 | Tail angle_Autocorrelation | CT | 0 | 6 | 0 | 0 | | 1 | ns | 3.45E-13 | 3.14E-10 | 4.79E-07 |
| 2 | Tail angle_Autocorrelation | A5 | 2 | 6 | 0.09561193 | 0.01742607 | 0.009775118 | 0.058650709 | ns | 3.45E-13 | 3.14E-10 | 4.79E-07 |
| 2 | Tail angle_Autocorrelation | CT | 2 | 6 | 0.03269221 | 0.00933625 | 0.009775118 | 0.058650709 | ns | 3.45E-13 | 3.14E-10 | 4.79E-07 |
| 2 | Tail angle_Autocorrelation | A5 | 4 | 6 | 0.09137207 | 0.01363908 | 0.432993649 | 1 | ns | 3.45E-13 | 3.14E-10 | 4.79E-07 |
| 2 | Tail angle_Autocorrelation | CT | 4 | 6 | 0.06762204 | 0.02567395 | 0.432993649 | 1 | ns | 3.45E-13 | 3.14E-10 | 4.79E-07 |
| 2 | Tail angle_Autocorrelation | A5 | 6 | 6 | 0.11437181 | 0.0244785 | 0.010348152 | 0.062088912 | ns | 3.45E-13 | 3.14E-10 | 4.79E-07 |
| 2 | Tail angle_Autocorrelation | CT | 6 | 6 | 0.03310391 | 0.00817154 | 0.010348152 | 0.062088912 | ns | 3.45E-13 | 3.14E-10 | 4.79E-07 |
| 2 | Tail angle_Autocorrelation | A5 | 8 | 6 | 0.28049632 | 0.04531416 | 0.003065643 | 0.018393855 | * | 3.45E-13 | 3.14E-10 | 4.79E-07 |
| 2 | Tail angle_Autocorrelation | CT | 8 | 6 | 0.1034635 | 0.00546772 | 0.003065643 | 0.018393855 | * | 3.45E-13 | 3.14E-10 | 4.79E-07 |
| 2 | Tail angle_Autocorrelation | A5 | 10 | 6 | 0.36977884 | 0.05547362 | 0.000411656 | 0.002469938 | ** | 3.45E-13 | 3.14E-10 | 4.79E-07 |
| 2 | Tail angle_Autocorrelation | CT | 10 | 6 | 0.07717747 | 0.01051198 | 0.000411656 | 0.002469938 | ** | 3.45E-13 | 3.14E-10 | 4.79E-07 |
| 3 | Neck acc._Wavelet std_4 | A5 | 0 | 6 | 0 | 0 | | 1 | ns | 1.55E-27 | 2.62E-32 | 1.07E-25 |
| 3 | Neck acc._Wavelet std_4 | CT | 0 | 6 | 0 | 0 | | 1 | ns | 1.55E-27 | 2.62E-32 | 1.07E-25 |
| 3 | Neck acc._Wavelet std_4 | A5 | 2 | 6 | 0.07421688 | 0.00969439 | 0.005100132 | 0.030600789 | * | 1.55E-27 | 2.62E-32 | 1.07E-25 |
| 3 | Neck acc._Wavelet std_4 | CT | 2 | 6 | 0.03404681 | 0.0057154 | 0.005100132 | 0.030600789 | * | 1.55E-27 | 2.62E-32 | 1.07E-25 |
| 3 | Neck acc._Wavelet std_4 | A5 | 4 | 6 | 0.15359882 | 0.01805963 | 2.76E-05 | 1.66E-04 | *** | 1.55E-27 | 2.62E-32 | 1.07E-25 |
| 3 | Neck acc._Wavelet std_4 | CT | 4 | 6 | 0.02177305 | 0.00213357 | 2.76E-05 | 1.66E-04 | *** | 1.55E-27 | 2.62E-32 | 1.07E-25 |
| 3 | Neck acc._Wavelet std_4 | A5 | 6 | 6 | 0.55646892 | 0.05201572 | 4.24E-06 | 2.55E-05 | **** | 1.55E-27 | 2.62E-32 | 1.07E-25 |
| 3 | Neck acc._Wavelet std_4 | CT | 6 | 6 | 0.06793186 | 0.01604118 | 4.24E-06 | 2.55E-05 | **** | 1.55E-27 | 2.62E-32 | 1.07E-25 |
| 3 | Neck acc._Wavelet std_4 | A5 | 8 | 6 | 0.66091673 | 0.03725616 | 1.17256E-08 | 7.03534E-08 | **** | 1.55E-27 | 2.62E-32 | 1.07E-25 |
| 3 | Neck acc._Wavelet std_4 | CT | 8 | 6 | 0.02483187 | 0.0067696 | 1.17256E-08 | 7.03534E-08 | **** | 1.55E-27 | 2.62E-32 | 1.07E-25 |
| 3 | Neck acc._Wavelet std_4 | A5 | 10 | 6 | 0.73545469 | 0.04466466 | 3.27E-08 | 1.96E-07 | **** | 1.55E-27 | 2.62E-32 | 1.07E-25 |
| 3 | Neck acc._Wavelet std_4 | CT | 10 | 6 | 0.04051667 | 0.01103669 | 3.27E-08 | 1.96E-07 | **** | 1.55E-27 | 2.62E-32 | 1.07E-25 |
| 4 | Body angle velocity_ECDF percentile 0 | A5 | 0 | 6 | 0 | 0 | | 1 | ns | 3.75E-09 | 3.73E-06 | 1.66E-03 |
| 4 | Body angle velocity_ECDF percentile 0 | CT | 0 | 6 | 0 | 0 | | 1 | ns | 3.75E-09 | 3.73E-06 | 1.66E-03 |
| 4 | Body angle velocity_ECDF percentile 0 | A5 | 2 | 6 | 0.02404809 | 0.00528348 | 0.774706661 | 1 | ns | 3.75E-09 | 3.73E-06 | 1.66E-03 |
| 4 | Body angle velocity_ECDF percentile 0 | CT | 2 | 6 | 0.02196881 | 0.00469833 | 0.774706661 | 1 | ns | 3.75E-09 | 3.73E-06 | 1.66E-03 |
| 4 | Body angle velocity_ECDF percentile 0 | A5 | 4 | 6 | 0.05367335 | 0.01466589 | 0.21998823 | 1 | ns | 3.75E-09 | 3.73E-06 | 1.66E-03 |
| 4 | Body angle velocity_ECDF percentile 0 | CT | 4 | 6 | 0.03258461 | 0.00668379 | 0.21998823 | 1 | ns | 3.75E-09 | 3.73E-06 | 1.66E-03 |
| 4 | Body angle velocity_ECDF percentile 0 | A5 | 6 | 6 | 0.12555558 | 0.0175272 | 1.11E-02 | 6.66E-02 | ns | 3.75E-09 | 3.73E-06 | 1.66E-03 |
| 4 | Body angle velocity_ECDF percentile 0 | CT | 6 | 6 | 0.05600679 | 0.01391638 | 1.11E-02 | 6.66E-02 | ns | 3.75E-09 | 3.73E-06 | 1.66E-03 |
| 4 | Body angle velocity_ECDF percentile 0 | A5 | 8 | 6 | 0.18448129 | 0.03012059 | 8.87E-03 | 0.053193546 | ns | 3.75E-09 | 3.73E-06 | 1.66E-03 |
| 4 | Body angle velocity_ECDF percentile 0 | CT | 8 | 6 | 0.05883925 | 0.02441882 | 8.87E-03 | 0.053193546 | ns | 3.75E-09 | 3.73E-06 | 1.66E-03 |
| 4 | Body angle velocity_ECDF percentile 0 | A5 | 10 | 6 | 0.17332734 | 0.04242629 | 2.62E-02 | 1.57E-01 | ns | 3.75E-09 | 3.73E-06 | 1.66E-03 |
| 4 | Body angle velocity_ECDF percentile 0 | CT | 10 | 6 | 0.05612191 | 0.01493762 | 2.62E-02 | 1.57E-01 | ns | 3.75E-09 | 3.73E-06 | 1.66E-03 |
| 5 | Body angle_min | A5 | 0 | 6 | 0 | 0 | | 1 | ns | 7.38E-18 | 1.39E-14 | 1.04E-07 |
| 5 | Body angle_min | CT | 0 | 6 | 0 | 0 | | 1 | ns | 7.38E-18 | 1.39E-14 | 1.04E-07 |
| 5 | Body angle_min | A5 | 2 | 6 | 0.06455932 | 0.00910821 | 0.021637462 | 0.129824771 | ns | 7.38E-18 | 1.39E-14 | 1.04E-07 |
| 5 | Body angle_min | CT | 2 | 6 | 0.03237961 | 0.00756454 | 0.021637462 | 0.129824771 | ns | 7.38E-18 | 1.39E-14 | 1.04E-07 |
| 5 | Body angle_min | A5 | 4 | 6 | 0.06967051 | 0.00709253 | 0.014873619 | 0.089241714 | ns | 7.38E-18 | 1.39E-14 | 1.04E-07 |
| 5 | Body angle_min | CT | 4 | 6 | 0.03530771 | 0.00930748 | 0.014873619 | 0.089241714 | ns | 7.38E-18 | 1.39E-14 | 1.04E-07 |
| 5 | Body angle_min | A5 | 6 | 6 | 0.20237378 | 0.01446254 | 3.41E-05 | 2.05E-04 | *** | 7.38E-18 | 1.39E-14 | 1.04E-07 |
| 5 | Body angle_min | CT | 6 | 6 | 0.06577093 | 0.01281053 | 3.41E-05 | 2.05E-04 | *** | 7.38E-18 | 1.39E-14 | 1.04E-07 |
| 5 | Body angle_min | A5 | 8 | 6 | 0.20804828 | 0.01872075 | 8.44E-05 | 5.06E-04 | *** | 7.38E-18 | 1.39E-14 | 1.04E-07 |
| 5 | Body angle_min | CT | 8 | 6 | 0.0622105 | 0.01335448 | 8.44E-05 | 5.06E-04 | *** | 7.38E-18 | 1.39E-14 | 1.04E-07 |
| 5 | Body angle_min | A5 | 10 | 6 | 0.17717344 | 0.01876867 | 5.35E-03 | 3.21E-02 | * | 7.38E-18 | 1.39E-14 | 1.04E-07 |
| 5 | Body angle_min | CT | 10 | 6 | 0.07804112 | 0.02077591 | 5.35E-03 | 3.21E-02 | * | 7.38E-18 | 1.39E-14 | 1.04E-07 |
| 6 | Left limb angle asym._Histogram 1 | A5 | 0 | 6 | 0 | 0 | | 1 | ns | 2.31E-07 | 1.03E-10 | 5.67E-06 |
| 6 | Left limb angle asym._Histogram 1 | CT | 0 | 6 | 0 | 0 | | 1 | ns | 2.31E-07 | 1.03E-10 | 5.67E-06 |
| 6 | Left limb angle asym._Histogram 1 | A5 | 2 | 6 | 0.03731306 | 0.01206259 | 0.599282662 | 1 | ns | 2.31E-07 | 1.03E-10 | 5.67E-06 |
| 6 | Left limb angle asym._Histogram 1 | CT | 2 | 6 | 0.0299387 | 0.00626075 | 0.599282662 | 1 | ns | 2.31E-07 | 1.03E-10 | 5.67E-06 |
| 6 | Left limb angle asym._Histogram 1 | A5 | 4 | 6 | 0.15195249 | 0.02211651 | 0.001464505 | 0.008787029 | ** | 2.31E-07 | 1.03E-10 | 5.67E-06 |
| 6 | Left limb angle asym._Histogram 1 | CT | 4 | 6 | 0.0419046 | 0.0123927 | 0.001464505 | 0.008787029 | ** | 2.31E-07 | 1.03E-10 | 5.67E-06 |
| 6 | Left limb angle asym._Histogram 1 | A5 | 6 | 6 | 0.21067546 | 0.02563964 | 2.67443E-05 | 0.000160466 | *** | 2.31E-07 | 1.03E-10 | 5.67E-06 |
| 6 | Left limb angle asym._Histogram 1 | CT | 6 | 6 | 0.02188173 | 0.00397691 | 2.67443E-05 | 0.000160466 | *** | 2.31E-07 | 1.03E-10 | 5.67E-06 |
| 6 | Left limb angle asym._Histogram 1 | A5 | 8 | 6 | 0.35667667 | 0.09140708 | 0.006636711 | 0.039820266 | * | 2.31E-07 | 1.03E-10 | 5.67E-06 |
| 6 | Left limb angle asym._Histogram 1 | CT | 8 | 6 | 0.04425295 | 0.00542579 | 0.006636711 | 0.039820266 | * | 2.31E-07 | 1.03E-10 | 5.67E-06 |
| 6 | Left limb angle asym._Histogram 1 | A5 | 10 | 6 | 0.32982536 | 0.063176 | 0.000755069 | 0.004530413 | ** | 2.31E-07 | 1.03E-10 | 5.67E-06 |
| 6 | Left limb angle asym._Histogram 1 | CT | 10 | 6 | 0.02782555 | 0.00378502 | 0.000755069 | 0.004530413 | ** | 2.31E-07 | 1.03E-10 | 5.67E-06 |
| 7 | Right limb angle asym._Histogram 1 | A5 | 0 | 6 | 0 | 0 | | 1 | ns | 2.98E-08 | 1.29E-09 | 3.71E-06 |
| 7 | Right limb angle asym._Histogram 1 | CT | 0 | 6 | 0 | 0 | | 1 | ns | 2.98E-08 | 1.29E-09 | 3.71E-06 |
| 7 | Right limb angle asym._Histogram 1 | A5 | 2 | 6 | 0.04192758 | 0.02786576 | 0.692717259 | 1 | ns | 2.98E-08 | 1.29E-09 | 3.71E-06 |
| 7 | Right limb angle asym._Histogram 1 | CT | 2 | 6 | 0.03029413 | 0.00642412 | 0.692717259 | 1 | ns | 2.98E-08 | 1.29E-09 | 3.71E-06 |
| 7 | Right limb angle asym._Histogram 1 | A5 | 4 | 6 | 0.08082089 | 0.02295092 | 0.161227658 | 0.967365951 | ns | 2.98E-08 | 1.29E-09 | 3.71E-06 |
| 7 | Right limb angle asym._Histogram 1 | CT | 4 | 6 | 0.04439967 | 0.00726229 | 0.161227658 | 0.967365951 | ns | 2.98E-08 | 1.29E-09 | 3.71E-06 |
| 7 | Right limb angle asym._Histogram 1 | A5 | 6 | 6 | 0.16131958 | 0.01154759 | 5.02719E-05 | 0.000301631 | *** | 2.98E-08 | 1.29E-09 | 3.71E-06 |
| 7 | Right limb angle asym._Histogram 1 | CT | 6 | 6 | 0.03665988 | 0.01440419 | 5.02719E-05 | 0.000301631 | *** | 2.98E-08 | 1.29E-09 | 3.71E-06 |
| 7 | Right limb angle asym._Histogram 1 | A5 | 8 | 6 | 0.24878075 | 0.04536917 | 0.001502661 | 0.009015968 | ** | 2.98E-08 | 1.29E-09 | 3.71E-06 |
| 7 | Right limb angle asym._Histogram 1 | CT | 8 | 6 | 0.05004002 | 0.00733203 | 0.001502661 | 0.009015968 | ** | 2.98E-08 | 1.29E-09 | 3.71E-06 |
| 7 | Right limb angle asym._Histogram 1 | A5 | 10 | 6 | 0.27082717 | 0.05774028 | 0.002139157 | 0.01283494 | * | 2.98E-08 | 1.29E-09 | 3.71E-06 |
| 7 | Right limb angle asym._Histogram 1 | CT | 10 | 6 | 0.0304976 | 0.0099679 | 0.002139157 | 0.01283494 | * | 2.98E-08 | 1.29E-09 | 3.71E-06 |
| 8 | Left limb angle asym._Histogram 2 | A5 | 0 | 6 | 0 | 0 | | 1 | ns | 1.99E-07 | 1.44E-10 | 7.91E-06 |
| 8 | Left limb angle asym._Histogram 2 | CT | 0 | 6 | 0 | 0 | | 1 | ns | 1.99E-07 | 1.44E-10 | 7.91E-06 |
| 8 | Left limb angle asym._Histogram 2 | A5 | 2 | 6 | 0.02358795 | 0.00963979 | 0.963278364 | 1 | ns | 1.99E-07 | 1.44E-10 | 7.91E-06 |
| 8 | Left limb angle asym._Histogram 2 | CT | 2 | 6 | 0.02306394 | 0.00550418 | 0.963278364 | 1 | ns | 1.99E-07 | 1.44E-10 | 7.91E-06 |
| 8 | Left limb angle asym._Histogram 2 | A5 | 4 | 6 | 0.09900293 | 0.02202031 | 0.017207834 | 0.103247004 | ns | 1.99E-07 | 1.44E-10 | 7.91E-06 |
| 8 | Left limb angle asym._Histogram 2 | CT | 4 | 6 | 0.03116195 | 0.00900894 | 0.017207834 | 0.103247004 | ns | 1.99E-07 | 1.44E-10 | 7.91E-06 |
| 8 | Left limb angle asym._Histogram 2 | A5 | 6 | 6 | 0.18666478 | 0.03640445 | 0.001657289 | 0.009943733 | ** | 1.99E-07 | 1.44E-10 | 7.91E-06 |
| 8 | Left limb angle asym._Histogram 2 | CT | 6 | 6 | 0.02907983 | 0.00645753 | 0.001657289 | 0.009943733 | ** | 1.99E-07 | 1.44E-10 | 7.91E-06 |
| 8 | Left limb angle asym._Histogram 2 | A5 | 8 | 6 | 0.23598235 | 0.05225041 | 0.003176701 | 0.019060207 | * | 1.99E-07 | 1.44E-10 | 7.91E-06 |
| 8 | Left limb angle asym._Histogram 2 | CT | 8 | 6 | 0.02918754 | 0.01203271 | 0.003176701 | 0.019060207 | * | 1.99E-07 | 1.44E-10 | 7.91E-06 |
| 8 | Left limb angle asym._Histogram 2 | A5 | 10 | 6 | 0.19336265 | 0.03426395 | 5.62E-04 | 3.37E-03 | ** | 1.99E-07 | 1.44E-10 | 7.91E-06 |
| 8 | Left limb angle asym._Histogram 2 | CT | 10 | 6 | 0.02086569 | 0.00555713 | 5.62E-04 | 3.37E-03 | ** | 1.99E-07 | 1.44E-10 | 7.91E-06 |
| 9 | Neck velocity_FFT mean coeff. 1 | A5 | 0 | 6 | 0 | 0 | | 1 | ns | 2.90E-09 | 5.01E-04 | 3.04E-04 |
| 9 | Neck velocity_FFT mean coeff. 1 | CT | 0 | 6 | 0 | 0 | | 1 | ns | 2.90E-09 | 5.01E-04 | 3.04E-04 |
| 9 | Neck velocity_FFT mean coeff. 1 | A5 | 2 | 6 | 0.05668572 | 0.01064155 | 0.104364306 | 0.626185837 | ns | 2.90E-09 | 5.01E-04 | 3.04E-04 |
| 9 | Neck velocity_FFT mean coeff. 1 | CT | 2 | 6 | 0.03455398 | 0.00634614 | 0.104364306 | 0.626185837 | ns | 2.90E-09 | 5.01E-04 | 3.04E-04 |
| 9 | Neck velocity_FFT mean coeff. 1 | A5 | 4 | 6 | 0.04974213 | 0.00878447 | 0.107401426 | 0.644408558 | ns | 2.90E-09 | 5.01E-04 | 3.04E-04 |
| 9 | Neck velocity_FFT mean coeff. 1 | CT | 4 | 6 | 0.03218789 | 0.00462082 | 0.107401426 | 0.644408558 | ns | 2.90E-09 | 5.01E-04 | 3.04E-04 |
| 9 | Neck velocity_FFT mean coeff. 1 | A5 | 6 | 6 | 0.03549342 | 0.00488556 | 8.76E-01 | 1.00E+00 | ns | 2.90E-09 | 5.01E-04 | 3.04E-04 |
| 9 | Neck velocity_FFT mean coeff. 1 | CT | 6 | 6 | 0.03438962 | 0.00489782 | 8.76E-01 | 1.00E+00 | ns | 2.90E-09 | 5.01E-04 | 3.04E-04 |
| 9 | Neck velocity_FFT mean coeff. 1 | A5 | 8 | 6 | 0.0269185 | 0.00505477 | 3.95E-01 | 1 | ns | 2.90E-09 | 5.01E-04 | 3.04E-04 |
| 9 | Neck velocity_FFT mean coeff. 1 | CT | 8 | 6 | 0.03496651 | 0.00752219 | 3.95E-01 | 1 | ns | 2.90E-09 | 5.01E-04 | 3.04E-04 |
| 9 | Neck velocity_FFT mean coeff. 1 | A5 | 10 | 6 | 0.0809141 | 0.01338732 | 0.002488797 | 0.014932784 | * | 2.90E-09 | 5.01E-04 | 3.04E-04 |
| 9 | Neck velocity_FFT mean coeff. 1 | CT | 10 | 6 | 0.02558123 | 0.00338222 | 0.002488797 | 0.014932784 | * | 2.90E-09 | 5.01E-04 | 3.04E-04 |
| 10 | Body length_FFT mean coeff. 1 | A5 | 0 | 6 | 0 | 0 | | 1 | ns | 2.10E-16 | 1.67E-17 | 6.64E-14 |
| 10 | Body length_FFT mean coeff. 1 | CT | 0 | 6 | 0 | 0 | | 1 | ns | 2.10E-16 | 1.67E-17 | 6.64E-14 |
| 10 | Body length_FFT mean coeff. 1 | A5 | 2 | 6 | 0.02470774 | 0.00441722 | 0.461265352 | 1 | ns | 2.10E-16 | 1.67E-17 | 6.64E-14 |
| 10 | Body length_FFT mean coeff. 1 | CT | 2 | 6 | 0.03360955 | 0.01074579 | 0.461265352 | 1 | ns | 2.10E-16 | 1.67E-17 | 6.64E-14 |
| 10 | Body length_FFT mean coeff. 1 | A5 | 4 | 6 | 0.10488117 | 0.01712052 | 0.001974196 | 0.011845174 | * | 2.10E-16 | 1.67E-17 | 6.64E-14 |
| 10 | Body length_FFT mean coeff. 1 | CT | 4 | 6 | 0.02894534 | 0.00643419 | 0.001974196 | 0.011845174 | * | 2.10E-16 | 1.67E-17 | 6.64E-14 |
| 10 | Body length_FFT mean coeff. 1 | A5 | 6 | 6 | 0.26944426 | 0.05348753 | 2.86E-03 | 1.72E-02 | * | 2.10E-16 | 1.67E-17 | 6.64E-14 |
| 10 | Body length_FFT mean coeff. 1 | CT | 6 | 6 | 0.05400598 | 0.01258049 | 2.86E-03 | 1.72E-02 | * | 2.10E-16 | 1.67E-17 | 6.64E-14 |
| 10 | Body length_FFT mean coeff. 1 | A5 | 8 | 6 | 0.33301638 | 0.03190248 | 3.77174E-06 | 2.26305E-05 | **** | 2.10E-16 | 1.67E-17 | 6.64E-14 |
| 10 | Body length_FFT mean coeff. 1 | CT | 8 | 6 | 0.03737335 | 0.00626943 | 3.77174E-06 | 2.26305E-05 | **** | 2.10E-16 | 1.67E-17 | 6.64E-14 |
| 10 | Body length_FFT mean coeff. 1 | A5 | 10 | 6 | 0.4743452 | 0.04916658 | 7.09E-06 | 4.25E-05 | **** | 2.10E-16 | 1.67E-17 | 6.64E-14 |
| 10 | Body length_FFT mean coeff. 1 | CT | 10 | 6 | 0.04496989 | 0.01226364 | 7.09E-06 | 4.25E-05 | **** | 2.10E-16 | 1.67E-17 | 6.64E-14 |
| 11 | U-body length_Negative turning points | A5 | 0 | 6 | 0 | 0 | | 1 | ns | 8.04E-23 | 5.33E-27 | 1.26E-21 |
| 11 | U-body length_Negative turning points | CT | 0 | 6 | 0 | 0 | | 1 | ns | 8.04E-23 | 5.33E-27 | 1.26E-21 |
| 11 | U-body length_Negative turning points | A5 | 2 | 6 | 0.039059 | 0.007846 | 0.521097 | 1 | ns | 8.04E-23 | 5.33E-27 | 1.26E-21 |
| 11 | U-body length_Negative turning points | CT | 2 | 6 | 0.033095 | 0.004346 | 0.521097 | 1 | ns | 8.04E-23 | 5.33E-27 | 1.26E-21 |
| 11 | U-body length_Negative turning points | A5 | 4 | 6 | 0.101707 | 0.019455 | 0.019627 | 0.117765 | ns | 8.04E-23 | 5.33E-27 | 1.26E-21 |
| 11 | U-body length_Negative turning points | CT | 4 | 6 | 0.036312 | 0.013302 | 0.019627 | 0.117765 | ns | 8.04E-23 | 5.33E-27 | 1.26E-21 |
| 11 | U-body length_Negative turning points | A5 | 6 | 6 | 0.285586 | 0.028675 | 7.52E-06 | 4.51E-05 | **** | 8.04E-23 | 5.33E-27 | 1.26E-21 |
| 11 | U-body length_Negative turning points | CT | 6 | 6 | 0.032165 | 0.009179 | 7.52E-06 | 4.51E-05 | **** | 8.04E-23 | 5.33E-27 | 1.26E-21 |
| 11 | U-body length_Negative turning points | A5 | 8 | 6 | 0.41087 | 0.029797 | 1.75E-07 | 1.05E-06 | **** | 8.04E-23 | 5.33E-27 | 1.26E-21 |
| 11 | U-body length_Negative turning points | CT | 8 | 6 | 0.028951 | 0.004569 | 1.75E-07 | 1.05E-06 | **** | 8.04E-23 | 5.33E-27 | 1.26E-21 |
| 11 | U-body length_Negative turning points | A5 | 10 | 6 | 0.321488 | 0.018589 | 2.24E-08 | 1.35E-07 | **** | 8.04E-23 | 5.33E-27 | 1.26E-21 |
| 11 | U-body length_Negative turning points | CT | 10 | 6 | 0.024104 | 0.00359 | 2.24E-08 | 1.35E-07 | **** | 8.04E-23 | 5.33E-27 | 1.26E-21 |
| 12 | Hand distance_Median diff | A5 | 0 | 6 | 0 | 0 | | 1 | ns | 1.26E-15 | 1.84E-20 | 7.46E-11 |
| 12 | Hand distance_Median diff | CT | 0 | 6 | 0 | 0 | | 1 | ns | 1.26E-15 | 1.84E-20 | 7.46E-11 |
| 12 | Hand distance_Median diff | A5 | 2 | 6 | 0.070775 | 0.010509 | 0.018412 | 0.11047 | ns | 1.26E-15 | 1.84E-20 | 7.46E-11 |
| 12 | Hand distance_Median diff | CT | 2 | 6 | 0.038999 | 0.004153 | 0.018412 | 0.11047 | ns | 1.26E-15 | 1.84E-20 | 7.46E-11 |
| 12 | Hand distance_Median diff | A5 | 4 | 6 | 0.130757 | 0.016764 | 0.000858 | 0.005146 | ** | 1.26E-15 | 1.84E-20 | 7.46E-11 |
| 12 | Hand distance_Median diff | CT | 4 | 6 | 0.045904 | 0.006829 | 0.000858 | 0.005146 | ** | 1.26E-15 | 1.84E-20 | 7.46E-11 |
| 12 | Hand distance_Median diff | A5 | 6 | 6 | 0.141016 | 0.012268 | 5.24E-05 | 0.000314 | *** | 1.26E-15 | 1.84E-20 | 7.46E-11 |
| 12 | Hand distance_Median diff | CT | 6 | 6 | 0.038422 | 0.009091 | 5.24E-05 | 0.000314 | *** | 1.26E-15 | 1.84E-20 | 7.46E-11 |
| 12 | Hand distance_Median diff | A5 | 8 | 6 | 0.192528 | 0.018743 | 1.01E-05 | 6.08E-05 | **** | 1.26E-15 | 1.84E-20 | 7.46E-11 |
| 12 | Hand distance_Median diff | CT | 8 | 6 | 0.033143 | 0.005683 | 1.01E-05 | 6.08E-05 | **** | 1.26E-15 | 1.84E-20 | 7.46E-11 |
| 12 | Hand distance_Median diff | A5 | 10 | 6 | 0.213521 | 0.020493 | 1.52E-05 | 9.12E-05 | **** | 1.26E-15 | 1.84E-20 | 7.46E-11 |
| 12 | Hand distance_Median diff | CT | 10 | 6 | 0.038855 | 0.009243 | 1.52E-05 | 9.12E-05 | **** | 1.26E-15 | 1.84E-20 | 7.46E-11 |
| 13 | Leg angle asym._MFCC 3 | A5 | 0 | 6 | 0 | 0 | | 1 | ns | 1.18E-08 | 4.87E-07 | 7.75E-04 |
| 13 | Leg angle asym._MFCC 3 | CT | 0 | 6 | 0 | 0 | | 1 | ns | 1.18E-08 | 4.87E-07 | 7.75E-04 |
| 13 | Leg angle asym._MFCC 3 | A5 | 2 | 6 | 0.019574 | 0.002092 | 0.442945 | 1 | ns | 1.18E-08 | 4.87E-07 | 7.75E-04 |
| 13 | Leg angle asym._MFCC 3 | CT | 2 | 6 | 0.023804 | 0.004865 | 0.442945 | 1 | ns | 1.18E-08 | 4.87E-07 | 7.75E-04 |
| 13 | Leg angle asym._MFCC 3 | A5 | 4 | 6 | 0.070528 | 0.02153 | 0.139448 | 0.836691 | ns | 1.18E-08 | 4.87E-07 | 7.75E-04 |
| 13 | Leg angle asym._MFCC 3 | CT | 4 | 6 | 0.035059 | 0.004948 | 0.139448 | 0.836691 | ns | 1.18E-08 | 4.87E-07 | 7.75E-04 |
| 13 | Leg angle asym._MFCC 3 | A5 | 6 | 6 | 0.14577 | 0.024179 | 0.004812 | 0.028874 | * | 1.18E-08 | 4.87E-07 | 7.75E-04 |
| 13 | Leg angle asym._MFCC 3 | CT | 6 | 6 | 0.052653 | 0.009099 | 0.004812 | 0.028874 | * | 1.18E-08 | 4.87E-07 | 7.75E-04 |
| 13 | Leg angle asym._MFCC 3 | A5 | 8 | 6 | 0.15398 | 0.031758 | 0.024671 | 0.148029 | ns | 1.18E-08 | 4.87E-07 | 7.75E-04 |
| 13 | Leg angle asym._MFCC 3 | CT | 8 | 6 | 0.057834 | 0.017784 | 0.024671 | 0.148029 | ns | 1.18E-08 | 4.87E-07 | 7.75E-04 |
| 13 | Leg angle asym._MFCC 3 | A5 | 10 | 6 | 0.173517 | 0.037206 | 5.47E-03 | 3.28E-02 | * | 1.18E-08 | 4.87E-07 | 7.75E-04 |
| 13 | Leg angle asym._MFCC 3 | CT | 10 | 6 | 0.039657 | 0.007463 | 5.47E-03 | 3.28E-02 | * | 1.18E-08 | 4.87E-07 | 7.75E-04 |
| 14 | Chest acc._Wavlet entropy | A5 | 0 | 6 | 0 | 0 | | 1 | ns | 2.28E-29 | 1.12E-31 | 2.66E-29 |
| 14 | Chest acc._Wavlet entropy | CT | 0 | 6 | 0 | 0 | | 1 | ns | 2.28E-29 | 1.12E-31 | 2.66E-29 |
| 14 | Chest acc._Wavlet entropy | A5 | 2 | 6 | 0.054689 | 0.008715 | 0.87588 | 1 | ns | 2.28E-29 | 1.12E-31 | 2.66E-29 |
| 14 | Chest acc._Wavlet entropy | CT | 2 | 6 | 0.051435 | 0.018336 | 0.87588 | 1 | ns | 2.28E-29 | 1.12E-31 | 2.66E-29 |
| 14 | Chest acc._Wavlet entropy | A5 | 4 | 6 | 0.104999 | 0.026778 | 0.076186 | 0.457115 | ns | 2.28E-29 | 1.12E-31 | 2.66E-29 |
| 14 | Chest acc._Wavlet entropy | CT | 4 | 6 | 0.043263 | 0.016049 | 0.076186 | 0.457115 | ns | 2.28E-29 | 1.12E-31 | 2.66E-29 |
| 14 | Chest acc._Wavlet entropy | A5 | 6 | 6 | 0.405187 | 0.032781 | 1.31E-06 | 7.85E-06 | **** | 2.28E-29 | 1.12E-31 | 2.66E-29 |
| 14 | Chest acc._Wavlet entropy | CT | 6 | 6 | 0.037651 | 0.014838 | 1.31E-06 | 7.85E-06 | **** | 2.28E-29 | 1.12E-31 | 2.66E-29 |
| 14 | Chest acc._Wavlet entropy | A5 | 8 | 6 | 0.379141 | 0.021217 | 1.22E-08 | 7.33E-08 | **** | 2.28E-29 | 1.12E-31 | 2.66E-29 |
| 14 | Chest acc._Wavlet entropy | CT | 8 | 6 | 0.02024 | 0.003189 | 1.22E-08 | 7.33E-08 | **** | 2.28E-29 | 1.12E-31 | 2.66E-29 |
| 14 | Chest acc._Wavlet entropy | A5 | 10 | 6 | 0.740841 | 0.032101 | 8.57E-10 | 5.14E-09 | **** | 2.28E-29 | 1.12E-31 | 2.66E-29 |
| 14 | Chest acc._Wavlet entropy | CT | 10 | 6 | 0.028569 | 0.00459 | 8.57E-10 | 5.14E-09 | **** | 2.28E-29 | 1.12E-31 | 2.66E-29 |
| 15 | Right limb angle asym._Histogram 2 | A5 | 0 | 6 | 0 | 0 | | 1 | ns | 9.58E-12 | 6.49E-12 | 1.55E-09 |
| 15 | Right limb angle asym._Histogram 2 | CT | 0 | 6 | 0 | 0 | | 1 | ns | 9.58E-12 | 6.49E-12 | 1.55E-09 |
| 15 | Right limb angle asym._Histogram 2 | A5 | 2 | 6 | 0.015403 | 0.001878 | 0.076061 | 0.456364 | ns | 9.58E-12 | 6.49E-12 | 1.55E-09 |
| 15 | Right limb angle asym._Histogram 2 | CT | 2 | 6 | 0.026177 | 0.005111 | 0.076061 | 0.456364 | ns | 9.58E-12 | 6.49E-12 | 1.55E-09 |
| 15 | Right limb angle asym._Histogram 2 | A5 | 4 | 6 | 0.036049 |

**Supplementary Table 17. Statistical summary of the feature values for the top 20 features identified by the TSFEL model, comparing the CT and PD (A5) groups.** For each feature, the values at each week were divided by the group's corresponding baseline (0 wk) mean value, and the normalised data were analysed over the experimental duration (0–10 wk). Each group consisted of 6 sampling sets, each containing 150 randomly selected clips. Two-way ANOVA (group × week) was performed for each feature on the normalised data, followed by weekly t-tests comparing the CT and A5 groups. P-values from weekly t-tests were corrected for multiple comparisons using the Bonferroni method. Source data are provided in the Source Data file (See S_Figure 37).

| Rank | Feature name | Week | group | n | Mean | SEM | raw_p | corrected_p | significant | ANOVA_p_ Week | ANOVA_p_ Group | ANOVA_p_ Interaction |
|---|---|---|---|---|---|---|---|---|---|---|---|---|
| 1 | Foot distance_Signal distance | 0 | CT | 746 | 1 | 0.00029934 | 1 | 1 | ns | 1.00E+00 | 1.00E+00 | 0.884164 |
| 1 | Foot distance_Signal distance | 2 | CT | 622 | 1.00005993 | 0.00032513 | 5.93018E-21 | 3.55811E-20 | **** | 1.00E+00 | 1.00E+00 | 0.884164 |
| 1 | Foot distance_Signal distance | 4 | CT | 489 | 1.00162711 | 0.00035107 | 1.87823E-27 | 1.12694E-26 | **** | 1.00E+00 | 1.00E+00 | 0.884164 |
| 1 | Foot distance_Signal distance | 6 | CT | 444 | 1.00001093 | 0.0003976 | 9.00327E-79 | 5.40196E-78 | **** | 1.00E+00 | 1.00E+00 | 0.884164 |
| 1 | Foot distance_Signal distance | 8 | CT | 443 | 1.00223356 | 0.00044519 | 1.00425E-58 | 6.02551E-58 | **** | 1.00E+00 | 1.00E+00 | 0.884164 |
| 1 | Foot distance_Signal distance | 10 | CT | 414 | 1.00226097 | 0.00042607 | 4.25965E-64 | 2.55579E-63 | **** | 1.00E+00 | 1.00E+00 | 0.884164 |
| 1 | Foot distance_Signal distance | 0 | A5 | 927 | 1 | 0.00038159 | 1 | 1 | ns | 1.00E+00 | 1.00E+00 | 0.884164 |
| 1 | Foot distance_Signal distance | 2 | A5 | 962 | 1.00587274 | 0.00044336 | 5.93018E-21 | 3.55811E-20 | **** | 1.00E+00 | 1.00E+00 | 0.884164 |
| 1 | Foot distance_Signal distance | 4 | A5 | 797 | 1.00918904 | 0.00048756 | 1.87823E-27 | 1.12694E-26 | **** | 1.00E+00 | 1.00E+00 | 0.884164 |
| 1 | Foot distance_Signal distance | 6 | A5 | 1000 | 1.01590043 | 0.00049886 | 9.00327E-79 | 5.40196E-78 | **** | 1.00E+00 | 1.00E+00 | 0.884164 |
| 1 | Foot distance_Signal distance | 8 | A5 | 1286 | 1.01682259 | 0.0004863 | 1.00425E-58 | 6.02551E-58 | **** | 1.00E+00 | 1.00E+00 | 0.884164 |
| 1 | Foot distance_Signal distance | 10 | A5 | 1233 | 1.01680069 | 0.00045484 | 4.25965E-64 | 2.55579E-63 | **** | 1.00E+00 | 1.00E+00 | 0.884164 |
| 2 | Tail angle_Autocorrelation | 0 | CT | 728 | 1 | 0.0063287 | 1 | 1 | ns | 1.00E+00 | 1 | 0.320196 |
| 2 | Tail angle_Autocorrelation | 2 | CT | 626 | 0.97293909 | 0.00664421 | 9.26049E-23 | 5.5563E-22 | **** | 1.00E+00 | 1 | 0.320196 |
| 2 | Tail angle_Autocorrelation | 4 | CT | 488 | 0.97030063 | 0.0073709 | 6.67576E-23 | 4.00546E-22 | **** | 1.00E+00 | 1 | 0.320196 |
| 2 | Tail angle_Autocorrelation | 6 | CT | 449 | 0.97148527 | 0.00813478 | 1.45067E-20 | 8.70403E-20 | **** | 1.00E+00 | 1 | 0.320196 |
| 2 | Tail angle_Autocorrelation | 8 | CT | 450 | 0.95330551 | 0.00731066 | 1.51629E-79 | 9.09771E-79 | **** | 1.00E+00 | 1 | 0.320196 |
| 2 | Tail angle_Autocorrelation | 10 | CT | 417 | 0.95285739 | 0.00854282 | 4.02882E-69 | 2.41729E-68 | **** | 1.00E+00 | 1 | 0.320196 |
| 2 | Tail angle_Autocorrelation | 0 | A5 | 931 | 1 | 0.00527932 | 1 | 1 | ns | 1.00E+00 | 1 | 0.320196 |
| 2 | Tail angle_Autocorrelation | 2 | A5 | 939 | 1.06154048 | 0.00574272 | 9.26049E-23 | 5.5563E-22 | **** | 1.00E+00 | 1 | 0.320196 |
| 2 | Tail angle_Autocorrelation | 4 | A5 | 798 | 1.06050024 | 0.00538551 | 6.67576E-23 | 4.00546E-22 | **** | 1.00E+00 | 1 | 0.320196 |
| 2 | Tail angle_Autocorrelation | 6 | A5 | 993 | 1.05082005 | 0.00429118 | 1.45067E-20 | 8.70403E-20 | **** | 1.00E+00 | 1 | 0.320196 |
| 2 | Tail angle_Autocorrelation | 8 | A5 | 1313 | 1.11973982 | 0.0042107 | 1.51629E-79 | 9.09771E-79 | **** | 1.00E+00 | 1 | 0.320196 |
| 2 | Tail angle_Autocorrelation | 10 | A5 | 1231 | 1.10554855 | 0.00385684 | 4.02882E-69 | 2.41729E-68 | **** | 1.00E+00 | 1 | 0.320196 |
| 3 | Neck acc._Wavelet std_4 | 0 | CT | 730 | 1 | 0.00887594 | 1 | 1 | ns | 1.00E+00 | 1.00E+00 | 8.44E-01 |
| 3 | Neck acc._Wavelet std_4 | 2 | CT | 623 | 1.0474096 | 0.00966708 | 8.80932E-14 | 5.28559E-13 | **** | 1.00E+00 | 1.00E+00 | 8.44E-01 |
| 3 | Neck acc._Wavelet std_4 | 4 | CT | 492 | 0.98932775 | 0.0107384 | 5.72811E-20 | 3.43687E-19 | **** | 1.00E+00 | 1.00E+00 | 8.44E-01 |
| 3 | Neck acc._Wavelet std_4 | 6 | CT | 453 | 0.94041074 | 0.01037503 | 1.77859E-55 | 1.06715E-54 | **** | 1.00E+00 | 1.00E+00 | 8.44E-01 |
| 3 | Neck acc._Wavelet std_4 | 8 | CT | 446 | 0.9577791 | 0.0107154 | 6.31E-59 | 3.78E-58 | **** | 1.00E+00 | 1.00E+00 | 8.44E-01 |
| 3 | Neck acc._Wavelet std_4 | 10 | CT | 414 | 0.96375573 | 0.01231025 | 1.28E-71 | 7.69E-71 | **** | 1.00E+00 | 1.00E+00 | 8.44E-01 |
| 3 | Neck acc._Wavelet std_4 | 0 | A5 | 953 | 1 | 0.00780846 | 1.00E+00 | 1.00E+00 | ns | 1.00E+00 | 1.00E+00 | 8.44E-01 |
| 3 | Neck acc._Wavelet std_4 | 2 | A5 | 953 | 0.94371546 | 0.00917521 | 8.81E-14 | 5.29E-13 | **** | 1.00E+00 | 1.00E+00 | 8.44E-01 |
| 3 | Neck acc._Wavelet std_4 | 4 | A5 | 792 | 0.86197114 | 0.00848128 | 5.72811E-20 | 3.43687E-19 | **** | 1.00E+00 | 1.00E+00 | 8.44E-01 |
| 3 | Neck acc._Wavelet std_4 | 6 | A5 | 979 | 0.73218132 | 0.00718421 | 1.77859E-55 | 1.06715E-54 | **** | 1.00E+00 | 1.00E+00 | 8.44E-01 |
| 3 | Neck acc._Wavelet std_4 | 8 | A5 | 1290 | 0.7547281 | 0.00605492 | 6.31E-59 | 3.78E-58 | **** | 1.00E+00 | 1.00E+00 | 8.44E-01 |
| 3 | Neck acc._Wavelet std_4 | 10 | A5 | 1238 | 0.75282912 | 0.00501445 | 1.28E-71 | 7.69E-71 | **** | 1.00E+00 | 1.00E+00 | 8.44E-01 |
| 4 | Body angle velocity_ECDF percentile 0 | 0 | CT | 733 | 1 | 0.01174164 | 1 | 1 | ns | 1.00E+00 | 2.56E-04 | 8.95E-01 |
| 4 | Body angle velocity_ECDF percentile 0 | 2 | CT | 619 | 0.99349508 | 0.01290055 | 0.950392836 | 1 | ns | 1.00E+00 | 2.56E-04 | 8.95E-01 |
| 4 | Body angle velocity_ECDF percentile 0 | 4 | CT | 487 | 0.96836973 | 0.01366167 | 0.028137735 | 0.16882641 | ns | 1.00E+00 | 2.56E-04 | 8.95E-01 |
| 4 | Body angle velocity_ECDF percentile 0 | 6 | CT | 448 | 0.93831997 | 0.01430956 | 2.67539E-09 | 1.60523E-08 | **** | 1.00E+00 | 2.56E-04 | 8.95E-01 |
| 4 | Body angle velocity_ECDF percentile 0 | 8 | CT | 447 | 0.93811006 | 0.01474517 | 1.90816E-08 | 1.1449E-07 | **** | 1.00E+00 | 2.56E-04 | 8.95E-01 |
| 4 | Body angle velocity_ECDF percentile 0 | 10 | CT | 424 | 0.9393209 | 0.01469519 | 2.68923E-09 | 1.61354E-08 | **** | 1.00E+00 | 2.56E-04 | 8.95E-01 |
| 4 | Body angle velocity_ECDF percentile 0 | 0 | A5 | 940 | 1 | 0.00999375 | 1.00E+00 | 1.00E+00 | ns | 1.00E+00 | 2.56E-04 | 8.95E-01 |
| 4 | Body angle velocity_ECDF percentile 0 | 2 | A5 | 950 | 0.99455936 | 0.01095283 | 9.50E-01 | 1.00E+00 | ns | 1.00E+00 | 2.56E-04 | 8.95E-01 |
| 4 | Body angle velocity_ECDF percentile 0 | 4 | A5 | 790 | 0.92951253 | 0.01103418 | 2.81E-02 | 0.16882641 | ns | 1.00E+00 | 2.56E-04 | 8.95E-01 |
| 4 | Body angle velocity_ECDF percentile 0 | 6 | A5 | 987 | 0.83327743 | 0.00987281 | 2.68E-09 | 1.60523E-08 | **** | 1.00E+00 | 2.56E-04 | 8.95E-01 |
| 4 | Body angle velocity_ECDF percentile 0 | 8 | A5 | 1299 | 0.84927352 | 0.00770961 | 1.91E-08 | 1.14E-07 | **** | 1.00E+00 | 2.56E-04 | 8.95E-01 |
| 4 | Body angle velocity_ECDF percentile 0 | 10 | A5 | 1239 | 0.84042631 | 0.00826035 | 2.69E-09 | 1.61E-08 | **** | 1.00E+00 | 2.56E-04 | 8.95E-01 |
| 5 | Body angle_min | 0 | CT | 739 | 1 | 0.02730972 | 1 | 1 | ns | 8.65E-01 | 1.00E+00 | 8.91E-01 |
| 5 | Body angle_min | 2 | CT | 622 | 1.03882994 | 0.02990078 | 4.39666E-06 | 2.6398E-05 | **** | 8.65E-01 | 1.00E+00 | 8.91E-01 |
| 5 | Body angle_min | 4 | CT | 481 | 1.11350007 | 0.0346349 | 0.030615211 | 0.183691268 | ns | 8.65E-01 | 1.00E+00 | 8.91E-01 |
| 5 | Body angle_min | 6 | CT | 450 | 1.19404807 | 0.0376951 | 1.46313E-10 | 8.77877E-10 | **** | 8.65E-01 | 1.00E+00 | 8.91E-01 |
| 5 | Body angle_min | 8 | CT | 453 | 1.1949386 | 0.03766088 | 5.03378E-09 | 3.02027E-08 | **** | 8.65E-01 | 1.00E+00 | 8.91E-01 |
| 5 | Body angle_min | 10 | CT | 413 | 1.25551707 | 0.04209797 | 5.49168E-06 | 3.29501E-05 | **** | 8.65E-01 | 1.00E+00 | 8.91E-01 |
| 5 | Body angle_min | 0 | A5 | 942 | 1 | 0.0253374 | 1.00E+00 | 1.00E+00 | ns | 8.65E-01 | 1.00E+00 | 8.91E-01 |
| 5 | Body angle_min | 2 | A5 | 955 | 1.21861548 | 0.02474501 | 4.40E-06 | 2.64E-05 | **** | 8.65E-01 | 1.00E+00 | 8.91E-01 |
| 5 | Body angle_min | 4 | A5 | 790 | 1.21117181 | 0.02819752 | 3.06E-02 | 1.84E-01 | ns | 8.65E-01 | 1.00E+00 | 8.91E-01 |
| 5 | Body angle_min | 6 | A5 | 989 | 1.49528508 | 0.02638764 | 1.46E-10 | 8.78E-10 | **** | 8.65E-01 | 1.00E+00 | 8.91E-01 |
| 5 | Body angle_min | 8 | A5 | 1290 | 1.45509204 | 0.02266055 | 5.03E-09 | 3.02E-08 | **** | 8.65E-01 | 1.00E+00 | 8.91E-01 |
| 5 | Body angle_min | 10 | A5 | 1239 | 1.47371043 | 0.02379651 | 5.49E-06 | 3.30E-05 | **** | 8.65E-01 | 1.00E+00 | 8.91E-01 |
| 6 | Left limb angle asym._Histogram 1 | 0 | CT | 740 | 1 | 0.02807589 | 1 | 1 | ns | 1.46E-02 | 4.65E-30 | 0.774775 |
| 6 | Left limb angle asym._Histogram 1 | 2 | CT | 629 | 1.02487049 | 0.0328808 | 0.001405871 | 0.008435228 | ** | 1.46E-02 | 4.65E-30 | 0.774775 |
| 6 | Left limb angle asym._Histogram 1 | 4 | CT | 490 | 1.12041828 | 0.03687113 | 2.48932E-22 | 1.49359E-21 | **** | 1.46E-02 | 4.65E-30 | 0.774775 |
| 6 | Left limb angle asym._Histogram 1 | 6 | CT | 449 | 0.96050556 | 0.03546293 | 1.15474E-20 | 6.92842E-20 | **** | 1.46E-02 | 4.65E-30 | 0.774775 |
| 6 | Left limb angle asym._Histogram 1 | 8 | CT | 457 | 1.15317203 | 0.03904622 | 3.73618E-53 | 2.24171E-52 | **** | 1.46E-02 | 4.65E-30 | 0.774775 |
| 6 | Left limb angle asym._Histogram 1 | 10 | CT | 427 | 1.06615263 | 0.03868835 | 4.66618E-38 | 2.79971E-37 | **** | 1.46E-02 | 4.65E-30 | 0.774775 |
| 6 | Left limb angle asym._Histogram 1 | 0 | A5 | 936 | 1 | 0.02651958 | 1 | 1 | ns | 1.46E-02 | 4.65E-30 | 0.774775 |
| 6 | Left limb angle asym._Histogram 1 | 2 | A5 | 957 | 0.89343873 | 0.02534477 | 0.001405871 | 0.008435228 | ** | 1.46E-02 | 4.65E-30 | 0.774775 |
| 6 | Left limb angle asym._Histogram 1 | 4 | A5 | 800 | 0.69257718 | 0.02516747 | 2.48932E-22 | 1.49359E-21 | **** | 1.46E-02 | 4.65E-30 | 0.774775 |
| 6 | Left limb angle asym._Histogram 1 | 6 | A5 | 1003 | 0.6031925 | 0.0196513 | 1.15474E-20 | 6.92842E-20 | **** | 1.46E-02 | 4.65E-30 | 0.774775 |
| 6 | Left limb angle asym._Histogram 1 | 8 | A5 | 1312 | 0.58004658 | 0.01640516 | 3.73618E-53 | 2.24171E-52 | **** | 1.46E-02 | 4.65E-30 | 0.774775 |
| 6 | Left limb angle asym._Histogram 1 | 10 | A5 | 1261 | 0.58874219 | 0.01642568 | 4.66618E-38 | 2.79971E-37 | **** | 1.46E-02 | 4.65E-30 | 0.774775 |
| 7 | Right limb angle asym._Histogram 1 | 0 | CT | 742 | 1 | 0.03317324 | 1 | 1 | ns | 1 | 1.00E+00 | 0.598228 |
| 7 | Right limb angle asym._Histogram 1 | 2 | CT | 625 | 1.00655937 | 0.03588926 | 0.137621953 | 0.825731721 | ns | 1 | 1.00E+00 | 0.598228 |
| 7 | Right limb angle asym._Histogram 1 | 4 | CT | 497 | 1.021066 | 0.03837517 | 3.82707E-11 | 2.29624E-10 | **** | 1 | 1.00E+00 | 0.598228 |
| 7 | Right limb angle asym._Histogram 1 | 6 | CT | 453 | 1.01078752 | 0.04464375 | 2.43938E-19 | 1.46363E-18 | **** | 1 | 1.00E+00 | 0.598228 |
| 7 | Right limb angle asym._Histogram 1 | 8 | CT | 453 | 1.24511345 | 0.04674309 | 3.15813E-59 | 1.89488E-58 | **** | 1 | 1.00E+00 | 0.598228 |
| 7 | Right limb angle asym._Histogram 1 | 10 | CT | 425 | 1.07655899 | 0.04395167 | 3.755E-31 | 2.253E-30 | **** | 1 | 1.00E+00 | 0.598228 |
| 7 | Right limb angle asym._Histogram 1 | 0 | A5 | 939 | 1 | 0.03045825 | 1 | 1 | ns | 1 | 1.00E+00 | 0.598228 |
| 7 | Right limb angle asym._Histogram 1 | 2 | A5 | 960 | 0.93766326 | 0.02923248 | 0.137621953 | 0.825731721 | ns | 1 | 1.00E+00 | 0.598228 |
| 7 | Right limb angle asym._Histogram 1 | 4 | A5 | 801 | 0.71303356 | 0.02751704 | 3.82707E-11 | 2.29624E-10 | **** | 1 | 1.00E+00 | 0.598228 |
| 7 | Right limb angle asym._Histogram 1 | 6 | A5 | 999 | 0.61376192 | 0.02120728 | 2.43938E-19 | 1.46363E-18 | **** | 1 | 1.00E+00 | 0.598228 |
| 7 | Right limb angle asym._Histogram 1 | 8 | A5 | 1320 | 0.58014228 | 0.016646 | 3.15813E-59 | 1.89488E-58 | **** | 1 | 1.00E+00 | 0.598228 |
| 7 | Right limb angle asym._Histogram 1 | 10 | A5 | 1257 | 0.5986892 | 0.01815118 | 3.755E-31 | 2.253E-30 | **** | 1 | 1.00E+00 | 0.598228 |
| 8 | Left limb angle asym._Histogram 2 | 0 | CT | 742 | 1 | 0.02168668 | 1 | 1 | ns | 1.00E+00 | 1.00E+00 | 5.28E-01 |
| 8 | Left limb angle asym._Histogram 2 | 2 | CT | 623 | 1.07786378 | 0.02532496 | 0.002216794 | 0.013300766 | * | 1.00E+00 | 1.00E+00 | 5.28E-01 |
| 8 | Left limb angle asym._Histogram 2 | 4 | CT | 490 | 1.13144679 | 0.02974029 | 8.65395E-22 | 5.19237E-21 | **** | 1.00E+00 | 1.00E+00 | 5.28E-01 |
| 8 | Left limb angle asym._Histogram 2 | 6 | CT | 448 | 1.07721274 | 0.02873923 | 2.6854E-37 | 1.61124E-36 | **** | 1.00E+00 | 1.00E+00 | 5.28E-01 |
| 8 | Left limb angle asym._Histogram 2 | 8 | CT | 456 | 1.07235598 | 0.02851367 | 3.99475E-41 | 2.39685E-40 | **** | 1.00E+00 | 1.00E+00 | 5.28E-01 |
| 8 | Left limb angle asym._Histogram 2 | 10 | CT | 422 | 1.0469387 | 0.03083233 | 9.77222E-27 | 5.86333E-26 | **** | 1.00E+00 | 1.00E+00 | 5.28E-01 |
| 8 | Left limb angle asym._Histogram 2 | 0 | A5 | 938 | 1 | 0.02105648 | 1 | 1 | ns | 1.00E+00 | 1.00E+00 | 5.28E-01 |
| 8 | Left limb angle asym._Histogram 2 | 2 | A5 | 959 | 0.97769291 | 0.0205772 | 0.002216794 | 0.013300766 | * | 1.00E+00 | 1.00E+00 | 5.28E-01 |
| 8 | Left limb angle asym._Histogram 2 | 4 | A5 | 800 | 0.7903888 | 0.02037109 | 8.65395E-22 | 5.19237E-21 | **** | 1.00E+00 | 1.00E+00 | 5.28E-01 |
| 8 | Left limb angle asym._Histogram 2 | 6 | A5 | 1001 | 0.65278762 | 0.01738146 | 2.6854E-37 | 1.61124E-36 | **** | 1.00E+00 | 1.00E+00 | 5.28E-01 |
| 8 | Left limb angle asym._Histogram 2 | 8 | A5 | 1318 | 0.65247247 | 0.01496114 | 3.99E-41 | 2.40E-40 | **** | 1.00E+00 | 1.00E+00 | 5.28E-01 |
| 8 | Left limb angle asym._Histogram 2 | 10 | A5 | 1253 | 0.69138393 | 0.01584709 | 9.77E-27 | 5.86E-26 | **** | 1.00E+00 | 1.00E+00 | 5.28E-01 |
| 9 | Neck velocity_FFT mean coeff. 1 | 0 | CT | 736 | 1 | 0.03376391 | 1 | 1 | ns | 1.00E+00 | 4.06E-01 | 7.34E-01 |
| 9 | Neck velocity_FFT mean coeff. 1 | 2 | CT | 620 | 1.06225131 | 0.03970176 | 0.006623869 | 0.039743213 | * | 1.00E+00 | 4.06E-01 | 7.34E-01 |
| 9 | Neck velocity_FFT mean coeff. 1 | 4 | CT | 491 | 0.98209504 | 0.04215344 | 3.91203E-06 | 2.34722E-05 | **** | 1.00E+00 | 4.06E-01 | 7.34E-01 |
| 9 | Neck velocity_FFT mean coeff. 1 | 6 | CT | 449 | 0.9626069 | 0.04249771 | 0.009185566 | 0.055113396 | ns | 1.00E+00 | 4.06E-01 | 7.34E-01 |
| 9 | Neck velocity_FFT mean coeff. 1 | 8 | CT | 447 | 1.05131447 | 0.04580083 | 0.181105255 | 1 | ns | 1.00E+00 | 4.06E-01 | 7.34E-01 |
| 9 | Neck velocity_FFT mean coeff. 1 | 10 | CT | 415 | 1.00647523 | 0.04765655 | 3.02313E-07 | 1.81388E-06 | **** | 1.00E+00 | 4.06E-01 | 7.34E-01 |
| 9 | Neck velocity_FFT mean coeff. 1 | 0 | A5 | 949 | 1 | 0.03204915 | 1.00E+00 | 1.00E+00 | ns | 1.00E+00 | 4.06E-01 | 7.34E-01 |
| 9 | Neck velocity_FFT mean coeff. 1 | 2 | A5 | 936 | 1.22240843 | 0.04008433 | 6.62E-03 | 3.97E-02 | * | 1.00E+00 | 4.06E-01 | 7.34E-01 |
| 9 | Neck velocity_FFT mean coeff. 1 | 4 | A5 | 790 | 1.27851717 | 0.04305883 | 3.91E-06 | 2.34722E-05 | **** | 1.00E+00 | 4.06E-01 | 7.34E-01 |
| 9 | Neck velocity_FFT mean coeff. 1 | 6 | A5 | 983 | 1.11965618 | 0.03575718 | 9.19E-03 | 0.055113396 | ns | 1.00E+00 | 4.06E-01 | 7.34E-01 |
| 9 | Neck velocity_FFT mean coeff. 1 | 8 | A5 | 1302 | 1.12672352 | 0.02904117 | 0.181105255 | 1 | ns | 1.00E+00 | 4.06E-01 | 7.34E-01 |
| 9 | Neck velocity_FFT mean coeff. 1 | 10 | A5 | 1245 | 1.35381533 | 0.0356058 | 3.02313E-07 | 1.81388E-06 | **** | 1.00E+00 | 4.06E-01 | 7.34E-01 |
| 10 | Body length_FFT mean coeff. 1 | 0 | CT | 732 | 1 | 0.03352943 | 1 | 1 | ns | 1.00E+00 | 2.04E-02 | 7.69E-01 |
| 10 | Body length_FFT mean coeff. 1 | 2 | CT | 620 | 0.95020333 | 0.03384413 | 0.365788319 | 1 | ns | 1.00E+00 | 2.04E-02 | 7.69E-01 |
| 10 | Body length_FFT mean coeff. 1 | 4 | CT | 490 | 0.90229104 | 0.03845192 | 4.13904E-07 | 2.48342E-06 | **** | 1.00E+00 | 2.04E-02 | 7.69E-01 |
| 10 | Body length_FFT mean coeff. 1 | 6 | CT | 448 | 0.8690146 | 0.0410015 | 8.38754E-16 | 5.03253E-15 | **** | 1.00E+00 | 2.04E-02 | 7.69E-01 |
| 10 | Body length_FFT mean coeff. 1 | 8 | CT | 451 | 0.86282848 | 0.04019393 | 7.36182E-24 | 4.41709E-23 | **** | 1.00E+00 | 2.04E-02 | 7.69E-01 |
| 10 | Body length_FFT mean coeff. 1 | 10 | CT | 417 | 0.83750533 | 0.03837667 | 2.14201E-27 | 1.28521E-26 | **** | 1.00E+00 | 2.04E-02 | 7.69E-01 |
| 10 | Body length_FFT mean coeff. 1 | 0 | A5 | 921 | 1 | 0.02940079 | 1.00E+00 | 1.00E+00 | ns | 1.00E+00 | 2.04E-02 | 7.69E-01 |
| 10 | Body length_FFT mean coeff. 1 | 2 | A5 | 959 | 0.91133772 | 0.02673068 | 3.66E-01 | 1.00E+00 | ns | 1.00E+00 | 2.04E-02 | 7.69E-01 |
| 10 | Body length_FFT mean coeff. 1 | 4 | A5 | 791 | 0.67974449 | 0.02484779 | 4.13904E-07 | 2.48342E-06 | **** | 1.00E+00 | 2.04E-02 | 7.69E-01 |
| 10 | Body length_FFT mean coeff. 1 | 6 | A5 | 990 | 0.55073999 | 0.01864069 | 8.38754E-16 | 5.03253E-15 | **** | 1.00E+00 | 2.04E-02 | 7.69E-01 |
| 10 | Body length_FFT mean coeff. 1 | 8 | A5 | 1295 | 0.49055743 | 0.01631295 | 7.36E-24 | 4.42E-23 | **** | 1.00E+00 | 2.04E-02 | 7.69E-01 |
| 10 | Body length_FFT mean coeff. 1 | 10 | A5 | 1249 | 0.46815026 | 0.01448021 | 2.14E-27 | 1.29E-26 | **** | 1.00E+00 | 2.04E-02 | 7.69E-01 |

| Rank | Feature name | Week | group | n | Mean | SEM | raw_p | corrected_p | significant | ANOVA_p_ Week | ANOVA_p_ Group | ANOVA_p_ Interaction |
|---|---|---|---|---|---|---|---|---|---|---|---|---|
| 11 | U-body length_Negative turning points | 0 | CT | 741 | 1 | 0.006075 | 1 | 1 | ns | 1.00E+00 | 9.63E-01 | 1.74E-01 |
| 11 | U-body length_Negative turning points | 2 | CT | 629 | 0.987775 | 0.006558 | 0.000135 | 0.000811 | *** | 1.00E+00 | 9.63E-01 | 1.74E-01 |
| 11 | U-body length_Negative turning points | 4 | CT | 494 | 1.010186 | 0.007116 | 2.79E-09 | 1.68E-08 | **** | 1.00E+00 | 9.63E-01 | 1.74E-01 |
| 11 | U-body length_Negative turning points | 6 | CT | 451 | 0.995584 | 0.007209 | 4.78E-42 | 2.87E-41 | **** | 1.00E+00 | 9.63E-01 | 1.74E-01 |
| 11 | U-body length_Negative turning points | 8 | CT | 453 | 1.006387 | 0.007282 | 4.06E-54 | 2.44E-53 | **** | 1.00E+00 | 9.63E-01 | 1.74E-01 |
| 11 | U-body length_Negative turning points | 10 | CT | 422 | 1.002038 | 0.007831 | 3.21E-42 | 1.93E-41 | **** | 1.00E+00 | 9.63E-01 | 1.74E-01 |
| 11 | U-body length_Negative turning points | 0 | A5 | 958 | 1 | 0.005434 | 1 | 1 | ns | 1.00E+00 | 9.63E-01 | 1.74E-01 |
| 11 | U-body length_Negative turning points | 2 | A5 | 963 | 1.020922 | 0.005538 | 0.000135 | 0.000811 | *** | 1.00E+00 | 9.63E-01 | 1.74E-01 |
| 11 | U-body length_Negative turning points | 4 | A5 | 798 | 1.065464 | 0.005779 | 2.79E-09 | 1.68E-08 | **** | 1.00E+00 | 9.63E-01 | 1.74E-01 |
| 11 | U-body length_Negative turning points | 6 | A5 | 994 | 1.133608 | 0.00576 | 4.78E-42 | 2.87E-41 | **** | 1.00E+00 | 9.63E-01 | 1.74E-01 |
| 11 | U-body length_Negative turning points | 8 | A5 | 1304 | 1.154967 | 0.004839 | 4.06E-54 | 2.44E-53 | **** | 1.00E+00 | 9.63E-01 | 1.74E-01 |
| 11 | U-body length_Negative turning points | 10 | A5 | 1254 | 1.143866 | 0.005251 | 3.21E-42 | 1.93E-41 | **** | 1.00E+00 | 9.63E-01 | 1.74E-01 |
| 12 | Hand distance_Median diff | 0 | CT | 728 | 1 | 0.117539 | 1 | 1 | ns | 1.00E+00 | 1.00E+00 | 9.70E-01 |
| 12 | Hand distance_Median diff | 2 | CT | 626 | 0.910835 | 0.119244 | 8.05E-05 | 0.000483 | *** | 1.00E+00 | 1.00E+00 | 9.70E-01 |
| 12 | Hand distance_Median diff | 4 | CT | 482 | 1.232448 | 0.14327 | 4.81E-08 | 2.89E-07 | **** | 1.00E+00 | 1.00E+00 | 9.70E-01 |
| 12 | Hand distance_Median diff | 6 | CT | 451 | 0.878286 | 0.146231 | 1.02E-10 | 6.14E-10 | **** | 1.00E+00 | 1.00E+00 | 9.70E-01 |
| 12 | Hand distance_Median diff | 8 | CT | 452 | 1.129434 | 0.15207 | 1.41E-15 | 8.46E-15 | **** | 1.00E+00 | 1.00E+00 | 9.70E-01 |
| 12 | Hand distance_Median diff | 10 | CT | 419 | 0.954634 | 0.139985 | 2.17E-14 | 1.3E-13 | **** | 1.00E+00 | 1.00E+00 | 9.70E-01 |
| 12 | Hand distance_Median diff | 0 | A5 | 958 | 1 | 0.110098 | 1.00E+00 | 1 | ns | 1.00E+00 | 1.00E+00 | 9.70E-01 |
| 12 | Hand distance_Median diff | 2 | A5 | 963 | 1.687542 | 0.138147 | 8.05E-05 | 0.000483 | *** | 1.00E+00 | 1.00E+00 | 9.70E-01 |
| 12 | Hand distance_Median diff | 4 | A5 | 794 | 2.534609 | 0.162997 | 4.81E-08 | 2.89E-07 | **** | 1.00E+00 | 1.00E+00 | 9.70E-01 |
| 12 | Hand distance_Median diff | 6 | A5 | 984 | 2.46328 | 0.150514 | 1.02E-10 | 6.14E-10 | **** | 1.00E+00 | 1.00E+00 | 9.70E-01 |
| 12 | Hand distance_Median diff | 8 | A5 | 1279 | 3.47654 | 0.164539 | 1.41E-15 | 8.46E-15 | **** | 1.00E+00 | 1.00E+00 | 9.70E-01 |
| 12 | Hand distance_Median diff | 10 | A5 | 1227 | 3.190061 | 0.16253 | 2.17E-14 | 1.3E-13 | **** | 1.00E+00 | 1.00E+00 | 9.70E-01 |
| 13 | Leg angle asym._MFCC 3 | 0 | CT | 739 | 1 | 0.032479 | 1 | 1 | ns | 1.00E+00 | 1.00E+00 | 2.02E-01 |
| 13 | Leg angle asym._MFCC 3 | 2 | CT | 619 | 1.125009 | 0.035868 | 0.001601 | 0.009604 | ** | 1.00E+00 | 1.00E+00 | 2.02E-01 |
| 13 | Leg angle asym._MFCC 3 | 4 | CT | 483 | 1.020833 | 0.040609 | 2.93E-07 | 1.76E-06 | **** | 1.00E+00 | 1.00E+00 | 2.02E-01 |
| 13 | Leg angle asym._MFCC 3 | 6 | CT | 444 | 0.875474 | 0.04166 | 2.63E-09 | 1.58E-08 | **** | 1.00E+00 | 1.00E+00 | 2.02E-01 |
| 13 | Leg angle asym._MFCC 3 | 8 | CT | 452 | 0.838696 | 0.042406 | 7.47E-08 | 4.48E-07 | **** | 1.00E+00 | 1.00E+00 | 2.02E-01 |
| 13 | Leg angle asym._MFCC 3 | 10 | CT | 421 | 0.83959 | 0.042569 | 4.5E-08 | 2.7E-07 | **** | 1.00E+00 | 1.00E+00 | 2.02E-01 |
| 13 | Leg angle asym._MFCC 3 | 0 | A5 | 942 | 1 | 0.028724 | 1 | 1 | ns | 1.00E+00 | 1.00E+00 | 2.02E-01 |
| 13 | Leg angle asym._MFCC 3 | 2 | A5 | 948 | 0.98162 | 0.028193 | 0.001601 | 0.009604 | ** | 1.00E+00 | 1.00E+00 | 2.02E-01 |
| 13 | Leg angle asym._MFCC 3 | 4 | A5 | 791 | 0.761251 | 0.030549 | 2.93E-07 | 1.76E-06 | **** | 1.00E+00 | 1.00E+00 | 2.02E-01 |
| 13 | Leg angle asym._MFCC 3 | 6 | A5 | 988 | 0.592545 | 0.025527 | 2.63E-09 | 1.58E-08 | **** | 1.00E+00 | 1.00E+00 | 2.02E-01 |
| 13 | Leg angle asym._MFCC 3 | 8 | A5 | 1303 | 0.601596 | 0.021256 | 7.47E-08 | 4.48E-07 | **** | 1.00E+00 | 1.00E+00 | 2.02E-01 |
| 13 | Leg angle asym._MFCC 3 | 10 | A5 | 1233 | 0.584443 | 0.022907 | 4.50E-08 | 2.70E-07 | **** | 1.00E+00 | 1.00E+00 | 2.02E-01 |
| 14 | Chest acc._Wavlet entropy | 0 | CT | 733 | 1 | 0.00016 | 1 | 1 | ns | 1.00E+00 | 1.00E+00 | 9.74E-01 |
| 14 | Chest acc._Wavlet entropy | 2 | CT | 620 | 1.000342 | 0.000169 | 7.71E-07 | 4.63E-06 | **** | 1.00E+00 | 1.00E+00 | 9.74E-01 |
| 14 | Chest acc._Wavlet entropy | 4 | CT | 488 | 1.000398 | 0.000185 | 1.16E-11 | 6.98E-11 | **** | 1.00E+00 | 1.00E+00 | 9.74E-01 |
| 14 | Chest acc._Wavlet entropy | 6 | CT | 451 | 1.000631 | 0.000181 | 4.44E-48 | 2.67E-47 | **** | 1.00E+00 | 1.00E+00 | 9.74E-01 |
| 14 | Chest acc._Wavlet entropy | 8 | CT | 449 | 0.999948 | 0.000212 | 7.94E-39 | 4.76E-38 | **** | 1.00E+00 | 1.00E+00 | 9.74E-01 |
| 14 | Chest acc._Wavlet entropy | 10 | CT | 417 | 0.999246 | 0.000248 | 1.31E-62 | 7.84E-62 | **** | 1.00E+00 | 1.00E+00 | 9.74E-01 |
| 14 | Chest acc._Wavlet entropy | 0 | A5 | 944 | 1 | 0.000184 | 1 | 1 | ns | 1.00E+00 | 1.00E+00 | 9.74E-01 |
| 14 | Chest acc._Wavlet entropy | 2 | A5 | 951 | 0.998736 | 0.000237 | 7.71E-07 | 4.63E-06 | **** | 1.00E+00 | 1.00E+00 | 9.74E-01 |
| 14 | Chest acc._Wavlet entropy | 4 | A5 | 794 | 0.998114 | 0.000235 | 1.16E-11 | 6.98E-11 | **** | 1.00E+00 | 1.00E+00 | 9.74E-01 |
| 14 | Chest acc._Wavlet entropy | 6 | A5 | 999 | 0.993007 | 0.000329 | 4.44E-48 | 2.67E-47 | **** | 1.00E+00 | 1.00E+00 | 9.74E-01 |
| 14 | Chest acc._Wavlet entropy | 8 | A5 | 1300 | 0.993489 | 0.000275 | 7.94E-39 | 4.76

**Supplementary Table 18. Statistical summary of group comparisons (A1O3) for the top 20 features (TSFEL model) at 10 wk.** One-way ANOVA was performed, followed by post-hoc comparisons using Welch's t-tests comparing each group to the reference (CT) group. Statistical significance is indicated by asterisks after Holm–Sidak correction for multiple comparisons. This PDF table displays only the top 20 features in ascending rank order for concise presentation. Additional features are included in the full version of the table, available in the Source Data file (see S_Table 18). The underlying source data for this table is provided in the same Source Data file (see S_Figure 39).

| Rank | Parameter | Group | n | Mean | SEM | ANOVA p-value | Raw Post-hoc p-value | Corrected Post-hoc p-value | Significance |
|---|---|---|---|---|---|---|---|---|---|
| 1 | Foot distance_Signal distance | CT | 414 | 120.9610938 | 0.05142103 | 1.32E-126 | | | |
| 1 | Foot distance_Signal distance | A5 | 1233 | 122.8990073 | 0.054976337 | 1.32E-126 | 9.45E-119 | 2.83E-118 | **** |
| 1 | Foot distance_Signal distance | A1 | 405 | 121.0505208 | 0.059591425 | 1.32E-126 | 0.256231259 | 0.256231259 | ns |
| 1 | Foot distance_Signal distance | A1O3 | 71 | 121.2484047 | 0.140981552 | 1.32E-126 | 0.058739901 | 0.114029426 | ns |
| 2 | Tail angle_Autocorrelation | CT | 417 | 621.0410193 | 5.567925837 | 4.43E-118 | | | |
| 2 | Tail angle_Autocorrelation | A5 | 1231 | 725.598803 | 2.531338775 | 4.43E-118 | 1.26E-53 | 3.77E-53 | **** |
| 2 | Tail angle_Autocorrelation | A1 | 408 | 617.4904705 | 5.921770687 | 4.43E-118 | 0.662361773 | 0.662361773 | ns |
| 2 | Tail angle_Autocorrelation | A1O3 | 73 | 573.3920942 | 14.08472479 | 4.43E-118 | 0.002204392 | 0.004403924 | ** |
| 3 | Neck acc._Wavelet std_4 | CT | 414 | 82.6602058 | 1.055835852 | 6.90E-37 | | | |
| 3 | Neck acc._Wavelet std_4 | A5 | 1238 | 71.22936308 | 0.474445343 | 6.90E-37 | 2.20E-21 | 4.40E-21 | **** |
| 3 | Neck acc._Wavelet std_4 | A1 | 409 | 66.48778717 | 0.982806596 | 6.90E-37 | 3.09E-27 | 9.26E-27 | **** |
| 3 | Neck acc._Wavelet std_4 | A1O3 | 69 | 74.18110168 | 1.797033519 | 6.90E-37 | 8.49E-05 | 8.49E-05 | **** |
| 4 | Body angle velocity_ECDF percentile 0 | CT | 424 | -0.664142414 | 0.010390164 | 5.44E-05 | | | |
| 4 | Body angle velocity_ECDF percentile 0 | A5 | 1239 | -0.609791259 | 0.005993496 | 5.44E-05 | 6.86E-06 | 2.06E-05 | **** |
| 4 | Body angle velocity_ECDF percentile 0 | A1 | 408 | -0.642360398 | 0.011623455 | 5.44E-05 | 0.162750099 | 0.287653734 | ns |
| 4 | Body angle velocity_ECDF percentile 0 | A1O3 | 72 | -0.627719176 | 0.023269171 | 5.44E-05 | 0.155993918 | 0.287653734 | ns |
| 5 | Body angle_min | CT | 413 | 6.500888549 | 0.217977295 | 6.34E-11 | | | |
| 5 | Body angle_min | A5 | 1239 | 7.74169535 | 0.125007834 | 6.34E-11 | 9.87E-07 | 2.96E-06 | **** |
| 5 | Body angle_min | A1 | 404 | 6.462713521 | 0.205533146 | 6.34E-11 | 0.898638274 | 0.898638274 | ns |
| 5 | Body angle_min | A1O3 | 69 | 5.596534226 | 0.468529268 | 6.34E-11 | 0.083178079 | 0.159437565 | ns |
| 6 | Left limb angle asym._Histogram 1 | CT | 427 | 11.33723653 | 0.411403553 | 1.73E-63 | | | |
| 6 | Left limb angle asym._Histogram 1 | A5 | 1261 | 5.154639175 | 0.143812472 | 1.73E-63 | 5.43E-39 | 1.63E-38 | **** |
| 6 | Left limb angle asym._Histogram 1 | A1 | 415 | 7.575903614 | 0.352441318 | 1.73E-63 | 7.77E-12 | 1.55E-11 | **** |
| 6 | Left limb angle asym._Histogram 1 | A1O3 | 72 | 9.819444444 | 0.972896871 | 1.73E-63 | 0.153930463 | 0.153930463 | ns |
| 7 | Right limb angle asym._Histogram 1 | CT | 425 | 9.249411765 | 0.377617115 | 7.03E-56 | | | |
| 7 | Right limb angle asym._Histogram 1 | A5 | 1257 | 4.161495625 | 0.12616908 | 7.03E-56 | 9.98E-33 | 2.99E-32 | **** |
| 7 | Right limb angle asym._Histogram 1 | A1 | 413 | 5.644067797 | 0.270177399 | 7.03E-56 | 2.63E-14 | 5.26E-14 | **** |
| 7 | Right limb angle asym._Histogram 1 | A1O3 | 73 | 6.356164384 | 0.605771915 | 7.03E-56 | 8.48E-05 | 8.48E-05 | **** |
| 8 | Left limb angle asym._Histogram 2 | CT | 422 | 18.1492891 | 0.53449628 | 5.24E-44 | | | |
| 8 | Left limb angle asym._Histogram 2 | A5 | 1253 | 10.56903432 | 0.242250967 | 5.24E-44 | 7.13E-34 | 2.14E-33 | **** |
| 8 | Left limb angle asym._Histogram 2 | A1 | 414 | 12.78019324 | 0.475856098 | 5.24E-44 | 1.62E-13 | 3.24E-13 | **** |
| 8 | Left limb angle asym._Histogram 2 | A1O3 | 72 | 15.23611111 | 1.136513946 | 5.24E-44 | 0.022300566 | 0.022300566 | * |
| 9 | Neck velocity_FFT mean coeff. 1 | CT | 415 | 12.65441844 | 0.599186101 | 6.24E-32 | | | |
| 9 | Neck velocity_FFT mean coeff. 1 | A5 | 1245 | 20.32873493 | 0.534652572 | 6.24E-32 | 7.60E-21 | 2.28E-20 | **** |
| 9 | Neck velocity_FFT mean coeff. 1 | A1 | 409 | 10.56500463 | 0.487137409 | 6.24E-32 | 0.006962391 | 0.013876307 | * |
| 9 | Neck velocity_FFT mean coeff. 1 | A1O3 | 69 | 12.54483707 | 1.376983242 | 6.24E-32 | 0.941981228 | 0.941981228 | ns |
| 10 | Body length_FFT mean coeff. 1 | CT | 417 | 1.241565677 | 0.056891772 | 5.78E-48 | | | |
| 10 | Body length_FFT mean coeff. 1 | A5 | 1249 | 0.737821489 | 0.022821329 | 5.78E-48 | 1.46E-15 | 4.39E-15 | **** |
| 10 | Body length_FFT mean coeff. 1 | A1 | 405 | 1.595640281 | 0.07316708 | 5.78E-48 | 0.000144069 | 0.000288117 | *** |
| 10 | Body length_FFT mean coeff. 1 | A1O3 | 71 | 1.043731885 | 0.115222877 | 5.78E-48 | 0.1266215 | 0.1266215 | ns |
| 11 | U-body length_Negative turning points | CT | 422 | 15.86492891 | 0.123990241 | 4.02E-37 | | | |
| 11 | U-body length_Negative turning points | A5 | 1254 | 17.87559809 | 0.082052092 | 4.02E-37 | 9.39E-38 | 2.82E-37 | **** |
| 11 | U-body length_Negative turning points | A1 | 402 | 17.01243781 | 0.131344057 | 4.02E-37 | 3.50E-10 | 7.01E-10 | **** |
| 11 | U-body length_Negative turning points | A1O3 | 73 | 16.34246575 | 0.294688636 | 4.02E-37 | 0.138439864 | 0.138439864 | ns |
| 12 | Hand distance_Median diff | CT | 419 | 0.001098357 | 0.00016106 | 1.43E-18 | | | |
| 12 | Hand distance_Median diff | A5 | 1227 | 0.004283188 | 0.000218223 | 1.43E-18 | 1.42E-30 | 4.26E-30 | **** |
| 12 | Hand distance_Median diff | A1 | 402 | 0.002470199 | 0.000254182 | 1.43E-18 | 6.09E-06 | 1.22E-05 | **** |
| 12 | Hand distance_Median diff | A1O3 | 71 | 0.00171892 | 0.000525653 | 1.43E-18 | 0.262226236 | 0.262226236 | ns |
| 13 | Leg angle asym._MFCC 3 | CT | 421 | -46.29394915 | 2.347180078 | 6.17E-07 | | | |
| 13 | Leg angle asym._MFCC 3 | A5 | 1233 | -32.50746682 | 1.274105511 | 6.17E-07 | 3.20E-07 | 9.61E-07 | **** |
| 13 | Leg angle asym._MFCC 3 | A1 | 411 | -34.74954104 | 2.207896049 | 6.17E-07 | 0.000360166 | 0.000653557 | *** |
| 13 | Leg angle asym._MFCC 3 | A1O3 | 72 | -27.16222923 | 4.594470222 | 6.17E-07 | 0.000326832 | 0.000653557 | *** |
| 14 | Chest acc._Wavlet entropy | CT | 417 | 2.183488911 | 0.00054217 | 3.56E-76 | | | |
| 14 | Chest acc._Wavlet entropy | A5 | 1217 | 2.157286841 | 0.000825998 | 3.56E-76 | 6.31E-129 | 1.89E-128 | **** |
| 14 | Chest acc._Wavlet entropy | A1 | 405 | 2.16464008 | 0.001143628 | 3.56E-76 | 1.09E-42 | 2.18E-42 | **** |
| 14 | Chest acc._Wavlet entropy | A1O3 | 72 | 2.18134925 | 0.001357257 | 3.56E-76 | 0.146499226 | 0.146499226 | ns |
| 15 | Right limb angle asym._Histogram 2 | CT | 424 | 16.54716981 | 0.499381038 | 1.77E-60 | | | |
| 15 | Right limb angle asym._Histogram 2 | A5 | 1258 | 8.46899841 | 0.208330629 | 1.77E-60 | 7.43E-43 | 2.23E-42 | **** |
| 15 | Right limb angle asym._Histogram 2 | A1 | 413 | 11.08474576 | 0.449708957 | 1.77E-60 | 1.58E-15 | 3.16E-15 | **** |
| 15 | Right limb angle asym._Histogram 2 | A1O3 | 72 | 13.22222222 | 1.084140584 | 1.77E-60 | 0.006355385 | 0.006355385 | ** |
| 16 | Chest 3D velocity_LPCC 9 | CT | 421 | 0.194585315 | 0.005375514 | 2.13E-13 | | | |
| 16 | Chest 3D velocity_LPCC 9 | A5 | 1243 | 0.246761648 | 0.003428944 | 2.13E-13 | 1.11E-15 | 3.32E-15 | **** |
| 16 | Chest 3D velocity_LPCC 9 | A1 | 401 | 0.228902479 | 0.006015333 | 2.13E-13 | 2.35E-05 | 4.70E-05 | **** |
| 16 | Chest 3D velocity_LPCC 9 | A1O3 | 71 | 0.216593161 | 0.012385624 | 2.13E-13 | 0.106305247 | 0.106305247 | ns |
| 17 | Arm angle asym._MFCC 0 | CT | 417 | 46.06249976 | 0.61693644 | 1.01E-24 | | | |
| 17 | Arm angle asym._MFCC 0 | A5 | 1234 | 38.23429325 | 0.403915516 | 1.01E-24 | 1.02E-24 | 3.05E-24 | **** |
| 17 | Arm angle asym._MFCC 0 | A1 | 404 | 42.25425361 | 0.683829417 | 1.01E-24 | 3.92E-05 | 7.84E-05 | **** |
| 17 | Arm angle asym._MFCC 0 | A1O3 | 71 | 45.77172474 | 1.450269276 | 1.01E-24 | 0.854007905 | 0.854007905 | ns |
| 18 | H-body length_Skewness | CT | 415 | -0.179018497 | 0.028972309 | 1.97E-08 | | | |
| 18 | H-body length_Skewness | A5 | 1242 | -0.364531523 | 0.016704044 | 1.97E-08 | 4.10E-08 | 1.23E-07 | **** |
| 18 | H-body length_Skewness | A1 | 407 | -0.242841757 | 0.026443056 | 1.97E-08 | 0.104104441 | 0.197371147 | ns |
| 18 | H-body length_Skewness | A1O3 | 70 | -0.210574464 | 0.073431285 | 1.97E-08 | 0.690272774 | 0.690272774 | ns |
| 19 | Hand distance_Histogram 5 | CT | 418 | 0.85645933 | 0.097805237 | 1.04E-06 | | | |
| 19 | Hand distance_Histogram 5 | A5 | 1256 | 1.442675159 | 0.07168403 | 1.04E-06 | 1.57E-06 | 4.71E-06 | **** |
| 19 | Hand distance_Histogram 5 | A1 | 412 | 0.86407767 | 0.099380013 | 1.04E-06 | 0.956440827 | 0.956440827 | ns |
| 19 | Hand distance_Histogram 5 | A1O3 | 71 | 1.070422535 | 0.31865155 | 1.04E-06 | 0.522687242 | 0.772172531 | ns |
| 20 | Chest velocity_LPCC 5 | CT | 416 | 0.235399593 | 0.005912266 | 1.65E-17 | | | |
| 20 | Chest velocity_LPCC 5 | A5 | 1246 | 0.294604769 | 0.003277813 | 1.65E-17 | 1.54E-17 | 4.61E-17 | **** |
| 20 | Chest velocity_LPCC 5 | A1 | 402 | 0.279363262 | 0.005664607 | 1.65E-17 | 1.03E-07 | 2.06E-07 | **** |
| 20 | Chest velocity_LPCC 5 | A1O3 | 72 | 0.260991255 | 0.013280089 | 1.65E-17 | 0.081344886 | 0.081344886 | ns |

**Supplementary Table 19. Statistical summary of group comparisons (A1O3) for the turning features at 10 wk.** One-way ANOVA was performed, followed by post-hoc comparisons using Welch's t-tests comparing each group to the reference (CT) group. Statistical significance is indicated by asterisks after Benjamini–Hochberg correction for multiple comparisons. The top 20 features are listed in ascending rank order, with additional features appended afterwards. Source data are provided in the Source Data file (See S_Figure 40).

| Parameter | Group | Mean | SEM | n | ANOVA p-value | Raw Post-hoc p-value | Corrected Post-hoc p-value | Significance |
|---|---|---|---|---|---|---|---|---|
| Turning angle | CT | 7.71 | 0.30 | 170 | 0.1624 | | | |
| Turning angle | A5 | 8.20 | 0.26 | 160 | 0.1624 | 0.2176 | 0.4480 | ns |
| Turning angle | A1 | 7.31 | 0.49 | 97 | 0.1624 | 0.4890 | 0.4890 | ns |
| Turning angle | A1O3 | 7.22 | 0.37 | 98 | 0.1624 | 0.2987 | 0.4480 | ns |
| Turning duration | CT | 0.25 | 0.01 | 173 | 0.0053 | | | |
| Turning duration | A5 | 0.31 | 0.02 | 162 | 0.0053 | 0.0081 | 0.0244 | * |
| Turning duration | A1 | 0.26 | 0.02 | 98 | 0.0053 | 0.7744 | 0.7744 | ns |
| Turning duration | A1O3 | 0.23 | 0.02 | 98 | 0.0053 | 0.2873 | 0.4310 | ns |
| Turning velocity | CT | 40.72 | 2.32 | 170 | 0.0424 | | | |
| Turning velocity | A5 | 34.37 | 1.74 | 160 | 0.0424 | 0.0291 | 0.0436 | * |
| Turning velocity | A1 | 33.72 | 1.60 | 97 | 0.0424 | 0.0135 | 0.0405 | * |
| Turning velocity | A1O3 | 37.51 | 1.81 | 98 | 0.0424 | 0.2757 | 0.2757 | ns |
| Turning direction | CT | -0.01 | 0.08 | 174 | 0.1582 | | | |
| Turning direction | A5 | -0.06 | 0.08 | 164 | 0.1582 | 0.6503 | 0.9270 | ns |
| Turning direction | A1 | -0.27 | 0.10 | 99 | 0.1582 | 0.0354 | 0.1063 | ns |
| Turning direction | A1O3 | 0.00 | 0.10 | 102 | 0.1582 | 0.9270 | 0.9270 | ns |

**Supplementary Table 20. Statistical summary of group comparisons (A1O3) for the rearing features at 10 wk.** One-way ANOVA was performed, followed by post-hoc comparisons using Welch's t-tests comparing each group to the reference (CT) group. Statistical significance is indicated by asterisks after Holm–Sidak correction for multiple comparisons. The top 20 features are listed in ascending rank order, with additional features appended afterwards. Source data are provided in the Source Data file (See S_Figure 41).

| Parameter | Group | Mean | SEM | n | ANOVA p-value | Raw Post-hoc p-value | Corrected Post-hoc p-value | Significance |
|---|---|---|---|---|---|---|---|---|
| Chest z velocity (mean)_in rearing period | CT | 3.02 | 0.23 | 18 | 0.4003 | | | |
| Chest z velocity (mean)_in rearing period | A5 | 3.22 | 0.23 | 11 | 0.4003 | 0.5385 | 0.7870 | ns |
| Chest z velocity (mean)_in rearing period | A1 | 3.71 | 0.28 | 6 | 0.4003 | 0.0775 | 0.2149 | ns |
| Chest z velocity (mean)_in rearing period | A1O3 | 3.00 | 0.41 | 5 | 0.4003 | 0.9792 | 0.9792 | ns |
| Chest z velocity (max)_in rearing period | CT | 3.46 | 0.30 | 18 | 0.0724 | | | |
| Chest z velocity (max)_in rearing period | A5 | 4.23 | 0.29 | 11 | 0.0724 | 0.0727 | 0.1401 | ns |
| Chest z velocity (max)_in rearing period | A1 | 4.73 | 0.34 | 6 | 0.0724 | 0.0143 | 0.0423 | * |
| Chest z velocity (max)_in rearing period | A1O3 | 3.57 | 0.48 | 5 | 0.0724 | 0.8473 | 0.8473 | ns |
| Chest z velocity (min)_in rearing period | CT | 16.00 | 0.14 | 18 | 0.0426 | | | |
| Chest z velocity (min)_in rearing period | A5 | 1.57 | 0.13 | 11 | 0.0426 | 0.0133 | 0.0395 | * |
| Chest z velocity (min)_in rearing period | A1 | 2.11 | 0.14 | 6 | 0.0426 | 0.8984 | 0.8984 | ns |
| Chest z velocity (min)_in rearing period | A1O3 | 1.71 | 0.13 | 5 | 0.0426 | 0.0746 | 0.1437 | ns |
| Chest z velocity (std)_in rearing period | CT | 0.46 | 0.07 | 18 | 0.0030 | | | |
| Chest z velocity (std)_in rearing period | A5 | 0.81 | 0.10 | 11 | 0.0030 | 0.0100 | 0.0199 | * |
| Chest z velocity (std)_in rearing period | A1 | 0.92 | 0.09 | 6 | 0.0030 | 0.0018 | 0.0055 | ** |
| Chest z velocity (std)_in rearing period | A1O3 | 0.53 | 0.13 | 5 | 0.0030 | 0.6583 | 0.6583 | ns |
| Rearing duration | CT | 0.67 | 0.11 | 18 | 0.0071 | | | |
| Rearing duration | A5 | 1.24 | 0.12 | 11 | 0.0071 | 0.0014 | 0.0042 | ** |
| Rearing duration | A1 | 1.03 | 0.14 | 6 | 0.0071 | 0.0694 | 0.1340 | ns |
| Rearing duration | A1O3 | 0.68 | 0.21 | 5 | 0.0071 | 0.9566 | 0.9566 | ns |
| Chest z velocity (mean)_in upward phase | CT | 5.27 | 0.44 | 9 | 0.0506 | | | |
| Chest z velocity (mean)_in upward phase | A5 | 3.00 | 0.25 | 2 | 0.0506 | 0.0023 | 0.0047 | ** |
| Chest z velocity (mean)_in upward phase | A1 | 7.13 | | 1 | 0.0506 | | | |
| Chest z velocity (mean)_in upward phase | A1O3 | 3.47 | 0.92 | 2 | 0.0506 | 0.2603 | 0.2603 | ns |
| Chest z velocity (max)_in upward phase | CT | 9.70 | 0.29 | 9 | 0.0002 | | | |
| Chest z velocity (max)_in upward phase | A5 | 6.17 | 0.31 | 2 | 0.0002 | 0.0029 | 0.0029 | ** |
| Chest z velocity (max)_in upward phase | A1 | 12.39 | | 1 | 0.0002 | | | |
| Chest z velocity (max)_in upward phase | A1O3 | 8.06 | 0.01 | 2 | 0.0002 | 0.0005 | 0.0009 | *** |
| Chest z velocity (std)_in upward phase | CT | 2.59 | 0.14 | 9 | 0.0498 | | | |
| Chest z velocity (std)_in upward phase | A5 | 1.82 | 0.07 | 2 | 0.0498 | 0.0011 | 0.0022 | ** |
| Chest z velocity (std)_in upward phase | A1 | 3.17 | | 1 | 0.0498 | | | |
| Chest z velocity (std)_in upward phase | A1O3 | 2.31 | 0.01 | 2 | 0.0498 | 0.0718 | 0.0718 | ns |
| Chest z velocity (mean)_in doward phase | CT | 3.13 | 0.44 | 5 | 0.1948 | | | |
| Chest z velocity (mean)_in doward phase | A5 | 2.33 | 0.24 | 8 | 0.1948 | 0.1589 | 0.4049 | ns |
| Chest z velocity (mean)_in doward phase | A1 | 2.91 | 0.29 | 5 | 0.1948 | 0.6814 | 0.8872 | ns |
| Chest z velocity (mean)_in doward phase | A1O3 | 3.34 | 0.04 | 2 | 0.1948 | 0.6642 | 0.8872 | ns |
| Chest z velocity (max)_in doward phase | CT | 12.11 | 1.00 | 5 | 0.0002 | | | |
| Chest z velocity (max)_in doward phase | A5 | 6.90 | 0.47 | 8 | 0.0002 | 0.0036 | 0.0106 | * |
| Chest z velocity (max)_in doward phase | A1 | 11.16 | 0.79 | 5 | 0.0002 | 0.4800 | 0.7296 | ns |
| Chest z velocity (max)_in doward phase | A1O3 | 12.06 | 1.59 | 2 | 0.0002 | 0.9809 | 0.9809 | ns |
| Chest z velocity (std)_in doward phase | CT | 3.70 | 0.35 | 5 | 0.0002 | | | |
| Chest z velocity (std)_in doward phase | A5 | 1.75 | 0.10 | 8 | 0.0002 | 0.0036 | 0.0108 | * |
| Chest z velocity (std)_in doward phase | A1 | 3.25 | 0.42 | 5 | 0.0002 | 0.4400 | 0.6864 | ns |
| Chest z velocity (std)_in doward phase | A1O3 | 3.77 | 0.39 | 2 | 0.0002 | 0.8945 | 0.8945 | ns |

**Supplementary Table 21. Definitions of the Gait model top 20 features.**

| Feature name | Unit | Definition |
|---|---|---|
| Stride length | cm | Distance covered during a full sequence of a paw's gait (stance and swing phases) |
| Stance distance | cm | Distance covered during a stance phase of a foot |
| Feet distance | cm | Distance between a foot at start of a stride and the controlateral foot's strike point |
| Stance_chest velocity | cm/s | 2D chest velocity during a stance phase |
| Swing velocity | cm/s | Distance covered during a swing phase of a foot devided by swing time |
| Stride_chest velocity | cm/s | 2D chest velocity during a full sequence of a stride |
| Stride leg angle_min | deg | The minimum leg angle during a full sequence of a stride of the foot |
| Stance width | cm | Distance between feet during full stance (perpendicular distance from the controlateral foot's stance point to the line, connecting the start and end points of a stride) |
| Stance_leg angle anticorr. | n/a | Correlation efficiency of legs angles during a stance phase |
| Swing_chest velocity | cm/s | 2D chest velocity during a swing phase |
| Stance velocity | cm/s | Stance distance devided by stance time |
| Swing distance | cm | Distance covered during a swing phase of a foot |
| Feet angle | cm | Angle between feet; foot position at the end of a stride, anus position and the controlateral foot poisition at the contrateral foot strike |
| Stride leg angle_max | deg | The maximum leg angle during a full sequence of a stride of the foot |
| Stride leg angle_std | deg | The std leg angle during a full sequence of a stride of the foot |
| Spatial diff._stance/swing | % | (stance_dist/stride_length)/(swing_dist/stride_length)*100 |
| Stride leg angle_mean | deg | The mean leg angle during a full sequence of a stride of the foot |
| Stance leg angle_velocity | deg/s | Mean angular velocity of a leg during a stance phase |
| Stride leg angle_anticorr. | n/a | Correlation efficiency of legs angles during a stride phase |
| Swing leg angle_anticorr. | n/a | Correlation efficiency of legs angles during a swing phase |

**Supplementary Table 22. Statistical summary of group comparisons (A1O3) for the top 20 features ( Gait model) at 10 wk.** One-way ANOVA was performed, followed by post-hoc comparisons using Welch's t-tests comparing each group to the reference (CT) group. Statistical significance is indicated by asterisks after Holm–Sidak correction for multiple comparisons. This PDF table displays only the top 20 features in ascending rank order for concise presentation. Additional features are included in the full version of the table, available in the Source Data file (see S_Table 22). The underlying source data for this table is provided in the same Source Data file (see S_Figure 44).

| | Parameter | Group | Mean | SEM | n | ANOVA p-value | Raw Post-hoc p-value | Corrected Post-hoc p-value | Significance |
|---|---|---|---|---|---|---|---|---|---|
| 1 | Stride length | CT | 3.67 | 0.07 | 421 | 0.0000 | | | |
| 1 | Stride length | A5 | 4.73 | 0.07 | 344 | 0.0000 | 0.0000 | 0.0000 | **** |
| 1 | Stride length | A1 | 3.59 | 0.10 | 194 | 0.0000 | 0.5100 | 0.5100 | ns |
| 1 | Stride length | A1O3 | 3.52 | 0.10 | 174 | 0.0000 | 0.1989 | 0.3583 | ns |
| 2 | Stance distance | CT | 0.63 | 0.02 | 421 | 0.0000 | | | |
| 2 | Stance distance | A5 | 1.08 | 0.04 | 348 | 0.0000 | 0.0000 | 0.0000 | **** |
| 2 | Stance distance | A1 | 0.83 | 0.04 | 194 | 0.0000 | 0.0000 | 0.0000 | **** |
| 2 | Stance distance | A1O3 | 0.74 | 0.03 | 174 | 0.0000 | 0.0106 | 0.0106 | * |
| 3 | Feet distance | CT | 2.98 | 0.02 | 421 | 0.0000 | | | |
| 3 | Feet distance | A5 | 3.34 | 0.04 | 344 | 0.0000 | 0.0000 | 0.0000 | **** |
| 3 | Feet distance | A1 | 3.23 | 0.04 | 194 | 0.0000 | 0.0000 | 0.0000 | **** |
| 3 | Feet distance | A1O3 | 3.16 | 0.04 | 174 | 0.0000 | 0.0001 | 0.0001 | **** |
| 4 | Stance_chest velocity | CT | 6.34 | 0.09 | 421 | 0.0000 | | | |
| 4 | Stance_chest velocity | A5 | 7.37 | 0.05 | 344 | 0.0000 | 0.0000 | 0.0000 | **** |
| 4 | Stance_chest velocity | A1 | 7.15 | 0.08 | 194 | 0.0000 | 0.0000 | 0.0000 | **** |
| 4 | Stance_chest velocity | A1O3 | 6.17 | 0.11 | 174 | 0.0000 | 0.2304 | 0.2304 | ns |
| 5 | Swing velocity | CT | 13.01 | 0.26 | 421 | 0.0000 | | | |
| 5 | Swing velocity | A5 | 15.25 | 0.34 | 344 | 0.0000 | 0.0000 | 0.0000 | **** |
| 5 | Swing velocity | A1 | 11.08 | 0.44 | 194 | 0.0000 | 0.0002 | 0.0004 | *** |
| 5 | Swing velocity | A1O3 | 12.00 | 0.45 | 174 | 0.0000 | 0.0535 | 0.0535 | ns |
| 6 | Stride_chest velocity | CT | 6.46 | 0.08 | 421 | 0.0000 | | | |
| 6 | Stride_chest velocity | A5 | 7.45 | 0.05 | 344 | 0.0000 | 0.0000 | 0.0000 | **** |
| 6 | Stride_chest velocity | A1 | 7.18 | 0.08 | 194 | 0.0000 | 0.0000 | 0.0000 | **** |
| 6 | Stride_chest velocity | A1O3 | 6.28 | 0.10 | 174 | 0.0000 | 0.1607 | 0.1607 | ns |
| 7 | Stride leg angle_min | CT | 37.56 | 0.40 | 421 | 0.0177 | | | |
| 7 | Stride leg angle_min | A5 | 39.61 | 0.71 | 344 | 0.0177 | 0.0121 | 0.0359 | * |
| 7 | Stride leg angle_min | A1 | 39.73 | 0.79 | 194 | 0.0177 | 0.0150 | 0.0359 | * |
| 7 | Stride leg angle_min | A1O3 | 39.71 | 0.81 | 174 | 0.0177 | 0.0183 | 0.0359 | * |
| 8 | Stance width | CT | 2.29 | 0.03 | 421 | 0.0000 | | | |
| 8 | Stance width | A5 | 2.45 | 0.04 | 344 | 0.0000 | 0.0026 | 0.0026 | ** |
| 8 | Stance width | A1 | 2.59 | 0.05 | 194 | 0.0000 | 0.0000 | 0.0000 | **** |
| 8 | Stance width | A1O3 | 2.59 | 0.05 | 174 | 0.0000 | 0.0000 | 0.0000 | **** |
| 9 | Stance_leg angle anticorr. | CT | 0.50 | 0.03 | 416 | 0.0376 | | | |
| 9 | Stance_leg angle anticorr. | A5 | 0.40 | 0.04 | 338 | 0.0376 | 0.0477 | 0.0622 | ns |
| 9 | Stance_leg angle anticorr. | A1 | 0.37 | 0.05 | 188 | 0.0376 | 0.0316 | 0.0622 | ns |
| 9 | Stance_leg angle anticorr. | A1O3 | 0.36 | 0.05 | 173 | 0.0376 | 0.0200 | 0.0588 | ns |
| 10 | Swing_chest velocity | CT | 6.51 | 0.09 | 421 | 0.0000 | | | |
| 10 | Swing_chest velocity | A5 | 7.48 | 0.05 | 344 | 0.0000 | 0.0000 | 0.0000 | **** |
| 10 | Swing_chest velocity | A1 | 7.14 | 0.09 | 194 | 0.0000 | 0.0000 | 0.0000 | **** |
| 10 | Swing_chest velocity | A1O3 | 6.40 | 0.11 | 174 | 0.0000 | 0.4425 | 0.4425 | ns |
| 11 | Stance velocity | CT | 2.76 | 0.14 | 420 | 0.0000 | | | |
| 11 | Stance velocity | A5 | 3.95 | 0.18 | 339 | 0.0000 | 0.0000 | 0.0000 | **** |
| 11 | Stance velocity | A1 | 2.59 | 0.17 | 193 | 0.0000 | 0.4414 | 0.4414 | ns |
| 11 | Stance velocity | A1O3 | 2.23 | 0.14 | 173 | 0.0000 | 0.0083 | 0.0166 | * |
| 12 | Swing distance | CT | 2.44 | 0.06 | 421 | 0.0000 | | | |
| 12 | Swing distance | A5 | 2.87 | 0.07 | 344 | 0.0000 | 0.0000 | 0.0000 | **** |
| 12 | Swing distance | A1 | 2.03 | 0.10 | 194 | 0.0000 | 0.0004 | 0.0008 | *** |
| 12 | Swing distance | A1O3 | 2.13 | 0.09 | 174 | 0.0000 | 0.0058 | 0.0058 | ** |
| 13 | Feet angle | CT | 47.39 | 1.10 | 421 | 0.0000 | | | |
| 13 | Feet angle | A5 | 58.60 | 2.05 | 344 | 0.0000 | 0.0000 | 0.0000 | **** |
| 13 | Feet angle | A1 | 64.46 | 2.25 | 194 | 0.0000 | 0.0000 | 0.0000 | **** |
| 13 | Feet angle | A1O3 | 54.24 | 1.90 | 174 | 0.0000 | 0.0020 | 0.0020 | ** |
| 14 | Stride leg angle_max | CT | 68.34 | 0.80 | 421 | 0.0000 | | | |
| 14 | Stride leg angle_max | A5 | 83.99 | 1.18 | 344 | 0.0000 | 0.0000 | 0.0000 | **** |
| 14 | Stride leg angle_max | A1 | 78.07 | 1.36 | 194 | 0.0000 | 0.0000 | 0.0000 | **** |
| 14 | Stride leg angle_max | A1O3 | 70.90 | 1.38 | 174 | 0.0000 | 0.1121 | 0.1121 | ns |
| 15 | Stride leg angle_std | CT | 10.06 | 0.23 | 421 | 0.0000 | | | |
| 15 | Stride leg angle_std | A5 | 14.20 | 0.36 | 344 | 0.0000 | 0.0000 | 0.0000 | **** |
| 15 | Stride leg angle_std | A1 | 12.08 | 0.41 | 194 | 0.0000 | 0.0000 | 0.0001 | **** |
| 15 | Stride leg angle_std | A1O3 | 9.88 | 0.40 | 174 | 0.0000 | 0.6980 | 0.6980 | ns |
| 16 | Spatial diff._stance/swing | CT | 46.22 | 3.76 | 420 | 0.0000 | | | |
| 16 | Spatial diff._stance/swing | A5 | 114.86 | 22.51 | 348 | 0.0000 | 0.0028 | 0.0056 | ** |
| 16 | Spatial diff._stance/swing | A1 | 230.64 | 49.99 | 194 | 0.0000 | 0.0003 | 0.0009 | *** |
| 16 | Spatial diff._stance/swing | A1O3 | 62.87 | 7.87 | 172 | 0.0000 | 0.0574 | 0.0574 | ns |
| 17 | Stride leg angle_mean | CT | 52.63 | 0.53 | 421 | 0.0000 | | | |
| 17 | Stride leg angle_mean | A5 | 61.41 | 0.83 | 344 | 0.0000 | 0.0000 | 0.0000 | **** |
| 17 | Stride leg angle_mean | A1 | 58.49 | 0.94 | 194 | 0.0000 | 0.0000 | 0.0000 | **** |
| 17 | Stride leg angle_mean | A1O3 | 54.87 | 0.94 | 174 | 0.0000 | 0.0390 | 0.0390 | * |
| 18 | Stance leg angle_velocity | CT | 53.50 | 0.59 | 420 | 0.0000 | | | |
| 18 | Stance leg angle_velocity | A5 | 63.06 | 0.91 | 339 | 0.0000 | 0.0000 | 0.0000 | **** |
| 18 | Stance leg angle_velocity | A1 | 60.38 | 1.10 | 193 | 0.0000 | 0.0000 | 0.0000 | **** |
| 18 | Stance leg angle_velocity | A1O3 | 55.28 | 1.02 | 173 | 0.0000 | 0.1309 | 0.1309 | ns |
| 19 | Stride leg angle_anticorr. | CT | 0.41 | 0.02 | 421 | 0.1300 | | | |
| 19 | Stride leg angle_anticorr. | A5 | 0.38 | 0.03 | 344 | 0.1300 | 0.3742 | 0.3742 | ns |
| 19 | Stride leg angle_anticorr. | A1 | 0.31 | 0.04 | 194 | 0.1300 | 0.0257 | 0.0751 | ns |
| 19 | Stride leg angle_anticorr. | A1O3 | 0.34 | 0.04 | 174 | 0.1300 | 0.1507 | 0.2786 | ns |
| 20 | Swing leg angle_anticorr. | CT | 0.67 | 0.03 | 421 | 0.1387 | | | |
| 20 | Swing leg angle_anticorr. | A5 | 0.62 | 0.03 | 344 | 0.1387 | 0.2152 | 0.3841 | ns |
| 20 | Swing leg angle_anticorr. | A1 | 0.61 | 0.05 | 194 | 0.1387 | 0.2237 | 0.3841 | ns |
| 20 | Swing leg angle_anticorr. | A1O3 | 0.55 | 0.05 | 173 | 0.1387 | 0.0369 | 0.1067 | ns |

# Supplementary Notes

List of Supplementary Notes:

1. Comparative evaluation of lesion types affecting the DA system
2. Model evaluation methods
3. Comparative evaluation of AI-based and conventional behavioural assessments
4. Stability and generalisability of the feature selection
5. Assessment of body size as a potential confounding factor
6. Basal activity of optoRET in A5 PD mice
7. Interpretation of a RET agonist (BT44) in the hA53T overexpression mouse PD model
8. Interpretation of L-DOPA in the hA53T overexpression mouse PD model

## 1. Comparative evaluation of lesion types affecting the DA system

Dopaminergic (DA) neurons are among the most vulnerable neuronal populations in the brain, partly due to their intrinsic properties, including high melanin content and the oxidative metabolism of dopamine, which contributes to elevated oxidative stress. In experimental settings – such as viral injections used in this study – DA neuron loss can be relatively high, primarily due to two distinct mechanisms: mechanical damage to the substantia nigra pars compacta (SNc) and protein overload per se, both of which are independent of the specific effects of the exogenous genes introduced.

To provide a better insight and improve the reproducibility of our study, we explicitly included and carefully compared control groups to distinguish the specific effects attributable to: mechanically induced lesion (MIL, i.e., EV group), protein overload lesion (POL, i.e., R1 or R5 groups), and bilateral alpha-Synuclein-induced lesion (AIL, i.e., A1 or A5 groups).

Comparative analysis of the Control (CT) subgroups suggested that MIL did not significantly impair the motor function nor reduce the nigral DA cell counts, showing only ~10% difference compared to the No injection (NI) group ($p$ = 0.6853; Fig. 1h; Table 1). Contrarily, the POL – particularly the R5 group – showed evidence of toxicity affecting motor function in rotarod test score (RRS; $p$ = 0.0254) and DA neuron integrity. Notably, the R5 group showed approximately 29% SNc DA neuronal loss ($p$ = 0.0325), despite no significant decrease in the striatal TH fibre density ($p$ = 0.9129), which is in line with the previous studies[1, 2] (Fig. 1g,h).

Additionally, beam walking test score (BWS) and AI-predicted PD score (APS) analyses revealed no significant differences among the subgroups within the CT animals (Fig. 1f,k). The varied outcomes the behavioural assessments suggest differing sensitivities: RRS may reflect generalised motor coordination, while BWS likely assesses fine coordination and balance[3].

Collectively, these results inform the interpretation of our PD models: the A1 group most likely reflects the effects of AIL, whilst the A5 group may present a combination of AIL and POL. As our primary objective was to distinguish PD-related (AIL) features from non-PD (NP) features, we trained the non-PD (NP) class using data from the NI, R1, and R5 groups. Accordingly, our XGB model and the derived APS (AI-predicted PD score) metric are specifically tuned to capture behavioural features associated with AIL, rather than those arising from POL.

## 2. Model evaluation methods

In our machine learning (ML) framework, we employed a cross-view (CV) evaluation, training models on CT (n = 10) and A5 (n = 11) mice and validating on unseen subjects from the same groups (CT, n = 4; A5, n = 6). Acknowledging that cross-subject (CS) evaluation is widely regarded as a more stringent test of generalisation, yet both methods are highly valid in the machine learning (ML) field, we repeated the ML processes to develop models with a CS method. Specifically, we included nine

additional mice (CT, n = 4; A5, n = 5) to maintain a subject-level split with approximately 70% training and 30% validation.

Notably, the compared model performances were almost the same with both validation methods (Supplementary Fig. 7a). A direct comparison of the top 20 features between the XGB-CV and XGB-CS models revealed a Spearman correlation of ≈ 0.9789 ($p$ ≈ 7.15e-14), indicating that the feature ranking is nearly identical with 100% of the top 20 features overlapping (Supplementary Fig. 7b). In addition, the absolute SHAP values (as measured by Pearson correlation) were nearly identical between the two protocols ($r$ ≈ 0.9999, $p$ ≈ 4.81e-114), further supporting the consistency of feature importance. Furthermore, one-way ANOVA with Holm–Sidak multiple comparisons showed no significant differences in prediction outcomes across all groups between the XGB-CV and XGB-CS models and highly correlated ($p$ > 0.05; Pearson's correlation, $r$ = 0.99; Supplementary Fig. 7c,d). Importantly, our original XGB-CV model consistently assessed all unseen A5 mice into the severe PD category (APS > 75% in rounded values), providing additional rationale for retaining our initial evaluation method.

Collectively, these findings robustly confirm the generalisability and stability of the CV-based XGB model. Given the close agreement in both feature ranking and predictive performance between the CV and CS evaluations, we remain confident in our model choice.

### 3. Comparative evaluation of AI-based and conventional behavioural assessments

We performed direct statistical comparisons between the AI approach (AI-predicted PD score [APS]) and traditional task-dependent assessments (rotarod test score [RRS] and beam walking test score [BWS]). These comparisons include: (1) sensitivity in discriminating between the two PD cohorts at the endpoint, (2) early detection of PD cohorts, and (3) correlation with histological data. The results of these comparisons are summarised in Fig. 1l.

(1) We compared the $p$-values for differences between the A1 and A5 groups at the 10 wk endpoint in RRS, BWS, and APS assessments (Fig. 1d,f,k). The $p$-values were 0.1896 (RRS), 0.0020 (BWS), and <0.0001 (APS), indicating that APS provides the most sensitive discrimination between PD severity cohorts.

(2) We assessed early-stage (2 wk) detection of the PD cohorts using RRS, BWS, and APS (Supplementary Fig. 8). At 2 wk post-surgery, RRS failed to distinguish any PD groups from EV, although the A5 group showed a trend toward significance ($p$ = 0.0521). BWS significantly distinguished the A5 group from EV ($p$ = 0.0018), but not the A1 group ($p$ = 0.0965). In contrast, APS successfully distinguished both PD groups from EV (A1: $p$ = 0.0074; A5: $p$ < 0.0001) and further detected a significant difference between the A1 and A5 groups ($p$ = 0.0015). These results indicate that APS enables earlier and more sensitive detection of PD compared to RRS and BWS.

(3) We evaluated the absolute Pearson correlation coefficients (|*r*|) between behavioural assessments (RRS, BWS, and APS) and histological data (Supplementary Figs. 10,11). For striatal TH intensity, |*r*| values were 0.61 (RRS), 0.74 (BWS), and 0.80 (APS). For nigral DA cell count, the values were 0.78 (RRS), 0.79 (BWS), and 0.85 (APS). Together, these results demonstrate that APS provides the strongest association with underlying PD pathology across all behavioural metrics.

**4. Stability and generalisability of the feature selection**

To assess the robustness of our feature selection, we compared the top 20 behavioural features in XGB model, derived from the combined train-validation (TV) dataset with those obtained from the unseen dataset (CT, n = 40; A5, n = 13).

The analysis revealed a 100% overlap in the top 20 features, with a Spearman correlation of ≈ 0.9835 ($p \approx 8.29e\text{-}15$). A separate comparison of the absolute SHAP values for these top 20 features yielded a Pearson correlation of about 0.2013 ($p \approx 0.3948$), indicating some variability in the absolute magnitudes; however, given the near-perfect consistency in ranking, this variation in magnitudes is considered of lesser concern.

Together, these results provide robust quantitative evidence that the top 20 features remain highly relevant across the TV and unseen datasets, thereby confirming the stability and generalisability of the feature selection approach.

**5. Assessment of body size as a potential confounding factor**

Our feature creation process yielded many distance-based behavioural features, raising potential confounds related to group-specific body size differences in PD classification by our models. To address this concern, we conducted an extensive analysis of body lengths using both the raw pose dataset and the motion filtered dataset (i.e. the primary dataset, see Motion processing in Methods). For this purpose, the body length was defined as the sum of the forebody (fbody; neck-chest distance) and hindbody (hbody; chest-anus distance) lengths in 3D, filtering for frames where the body angle was within ± 10 degree before averaging the body lengths for each mouse at each week. Please note that this measure differs from the ‘body length (neck-anus distance)’ presented in the manuscript (see, Fig. 2a and Supplementary Fig. 5b).

In the raw pose dataset (Supplementary Fig. 13a, left), mean body lengths at 0 wk were highly consistent across groups (CT: 6.58 ± 0.02, A1: 6.58 ± 0.04, A5: 6.6 ± 0.04 cm; n = 46, 15, 16, respectively). However, significant differences emerged at 10 wk (CT: 6.45 ± 0.04, A1: 6.76 ± 0.07, A5: 6.99 ± 0.06 cm; n = 48, 15, 18, respectively), likely due to variations in body posture during non-moving (freeze) states (accounting approximately 60% of the raw pose dataset). Crucially, analysis of the move dataset (Supplementary Fig. 13a, right) showed no significant differences in body lengths

between groups at either 0 wk (CT: 6.95 ± 0.05, A1: 6.99 ± 0.12, A5: 7.06 ± 0.05 cm; n = 45, 14, 13) or 10 wk (CT: 7.02 ± 0.06, A1: 7.28 ± 0.12, A5: 7.13 ± 0.21 cm; n = 41, 9, 11). The 2-way ANOVA tests supported these observations (Supplementary Fig. 13b): the pose dataset showed significant effects for time ($p$ = 0.0006), group ($p$ < 0.0001), and their interactions ($p$ <0.0001), whereas the move dataset showed no significant effects for group (time: $p$ = 0.0456; group: $p$ = 0.2201; interaction: $p$ = 0.4359).

Additionally, we re-analysed preliminary data to further assess the robustness of our APS (AI-prediction of PD scores). In this exploratory analysis, we compared data from three individual mice: R1(50), low dose RFP injection at 50 wk; A1(10), low dose A53T injection at 10 wk; and A1(50), low dose A53T injection at 50 wk. Although these analyses involved only a single mouse per condition (thus preliminary), the results were consistent with our expectations: A1(10) exhibited a smaller body length consistent with younger age, whilst R1(50) and A1(50) had similar lengths to our primary dataset (Supplementary Fig. 13c). Importantly, despite the variations in body lengths, APS measurements remained robust: R1(50) maintained APS within non-PD status, whilst both A1(10) and A1(50) exhibited APS consistent with mild PD health status (Supplementary Fig. 13d).

Collectively, these findings provide robust evidence that our distance-based features are unlikely to be confounded by body size (neck-chest-anus) differences, particularly within the move dataset used for our primary analysis. Although the raw pose dataset exhibited differences (likely related to postural variations in the non-moving periods), our core analyses on the move dataset did not reflect significant confounds related to body size.

**6. Basal activity of optoRET in A5 PD mice**

Statistically, optoRET activation was ineffective in the A5 mice (see Supplementary Table 8), although a subtle, non-significant trend was observed in the A5OD (A5+optoRET+dark) and A5O2 (A5+optoRET+S#1) groups. Our *in vitro* studies suggest that the effects of optoRET are non-linear, with optimal light conditions yielding the most beneficial effects[4]. Although the light-sensitive domain of optoRET has been engineered to minimise basal activity, some residual effect remains. In severe PD states (A5), this basal activity may confer a modest benefit compared to daily, full light activation (A5O1), whereas in milder PD stages the effect appears negligible. We postulate that the basal effect may have protected A5 mice from the high protein overload lesion (POL) rather than the alpha-Synuclein-induced lesion (AIL; see Fig.1 and Supplementary Note 1). Further studies are required to elucidate these state-dependent dynamics; for instance, future experiments could investigate whether overexpression of R5 with optoRET can prevent motor dysfunction caused by POL.

Given that these trends did not reach statistical significance, our detailed analyses focused on the condition exhibiting the most robust response (A1O3).

## 7. Interpretation of a RET agonist (BT44) in the hA53T overexpression mouse PD model

Although optogenetic activation of RET signalling using optoRET provides valuable proof-of-concept and mechanistic insights, its direct clinical translation remains challenging (despite the FDA approval of channelrhodopsin and the clinical use of deep-brain implanted devices). Alternative RET-targeted therapeutics, such as pharmacologically validated RET agonists, may offer more immediate translational promise. However, currently available RET agonists lack the capacity for temporal control and face substantial limitations regarding pharmacokinetics[5-7], including poor systemic delivery and potential off-target effects – particularly in tissues with high RET expression, such as the gastrointestinal tract. One of the most extensively validated preclinical RET agonists, BT44, has thus far only been shown to be effective in a rat 6-OHDA model when delivered directly to the brain via infusion[6].

To test the efficacy of a RET agonist in our hA53T overexpression mouse PD model, we included an experimental group, A1BT, in which BT44 (120 µM) was infused bilaterally into the brains of A1 mice at a constant flow rate of 0.18 µL/hr using osmotic pumps (see Methods). Due to the technical limitations of the pumps' capacity, the experiment concluded at 6 wk post-virus injection. Despite these constraints, we evaluated the therapeutic efficacy of BT44 relative to the optoRET group (A1O3).

Our findings indicated that BT44 was overall ineffective in the A1 PD model (Supplementary Figs. 26, 31). An initial beneficial trend was observed in the elevated beam walking test score (BWS) and AI-predicted PD score (APS), albeit smaller in magnitude than in the A1O2 group (Supplementary Fig. 25f). Additionally, the rotarod test score (RRS) showed improvement, although this did not reach statistical significance compared to the A1 group (Supplementary Fig. 26d). These results suggest that BT44 may moderately improve general motor coordination (RRS) but fails to significantly enhance fine motor control or balance (BWS) or broader PD-related features (APS).

The early beneficial trend could reflect the agonist's dependency on endogenous RET receptors, which are known to be downregulated during PD progression – particularly in aSyn overexpression models[8-10]. We propose that the limited efficacy results from a combination of factors: (1) a reduction in endogenous RET expression in our model, where aSyn overexpression likely exceeds the levels typically seen in human PD pathology[10]; and (2) diminished neuroprotective efficacy following prolonged ligand exposure[11, 12]. To distinguish whether these effects arise primarily from receptor downregulation or prolonged stimulation, further studies are warranted using alternative aSyn models, such as the aSyn-preformed fibril model, in which GDNF/RET signalling has shown therapeutic benefit[13].

Finally, treatment response evaluation (TRE) for the A1BT group indicated that only approximately 10% of behavioural features were marked as treated (Supplementary Fig. 31), further supporting the limited efficacy of BT44 in this context. A comparative TRE analysis across optoRET (A1O2, A1O3) and RET agonist (A1BT) groups also revealed common off-target effects on

locomotion, potentially reflecting RET signalling activation in brain circuits that influence motor behaviour. Collectively, these results highlight the comparative efficacy of optoRET over pharmacological RET agonists and offer mechanistic insights that may help inform future RET-targeted therapeutic strategies for PD.

## 8. Interpretation of L-DOPA in the hA53T overexpression mouse PD model

Levodopa (L-DOPA; 3,4-Dihydroxy-L-phenylalanine), a dopamine precursor, remains the gold-standard symptomatic treatment for PD, particularly effective in alleviating akinesia and rigidity[14-16]. However, L-DOPA is less effective for certain axial and non-motor symptoms, and its clinical utility becomes increasingly limited as PD progresses, primarily due to the progressive loss of dopaminergic neurons, which narrows the therapeutic window[14]. Over time, the therapeutic benefits of L-DOPA often diminish ('wearing-off' between medications), whilst side effects such as L-DOPA-induced dyskinesia (LID) emerge at peak concentrations[14, 16]. There is general agreement that LID arises from pronounced, intermittent fluctuations in brain DA levels, leading to abnormal stimulation of striatal dopamine receptors[16].

We evaluated L-DOPA in our hA53T overexpression mouse PD model if the intermittent administrations of a high dose (50 mg/kg) could improve PD symptoms. We included two L-DOPA treatment cohorts of A1 mice (A1L1 and A1L3 groups), in which L-DOPA (50 mg/kg) was administered intraperitoneally either daily or on alternate days, respectively. In our hA53T overexpression PD mouse model, we observed no significant therapeutic improvements across all assessed metrics, including RRS, BWT, and APS (Supplementary Fig. 26). Notably, the rotarod test score (RRS) showed an early trend towards worsening, although this effect was not significant at the endpoint. Furthermore, a significant increase in neck/trunk dystonia was observed, measured by the axial bending angle[16] (Supplementary Fig. 26j–m). These findings may reflect the consequences of our high-dose intermittent dosing protocols, potentially exacerbating side effects through dramatic fluctuations in striatal dopamine levels. Finally, treatment response evaluation (TRE) further revealed notable off-target effects on overall motor coordination (Supplementary Fig. 31).

Collectively, these results may highlight the importance of selecting appropriate medication protocols based on therapeutic strategy – continuous delivery may be more suitable for L-DOPA[17], whereas intermittent activation appears more appropriate for c-RET stimulation[11, 12] via optoRET.

## Supplementary References


1. Koprich, J.B., Johnston, T.H., Reyes, M.G., Sun, X. & Brotchie, J.M. Expression of human A53T alpha-synuclein in the rat substantia nigra using a novel AAV1/2 vector produces a rapidly evolving pathology with protein aggregation, dystrophic neurite architecture and nigrostriatal degeneration with potential to model the pat. *Molecular Neurodegeneration* **5**, 43 (2010).

2. Sanchez-Guajardo, V., Febbraro, F., Kirik, D. & Romero-Ramos, M. Microglia acquire distinct activation profiles depending on the degree of alpha-synuclein neuropathology in a rAAV based model of Parkinson's disease. *PLoS One* **5**, e8784 (2010).

3. Aniszewska, A., Bergstrom, J., Ingelsson, M. & Ekmark-Lewen, S. Modeling Parkinson's disease-related symptoms in alpha-synuclein overexpressing mice. *Brain Behav* **12**, e2628 (2022).

4. Hyeon, B., Lee, H., Kim, N. & Heo, W.D. Optogenetic dissection of RET signaling reveals robust activation of ERK and enhanced filopodia-like protrusions of regenerating axons. *Mol Brain* **16**, 56 (2023).

5. Viisanen, H. et al. Novel RET agonist for the treatment of experimental neuropathies. *Mol Pain* **16**, 1744806920950866 (2020).

6. Renko, J.M. et al. Neuroprotective Potential of a Small Molecule RET Agonist in Cultured Dopamine Neurons and Hemiparkinsonian Rats. *J Parkinsons Dis* **11**, 1023-1046 (2021).

7. Haider, M.S. et al. Biological Activity In Vitro, Absorption, BBB Penetration, and Tolerability of Nanoformulation of BT44:RET Agonist with Disease-Modifying Potential for the Treatment of Neurodegeneration. *Biomacromolecules* **24**, 4348-4365 (2023).

8. Decressac, M. et al. alpha-Synuclein-induced down-regulation of Nurr1 disrupts GDNF signaling in nigral dopamine neurons. *Sci Transl Med* **4**, 163ra156 (2012).

9. Decressac, M., Volakakis, N., Bjorklund, A. & Perlmann, T. NURR1 in Parkinson disease--from pathogenesis to therapeutic potential. *Nat Rev Neurol* **9**, 629-636 (2013).

10. Conway, J.A. & Kramer, E.R. Is activation of GDNF/RET signaling the answer for successful treatment of Parkinson's disease? A discussion of data from the culture dish to the clinic. *Neural Regeneration Research* **17**, 1462-1467 (2022).

11. Mesa-Infante, V., Afonso-Oramas, D., Salas-Hernandez, J., Rodriguez-Nunez, J. & Barroso-Chinea, P. Long-term exposure to GDNF induces dephosphorylation of Ret, AKT, and ERK1/2, and is ineffective at protecting midbrain dopaminergic neurons in cellular models of Parkinson's disease. *Mol Cell Neurosci* **118**, 103684 (2022).

12. Azevedo, M.D. et al. Oxidative stress induced by sustained supraphysiological intrastriatal GDNF delivery is prevented by dose regulation. *Molecular Therapy Methods & Clinical Development* **31** (2023).

13. Chmielarz, P. et al. GDNF/RET Signaling Pathway Activation Eliminates Lewy Body Pathology in Midbrain Dopamine Neurons. *Mov Disord* **35**, 2279-2289 (2020).

14. Armstrong, M.J. & Okun, M.S. Diagnosis and Treatment of Parkinson Disease: A Review. *JAMA* **323**, 548-560 (2020).

15. Blosser, J.A., Podolsky, E. & Lee, D. L-DOPA-Induced Dyskinesia in a Genetic Drosophila Model of Parkinson's Disease. *Exp Neurobiol* **29**, 273-284 (2020).

16. Andreoli, L., Abbaszadeh, M., Cao, X. & Cenci, M.A. Distinct patterns of dyskinetic and dystonic features following D1 or D2 receptor stimulation in a mouse model of parkinsonism. *Neurobiol Dis* **157**, 105429 (2021).

17. Olanow, C.W., Calabresi, P. & Obeso, J.A. Continuous Dopaminergic Stimulation as a Treatment for Parkinson's Disease: Current Status and Future Opportunities. *Mov Disord* **35**, 1731-1744 (2020).